



<https://theses.gla.ac.uk/>

Theses Digitisation:

<https://www.gla.ac.uk/myglasgow/research/enlighten/theses/digitisation/>

This is a digitised version of the original print thesis.

Copyright and moral rights for this work are retained by the author

A copy can be downloaded for personal non-commercial research or study,  
without prior permission or charge

This work cannot be reproduced or quoted extensively from without first  
obtaining permission in writing from the author

The content must not be changed in any way or sold commercially in any  
format or medium without the formal permission of the author

When referring to this work, full bibliographic details including the author,  
title, awarding institution and date of the thesis must be given

Enlighten: Theses

<https://theses.gla.ac.uk/>  
[research-enlighten@glasgow.ac.uk](mailto:research-enlighten@glasgow.ac.uk)

*DIRECT DESIGN OF REINFORCED CONCRETE SLABS  
USING NON ELASTIC STRESS FIELDS*

by

*MUSTAPHA BENREDOUANE*

*Ingenieur d'Etat des Travaux Publics*

*Ecole Nationale des Travaux Publics d'ALGER*

*A Thesis Submitted for the Degree of  
Master of Science*

*Department of Civil Engineering,  
University of Glasgow.*

*OCTOBER, 1988.*

ProQuest Number: 10998015

All rights reserved

INFORMATION TO ALL USERS

The quality of this reproduction is dependent upon the quality of the copy submitted.

In the unlikely event that the author did not send a complete manuscript and there are missing pages, these will be noted. Also, if material had to be removed, a note will indicate the deletion.



ProQuest 10998015

Published by ProQuest LLC (2018). Copyright of the Dissertation is held by the Author.

All rights reserved.

This work is protected against unauthorized copying under Title 17, United States Code  
Microform Edition © ProQuest LLC.

ProQuest LLC.  
789 East Eisenhower Parkway  
P.O. Box 1346  
Ann Arbor, MI 48106 – 1346

**BY THE NAME OF 'GOD' THE COMPASSIONATE, THE  
MERCIFUL**

## CONTENTS

ACKNOWLEDGEMENTS	I
SUMMARY	II
NOTATIONS	III
CHAPTER ONE: INTRODUCTION	1
1-1 General introduction	1
1-2 Methods of analysis and design	1
1-2-1 Elastic methods	1
1-2-2 Plastic methods(or limit state methods)	3
1-2-2-1 Upper bound method	4
1-2-2-2 Lower bound method	5
1-3 Purpose and scope of the present investigation	7
CHAPTER TWO: DIRECT DESIGN METHOD	10
2-1 Introduction	10
2-2 The direct design method	10
2-2-1 The equilibrium condition	10
2-2-2 The yield criterion	12
2-2-3 Design equations	21
2-2-4 Rules for placing reinforcement	25
2-2-5 Multiple load cases	26
2-2-6 The mechanism condition	29
2-2-7 Ductility demand	29
2-2-8 Conclusion	30

<b>CHAPTER THREE: FINITE ELEMENT METHOD</b>	<b>32</b>
3-1 Introduction	32
3-2 Review of the Mindlin finite element program	32
3-2-1 Mindlin plate element	33
3-2-2 Finite element formulation	35
3-2-3 Plasticity	42
3-2-4 Solution of nonlinear problem	46
3-2-5 Solution procedure adopted in the Mindlin program	48
3-2-6 Convergence criterion	49
3-2-7 Enhancements to the program	50
3-3 Review of the 'Layer' program	51
3-3-1 Introduction	51
3-3-2 Nonlinear finite element models	51
3-3-3 Review of the layer approach	53
3-3-3-1 Layered finite element formulation	53
3-3-3-2 Modeling the material	58
A- Concrete	58
B- Steel	75
3-3-3-3 Solution of the nonlinear problem	78
3-3-3-4 Solution procedure	79
3-3-3-5 Convergence criterion	79
3-3-4 Conclusion	80
 <b>CHAPTER FOUR: ELASTO- PLASTIC STRESS FIELD</b>	 <b>81</b>
4-1 Introduction	81
4-2 Description of the analysis	81

4-3	Analysis and results	82
4-4	Discussion of results	83
4-4-1	Load deflection curve	83
4-4-2	Table and figure	84
4-4-3	Isometric views	85
4-5	Conclusions	86

## CHAPTER FIVE: NONLINEAR ANALYSIS 122

5-1	Introduction	122
5-2	Designation of slabs studied	123
5-3	Proportioning and loading	123
5-4	Steel layout	125
5-5	Analysis	125
5-6	Results , discussion and conclusions	131
5-6-1	Test series 1	131
5-6-2	Conclusions	131
5-6-3	Test series 2	140
5-6-4	Conclusions	140
5-6-5	Test series 3	149
5-6-6	Conclusions	149

## CHAPTER SIX: ELASTO- PLASTIC ANALYSIS OF REINFORCED CONCRETE

### SLABS BASED ON WOOD-ARMER YIELD CRITERION. 161

6-1	Introduction	161
6-2	Program	161
6-2-1	Mathematical formulation of the yield criteria	163
6-2-2	Alterations to the Mindlin program	164

6-3	Convergence study	172
6-3-1	Mesh size	172
6-3-2	Tolerance	172
6-4	Numerical application	175
6-4-1	A simply supported slab under a central point load	175
6-4-2	Hago's model three	179
6-5	Conclusion	183

## CHAPTER SEVEN: GENERAL CONCLUSIONS

	AND RECOMMENDATIONS FOR FUTURE WORK	184
--	-------------------------------------	-----

7-1	General conclusions	184
7-2	Recommendations for future work	185

	References	187
--	------------	-----

	Appendices	197
--	------------	-----

A	Wood-Armer program	197
B	Evaluation of pseudo- thickness	210



## ACKNOWLEDGEMENTS

The work described herein was carried out in the Department of Civil Engineering at the University of Glasgow, under the general guidance of Professor A.Coull.

The author would like to express his appreciation to Professor A.Coull and Dr D.R.Green for the facilities of the department.

The author is greatly indebted to Dr P.Bhatt for his valuable supervision, encouragement and advice during the course of this study.

My grateful thanks are also due to :

\* The staff of the advisory at the computer centre, especially Mr John Buchanan, Mr Jim.Berck and Dr William. Sharp for their help and assistance in programming and running softwares.

\* Dr I.McConnochie for the administrative matters.

\* My friends R.Manaa, S.Djellab and M.Bendahgane for their useful discussion and comments.

\* My friends J.Moussa, Z.Merouani, A.Bouazza, R.Saadi, M.Souici, A.Salamani, A.Bensmail, E.Guechi, D.Abderahmane and Y.K.To for their encouragement.

\* My wife and my sons MAHMOUD and OUSSAMA for their boundless patience and moral support.

\* My family and my wife's family for their encouragement.

\* My father MOHAMED and my brother M'HAMED for their moral and material support and their encouragement throughout the years.

\* Finally my thanks are to 'ALLAH' for giving me the opportunity to do this study and helping me to accomplish it with succes.

## SUMMARY

Ultimate strength design of reinforced concrete can be carried out using elastic stress field in conjunction with Wood–Armer yield criterion. This procedure is known as Direct Design Method and has shown to produce well designed slabs. The object of this work is to explore in particular the effect on serviceability limit and ductility demand of using non elastic stress fields. This is the main object of the present work.

The work divides into two convenient parts:

- i– Determination of elasto–plastic stress fields as input to Wood–Armer equations. This is accomplished using a nonlinear finite element program based on Mindlin plate element and Von–Mises criterion.
- ii– Assessment of these designed slabs using a nonlinear finite element program based on 'Layer' approach. This analysis and assessment has been done for slabs with various boundary conditions and loading systems.

The results show that use of nonlinear stress fields has the following advantages:

- a) The distribution of the design moments ( $M_x^*$ ,  $M_y^*$ ) is more uniform.
- b) The congestion of reinforcement is avoided by smoothing out the peaks.
- c) The maximum design moment is reduced by an average of 26%.
- d) The slabs designed by non elastic stress field behaved satisfactorily at the service load (0.625 x design load) in terms of deflection and steel strain.
- e) The average load at first yield of steel for all the tested slabs was 0.86 times the design load.
- f) The results indicate that the ductility demand is not much different for all the slabs designed using elastic or non elastic stress field.
- g) The average ultimate load for all the analysed slabs was 1.07 times the design load.

-h) The sensitivity of the results to the level of plasticity spread was insignificant.

A second part of this work consists of developing a nonlinear finite element program for the analysis of reinforced concrete slabs based on Wood-Armer criterion. This program has the advantage that in terms of the time required for a full analysis to determine the ultimate load, it is much faster than any standard nonlinear finite element programs based on layer analysis.

## NOTATIONS

Major symbols used in the text are listed below. Others are defined when they first appear.

$\{a\}$	Flow vector.
$\{a_b\}, \{a_t\}$	Flow vector for positive yield surface and negative yield surface respectively.
A	Area of rigid region.
$A_s$	Area of steel in the longitudinal direction.
b	Section breath.
$b_s$	Body forces.
[B]	Strain matrix.
[ $B_f$ ]	Strain matrix associated with flexural deformation.
[ $B_p$ ]	Strain matrix associated with plane stress deformation.
[ $B_s$ ]	Strain matrix associated with shear deformation.
C	Shear strain coefficient.
$C_1, C_2$	Coefficients for the tension stiffening.
D	Flexural stiffness per unit width.
[D]	Elasticity matrix.
[D']	Instantaneous elasticity matrix.
[D]*	Rigidity inplane matrix for cracked concrete.
[ $D_{ep}$ ]	Elasto- plastic stress- strain matrix.
d	Effective depth.
$d_n$	Depth of neutral axis.
$d_{zi}$	Thickness of the $i^{th}$ layer.
$\{d_i\}$	Displacement vector.

$E$	Young's modulus.
$E_c$	Young's modulus for concrete.
$E_i$	Instantaneous Young's modulus for concrete.
$E_s$	Young's modulus for steel.
$E_x, E_y$	Young's modulus in X and Y directions in an anisotropic plate.
$E_{x1}$	An off diagonal term in material properties matrix.
$f$	Load increment.
$f_c$	Cylinder compressive strength of concrete.
$f_{cc}$	Intermediate surface strength of concrete.
$f_{cu}$	Cube strength of concrete.
$f_d$	Equivalent biaxial compressive strength of concrete.
$f_y$	Yield strength of steel.
$f_t$	Tensile strength of concrete.
$\{F\}$	Vector of nodal forces in the cartesian coordinate system.
$\{F'\}$	Vector of nodal forces in the local coordinate system (n,t).
$G$	Shear modulus.
$h$	Plate thickness.
$H$	Strain hardening parameter for steel.
$I$	Moment of inertia.
$I_{cr}$	Moment of inertia of a cracked section.
$I_g$	Gross moment of inertia of uncracked section.
$I_{eff}$	Effective moment of inertia of a section.
$[K]$	Stiffness matrix.
$[K]'$	Stiffness matrix related to the local axes.
$[K_T]$	Tangential stiffness matrix.
$L_x$	Length of the slab in X direction.
$L_y$	Length of the slab in Y direction.

$m$  Ratio between tensile and compressive strengths of concrete  
 $M$  Bending moment at any stage of loading.  
 $M_{cr}$  Cracking moment.  
 $M_x, M_y, M_{xy}$  Applied moment components at a point in cartesian coordinate.  
 $M_x^*, M_\alpha^*$  Design moments in X and  $\alpha$  directions respectively.  
 $M_{y0}^*$  Design moment in Y direction  
 $M_n^*$  Flexural yield strength of the section at an yield line.  
 $M_n, M_t, M_{nt}$  Applied moment components at a point in local coordinate system (n,t).  
 $M_p$  Plastic moment.  
 $M_1, M_2$  Principal moments.  
 $N$  Total number of nodal points.  
 $N_i$  Shape function associated with node i.  
 $P$  Applied load.  
 $P_{cr}$  Cracking load.  
 $P_d$  Design load.  
 $P_y$  First yield load.  
 $P_{ult}$  Ultimate load.  
 $q$  Uniformly distributed load intensity.  
 $Q_x, Q_y$  Shear force components in cartesian coordinate.  
 $S$  Loaded surface area.  
 $S_x, S_y$  Effective shear moduli in the X and Y directions.  
 $[T]$  Transformation matrix for cracks.  
 $[T_b]$  Transformation matrix for boundary condition.  
 $V$  Volume of the plate.  
 $U.L.T$  Ultimate load.  
 $u, v, w$  Displacements at a point in the plate in (X,Y,Z)

directions respectively.

- $u_0, v_0, w_0$  Displacements at a point in the plate on the reference plane.
- $X, Y, Z$  Rectangular cartesian coordinates.
- $x, y, z$  Coordinates of point in  $X, Y, Z$  system.
- $z_i$  Distance from the reference plane to centre of the  $i^{\text{th}}$  layer.
- $\alpha$  Angle of skew.
- $\beta$  Shear retention factor.
- $d\lambda$  Plastic multiplier.
- $\gamma_{xy}, \gamma_{yz}$  Shear strain components in the cartesian coordinates.
- $\{\delta\}$  Nodal displacement vector in the cartesian coordinates.
- $\epsilon_e$  Elastic strain.
- $\{\epsilon_f\}$  Strain vector associated with flexural deformations.
- $\{\epsilon_s\}$  Strain vector associated with shear deformations.
- $\epsilon_x, \epsilon_y, \gamma_{xy}$  Strain components in cartesian coordinates.
- $\epsilon_{pk}$  Peak strain.
- $\epsilon_p$  Plastic strain.
- $\epsilon_0$  Yielding strain of steel.
- $\xi, \eta$  Nondimensional local coordinate system.
- $\theta$  Angle of principal plane.
- $\theta_{cr}$  Angle of crack with respect to X axis.
- $\theta_x, \theta_y$  Rotations of the normal in the XZ and YZ planes respectively.
- $\nu$  Poisson's ratio.
- $\Phi_x, \Phi_y$  Transverse shear rotations in the XZ and YZ plane respectively.
- $\{\sigma\}$  Stress vector.

$\sigma$  Stress at a point.

$\sigma_f$  Incremental stress associated with flexural deformations.

$\sigma_s$  Incremental stress associated with shear deformations.

$\sigma_{oct}$  Octahedral normal stress.

$\sigma_{pk}$  Peak stress.

$\sigma_x, \sigma_y, \tau_{xy}$  Stress components in cartesian coordinates.

$\sigma_n, \sigma_t, \sigma_{nt}$  Stress components in local coordinate system (n,t).

$\sigma_1, \sigma_2$  Principal stresses.

$\tau_{oct}$  Octahedral shearing stress.

$\Pi$  Total potential energy.

$\Pi_e$  Total potential energy associated with element e.

$\{\Psi\}$  Residual force vector.

$\Omega$   $\sigma_1/\sigma_2$

$F$  Yield function.

$\kappa$  Work hardening parameter.

$Pl^t$  Plasticity.

$El^t$  Element.



CHAPTER ONE :

INTRODUCTION

1.1 General introduction:

Reinforced concrete slabs are among the most common structural elements, relatively thin and flat, whose main function is to transmit loading acting normal to their plane. Slabs are used as floors and roofs of buildings, as wall in tanks and buildings, and as bridge decks to carry traffic loads.

To design or analyse a reinforced concrete slab system, there are a number of possible approaches. These are based on elastic theory, limit analysis theory and modifications to elastic and limit analysis theory.

A brief summary of the methods of analysis and design is given in this chapter. Finally the aim of the present work is presented.

1.2 Methods of analysis and design:

1.2.1– Elastic methods:

The classical plate theory applies to isotropic and anisotropic slabs which are sufficiently thin for shear deformations to be insignificant and sufficiently thick for the effect of in-plane forces which may cause buckling to be unimportant.

Elastic methods use the biharmonic equation given by:

$$\frac{q}{D} = \frac{\partial^4 w}{\partial x^4} + 2.0 \frac{\partial^4 w}{\partial x^2 \cdot \partial y^2} + \frac{\partial^4 w}{\partial y^4} \quad (1.1)$$

where  $q$  = loading imposed on plate per unit area,  
 $w$  = deflection of plate in direction of loading at point  
( $X, Y$ ) in  $Z$  direction.  
 $D$  = flexural rigidity of the plate.

for the case of isotropic plate, which is the result of the combination of the equilibrium equations and the constitutive equations of the plate shown in Fig(1.1).

To solve this equation either the harmonic analysis or numerical methods are used, and the solution gives a distribution of moments and shears such that:

- 1- Equilibrium is satisfied at every point in the slab.
- 2- The boundary conditions are complied with.
- 3- Stress is proportional to strain; that is, bending moments proportional to curvature.

Although a lot of work has been done in the past to solve the biharmonic equation analytically, such as the work by Navier<sup>(59)</sup> (1820), Levy<sup>(66, 63)</sup>, Newmark<sup>(59, 63, 66)</sup>, Ritz<sup>(59)</sup> and many others, unfortunately, the solution is not straightforward, and until now the solutions were restricted to very limited shapes of slabs and loading systems. This is due to the mathematical complications involved in the solution procedure.

Using the numerical techniques, mainly the finite element method, which is nowadays the most powerful tool for the solution of engineering problems, such difficulties can be easily overcome.

However, the elastic methods are further limited by the assumption of linear elasticity, which consequently limits their use in practical design problems.

### 1.2.2– Plastic methods (or limit state methods):

The assumption of linear elasticity is valid for low levels of stress, and as the load increases, concrete cracks due to the limited strength of concrete in tension, and accordingly, the slab flexural rigidity deteriorates. Cracking induces nonlinearity, and at higher loads, the degree of nonlinearity is increased by plastification of reinforcing steel. To account for this material changes, plasticity or limit state theory is used.

In plastic theory it is assumed that the material of the slab is capable of indefinite plastic straining once the conditions of yielding have been reached. Any solution to the ultimate load has to satisfy the conditions of classical plasticity:

- 1– The equilibrium condition: the internal stresses must be in equilibrium with the externally applied loads.
- 2– The mechanism condition: under ultimate load, sufficient plastic regions must exist to transform the structure into mechanism.
- 3– The yield criterion: the ultimate strength of the member must nowhere be exceeded.

But in general, it is extremely difficult to obtain such a solution analytically, and two different procedures for obtaining approximate solutions have been proposed based on the well-known upper bound and lower bound theorems in the theory of limit analysis. They were originally proposed by Prager, Drucker and many others. Thus the theory of plasticity permits the structural analyst to establish bounds on the calculated collapse load and thus ultimately works towards the true collapse load.

### 1.2.2.1 Upper bound method:

Upper bound method postulates a collapse mechanism for the slab system at the ultimate load such that:

- a– The moments at the "plastic hinges" are not greater than the ultimate moments of resistance of the sections.
- b– The collapse mechanism is compatible with the boundary conditions.

Consequently, the upper bound method gives an ultimate load which is either correct or too high, but if all the possible collapse mechanisms for the slab system are examined, the mechanism giving the lowest load is the correct one. Yield line theory after Johansen<sup>(44,14,70)</sup> falls into this category.

The method in practice suffers from four main disadvantages as follows:

- i) It is difficult to handle cases where a variable reinforcement pattern is used.
- ii) No information is provided on the forces transmitted to the supports.
- iii) This method does not provide any information about the state of stress in parts of the slab other than at yield lines.
- iv) It is not at all easy to use when the mechanism is governed by more than three geometrical parameters.

In general, this method is mostly used in assessing the strength of existing slabs, although it can be used as a limited design method.

### 1.2.2.2 Lower bound method:

Lower bound method postulates a distribution of moments in the slab at the ultimate load such that the following three conditions are satisfied:

- a– Equilibrium condition
- b– Yield criterion
- c– The boundary conditions are complied with.

Then the ultimate load is calculated from the equilibrium equations and the postulated distribution of moments. For a given slab system, the lower bound method gives an ultimate load which is either correct or too low; that is, the ultimate load is never overestimated.

In any lower bound design method, a designer is free to choose any moment distribution that he wishes, provided that it satisfies the equilibrium of the slab.

The method of slab design proposed by Hillerborg (1956) in its simple version is suitable for slabs without concentrated supports or re-entrant corners. In this method the slab is essentially designed as a torsionless grid of beams. Caution is necessary here because the freedom of choosing the load dispersion which may depart far from the elastic (working) conditions leading to unserviceability due to early cracking or large deflections.

For the case of fairly simple slabs this can easily be satisfied by assumed load distribution to the grillage beams, but in more complex cases either a torsionless grillage analysis or the strip deflection method of Fernando and Kemp<sup>(25, 26)</sup> can be used.

In the case of slabs with concentrated loads and supports, several options are open such as Hillerborg's advanced strip method<sup>(32)</sup>.

The only reason for neglecting the torsional moment in the strip methods is that it leads to a simple procedure for hand calculations. Once the calculations

become too complicated because of the boundary conditions and loading systems, it is convenient to use the computer. Consequently, the twisting moment  $M_{xy}$  is to be considered. This moment ( $M_{xy}$ ) exists in the theory of elasticity and it is particularly high in the corner regions of slabs simply supported on stiff beams or walls.

Another lower bound method is that based on elastic stress field (Direct Design Approach), where the elastic stress distribution at the ultimate load is used in conjunction with the yield criterion for reinforced concrete slabs to determine the steel reinforcement.

This approach was first proposed by Hillerborg<sup>(33)</sup> and later reconsidered and restated by Wood<sup>(71)</sup> for the case of orthogonal steel.

Nielson<sup>(58)</sup> has also developed equations for the optimum design of orthogonal steel and subsequently Armer<sup>(72)</sup> derived equations for the case in which the steel lies in a predetermined skew directions.

This latter method can be shown to be the most appropriate method for the purposes of CAD (Computer Aided Design) since the elastic stress analysis is more conveniently carried out using the finite element method, and the design equations mentioned above are readily implemented in a computer code to provide the necessary reinforcement at each point on the slab.

From their experimental work, A.W. Hago<sup>(30)</sup> and the L.M.A. Hafez<sup>(1)</sup> concluded that the direct design method is a highly practical design procedure for reinforced concrete slabs.

### 1.3– Purpose and scope of the present investigation:

So far the work done on the direct design approach was only confined to the use of elastic stress field. However, any stress field satisfying the slab equilibrium can be used with the direct design method. So the idea of using a stress field other than elastic might be more meaningful in terms of yielding a steel layout which can be thought as being more convenient.

The work presented in this thesis attempts to study this idea, by analysing the results of using non elastic stress field with the direct design method. Two areas were investigated, first the effect of using non elastic stress field on the distribution of the resisting moments over the slab and secondly the behaviour of the slabs so designed.

The non elastic stress field that are possible are :

i– Elastic– plastic stress fields obtained from the analysis of metallic plates.

ii– Elastic–plastic stress fields obtained from the analysis of reinforced concrete plates using Wood–Armer criterion:

$$(M_x^* - M_x)(M_y^* - M_y) - M_{xy}^2 = 0.0$$

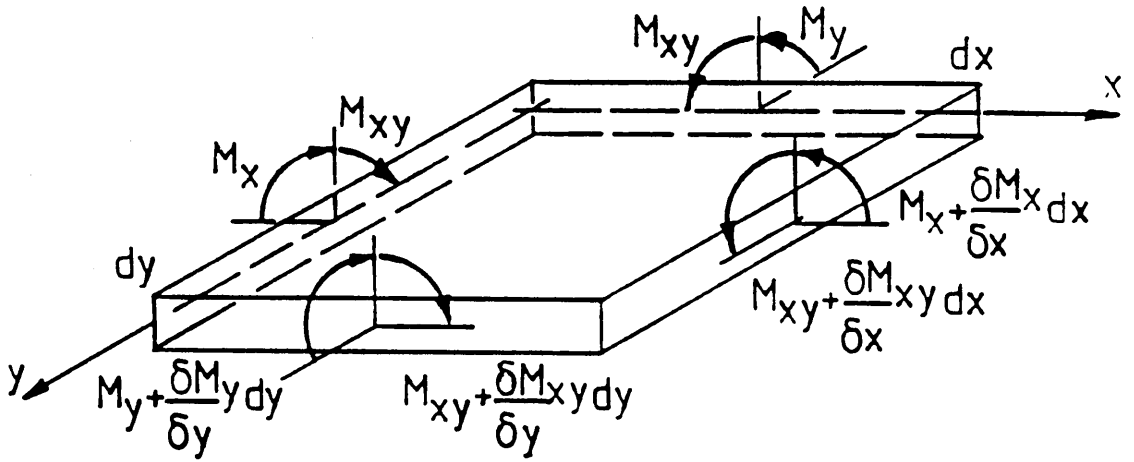
where  $M_x^*$  and  $M_y^*$  are the design moments which are predetermined for large sections of the slab.

iii– Any linear combination of the elastic stress field and the above stress fields.

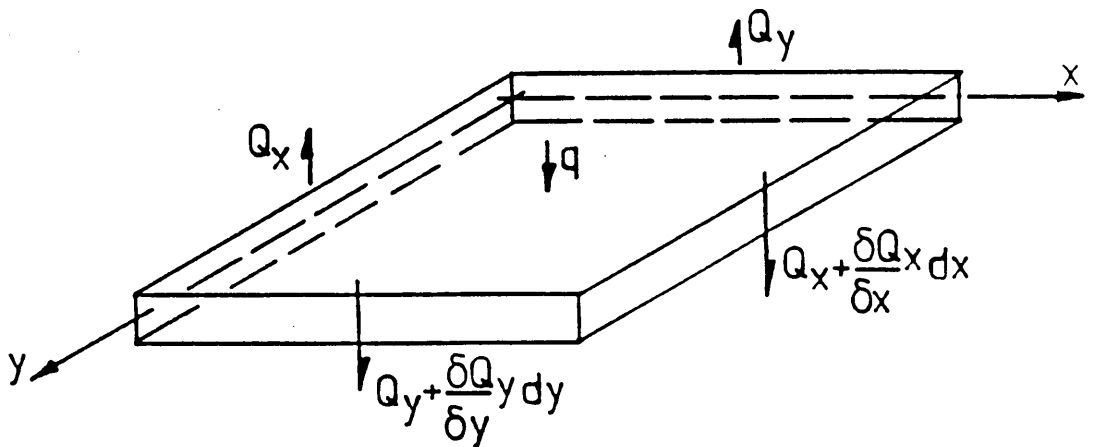
The present study has been restricted to the exploration of the elasto–plastic stress field resulting from the analysis of metallic plates, because it can be obtained by a rational and straightforward method. In addition, it will not require a predetermination of the steel reinforcement, as in the case of the analysis of a reinforced concrete plates.

This thesis is organised in seven chapters. Chapter one describes the methods available for analysing and designing slabs. Chapter two presents a discussion of the direct design method with its assumptions and applications. In chapter three the finite element method is reviewed with particular reference to the computer programs used in this study. The results of using the direct design method with elasto-plastic stress field are presented in chapter four. The predicted behaviour of the slabs so designed using the nonlinear finite element program, presented in chapter three, is discussed in chapter five. Chapter six describes a finite element program based on Wood-Armer criterion, developed to predict the ultimate load of reinforced concrete slabs. Finally, conclusions and recommendations for the future work are presented in chapter seven.





MOMENTS PER UNIT LENGTH



SHEAR FORCES PER UNIT LENGTH

Figure (1-1)

## CHAPTER TWO :

### DIRECT DESIGN METHOD

#### 2.1 Introduction :

In the previous chapter, the various methods available for the design of reinforced concrete slabs have been briefly discussed. Since the aim of the present study is to investigate the direct design method when used with non elastic stress field, the first step was then to study this method in detail.

The principle of the direct design approach and the rules used for placing the reinforcement are discussed in the following sections of this chapter.

#### 2.2 The direct design approach:

The direct design approach is very simple and straightforward. It is a design oriented method based on plasticity concepts and will satisfy the three conditions of the theory of plasticity.

The steps in the method will be discussed in relation to these conditions in the following manner:

##### 2.2.1 The equilibrium condition:

The equilibrium condition for the slab system shown in Fig(1.1) is derived as follows:

- i– For vertical equilibrium:

$$0.0 = q \cdot dx \cdot dy + \left[ Q_x + \frac{\partial Q_x}{\partial x} \cdot dx \right] dy + \left[ Q_y + \frac{\partial Q_y}{\partial y} \cdot dy \right] dx - Q_y \cdot dx - Q_x \cdot dy$$

$$\text{therefore : } -q = \frac{\partial Q_x}{\partial x} + \frac{\partial Q_y}{\partial y} \quad \dots (2.1)$$

ii- For moment equilibrium about the X axis:

$$0.0 = q \cdot dx \cdot dy \cdot \frac{dy}{2} + \left[ Q_y + \frac{\partial Q_y}{\partial y} \cdot dy \right] dx \cdot dy + \frac{\partial Q_x}{\partial x} dx \frac{dy^2}{2} + M_y \cdot dy - \left[ M_y + \frac{\partial M_y}{\partial y} dy \right] dx - M_{xy} dy + \left[ M_{xy} + \frac{\partial M_{xy}}{\partial x} dx \right] dy$$

therefore, as,  $dx$  and  $dy \Rightarrow 0.0$  :

$$Q_y = \frac{\partial M_y}{\partial y} - \frac{\partial M_{xy}}{\partial x} \quad \dots (2.2)$$

iii- Similarly, moment equilibrium about the Y axis gives:

$$Q_x = \frac{\partial M_x}{\partial x} - \frac{\partial M_{xy}}{\partial y} \quad \dots (2.3)$$

These three order differential equilibrium equations can be combined to give a second order equation relating moments to load intensity as:

$$-q = \frac{\partial^2 M_x}{\partial x^2} - 2.0 \frac{\partial^2 M_{xy}}{\partial x \cdot \partial y} + \frac{\partial^2 M_y}{\partial y^2} \quad \dots (2.4)$$

In the direct design procedure the stress distribution should satisfy the equilibrium equation (2.4) at every point on the slab.

If the stress distribution under the design load is obtained from a finite element analysis, the equilibrium condition (Eq- 2.4) will automatically be satisfied as the method is derived from equilibrium considerations. Owing to its simplicity and versatility, the method can be applied to any type of slab problem with any edge conditions.

### 2.2.2 The yield criterion:

The yield criterion defines the behaviour of the slab element under a given loading condition and mathematically relates the resisting and applied moment components at the formation of the yield lines. The stress analysis of the slab under the ultimate load provides at each point the stress triad  $M_x$ ,  $M_y$ , and  $M_{xy}$  for laterally loaded plate. To provide the reinforcement to fit the predicted moment field at ultimate limit state, the steel should be proportioned as required by the yield criterion.

Accordingly, it becomes necessary to derive the yield criterion in terms of the three moment components, such as:

$$F (M_x, M_y, M_{xy}, M_x^*, M_y^*) = 0.0 \quad \dots (2.5)$$

where  $M_x^*$  and  $M_y^*$  are the uniaxial flexural strength of the slab in X- and Y- directions respectively. The derivation of such yield criterion will be considered in this section.

Consider the slab element shown in Fig- (2.1) under the moment field  $(M_x, M_y, M_{xy})$  per unit width. The sign convention adopted is such that all

moments acting in the element are positive.

Simplifying assumptions are further made, and these can be summarized as follows:

- (1)– The concrete is assumed to have a zero tensile strength.
- (2)– Bar diameters are small in comparison with slab depth, and they can carry stresses only in their original direction. Accordingly, kinking of bars across a yield line is not considered.
- (3)– The slab element is lightly reinforced, so that compression failure is not permissible and only ductile failures are allowed. This is necessary for moment redistribution, so that the slab elements can reach their ultimate strength at sufficient number of sections, to convert the slab into a mechanism.
- (4)– Membrane forces do not exist, it is acknowledged that the co-existence of such forces with flexural fields on the slab elements, will considerably affect the resisting moment of the slab element – depending on whether they are compressive or tensile and the restraints existing at the boundary of the slab.

The basic idea is that, if at any point P in a slab (Fig– 2.2) a line with normal  $n$  and direction  $t$  is examined, the normal moment  $M_n$ , due to the applied moments ( $M_x, M_y, M_{xy}$ ) must not exceed the value of  $M_n^*$  which is the moment of resistance that the reinforcement in the slab could develop in direction  $n$ . This therefore is a normal moment criterion which is tested in every direction<sup>(45)</sup>.

For generality the yielding criterion will be derived in the following for the case of skew reinforcement as shown in Fig– (2.2).

Taking the normal to the yield line at an angle  $\alpha$  to the X– axis and considering the equilibrium of the element shown in Fig– (2.3), we have:

$$M_n = M_x \cdot \cos^2 \theta + M_y \cdot \sin^2 \theta - 2.0 \cdot M_{xy} \cdot \sin \theta \cdot \cos \theta \quad \dots (2.6)$$

$$M_t = M_x \cdot \sin^2 \theta + M_y \cdot \cos^2 \theta + 2.0 \cdot M_{xy} \cdot \sin \theta \cdot \cos \theta \quad \dots (2.7)$$

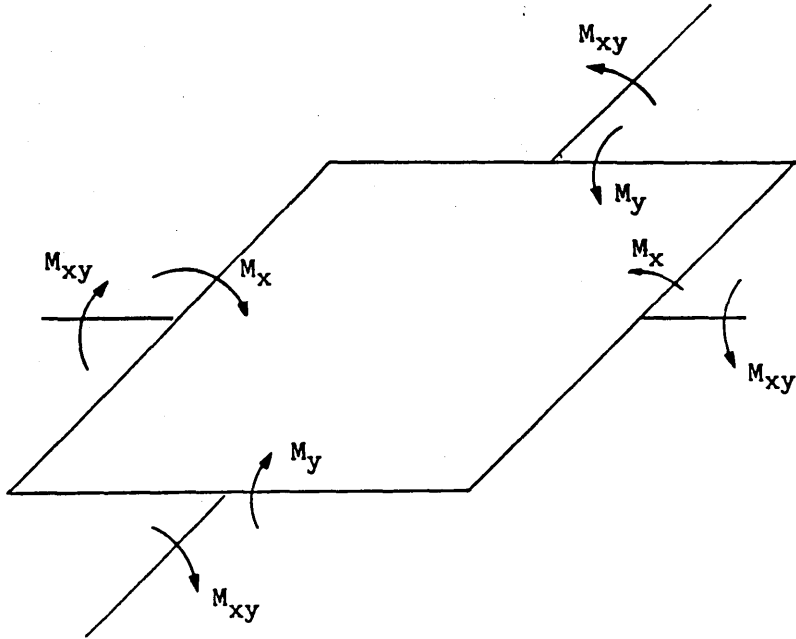


Figure (2-1) Notation for moments on an element  
(positive as shown)

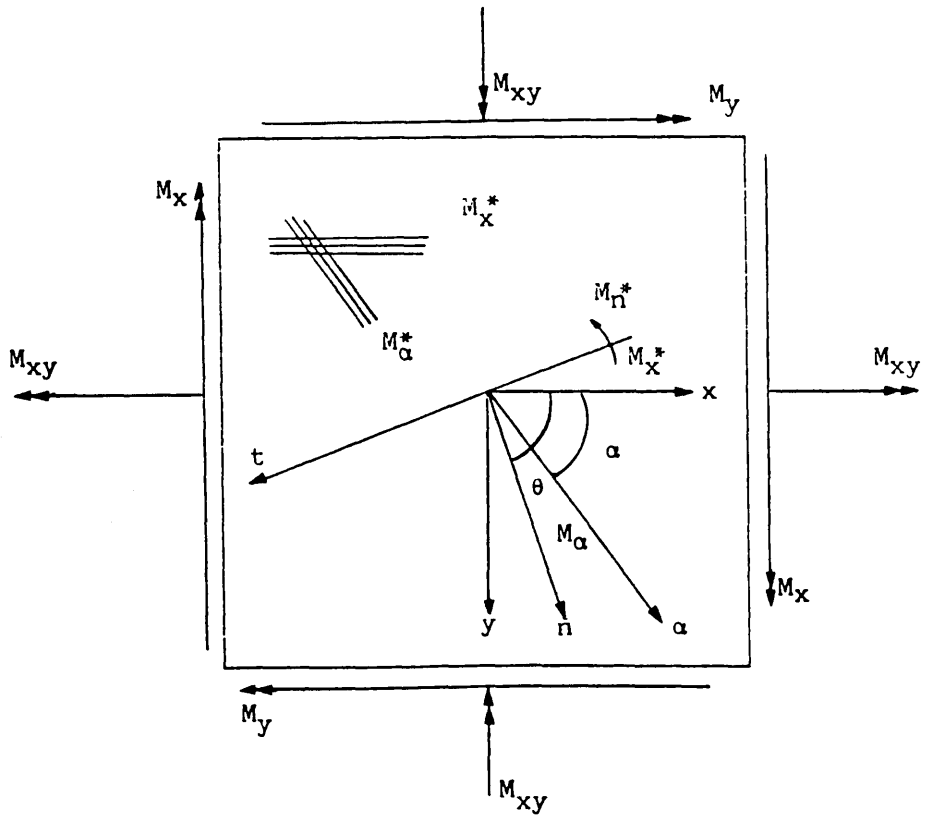


Figure (2-2) Element with skew reinforcement

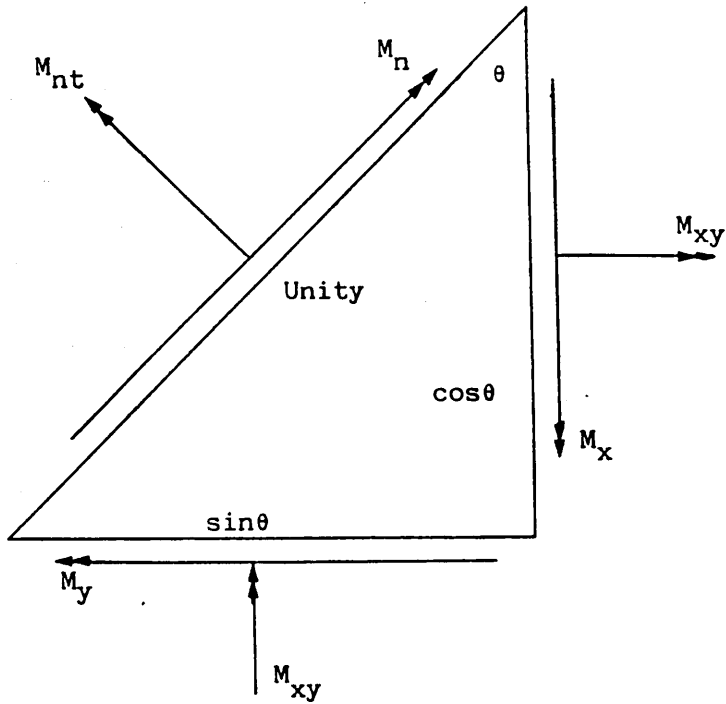


Figure (2-3) Equilibrium of a slab element under a moment field.

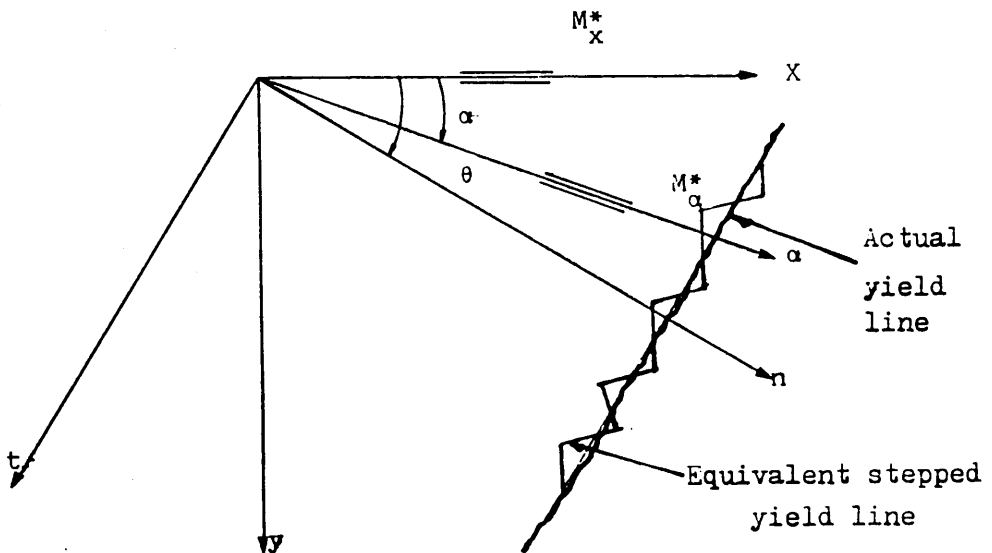


Figure (2-4) Idealized yield line

( Johansen's stepped yield criterion )

$$M_{nt} = (M_x - M_y) \sin\theta \cdot \cos\theta + M_{xy}(\cos^2\theta - \sin^2\theta) \quad \dots(2.8)$$

the resisting moments at the yield line can be expressed using the Johansen's "stepped" yield criterion<sup>(44)</sup> which is based on the following assumptions:

(1)– The normal moment on a yield line can be obtained by considering each band of reinforcement in turn, the total effect being the addition of the individual effects.

(2)– For each band of reinforcement taken on its own the yield line may be considered to be divided into small steps parallel to, and at right angles to the reinforcement, as shown in figure (2.1).

(3)– All reinforcement crossing the yield line is assumed to yield.

(4)– All reinforcement is assumed to stay in its original straight line when the steel yield, i.e there is no "kinking", or change in direction of the steel in crossing the yield line.

(5)– When each band of reinforcement is considered on its own, on the small steps at right angles to the reinforcement there is only a normal moment/unit width whilst on the steps parallel to the reinforcement there is neither normal nor twisting moment.

(6)– The values of normal and twisting moments on the yield line are such that they are equivalent to the components of the normal moment on the steps.

On the basis of these assumptions, the resisting moments can be written as:

$$M_n^* = M_x^* \cos^2\theta + M_\alpha^* \cos^2(\theta - \alpha) \quad \dots(2.9)$$

$$M_t^* = M_x^* \sin^2\theta + M_\alpha^* \sin^2(\theta - \alpha) \quad \dots(2.10)$$

Hence the value of  $M_n^*$  obtained from equation (2.9) must always be greater than that for  $M_n$  calculated from equation (2.6); that is,

$$M_n^* - M_n \geq 0.0 \quad \dots(2.11)$$



Substituting Eq- (2.6) and Eq- (2.9) in Eq- (2.11) we have :

$$\begin{aligned} \text{Excess strength} &= (M_x^* - M_x + M_\alpha^* \cos^2 \alpha) \cos^2 \theta + (M_\alpha^* \sin^2 \alpha - M_y) \sin^2 \theta + \\ &2(M_{xy} + M_\alpha^* \sin \alpha \cdot \cos \alpha) \sin \theta \cdot \cos \theta \geq 0.0 \end{aligned}$$

or

$$F = A \cdot \cos^2 \theta + B \cdot \sin^2 \theta + 2.0 \cdot C \cdot \cos \theta \cdot \sin \theta \geq 0.0$$

where  $A = M_x^* - M_x + M_\alpha^* \cdot \cos^2 \alpha$

$$B = M_\alpha^* \cdot \sin^2 \alpha - M_y$$

$$C = M_{xy} + M_\alpha^* \cdot \sin \alpha \cdot \cos \alpha$$

dividing by  $\cos \theta$  and putting  $K = \tan \theta$  the latter equation reduces to :

$$F = A + BK^2 + 2CK \geq 0.0 \quad \dots(2.12)$$

For optimum steel, excess strength must be a minimum, that is to say :

$$\frac{dF}{d \tan \theta} = 0 \quad \text{and} \quad \frac{d^2F}{d \tan^2 \theta} \succ 0.0$$

Differentiating Eq- (2.12) with respect to  $\tan \theta$ , we have

$$BK + C = 0.0 \quad \text{or} \quad K = - C / B \quad \dots(2.13a)$$

and  $B \succ 0$  since  $M_\alpha^* \sin^2 \alpha \succ M_y$

Substituting the values of B and C in Eq- (2.13a), one gets

$$K = - \frac{M_{xy} + M_\alpha^* \sin \alpha \cdot \cos \alpha}{M_\alpha^* \sin^2 \alpha - M_y} \quad \dots(2.13b)$$

This gives the orientation of the plane of minimum resistance of skew steel. For the case of orthogonal steel  $\alpha = 90^\circ$  then :

$$K = - \frac{M_{xy}}{M_{90}^* - M_y} \quad \dots(2.13c)$$

Substituting Eq- (2.13a) in Eq- (2.12) and using equality sign for minimum resistance, then :

$$A + B(-C/B)^2 + 2C(-C/B) = 0.0$$

or

$$AB - C^2 = 0.0 \quad \dots(2.14)$$

Substituting the value of A and B in Eq- (2.14), one gets:

$$(M_x^* - M_x + M_\alpha^* \cos^2 \alpha)(M_\alpha^* \sin^2 \alpha - M_y) - (M_{xy} + M_\alpha^* \sin \alpha \cos \alpha)^2 \geq 0$$

or

$$-(M_x^* - M_x + M_\alpha^* \cos^2 \alpha)(M_\alpha^* \sin^2 \alpha - M_y) + (M_{xy} + M_\alpha^* \sin \alpha \cos \alpha)^2 \leq 0$$

$$\dots(2.15a)$$

in order to have a safe design inside the yield surface.

Eq- (2.15a) is the yield criterion for skew reinforced concrete slabs. The yield criterion of orthogonal steel case ( $\alpha = 90^\circ$ ) is given by:

$$-(M_x^* - M_x)(M_{90}^* - M_y) + M_{xy}^2 \leq 0.0 \quad \dots(2.15b)$$

which is the same equation arrived at by Save<sup>(61)</sup>, Nielson<sup>(58)</sup>, Lenschow et al<sup>(49)</sup>, and Kemp<sup>(45)</sup>.

The extensive experimental work carried out by the research workers, Lenschow et al<sup>(49)</sup>, Cardenas and Sozen<sup>(8)</sup>, Lenkei<sup>(50)</sup>, and Salish Jain et al<sup>(40)</sup>, on the derived yield criterion for the case of orthogonal steel, confirmed the validity of this criterion. It has further been established that the yield line orientation do not necessarily coincide with the principal direction of either the applied or resisting moments in the case of nonisotropic reinforcement. Consequently, twisting moments do exist at the yield lines in addition to the flexural moments, but no decrease in flexural yield capacity due to the interaction between flexural and torsional moments is observed.

For yield in the negative steel at the top of the slab, similar procedure to the one just described for positive yield, can be applied.

If the top steel layers are laid in X- and  $\alpha$ - directions to provide the resisting moments  $M_x^{*t}$  and  $M_\alpha^{*t}$  respectively, then the yield condition with negative steel can be written as:

$$-(M_x^{*t} + M_x - M_\alpha^{*t} \cos^2 \alpha)(M_\alpha^{*t} \sin^2 \alpha + M_y) + (M_{xy} - M_\alpha^{*t} \sin \alpha \cos \alpha) \leq 0.0$$

....(2.16a)

If  $\alpha = 90^\circ$  for orthogonal steel case, the yield criterion is given by :

$$-(M_x^{*t} + M_x)(M_{90}^{*t} + M_y) + M_{xy}^2 \leq 0.0$$

....(2.16b)

where both  $M_x$  and  $M_y$  are negative moments.

Equation (2.15b) and Equation (2.16b) represents a pair of intersecting cones in the  $(M_x, M_y, M_{xy})$  space, as shown in figure (2.5).

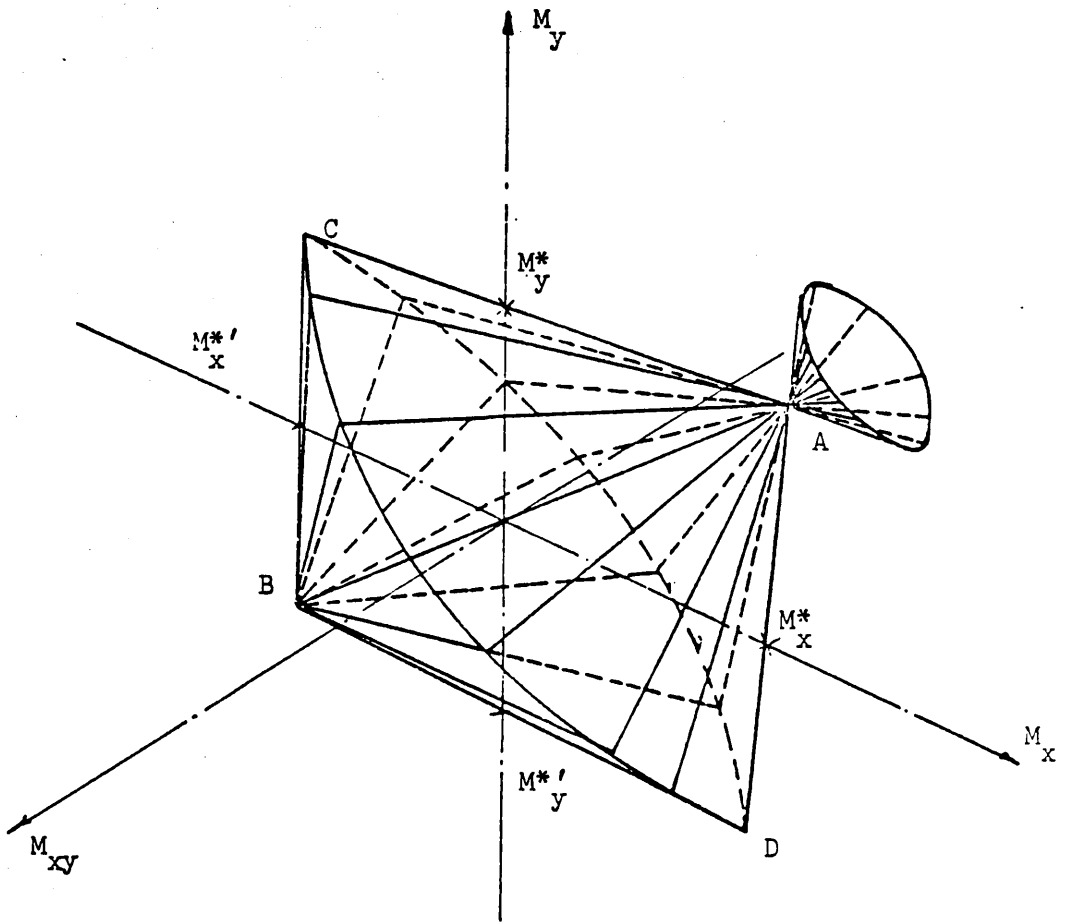


**Figure (2-5) Yield surface**

### 2.2.3 Design equations:

From the yield criterion derived previously the following equations can be used for design.

#### a- positive moment fields:

Referring to Eq- (2.15a):

$$M_x^* = \frac{(M_{xy} + M_\alpha^* \cos\alpha \cdot \sin\alpha)^2}{M_\alpha^* \sin^2\alpha - M_y} + M_x - M_\alpha^* \cos^2\alpha \quad \dots(2.17)$$

$$M_x^* + M_\alpha^* = \frac{(M_{xy} + M_\alpha^* \cos\alpha \cdot \sin\alpha)^2}{M_\alpha^* \sin^2\alpha - M_y} + M_x + M_\alpha^* (1 - \cos^2\alpha) \quad \dots(2.18)$$

For a minimum steel  $\frac{d(M_x^* + M_\alpha^*)}{d(M_\alpha^*)} = 0.0 \quad \dots(2.19)$

From Eq- (2.18) and Eq- (2.19) we get :

$$M_\alpha^* = \frac{M_y}{\sin^2\alpha} \mp \frac{M_y \cdot \cos\alpha + M_{xy} \cdot \sin\alpha}{\sin^2\alpha}$$

and since  $M_\alpha^* \succ [M_y / \sin^2\alpha]$  , thus:

$$M_\alpha^* = \frac{M_y}{\sin^2\alpha} + \left| \frac{M_{xy} + M_y \cot\alpha}{\sin\alpha} \right| \quad \dots(2.20)$$

Substituting Eq- (2.20) in Eq- (2.17) we get :

$$M_x^* = M_x + M_y \cdot \cot^2 \alpha + 2 M_{xy} \cot \alpha + \left| \frac{M_{xy} + M_y \cdot \cot \alpha}{\sin \alpha} \right| \quad \dots(2.21)$$

For orthogonal steel  $\alpha = 90^\circ$  the two equations (2.20) and (2.21) will be reduced to :

$$M_x^* = M_x + |M_{xy}| \quad \dots(2.22)$$

$$M_{90}^* = M_y + |M_{xy}| \quad \dots(2.23)$$

b- negative moment fields:

For negative steel at the top of the slab, similar procedure to the one just described for positive steel can be applied using the negative yield criterion.

The corresponding Eqns to (2.20) and (2.21) are:

$$M_x^{*t} = M_x + 2 M_{xy} \cot \alpha + M_y \cot^2 \alpha - \left| \frac{M_{xy} + M_y \cot \alpha}{\sin \alpha} \right| \quad \dots(2.24)$$

$$M_{\alpha}^{*t} = \frac{M_y}{\sin^2 \alpha} - \left| \frac{M_{xy} + M_y \cot \alpha}{\sin \alpha} \right| \quad \dots(2.25)$$

For  $\alpha = 90^\circ$  :

$$M_x^{*t} = M_x - |M_{xy}| \quad \dots(2.26)$$

$$M_{90}^{*t} = M_y - |M_{xy}| \quad \dots(2.27)$$

c- mixed moment fields:

For positive moment fields if  $M_{\alpha}^* \leq 0.0$  then from yield criterion equation (2.15a)

$$M_{\alpha}^* = M_x + 2 M_{xy} \cot\alpha + M_y \cot^2\alpha + \left| \frac{(M_{xy} + M_y \cot\alpha)^2}{M_y} \right| \dots(2.28)$$

For orthogonal steel  $\alpha = 90^\circ \Rightarrow$

$$M_{\alpha}^* = M_x + \left| \frac{M_{xy}^2}{M_y} \right| \dots(2.29)$$

If  $M_{\alpha}^* \leq 0.0$  then from yield criterion Eq- (2.15a)

$$M_{\alpha}^* = \frac{M_x \cdot M_y - M_{xy}^2}{M_x \sin^2\alpha + M_y \cos^2\alpha + 2 M_{xy} \sin\alpha \cdot \cos\alpha}$$

After rearranging it reduces to :

$$M_{\alpha}^* = \frac{M_y}{\sin^2\alpha} + \frac{(M_{xy} + M_y \cot\alpha)^2}{\sin^2\alpha (M_x + 2 M_{xy} \cot\alpha + M_y \cot^2\alpha)}$$

and since  $M_{\alpha}^* \geq [M_y / \sin^2\alpha]$  thus

$$M_{\alpha}^* = \frac{1.0}{\sin^2\alpha} \left[ M_y + \left| \frac{(M_{xy} + M_y \cot\alpha)^2}{(M_x + 2 M_{xy} \cot\alpha + M_y \cot^2\alpha)} \right| \right] \dots(2.30)$$

For orthogonal steel  $\alpha = 90^\circ \Rightarrow$

$$M_{90}^* = M_y + \left| \frac{M_{xy}^2}{M_x} \right| \quad \dots(2.31)$$

For negative moment fields considering the negative yield criterion and following the same procedure the corresponding expressions for negative steel are:

$$M_x^{*t} = M_x + 2 M_{xy} \cdot \cot \alpha + M_y \cdot \cot^2 \alpha - \left| \frac{(M_{xy} + M_y \cdot \cot \alpha)^2}{M_y} \right| \dots$$

....(2.32)

and for  $\alpha = 90^\circ$

$$M_x^{*t} = M_x - \left| \frac{M_{xy}^2}{M_y} \right| \quad \dots(2.33)$$

$$M_\alpha^{*t} = \frac{1.0}{\sin^2 \alpha} \left[ M_y - \left| \frac{(M_{xy} + M_y \cdot \cot \alpha)^2}{(M_x + 2 M_{xy} \cdot \cot \alpha + M_y \cdot \cot^2 \alpha)} \right| \right]$$

....(2.34)

and for  $\alpha = 90^\circ$

$$M_{90}^{*t} = M_y - \left| \frac{M_{xy}^2}{M_x} \right| \quad \dots(2.35)$$

If  $M_\alpha^* = 0.0 = M_x^* = 0.0$ , then no reinforcement is needed.



### 2.2.4 Rules for placing reinforcement :

Given the stress field  $(M_x, M_y, M_{xy})$  with the angle of skew equal  $\alpha$  at any point on the slab, the reinforcements in the X- and  $\alpha$ - directions respectively, will be placed according to the following rules:

#### a- Bottom steel:

- (1) Compute the design moments  $M_x^*$  and  $M_\alpha^*$  from Eq- (2.21) and Eq- (2.20).
- (2) If  $M_x^* < 0.0$  then set  $M_x^* = 0.0$  and calculate  $M_\alpha^*$  according to Eq- (2.30). If the calculated value of  $M_\alpha^*$  is  $< 0.0$ , then  $M_x^* = M_\alpha^* = 0.0$  (no reinforcement is needed).

Or,

- (3) If  $M_\alpha^* < 0.0$  then set  $M_\alpha^* = 0.0$  and calculate  $M_x^*$  according to Eq- (2.28). If the calculated  $M_x^* < 0.0$  then  $M_x^* = M_\alpha^* = 0.0$  (no reinforcement is needed).

Or,

- (4) If both  $M_x^*$  and  $M_\alpha^*$  are positive, then adopte the calculated values as the design moments.

Or,

- (5) If both  $M_x^*$  and  $M_\alpha^*$  are negative then no reinforcement is needed.

#### b- Top reinforcement:

- (1) Compute the design moments  $M_x^{*t}$  and  $M_\alpha^{*t}$  from Eq- (2.24) and Eq- (2.25).
- (2) If  $M_x^{*t} > 0.0$  then set  $M_x^{*t} = 0.0$  and calculate  $M_\alpha^{*t}$  from Eq- (2.34). If the resulting value of  $M_\alpha^{*t}$  is  $> 0.0$  then  $M_x^{*t} = M_\alpha^{*t} = 0.0$  (no reinforcement is needed).

Or,if

- (3)  $M_\alpha^{*t} > 0.0$  then set  $M_\alpha^{*t} = 0.0$  and calculate  $M_x^{*t}$  from Eq- (2.32). If the resulting value of  $M_x^{*t}$  is  $> 0.0$  then  $M_x^{*t} = M_\alpha^{*t} = 0.0$  (no reinforcement is needed).

Or,if

- (4) both  $M_x^{*t}$  and  $M_\alpha^{*t}$  are negative, then adopt the calculated values as design

moments.

Or, if

(5) both  $M_x^{*t}$  and  $M_\alpha^{*t}$  are positive, then no reinforcement is needed at the top.

For bottom and top reinforcement if the design moments are found to be equal to zero then the minimum steel may be provided according to the code of practice<sup>(22)</sup>.

### 2.2.5 Multiple load cases:

The above rules apply only when the slab is subjected to a moment field resulting from a single load case. In practice, however, many slabs and particularly bridge decks are subjected to multiple loading. The reinforcement must then be proportioned to satisfy the multiple moments triads  $(M_{xi}, M_{yi}, M_{xyi})$   $i = 1, n$  produced by the multiple loading, where  $n$  is the number of such loading cases.

(1) Using the design equations (as described previously), for the  $i^{\text{th}}$  load case, calculate the corresponding  $M_{xi}^*$  and  $M_{\alpha i}^*$ .

(2) Calculate the maximum of all the  $M_{xi}^*$  and  $M_{\alpha i}^*$  taking into consideration all the load cases. Let these be  $M_{x-\max}^*$  and  $M_{\alpha-\max}^*$ .

Evidently if we use these as the design moments, then we will get a safe design but not necessarily an optimum design. So we can move towards an optimum design as follows:

(3) Assume that in the X- direction we provide  $M_{x-\max}^*$ , but in the  $\alpha$ - direction we provide  $M_{\alpha i}^*$  so as to satisfy the yield criterion in each case.  $M_{\alpha i}^*$  is given for each case by:

$$M_{\alpha i}^* = \frac{1.0}{\sin^2 \alpha} \left[ M_y + \frac{(M_{xy} + M_{\alpha i}^* \sin \alpha \cos \alpha)^2}{(M_{x-\max}^* - M_x + M_{\alpha i}^* \cos^2 \alpha)} \right]$$

Calculate the maximum of  $M_{\alpha i}^*$  that satisfies the yield criterion and let it be  $M_{\alpha-\text{emax}}^*$ . Evidently a safe design is produced if we use  $M_{x-\text{max}}^*$  in conjunction with the maximum  $M_{\alpha-\text{emax}}^*$  determined so as to satisfy the yield criterion.

(4) A similar procedure to (3) above can be done if we choose  $M_{\alpha-\text{max}}^*$  as the design moment in  $\alpha$ - direction, and calculate  $M_{xi}^*$  that satisfy the yield criterion in each case.  $M_{xi}^*$  will be given by :

$$M_{xi}^* = M_x - M_{\alpha-\text{max}}^* \cos^2 \alpha - \frac{(M_{xy} + M_{\alpha-\text{max}}^* \sin \alpha \cdot \cos \alpha)^2}{M_{\alpha-\text{max}}^* \sin \alpha - M_y}$$

Let the maximum one that satisfies the yield criterion be  $M_{x-\text{emax}}^*$ .

Therefore a better design is to choose that set of design moment where the  $(M_x^* + M_{\alpha}^*)$  is the smallest.

We can stop at this stage but if need be we can improve on this by assuming that other combinations are possible and use a simple search technique (i.e. examining the feasible design region as shown in figure (2.6) ). For each load case, we see if the design moments at the grid points are a better minimum. If it is not, we reject it. If it is, we check to see if it violates the yield criterion for the load case considered. If it does, we reject it. If not, we see at which grid point we can get minimum of  $(M_x^* + M_{\alpha}^*)$ . This gives us the optimum design moments.

The above procedure is adopted for positive steel (bottom layers), the same procedure can be used for negative steel, in which case, the minimum replaces the maximum in the above steps.

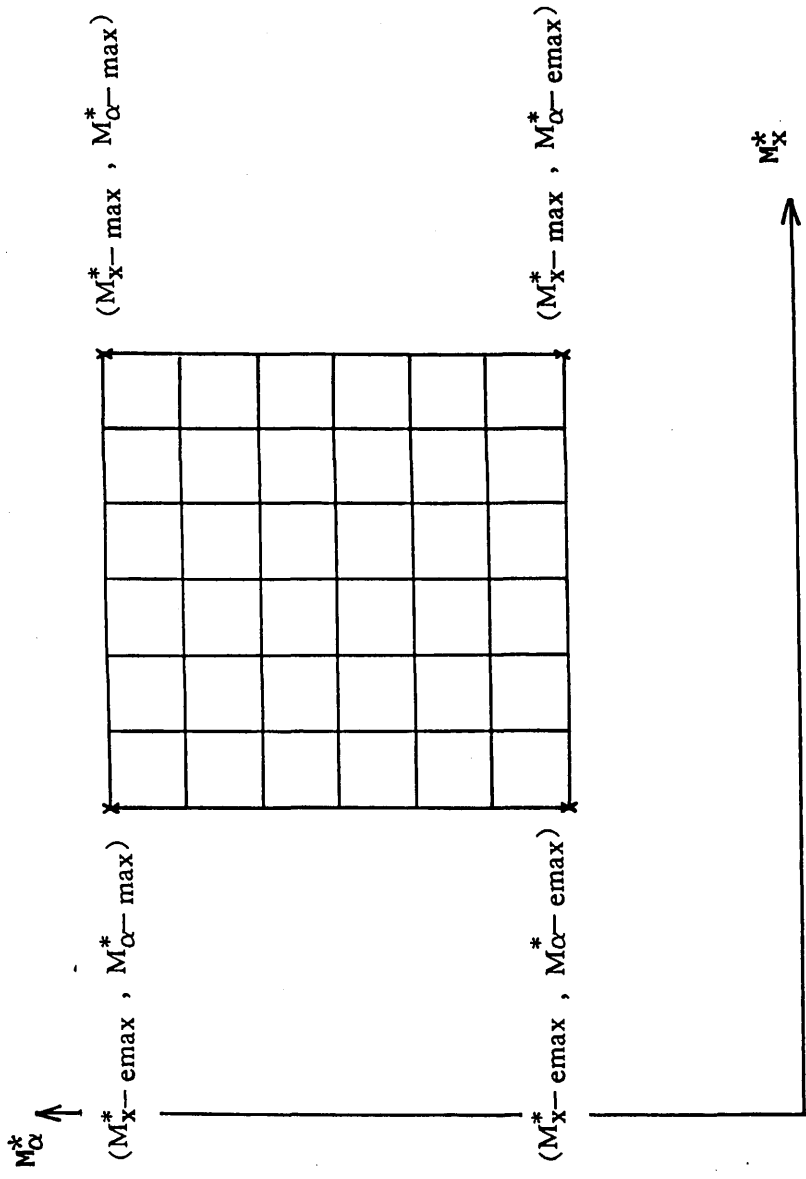


Figure (2-6) Simple search technique

### 2.2.6 The mechanism condition:

At ultimate load it is necessary that the slab must become a mechanism signifying that the slab cannot carry any further load.

In the direct design approach any stress field in equilibrium with the applied load is linked with the yield conditions previously derived to provide the necessary strength. So the necessary strength is made equal to the calculated stress at every point in the slab. Accordingly, if elastic moment field is used at ultimate load, almost all the points attain their ultimate strength with a minimum redistribution of the stresses. Thus converting the slab into a mechanism.

However, if elasto-plastic field of moments is used, then some points of the slab may start yielding well before the design load is reached. So when elasto-plastic stress field is used in the design method, the simultaneous yield at the design load will not happen. This represents the major difference between designing with elastic and non elastic stress field although in both cases the mechanism condition is satisfied at design load.

A similar phenomenon is noticed in the case of multiple loading, where all points of the slab may not reach their ultimate strength at the same level of loading.

### 2.2.7 Ductility demand:

In the classical plasticity theory it is assumed that the material possesses unlimited ductility. This means that portions of the slab which yield early on in the load history continue to deform without any reduction in their ultimate strength. Unfortunately, in the case of reinforced concrete slabs this assumption cannot be accepted without reservation.

What is needed is that the difference between the load at which the first yielding of the slab occurs at a point and the ultimate load of the whole slab is made as small as possible. This will reduce the load range during which sections that

yield early are required to deform at constant stress without losing their strength due to strain softening of the concrete.

Theoretically, this ideal situation will be satisfied automatically as all the points of the slab will yield simultaneously when elastic distribution is used in the design.

However, in practice limitations on the size of bars, spacing of bars for example prevent the simultaneous yield being reached.

It is possible that the ductility demand increases when elasto– plastic stress field is used in the design method. The chosen distribution of the stress field over the elastic range will induce some points to yield before the design load is reached and also probably at an earlier stage than the one corresponding to an elastic moment field. Consequently, the difference between the ultimate load and the onset of yielding could be relatively large in comparison with the design using elastic stress field and thus it may lead to an undesirable behaviour of the slab. In other words in the case of elasto– plastic moment field , more ductility may be required than for the case of elastic moment field, and the difference will depend upon the degree of plasticity of the moment field chosen in the design method.

In the present study, this problem will be investigated in detail and an attempt will be made to see how far we can depart from the elastic distribution without violating the serviceability requirements of the slab.

Another problem which will not be treated here is the one related to the multiple load cases.

#### 2.2.8 Conclusion:

The rules set in this chapter provide either an optimum design or a close upper bound to the minimum reinforcement in concrete slabs. These rules will ensure that the yield criterion is nowhere exceeded, and that a state of yield will exist in most slab regions, sufficient to convert it into mechanism at design load.

Design for membrane forces and the result of combining bending and membrane forces have not been mentioned in this chapter for the simple reason that the present investigation is restricted to the design for bending moments only.

The conditions of equilibrium and boundary conditions will be satisfied by a stress field obtained from a finite element program, which will be discussed in the next chapter.

The mechanism condition and ductility demand will be analysed in chapter five.

## CHAPTER THREE :

### THE FINITE ELEMENT METHOD

#### 3.1 Introduction:

In the previous chapter, the rules for designing the reinforcement in concrete slabs for a given moment triad ( $M_x, M_y, M_{xy}$ ) were established.

The elastic or non elastic moments triads ( $M_x, M_y, M_{xy}$ ) are obtained by means of a finite element program which will be described in this chapter.

The mechanism condition and ductility demand discussed in the previous chapter will be investigated for the case of non elastic stress field using a nonlinear finite element program which also will be described.

#### 3.2 Review of Mindlin finite element program:

As mentioned above, the distribution of the stress field is obtained by a finite element program which will be discussed in detail here. The finite element program used in this study is the one given by reference<sup>(36)</sup> known as Mindlin program.

As the standard procedure of finite element analysis is well known it is not described in detail here, but in order to define terms, a brief review of the method is included. This is done with particular reference to the formulation of the Mindlin plate bending elements.

The finite element method is an approximation technique which represents continua by equivalent discrete systems. Consequently, continua with infinite degrees of freedom are approximated by equivalent systems with finite numbers of degrees of freedom.



Thus, a slab to be analysed by finite element method is first divided into a series of elements of simple geometric shape which are connected at a finite number of points known as nodal points. This process is known as discretisation. A displacement function in terms of the coordinate variables  $(x,y)$  and the nodal displacement parameter (eg.  $u,v$ ), is chosen to represent the displacement variations within each element, and, by using the principle of minimum total potential, a stiffness matrix relating the nodal 'forces' to the nodal 'displacements' can be derived. Such a displacement function will try to approximate the actual displacement field over the whole element.

### 3.2.1 Mindlin plate elements:

Mindlin plate theory allows for transverse shear deformation effects and thus offers an alternative to classical Kirchoff thin plate theory. The main assumptions are that :

- a– Displacements are small compared to the plate thickness.
- b– The stress normal to the plate mid– surface is negligible.
- c– Normals to mid– surface before deformation remain straight but not necessarily normal to the mid– surface after deformation.

A typical Mindlin plate is shown in Fig– (3.1)

Finite elements based on Mindlin's assumptions have one important advantage over elements based on classical thin plate theory. Mindlin plate elements require only  $c(0)$  continuity of the lateral displacement  $w$  and the independent rotations  $\theta_x$  and  $\theta_y$  . However, elements based on the classical Kirchoff thin plate theory require  $c(1)$  continuity. In other words  $(\partial w / \partial x)$  and  $(\partial w / \partial y)$  as well as  $w$  should be continuous across element interfaces, although this condition is relaxed in non– conforming plate elements. Thus, it would appear that Mindlin

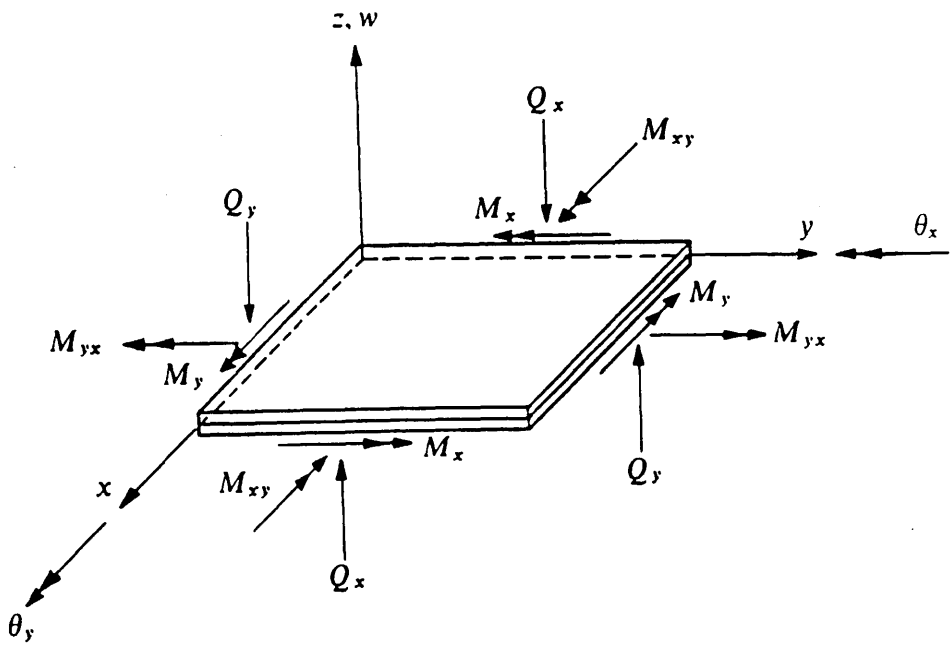


**Figure (3-1) Sign convention for Mindlin plate theory**

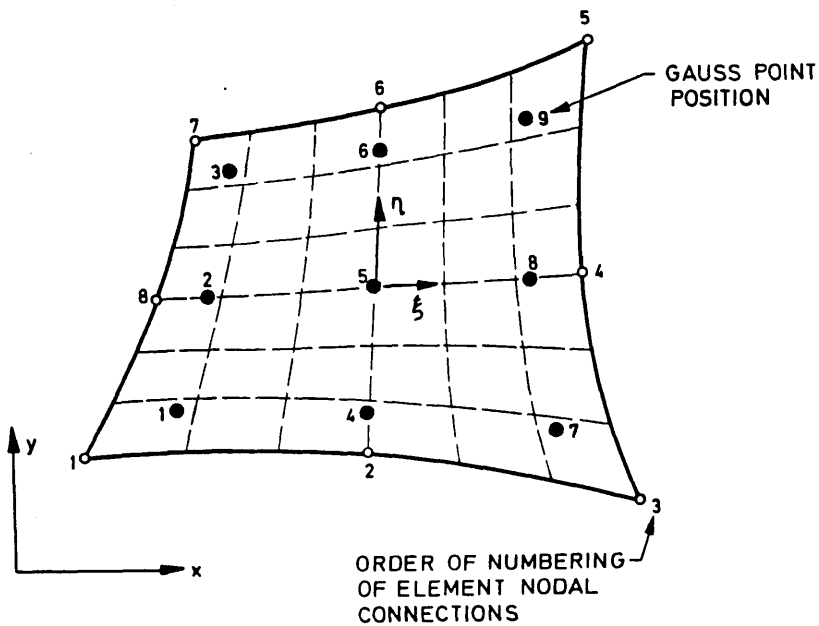


**Figure (3-2) Parabolic isoparametric plate bending element**

plate elements are simpler to formulate and they have the added advantage of being able to model shear-weak as well as shear-stiff plates – if transverse shear effects are present in the plate they are automatically modelled with Mindlin plate elements.

Using the well known and tested<sup>(24)</sup> isoparametric formulations, the eight noded parabolic elements in the XY plane are chosen (Fig- 3.2) in this study.

### 3.2.2 Finite element formulation:

On the basis of the Mindlin's assumptions, and with reference to the figure (3.3) the displacement field can be written as:

$$\delta = \begin{bmatrix} w \\ \theta_x \\ \theta_y \end{bmatrix} = \begin{bmatrix} w \\ \frac{\partial w}{\partial x} + \Phi_x \\ \frac{\partial w}{\partial y} + \Phi_y \end{bmatrix} \quad \dots\dots(3.1)$$

where  $w$  = independent variation of the lateral displacement,

$(\theta_x, \theta_y)$  = angles defining the direction of the line originally normal to mid-surface of the plate as shown in Fig- (3.3). They are considered as average rotations and a correction will be made subsequently to allow for non-uniform shear distribution,

$(\Phi_x, \Phi_y)$  = denote the average shear deformations.

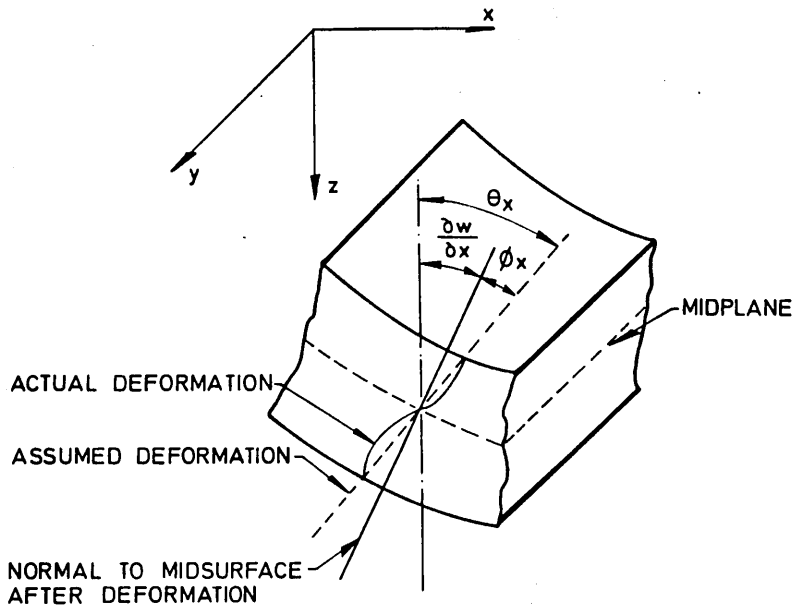


Figure (3-3) Deformation of the cross-section of plate of homogenous section

The in- plane strains are given by :

$$\begin{bmatrix} \epsilon_x \\ \epsilon_y \\ \gamma_{xy} \end{bmatrix} = \begin{bmatrix} \frac{\partial u}{\partial x} \\ \frac{\partial v}{\partial y} \\ \frac{\partial u}{\partial y} + \frac{\partial v}{\partial x} \end{bmatrix} = \begin{bmatrix} -z \frac{\partial \theta_x}{\partial x} \\ -z \frac{\partial \theta_y}{\partial y} \\ -z \left[ \frac{\partial \theta_x}{\partial y} + \frac{\partial \theta_y}{\partial x} \right] \end{bmatrix} \quad \dots(3.2)$$

For plane stress condition, if the stress corresponding to the strains  $(\epsilon_x, \epsilon_y, \gamma_{xy})$  are  $(\sigma_x, \sigma_y, \tau_{xy})$  then,

$$\begin{bmatrix} \sigma_x \\ \sigma_y \\ \tau_{xy} \end{bmatrix} = \begin{bmatrix} E_x & E_{x1} & 0 \\ E_{x1} & E_y & 0 \\ 0 & 0 & G \end{bmatrix} \begin{bmatrix} \epsilon_x \\ \epsilon_y \\ \gamma_{xy} \end{bmatrix} \quad \dots(3.3)$$

where  $E_x$  ,  $E_y$  ,  $G$  and  $E_{x1}$  are independent material constants which are needed to define the elastic properties of the plate.

These stresses produce the bending and twisting moment stress resultants  $(M_x, M_y, M_{xy})$

$$\begin{bmatrix} M_x \\ M_y \\ M_{xy} \end{bmatrix} = \int_{-t/2}^{t/2} \begin{bmatrix} \sigma_x \\ \sigma_y \\ \tau_{xy} \end{bmatrix} dz$$

By substituting the Eq- (3.3) into the previous relation, we obtain:

$$\begin{bmatrix} M_x \\ M_y \\ M_{xy} \end{bmatrix} = \begin{bmatrix} D_x & D_{x1} & 0 \\ D_{x1} & D_y & 0 \\ 0 & 0 & D_{xy} \end{bmatrix} \begin{bmatrix} -\partial\theta_x / \partial x \\ -\partial\theta_y / \partial y \\ -\left[ \frac{\partial\theta_x}{\partial y} + \frac{\partial\theta_y}{\partial x} \right] \end{bmatrix}$$

....(3.4)

where  $D_x = \frac{E_x \cdot t^3}{12}$  ;  $D_y = \frac{E_y \cdot t^3}{12}$  ;  $D_{xy} = \frac{G \cdot t^3}{12}$  and

$$D_{x1} = \frac{E_{x1} \cdot t^3}{12}$$

The above Eq- (3.4) can be rewritten as :

$$M = D_f \cdot \epsilon_f \quad \text{....(3.5)}$$

And the shear forces ( $Q_x$  ,  $Q_y$ ) are obtained by the following equation :

$$\begin{bmatrix} Q_x \\ Q_y \end{bmatrix} = \begin{bmatrix} S_x & 0 \\ 0 & S_y \end{bmatrix} \begin{bmatrix} \theta_x - \partial w / \partial x \\ \theta_y - \partial w / \partial y \end{bmatrix} \quad \text{.....(3.6)}$$

where  $S_x$  and  $S_y$  are the effective shear moduli in the X- and Y- directions respectively. For an isotropic material

$$S_x = S_y = \frac{E}{2(1+\nu)} \left( \frac{5}{6} \right)$$

where  $E$  and  $\nu$  are the Young's modulus and the Poisson's ratio respectively.

Equation (3.6) may be rewritten as :

$$Q = D_s \cdot \epsilon_s \quad \text{....(3.7)}$$

The above two equations (3.5) and (3.7) can be grouped as :

$$\begin{bmatrix} M_x \\ M_y \\ M_{xy} \end{bmatrix} = \begin{bmatrix} D_f & | & 0 \\ \hline & & \\ 0 & | & D_s \end{bmatrix} \begin{bmatrix} \epsilon_f \\ \hline \\ \epsilon_s \end{bmatrix} \quad \dots\dots(3.8)$$

Or in a more general form :

$$\sigma = D \cdot \epsilon \quad \dots\dots(3.9)$$

The governing equilibrium equations can be obtained by minimising the total potential of the system. The total potential,  $\pi$ , can be expressed as:

$$\pi = \frac{1}{2} \int_V [\sigma]^T \epsilon \, dv - \int_V [\delta]^T p \, dv - \int_A [\delta]^T q \, ds \quad \dots\dots(3.10)$$

where  $\sigma$  and  $\epsilon$  are the stress and strain vectors respectively,  $\delta$  the displacements at any point,  $p$  the body forces per unit volume and  $q$  the applied surface tractions.

Integrations are taken over the volume  $V$  of the structure and loaded surface area,  $A$ .

In the isoparametric formulation, the displacement variation over the element is defined in terms of the nodal displacement components by the expression :

$$\begin{bmatrix} w \\ \theta_x \\ \theta_y \end{bmatrix} = \sum_{i=1}^8 N_i \cdot \delta_i \quad \dots\dots(3.11)$$

where  $N_i$  is the shape function associated with node  $i$ , function of  $(\xi, \eta)$  and which are given by Zienkiewicz<sup>(74)</sup>,

$\delta_i = [w_i, \theta_{xi}, \theta_{yi}]^T$  is the vector of displacements at node  $i$ .

The strains within any element can be expressed in terms of element nodal displacements as :

$$\epsilon = \sum_{i=1}^8 B_i \cdot \delta_i \quad \dots(3.12)$$

where  $B_i$  is the strain matrix of node  $i$ , generally composed of derivatives of the shape functions:

$$\begin{bmatrix} B_{fi} \\ \dots \\ B_{si} \end{bmatrix} = \begin{bmatrix} 0 & -\frac{\partial N_i}{\partial x} & 0 \\ 0 & 0 & -\frac{\partial N_i}{\partial y} \\ 0 & -\frac{\partial N_i}{\partial y} & -\frac{\partial N_i}{\partial x} \\ \dots \\ \frac{\partial N_i}{\partial x} & -N_i & 0 \\ \frac{\partial N_i}{\partial y} & 0 & -N_i \end{bmatrix} \quad \dots(3.13)$$

$B_{fi}$  is the strain matrix associated with bending deformation  $\epsilon_f$  and  $B_{si}$  is the strain matrix associated with shear deformation  $\epsilon_s$ .

The equation (3.10) can now be rewritten for each element :



$$\begin{aligned} \pi_e = & \frac{1}{2} \int_{V_e} [ \delta^e ]^T [ B ]^T D.B. \delta^e dV - \\ & \int_{V_e} [ \delta^e ]^T [ N ]^T p.dV - \int_{A_e} [ \delta^e ]^T [ N ]^T q.dS \end{aligned} \quad \dots(3.14a)$$

where  $V_e$  is the element volume and  $A_e$  the loaded element area.

Performance of the minimisation for element  $e$  with the nodal displacement  $\delta^e$  for the element result in :

$$\begin{aligned} \frac{\partial \pi_e}{\partial \delta^e} = & \int_{V_e} ( [ B ]^T D B ) \delta^e.dV - \int_{V_e} [ N ]^T p.dV - \\ & \int_{A_e} [ N ]^T q.dS \end{aligned} \quad \dots(3.14b)$$

$$= K^e \delta^e - F^e \quad \dots(3.15)$$

$$\text{where } F^e = \int_{V_e} [ N ]^T p.dV + \int_{A_e} [ N ]^T q.dS \quad \dots(3.16)$$

are the equivalent nodal forces for the element, and

$$K^e = \int_{V_e} [ B ]^T D B dV \quad \dots(3.17)$$

is termed the element stiffness matrix.

The summation of the terms in Eq- (3.14b) when equated to zero, results in a system of equilibrium equations for complete continuum. These equations are then solved by any standard technique to yield the nodal displacements.

Note here, that the stiffness matrix is obtained by Gauss quadrature integration. A 3 x 3 Gauss rule is used with the flexural strain energy contribution and 2 x 2 Gauss rule with the shear strain energy contribution. This method is known as 'reduced integration' scheme, and has been tested<sup>(35)</sup> to provide the correct contribution for the shear components of the stiffness matrix for rectangular and parallelogram shaped elements.

### 3.2.3 Plasticity:

In the present program (Mindlin) the material obeys the Von- Mises criterion given by the equation :

$$F = M_x^2 + M_y^2 - M_x.M_y + 3 M_{xy}^2 - M_p^2 = 0.0 \quad (3.18)$$

where (  $M_x, M_y, M_{xy}$  ) are the moment triad, and  $M_p$  is the plastic moment. It defines the stress level at which plastic deformation begins. The equation indicates that when bending moment reaches the yield moment  $M_p$  , the whole section of the plate becomes plastic instantaneously although we know that this is a convenient fiction since there is always a gradual spread of plasticity over the depth of plate.

Von- Mises criterion simulates very well metallic materials, and good agreement with experimental data have been obtained for most metals. However, for concrete the applicability of Von- Mises criterion is debatable because nonlinear action in concrete is not caused by actual plastic flow as in metals, but is dictated by the cumulative effect of microcrack propagation. However, these reservations are irrelevant in the present context because the object is to obtain elasto- plastic stress distribution in equilibrium with the applied load, and without any knowledge of the reinforcement in the slab being analysed. The output from this analysis will simply serve as input to the determination of the design moments.

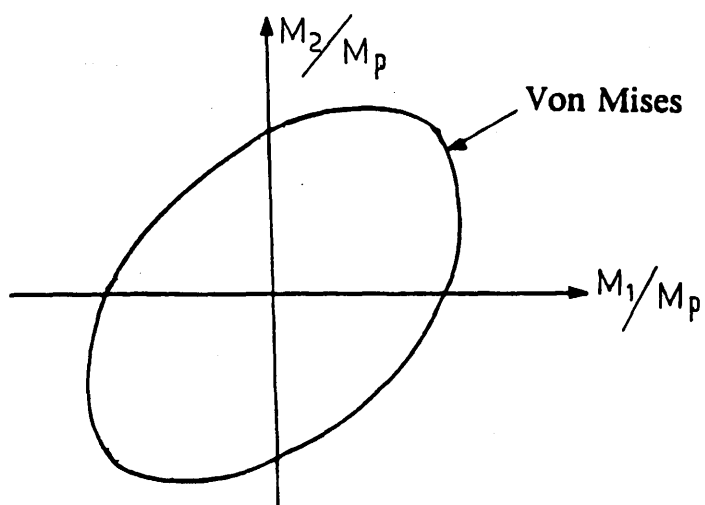


Figure (3-4) 2-D representation of the Von-Mises yield surface

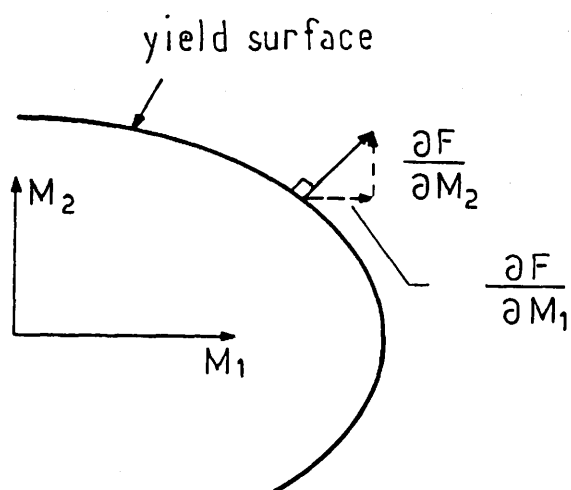


Figure (3-5) Geometrical representation of the normality rule of associated plasticity

– Elasto– plastic stress / strain relation:

For the post yield state, the material behaviour will be partly elastic and partly plastic. During any increment of stress during the load history, the changes of strain are :

$$d\epsilon = d\epsilon_e + d\epsilon_p \quad \dots(3.19)$$

where  $d\epsilon_e$  represents the elastic component of the strain and is given by :

$$d\epsilon_e = [ D ]^{-1} d\sigma \quad \dots(3.20)$$

where  $[ D ]$  is the elastic constitutive matrix,

and  $d\epsilon_p$  represents the plastic component of the incremental strain  $d\epsilon$ .

In order to derive the relationship between the plastic strain component  $d\epsilon_p$  and the stress increment  $d\sigma$ , it will be assumed that the material obeys the flow rule (normality rule), as shown in Fig– (3.5). The flow rule states that the incremental strain increment, has a direction normal to the yield surface at the point considered, and is given by the relation :

$$d\epsilon_p = d\lambda \frac{\partial F}{\partial \sigma} \quad \dots(3.21)$$

where  $d\lambda$  is a proportionality constant termed the plastic multiplier.

Thus on use of Eq– (3.19), Eq– (3.20) and Eq– (3.21) the complete incremental relationship between stress and strain for elasto– plastic deformation is found to be :

$$d\epsilon = [D]^{-1} d\sigma + d\lambda \frac{\partial F}{\partial \sigma} \quad \dots(3.22)$$

The vector  $a^T = \frac{\partial F}{\partial \sigma} = \left[ \frac{\partial F}{\partial M_x}, \frac{\partial F}{\partial M_y}, \frac{\partial F}{\partial M_{xy}} \right]$  is termed

the flow vector.

If the hardening phenomenon is taken into consideration, then the yield function  $F$  in terms of the stresses  $\sigma$  and work hardening parameter  $\kappa$  is given as :

$$F(\sigma, \kappa) = 0.0$$

and the total derivative of the yield function is given as :

$$dF = \frac{\partial F}{\partial \sigma} d\sigma + \frac{\partial F}{\partial \kappa} d\kappa = 0.0 \quad \dots(3.23)$$

or  $a^T d\sigma - A d\lambda = 0.0$

with  $A = - \frac{1}{d\lambda} \frac{\partial F}{\partial \kappa} d\kappa \quad \dots(3.24)$

Premultiplying both sides of Eq- (3.22) by  $a^T D$  and eliminating  $a^T d\sigma$  using Eq- (3.24) we obtain the plastic multiplier  $d\lambda$  to be :

$$a^T D d\epsilon = a^T D [D]^{-1} d\sigma + a^T D d\lambda a$$

then  $a^T D d\epsilon = d\lambda \{ A + a^T D a \} \Rightarrow$

$$d\lambda = \frac{1}{A + a^T D a} a^T D d\epsilon \quad \dots(3.25)$$

Using Eq- (3.25) into Eq- (3.22) then :

$$d\epsilon = [D]^{-1} d\sigma + \frac{1}{A + a^T D a} a^T D d\epsilon a$$

and by premultiplying the above equation by  $D$  , we get :

$$D d\epsilon = d\sigma + \frac{1}{A + a^T D a} D a a^T D$$

$$\text{Thus } d\sigma = d\epsilon \left[ D - \frac{1}{A + a^T D a} D a a^T D \right]$$

$$\text{Or } d\sigma = D_{ep} d\epsilon \quad \dots(3.26)$$

$$\text{with } D_{ep} = D - \frac{1}{A + a^T D a} D a a^T D \quad \dots(3.27)$$

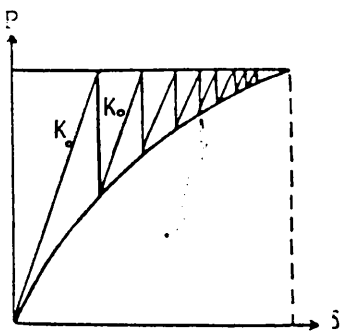
$D_{ep}$  represents the elasto- plastic " stress- strain " matrix.

#### 3.2.4 Solution of nonlinear problems:

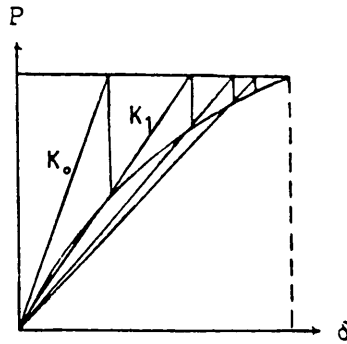
The solution of nonlinear problems by finite element method is usually attempted by one of the three following techniques: (see Figure 3.6)

- (i) Incremental ( step wise procedure)
- (ii) Iterative ( Newton- Raphson method )
- (iii) Increment - Iterative ( mixed procedure )

In this program all these three methods are available, and the mixed procedure will be used in this study where the stiffness matrix is updated for the second iteration of each load increment only. Consequently economies in computation time are gained.

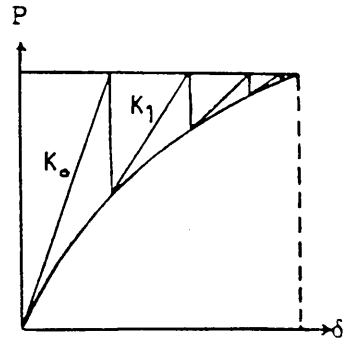


constant stiffness  
procedure



variable stiffness  
procedure

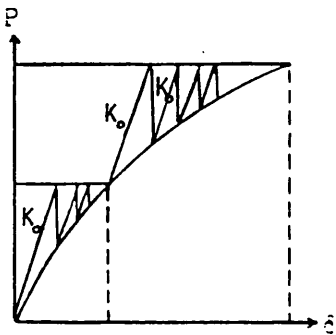
Secant Modulus  
Approach



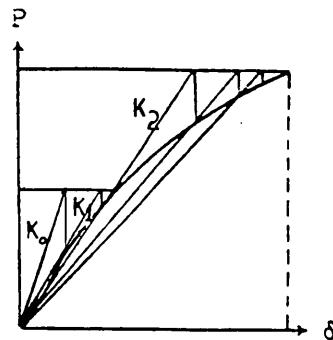
variable stiffness  
procedure

Tangent Modulus  
Approach

### ITERATION PROCESS

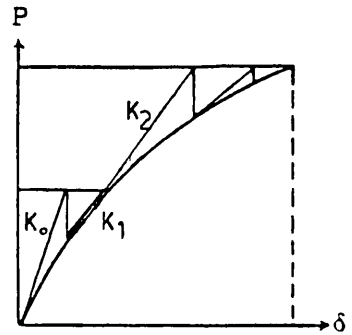


constant stiffness  
procedure



variable stiffness  
procedure

Secant Modulus  
Approach



variable stiffness  
procedure

Tangent Modulus  
Approach

### MIXED PROCEDURE

Figure (3-6) Basic procedure for nonlinear solution

### 3.2.5 Solution procedure adopted in the Mindlin program:

The solution procedure followed by this program is summarized in the following two tables:

Table (3.1) Equation solving technique for Mindlin program

- (1) Begins new load increment,  $f = f + \Delta f$
- (2) Set  $\Delta f$  equal to the current load increment vector.
- (3) Set  $\delta^0$  equal to 0.0 for the first increment or equal to the total displacement vector at the end of the last load increment.
- (4) Set the residual force vector  $\Psi^0$  to zero for the first load increment, where  $\Psi$  represents the unbalanced load vector given by the difference  $\{ K^e \delta^e - F^e \}$  (see Eq- 3.15)
- (5) Set  $\Psi^0 = \Psi^0 + \Delta f$
- (6) Solve  $\Delta d^0 = - [ K_T ]^{-1} \Psi^0$ ,  $K_T$  represent the old or updated tangential stiffness matrix.
- (7) Set  $d^1 = d^0 + \Delta d^0$
- (8) Evaluate  $\Psi^1(d^1)$  ( the current residual force ).
- (9) If the solution has converged go to 11 ; otherwise continue.
- (10) Iterate until solution has converged.
- (11) If this is not the last increment go to 1 ; otherwise stop.

Table (3.20) The iteration loop

- (1) Set iteration number  $i = 1$
- (2) Solve  $\Delta d^i = - [ K_T ]^{-1} \Psi^i$ , use old or updated  $K_T$ .
- (3) Set  $d^{i+1} = d^i + \Delta d^i$ .



(4) For each Gauss point, evaluate the increments in strain resultants :

$$\Delta \epsilon_f^i = B_f ( \Delta d^i )$$

$$\Delta \epsilon_s^i = B_s ( \Delta d^i )$$

(5) Using the elastic rigidities estimate at each Gauss point, the increments in stress resultants and hence the total stress resultants :

$$\Delta \sigma_f^i = D_f \epsilon_f^i \Rightarrow \sigma_f^{i+1} = \sigma_f^i + \Delta \sigma_f^i$$

$$\Delta \sigma_s^i = D_s \epsilon_s^i \Rightarrow \sigma_s^{i+1} = \sigma_s^i + \Delta \sigma_s^i$$

(6) At each Gauss point depending on the states of  $\sigma_f^i$  and  $\sigma_s^{i+1}$  , adjust  $\sigma_f^{i+1}$  to satisfy the yield criterion and preserve the normality condition.

(7) Evaluate the residual force vector:

$$\Psi^{i+1} = \int_A \left\{ [ B_f ]^T \sigma_f + [ B_s ]^T \sigma_s \right\} dA - f$$

(8) If the solution has converged, continue, otherwise set  $i = i + 1$  and go to 2

(9) Move to the next increment.

### 3.2.6 Convergence criteria:

Because of equilibrium violation, extraneous residual forces develop in iterative process of solution, The convergence criterion is based on a 'tolerable' value of the residual. The criterion employed states that convergence occurs if the norm of the residual forces becomes less than the tolerance  $t$  :

$$\frac{\left[ \sum_{i=1}^N \left( \Psi_i^r \right)^2 \right]^{\frac{1}{2}}}{\left[ \sum_{i=1}^N \left( f_i \right)^2 \right]^{\frac{1}{2}}} \times 100 \leq t \quad \dots (3.28)$$

where  $f$  is the applied force vector,  $\Psi$  is the residual force vector,  $r$  denotes the iteration number and  $N$  is the total number of nodal points.

### 3.2.7 Enhancements to the program:

Some modifications were necessary before the program could be used for this study. It involved the writing of a code to set up the design of slabs in accordance to the direct design approach. In consequence the design equations given in chapter two have been incorporated within Mindlin program in such a way that at each increment level, the required reinforcement for the slab is obtained (this task will be detailed in the following chapter).

The moment volume giving the amount of reinforcement for the whole slab at each stage of loading is also given.

Finally, a mesh generation routine was also added to the program. This saved time and helped to avoid errors during the rather tedious task of data input.

### 3.3 Review of the ' LAYER ' program:

#### 3.3.1 Introduction:

In the previous section, a rational manner of obtaining the stress fields ( elastic and non- elastic ) has been established.

To test the slabs designed by the direct design approach using non- elastic stress field, one can do it theoretically and then confirm the results experimentally.

Analytical procedures which accurately determine stress and deformation states in reinforced concrete members are complicated due to many factors.

Among them are:

- (1) The nonlinear load- deformation response of concrete and difficulty in forming suitable constitutive relationships under combined stresses.
- (2) Progressive cracking of concrete under increasing load and the complexity in formulating the failure behaviour for various stress states.
- (3) Consideration of steel reinforcement and the interaction between concrete and steel constituents that form the composite system.
- (4) Time dependent effects such as creep and shrinkage of concrete.

Because of the complexities, analytical studies on reinforced concrete were based on either empirical approaches, or on simple analysis assumptions such as those of linear elastic behaviour for the system. However, finite element method offers an adaptable means whereby such complex systems can be analysed.

#### 3.3.2 Nonlinear finite element models:

In this review we limit ourselves to the material nonlinearities because they occur in all reinforced concrete structures and should be considered in any accurate rational analysis.

To model mathematically the nonlinear reinforced concrete behaviour, three areas must be examined:

(1) Since steel reinforcement is comparatively thin, it is generally assumed capable of transmitting axial force only and thus, a uniaxial stress-strain relationship is sufficient for general use.

(2) For concrete, however, a knowledge of multiaxial stress-strain behaviour is required. Although a variety of models have been proposed, this is still far from being complete.

(3) The bond slip phenomenon between steel and concrete is not considered. Most practical applications assume perfect bond.

Once the stress-strain relation of each material is available and a perfect bond is assumed, steel reinforcement can then be placed in proper positions in concrete elements. Constitutive equations for the composite response of concrete elements can then be formulated.

Having derived the nonlinear constitutive relationships, the next step is to solve the nonlinear problem using the finite element techniques.

In the literature, two distinctly different viewpoints have been reported in an effort to obtain the necessary constitutive relations. In the first approach, exemplified by the work of Jofriet and Mc Niece<sup>(43)</sup> and Bell<sup>(5)</sup>, a semi-empirical overall moment-curvature relation is employed which attempts to take into consideration the various stages of material behaviour. This approach is limited due to the assumption of a macroscopic equivalent moment-curvature relationship.

The second approach is based on idealized stress-strain relations for concrete and steel, together with some assumptions regarding compatibility of deformation between the two constituent materials. Cervenka has analysed reinforced concrete panels under in-plane loads using this technique.

For flexural deformation, material property variation through the thickness must be taken into account. This can be accomplished in a discretized fashion via a

layering approach or by the introduction of numerical integration points through the thickness. The layering concept was applied by Whang<sup>(68)</sup> to the elasto-plastic analysis of shells, and is a physically interpretable special case of the integration point approach suggested by Marcal<sup>(52)</sup>.

Dotreppe.J.C<sup>(20)</sup>, Johnarry<sup>(41)</sup>, Hago.A.W.<sup>(29)</sup> and L.M.A.Hafez<sup>(1)</sup> and others have used the layer approach and have reported good agreement with experimental results. So in this study the layering concept will be used.

### 3.3.3 Review of the layer approach:

In such models the slab thickness is divided hypothetically into a number of layers parallel to its middle plane.(Fig 3.7)

Each layer is assumed to be in a state of plane stress condition, and a linear strain variation with the depth is assumed for the small deflection theory. Each layer can be of a different material, thus for a reinforced concrete element, each constituent material is assigned a different layer. Perfect bond between all layers is normally assumed, although in some cases, bond slip can easily be accommodated.

The deterioration in the slab stiffness is represented by appropriately changing the layer properties, whenever nonlinearity occurs. Crack penetration through the slab can thus be conveniently reflected by this model.

Various layered finite element models have been used and are reported in the literature such as A.W.Hago's or L.M.A.Hafez's models.

In the present study the model given by reference<sup>(1)</sup> has been used and it is defined in the following.

#### 3.3.3.1 Layered finite element formulation:

Layer approach is used widely with various types of elements. The first element used by Wegmuller<sup>(69)</sup> is a rectangular element with three degrees of freedom ( $\theta_x, \theta_y, w$ ). The element ignores in-plane effects, and thus assumes a fixed

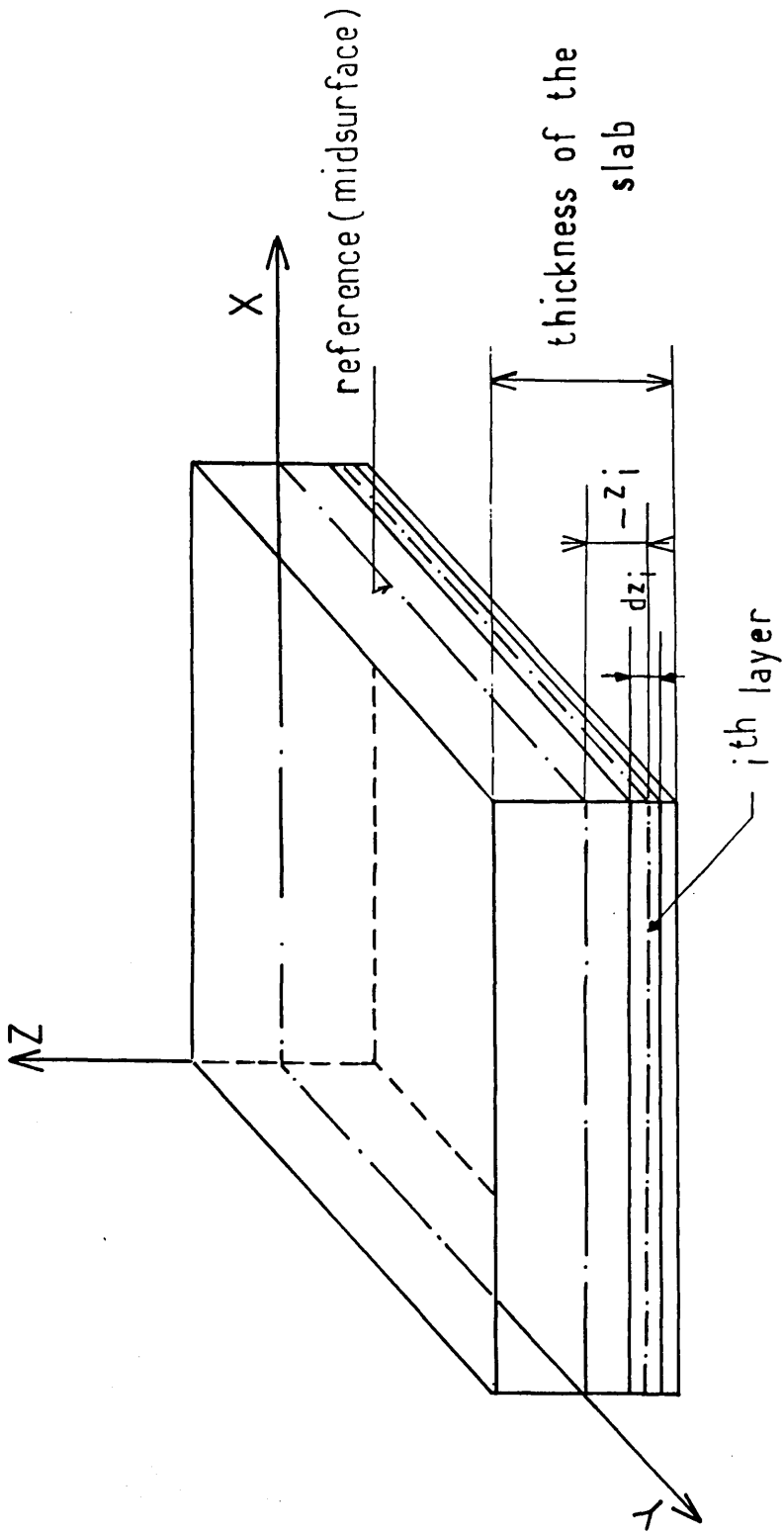


Figure (3-7) Layer idealization

position of the middle plane of plate, such an assumption will be restricted only to problems in which membrane forces are negligible or there is little shift in neutral axis position.

For bending problems, as the cracking progresses deeper into the slab depth, the neutral axis shifts from its initial position towards the compression face. The layer approach has been used to solve this problem by taking the effect of membrane stresses into consideration.

Wegmuller<sup>(69)</sup>, Hand<sup>(31)</sup>, Johnarry<sup>(41)</sup>, Cope<sup>(17)</sup> and Hago<sup>(30)</sup> have used a rectangular element with five degrees of freedom ( $u, v, w, \theta_x, \theta_y$ ) at each node.

L.M.A.Hafez<sup>(1)</sup> used an isoparametric eight noded elements with five degrees of freedom ( $u, v, w, \theta_x, \theta_y$ ), based on the Mindlin theory. In this study this model is used.

In the following, formulations are made separately for each layer.

- Displacement representation:

The displacements  $u, v, w$  at any point in the plate with coordinates  $(x, y, z)$  can be expressed as :

$$\begin{bmatrix} u(x, y, z) \\ v(x, y, z) \\ w(x, y, z) \end{bmatrix} = \begin{bmatrix} u_0(x, y) - z \theta_x(x, y) \\ v_0(x, y) - z \theta_y(x, y) \\ w_0(x, y) \end{bmatrix} \quad \dots (3.29)$$

where  $u_0$  ,  $v_0$  and  $w_0$  represent the displacement at the plate reference in the X- , Y- and Z- directions respectively.

So the strain– displacement relationships are given as :

(using the finite element idealization)

$$\begin{bmatrix} \epsilon_x \\ \epsilon_y \\ \epsilon_{xy} \\ \gamma_{xy} \\ \gamma_{yz} \end{bmatrix} = \sum_{i=1}^8 \begin{bmatrix} \frac{\partial N_i^e}{\partial x} & 0 & 0 & -z \frac{\partial N_i^e}{\partial x} & 0 \\ 0 & \frac{\partial N_i^e}{\partial y} & 0 & 0 & -z \frac{\partial N_i^e}{\partial y} \\ \frac{\partial N_i^e}{\partial y} & \frac{\partial N_i^e}{\partial x} & 0 & -z \frac{\partial N_i^e}{\partial y} & -z \frac{\partial N_i^e}{\partial x} \\ 0 & 0 & \frac{\partial N_i^e}{\partial x} & -N_i^e & 0 \\ 0 & 0 & \frac{\partial N_i^e}{\partial y} & 0 & -N_i^e \end{bmatrix} \begin{bmatrix} u_i \\ v_i \\ w_i \\ \theta_{xi} \\ \theta_{yi} \end{bmatrix}$$

....(3.30)

In which  $\epsilon_x, \epsilon_y, \epsilon_{xy}$  are the inplane strains components, and  $\gamma_{xy}, \gamma_{yz}$  are the transverse shear strain components,  $z$  is the distance from the reference plane to the layer centre, as shown in figure (3.7), and  $N_i^e$  are the usual shape functions.

Eq– (3.30) can be rewritten as :

$$\{ \epsilon \} = \sum_{i=1}^8 B_i \{ \delta_i \}$$

for each layer, where  $B_i = \begin{bmatrix} B_{pi} & B_{fi} \\ 0 & B_{si} \end{bmatrix}$  ....(3.31)

where  $B_{pi}$  represents the strain matrix associated with plane stress deformation, and  $B_{fi}$  and  $B_{si}$  are as defined previously.



For linear analysis of uncracked concrete and in the absence of initial stresses and strains, the stress-strain relationship for each layer may be written as :

$$\{ \sigma \} = [ D' ] \{ \epsilon \} \quad \dots(3.32)$$

which is similar to Eq- (3.9), but here the constitutive matrix for a concrete layer is given by :

$$D' = \frac{E_c}{1 - \nu^2} \begin{bmatrix} 1 & \nu & 0 & 0 & 0 \\ \nu & 1 & 0 & 0 & 0 \\ 0 & 0 & \frac{1 - \nu}{2} & 0 & 0 \\ 0 & 0 & 0 & \frac{5(1 - \nu)}{6 \times 2} & 0 \\ 0 & 0 & 0 & 0 & \frac{5(1 - \nu)}{6 \times 2} \end{bmatrix} \quad \dots(3.32)$$

where  $E_c$  is the Young modulus of concrete and  $\nu$  is the Poisson's ratio.

For steel layer  $[ D' ]$  is given by :

$$D' = \frac{\rho E_s}{1 - \nu^2} \begin{bmatrix} \cos^4\alpha & \cos^2\alpha \sin^2\alpha & \cos^3\alpha \sin\alpha & 0 & 0 \\ & \sin^4\alpha & \cos\alpha \sin^3\alpha & 0 & 0 \\ & & \cos^2\alpha \sin^2\alpha & 0 & 0 \\ \text{Symmetric} & & & 0 & 0 \\ & & & & 0 \end{bmatrix} \quad \dots(3.33)$$

where  $\rho$  represents the percentage of steel in the direction considered,  $E_s$  the Young's modulus of steel reinforcement, and  $\alpha$  the angle of inclination of the steel to X- axis measured from X- axis to the steel direction anticlockwise.

Consequently, the stiffness matrix is computed for each layer and then a summation for all the layers is done :

$$K = \sum_{i=1}^n \left\{ \int \int \int [B]^T D' [B] dx \cdot dy \right\} dz_i \quad \dots (3.34)$$

where  $dz_i$  is the thickness of the  $i^{\text{th}}$  layer,  $n$  is the total number of the layers,  $B$  is the strain matrix and  $D'$  is the constitutive matrix depending on the type of the material and the state of stress (steel or concrete, elastic , cracked or plastic ) in respect of each layer.

### 3.3.3.2 Modeling the material:

To trace the nonlinear behaviour of the composite material (reinforced concrete), uniaxial and biaxial stress– strain relationships for different materials and the corresponding yield criterion are required in the layer finite element model.

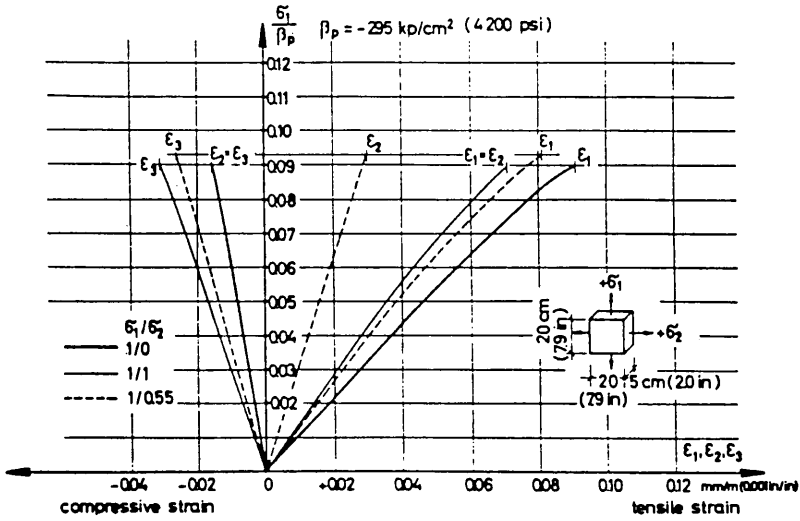
#### A– Concrete:

##### **A.1– Yield criterion:**

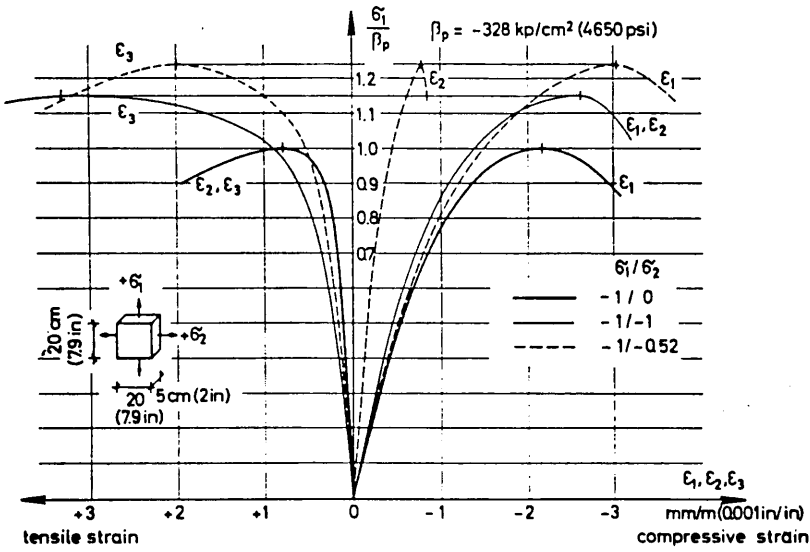
Studies of the behaviour of concrete under multiaxial stress states are essential to develop a universal failure criterion for concrete. For slab studies, in general, a knowledge of behaviour under biaxial state of stress is sufficient.

From experimental studies, it has been concluded that strength of concrete under biaxial compression is greater than the uniaxial compressive strength; and the strength under biaxial tension is independent of the stress ratio in the principal directions and equal to the uniaxial tensile strength.(Figure 3.8)

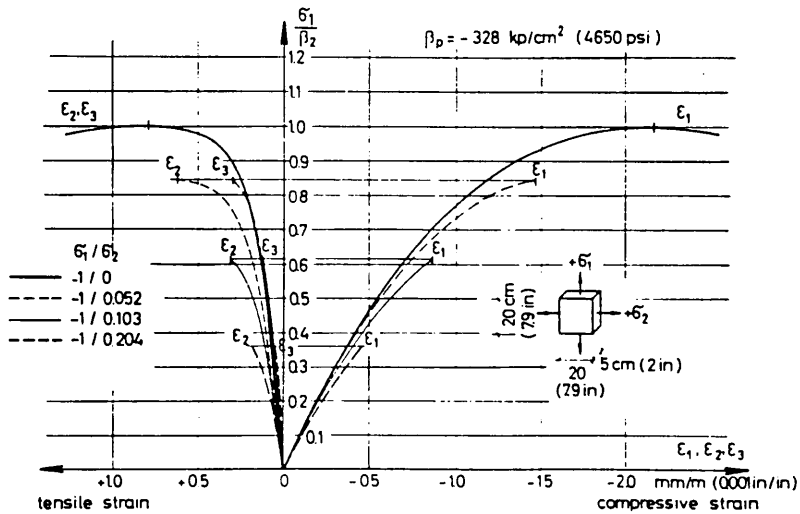
Widely accepted experimental data (regarding the strength, deformational characteristics and microcracking of concrete subjected to biaxial stresses) have been provided by Kupfer, Hillerdorf, and Rush<sup>(48)</sup> (Fig– 3.9) and these are



--Stress-strain relationships of concrete under biaxial tension



--Stress-strain relationships of concrete under biaxial compression



--Stress-strain relationships of concrete under combined tension and compression

Figure (3-8) Stress-strain relationships

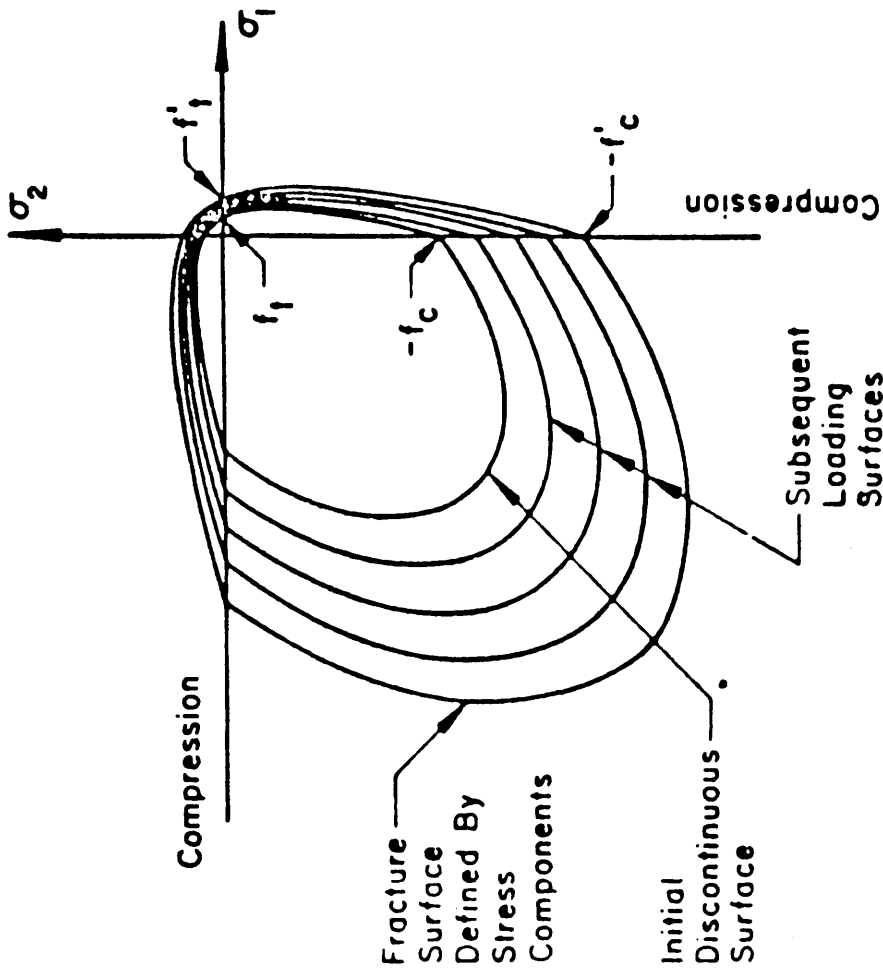


Figure (3-10) The yield surface and boundaries between different material behaviour regions.

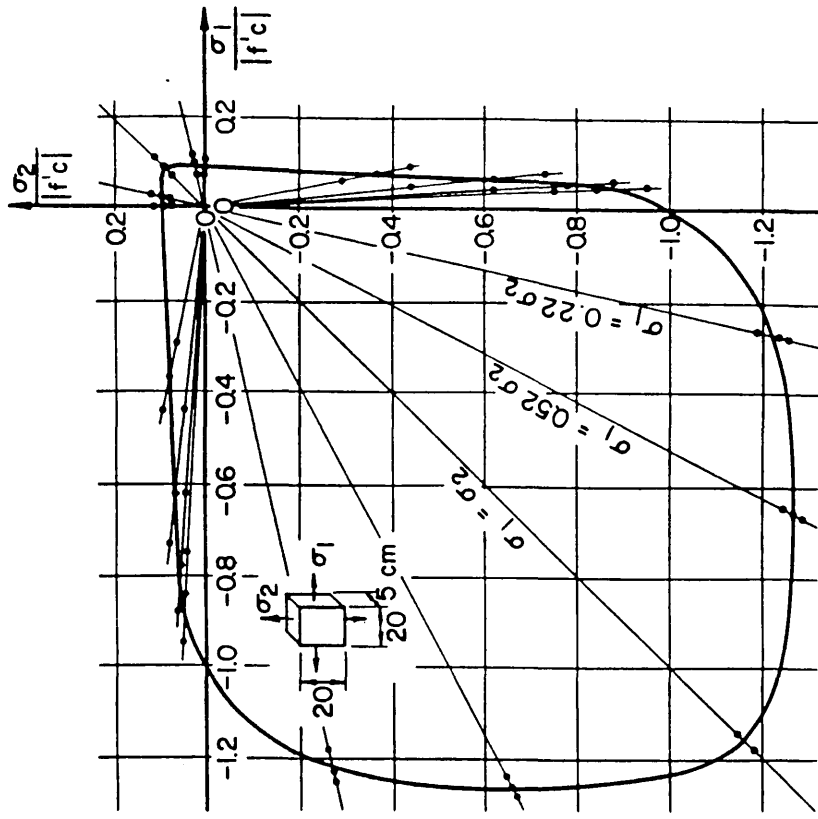


Figure (3-9) Yield surface for biaxial stress in plain concrete proposed by Kupfer, Hilsdorf, and Rush

adopted in this study.

This yield surface can be expressed in terms of octahedral shearing stress criterion of the form:

$$\tau_{\text{oct}} = a + b \sigma_{\text{oct}} \quad \dots(3.35)$$

in which  $\tau_{\text{oct}}$  = the octahedral shearing stress;  $\sigma_{\text{oct}}$  = the octahedral normal stress; and a and b = material constants.

Taking  $f_c$  as the uniaxial compressive strength of concrete and  $f_d$  as the equivalent compressive strength under biaxial compression, and defining the ratio  $m = f_t / f_c$ , Eq- (3.35) can be established in the following manner :

a- Compression- Compression:

(i) For uniaxial compression  $\tau_{\text{oct}} = [\sqrt{2} / 3] f_c$  and  $\sigma_{\text{oct}} = -f_c / 3$ , then

$$\frac{\sqrt{2}}{3} f_c = - \frac{b \cdot f_c}{3} + a \quad \dots(3.36)$$

(ii) For biaxial compression  $\tau_{\text{oct}} = [\sqrt{2} / 3] f_d$  and  $\sigma_{\text{oct}} = (-2 f_d) / 3$ , then

$$\frac{\sqrt{2}}{3} f_c = - \frac{2 \cdot b \cdot f_d}{3} + a \quad \dots(3.37)$$

Solving (3.36) and (3.37), and by assuming  $f_d = 1.16 f_c$  then

$$\frac{\tau_{\text{oct}}}{f_c} + 0.1714 \frac{\sigma_{\text{oct}}}{f_c} - 0.4143 = 0.0 \quad \dots(3.38)$$

b- Tension- Compression :

(i) For uniaxial compression  $\tau_{\text{oct}} = [\sqrt{2} / 3] f_c$  and  $\sigma_{\text{oct}} = - f_c / 3$

$$\frac{\sqrt{2}}{3} f_c = - \frac{b \cdot f_c}{3} + a \quad \dots (3.39)$$

(ii) For uniaxial tension and with  $f_t = m \cdot f_c$  :  $\tau_{\text{oct}} = [\sqrt{2} / 3] m \cdot f_c$  and

$$\sigma_{\text{oct}} = [m \cdot f_c] / 3$$

$$\frac{\sqrt{2}}{3} m \cdot f_c = \frac{m \cdot f_c \cdot b}{3} + a \quad \dots (3.40)$$

Solving (3.39) and (3.40) then :

$$\frac{\tau_{\text{oct}}}{f_c} + \sqrt{2} \frac{1 - m}{1 + m} \frac{\sigma_{\text{oct}}}{f_c} - \frac{2\sqrt{2}}{3} \frac{m}{1 + m} = 0.0 \quad \dots (3.41)$$

c- Tension- Tension:

Since there is no increase in ultimate strength due to biaxial tensile stressing, the simple circular condition :

$$\left[ \frac{\sigma_1}{f_t} \right]^2 + \left[ \frac{\sigma_2}{f_t} \right]^2 - 1.0 = 0.0 \quad \dots (3.42)$$

is sufficient.

The resulting yield surface known as the limiting yield surface is shown in Fig- (3.10). However unlike steel, plasticity in concrete begins well before the limiting or failure surface is reached. To accommodate this phenomenon into the analysis, the intermediate loading surfaces given in Fig- (3.10) have been adopted. Accordingly, the loading surface is divided into initial, subsequent and limiting yield surface. This was accomplished by simply scaling the yield surface, and is

further explained in the following section.

## A.2 Nonlinear constitutive material properties :

### A.2.1 – Concrete in compression:

Experimental results show<sup>(64,65)</sup> that an initial linear elastic behaviour for concrete under compression is limited only to small load range up to 30% of the ultimate capacity. Beyond this range nonlinear behaviour is involved.

To deal with the stress– strain relationship of concrete under compressive forces, there are several possible ways of representing the change in stiffness with increasing strain. The model proposed by Liu, Nilson and Slate<sup>(51)</sup> taking into account these changes was adopted in this study.

The basic concept of this model is to treat the biaxial stress– strain behaviour of concrete as an equivalent uniaxial case. According to this approach, the stress in each principal direction is evaluated solely by the principal strain increment in the same direction and the corresponding tangent stiffness, which is a function of the principal stress ratio, accounts for all the biaxial effects.

The relation between stress– strain is of the form :

$$\sigma = \frac{A + B.E. \epsilon}{(1 - \nu.\Omega)(1 + C. \epsilon + D. \epsilon^2)} \quad \dots(3.43)$$

where A,B,C and D are found from the following conditions on the stress– strain curve in compression :

$$(i) \quad \text{For } \epsilon = 0 \quad \Rightarrow \quad \sigma = 0$$

$$(ii) \quad \text{For } \epsilon = 0 \quad \Rightarrow \quad \frac{d\sigma}{d\epsilon} = \frac{E}{(1 - \nu.\Omega)}$$

which accounts for biaxial stress by the parameter  $\Omega$  , which is the ratio of principal stress in the orthogonal direction to the principal stress in the direction considered (  $\sigma_1 / \sigma_2$  ).

(iii) For  $\epsilon = \epsilon_{pk} \Rightarrow \sigma = \sigma_{pk}$

(iv) For  $\epsilon = \epsilon_{pk} \Rightarrow (d\sigma / d\epsilon) = 0$

where  $\sigma_{pk}$  and  $\epsilon_{pk}$  are the peak stress in biaxial compression and the strain at peak stress, respectively.

Substituting the resulting values in Eq- (3.43) and introducing the secant modulus

$E_s = \sigma_{pk} / \epsilon_{pk}$ , one obtains:

$$\sigma = \frac{E \cdot \epsilon}{(1 - \nu\Omega) \left[ 1 + \left[ \frac{1}{1 - \nu\Omega} \frac{E}{E_s} - 2 \right] \left[ \frac{\epsilon}{\epsilon_{pk}} + \frac{\epsilon}{\epsilon_{pk}} \right]^2 \right]}$$

....(3.44)

where  $\sigma$ ,  $\epsilon$  = stress and strain, respectively, in biaxial loading,

$E$  = modulus of elasticity of concrete for uniaxial loading,

$\nu$  = Poisson's ratio,

$\epsilon_{pk}$  = the strain at maximum stress of concrete for biaxial compression ( = .0025)

$\Omega$  = the ratio of principal stress in the orthogonal direction to the principal stress in the direction considered. ( =  $\sigma_1 / \sigma_2$  )

$E_\sigma$  = secant modulus =  $\sigma_{pk} / \epsilon_{pk}$

$\sigma_{pk}$  = ultimate strength of concrete for biaxial compression (taken equal to  $f_{cu}$  )



This equation describes the stress strain behaviour of concrete in biaxial compression up to peak strain equal to 0.0025 . Beyond this peak, the equation ceases to be valid due to strain softening of concrete. Since the major effect on the response of under reinforced flexural members is due to cracking, post- peak behaviour of concrete in compression can be safely ignored. Accordingly, in this study the softening of concrete is neglected by assuming perfectly plastic behaviour.

For the numerical model, to allow for a gradual reduction of stiffness and also to overcome the uncertainty always involved in the choice of a single point about which to make an intermediate stiffness reduction , several intermediate loading surfaces may be used. This essentially was what has been done by Bell and Elm<sup>(6)</sup> , and Chen et al <sup>(9)</sup> .

A scheme employing this concept which has been proposed by Johnarry<sup>(41)</sup> is as follows:

The intermediate surface strength  $f_{cc}$  to be used in place of  $f_c$  in the yield surface given by the Eq- (3.38) is defined as:

$$f_{cc} = f_{co} - f_t + \frac{E_c}{E_i} f_t \quad \dots(3.45)$$

subject that  $f_{cc} \geq f_c$

where  $f_{co} = 0.5f_c$

$E_c$  = initial Young modulus of elasticity,

$f_t$  = tensile strength of concrete,

$E_i$  = instantaneous elasticity modulus.

When a yield condition is satisfied from Eq- (3.38), the instantaneous modulus,  $E_i$  , is determined as follows:

$$\text{If } \epsilon_i \leq 0.0025 \quad \Rightarrow \quad E_i = \frac{d\sigma_i}{d\epsilon_i} \quad \text{from Eq- (3.44)}$$

$$\text{If } 0.0025 \leq \epsilon_i \leq 0.0035 \quad \Rightarrow \quad E_i = \frac{f_{cu}}{\epsilon_i}$$

$$\text{If } \epsilon_i \geq 0.0035 \quad \Rightarrow \quad E_i = 0.0$$

(\*) Note that the Eq- (3.44) was further investigated by Tasuji et al<sup>(64)</sup> and was found to represent the behaviour of concrete in both compression and tension.

### A.2.2 – Concrete under tensile forces:

In any well designed under-reinforced concrete structure, the cracking of concrete and tensile yielding of steel reinforcement are the major sources of nonlinearity. In general, two main approaches have been used to model concrete cracking viz the discrete and the smeared crack representation.

To produce a more detailed representation of behaviour it would be necessary to model the discrete nature of cracks and this is not economic or necessary for slabs. In addition the smeared crack representation is more popular because of ease of adoption in numerical work and it doesn't require the alteration of the finite element mesh.

In the smeared crack representation which was used in this model, it is assumed that at the instant of the crack formation, only the normal stress perpendicular to the cracked plane and the shear stress parallel to the cracked direction are released and the other stresses are assumed to remain unchanged.

Before going further into the modeling of crack, we need to define two factors:

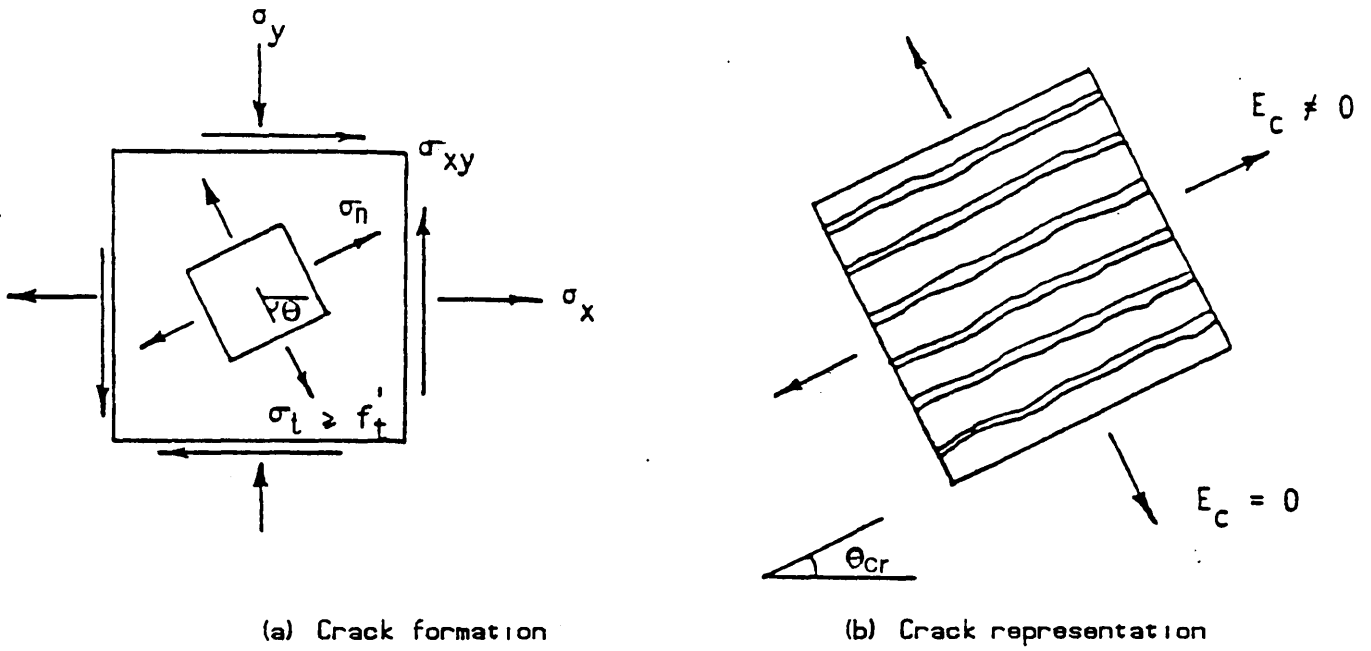
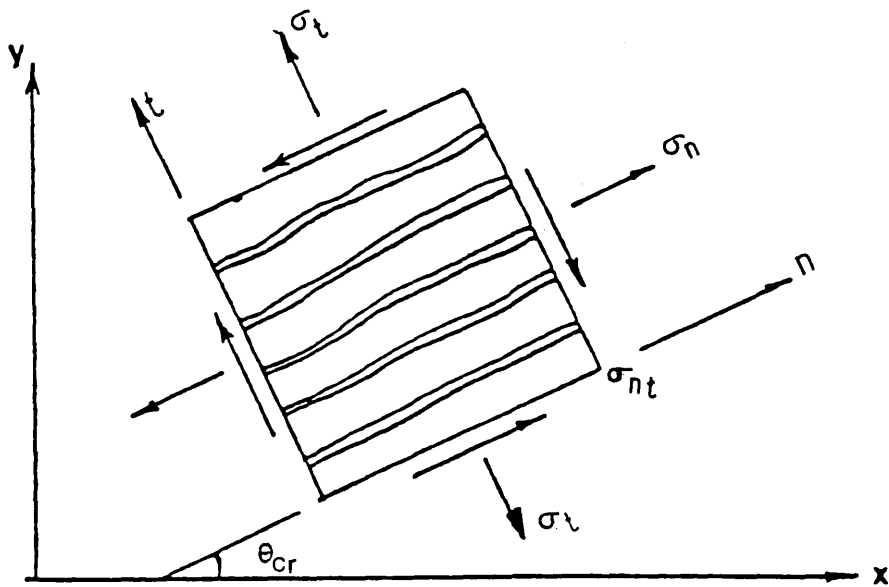


Figure (3-12) Smearred single crack.



Local coordinates for cracked concrete

First— The shear retention:

The surfaces of cracks that develop due to excess tensile stress in concrete are usually rough. When a force  $V$  is applied at a crack, both a tangential sliding  $\delta$  and a normal displacement  $w$  result as shown in Fig— (3.13):

When the normal displacement is restrained by reinforcing bars crossing the crack, axial tensile stresses will develop in the reinforcement, which will then induce compressive stresses in concrete. The resistance to sliding will then be provided by frictional force generated by the compressive stresses in the concrete.

This mechanism of shear transfer in cracked concrete is called the interface shear transfer mechanism. So cracked concrete faces are capable of transmitting shear forces across cracks by friction, and in order to take the shear stiffness of concrete into account, a reduced shear modulus  $G$  equal to  $\beta G$  is retained in the stress—strain relationships.

In the model used in this study, AL. Mahaidi's<sup>(2)</sup> suggestion which states a hyperbolic variation of  $G$  with the friction strain normal to the crack have been used.

$$\beta = \frac{0.4}{\epsilon_f / \epsilon_{cr}} \quad \dots (3.46)$$

where  $\epsilon_{cr} =$  concrete cracking strain  $= f_t / E_c$ ,

and  $\epsilon_{fic} =$  fictitious strain normal to the crack and is given by the following equation:

$$\epsilon_{fic} = \epsilon_x \cdot \sin^2 \theta_{cr} + \epsilon_y \cdot \cos^2 \theta_{cr} - \epsilon_{xy} \cdot \sin \theta_{cr} \cdot \cos \theta_{cr} \dots (3.47)$$

where  $(\epsilon_x, \epsilon_y, \epsilon_{xy})$  are the in—plane strains, and  $\theta_{cr}$  is the angle of crack.

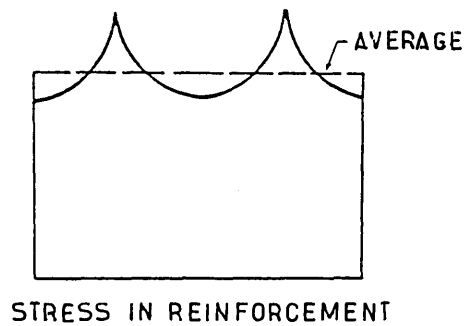
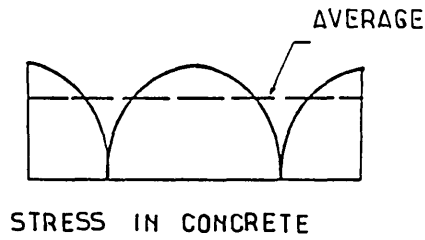
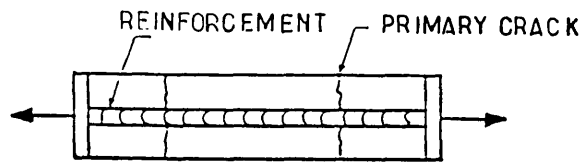


Figure (3-14) Stress distribution in cracked reinforced concrete.

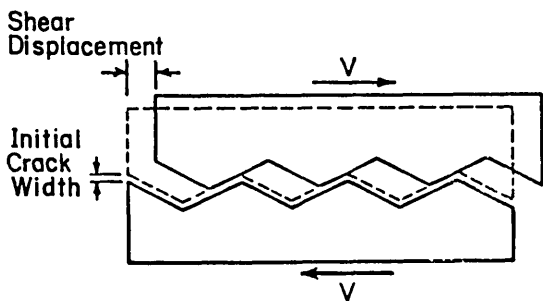


Figure (3-13) Shear retention phenomenon

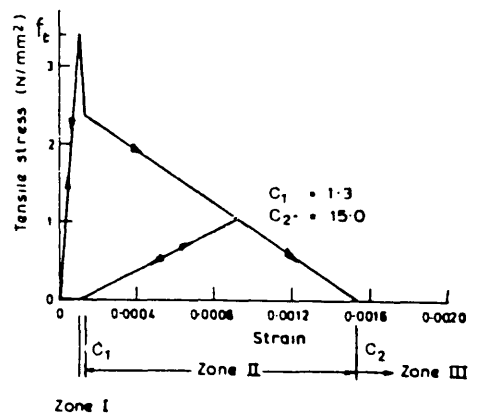


Figure (3-15) Concrete tensile stress-strain curve

Second— Tension stiffening:

Figure (3.14) shows the physical situation in the vicinity of a crack in a reinforced tension member, and indicates that at a crack the full load is carried by the reinforcement only, whereas between the cracks the load is shared between steel and concrete. This ability of concrete between cracks to share the tensile load with the reinforcement is termed tension stiffening.

Tension stiffening is dependent on many factors and is adopted in the model used in this study is the same as given by (13) with reference to Fig— (3.15)

$$\text{Zone I} \quad \epsilon_{cr} < \epsilon \leq C_1 \cdot \epsilon_{cr} \quad \sigma = 2 - \frac{\epsilon}{\epsilon_{cr}} f_t$$

$$\text{Zone II} \quad C_1 \cdot \epsilon_{cr} < \epsilon \leq C_2 \cdot \epsilon_{cr} \quad \sigma = \frac{2 - C_1}{C_2 - C_1} \left[ C_2 - \frac{\epsilon}{\epsilon_{cr}} \right] f_t$$

$$\text{Zone III} \quad \epsilon > C_2 \cdot \epsilon_{cr} \quad \sigma = 0.0$$

where  $f_t$  is the tensile strength of concrete and  $\epsilon_{cr}$  equal to cracking strain (0.0001).

The coefficient  $C_1 = 1.3$  and  $C_2 = 15.0$  were derived empirically to ensure good predictions for slabs and beams (13).

In the smeared crack representation many different theories of handling the formation of cracks and their orientation are used.

In the conventional analysis once a crack forms, it is assumed that the direction  $\theta_{cr}$  remains constant throughout subsequent analysis, and in some cases a crack may close, and a new or secondary crack may be formed, but with the restriction that the second crack is normal to the initial crack direction.

In the other extreme, the concrete is treated as a no-tension material, where the principal tensile stress is brought back to zero at every stage of the analysis.

And thus, it defines at each stage of the analysis a new crack angle without any reference to the previous one. (no-memory crack analysis)

This technique is quite simple due to the fact that no modification in the material stiffness matrix is involved in this type of analysis. It reflects to a certain extent the physical process of cracking but the lack of dependence on the loading path is an approximation and leads in some cases to an early yielding of steel which is presumably due to the release of the concrete tensile stresses.

A better illustration of the problem lies between these two techniques.

In this study the fixed crack analysis has been used by allowing second orthogonal cracks to occur. A theoretical investigation was carried out by L.M.A.Hafez<sup>(1)</sup> on this technique for the analysis of reinforced concrete slabs. She concluded that the fixed crack analysis is suitable when orthogonal reinforcement case is used.

Cracking takes place when the stress at a point satisfies the biaxial criterion, either in tension-tension zone or in tension-compression zone.

In the tension-tension zone, concrete is assumed to crack if the yield criterion in Eq- (3.42) is violated. Two orthogonal cracks may form if both the principal stresses exceed the tensile strength of concrete at the same time.

Under tension-compression states of stress, cracking of concrete takes place if the yield criterion using Eq- (3.41) with  $f_c = f_{cu}$  is violated.

On further loading, concrete which has already cracked in one direction may also

crack in another direction, which must be at an angle of  $30^\circ$  if no-orthogonal cracks are considered. Otherwise, if the concrete is subjected to high compressive stresses parallel to the crack direction, yielding and subsequent crushing of concrete may occur.

#### A.2.2.1 Singly cracked concrete:

The cracked concrete is treated as an orthotropic material with axes of orthotropy parallel and normal to the crack direction. The Poisson effect is neglected due to the lack of interaction between the two orthogonal directions after cracking and the modulus of elasticity of concrete normal to the crack direction is reduced to zero.

Thus, the total stress at the onset of cracking are given with respect to the local coordinate system  $n, t$  (shown Fig- 3.12)

$$\begin{bmatrix} \sigma_n \\ \sigma_t \\ \tau_{nt} \end{bmatrix} = \begin{bmatrix} E_c & 0 & 0 \\ 0 & 0 & 0 \\ 0 & 0 & \beta G \end{bmatrix} \begin{bmatrix} \epsilon_n \\ \epsilon_t \\ \gamma_{nt} \end{bmatrix} \quad \dots (3.48)$$

where  $E_c$  = modulus of elasticity of concrete,

$\beta$  = shear retention factor ( $0 \leq \beta \leq 1$ ),

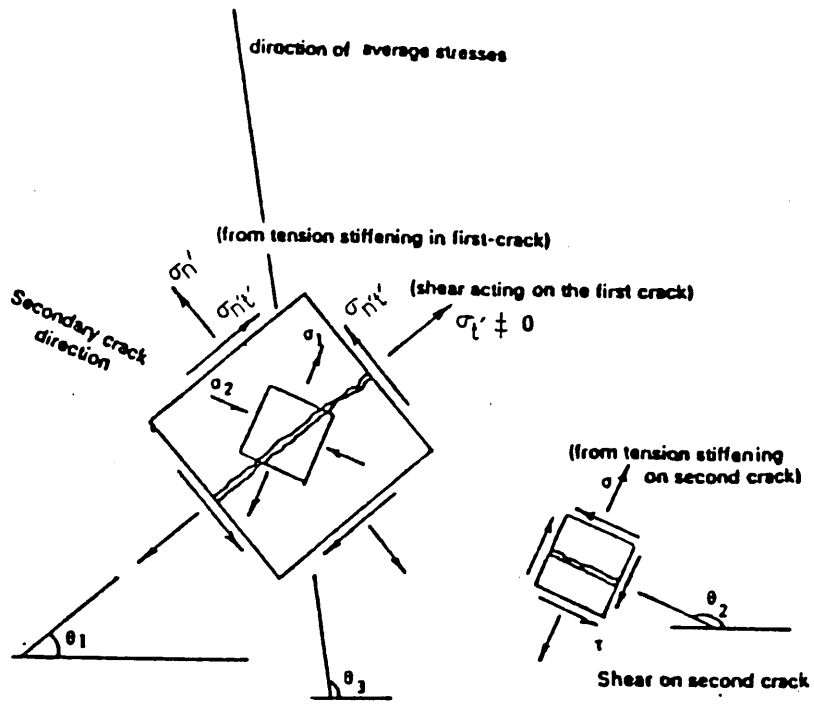
$G$  = shear modulus of concrete.

The diagonal term assumed with direction normal to the crack in the above matrix may then be updated if the tension stiffening is used.

#### A.2.2.2 Doubly cracked concrete:

In the model used in this study, concrete is allowed to crack in two orthogonal directions. Two smeared cracks in two orthogonal directions may develop in a





Formation of secondary crack

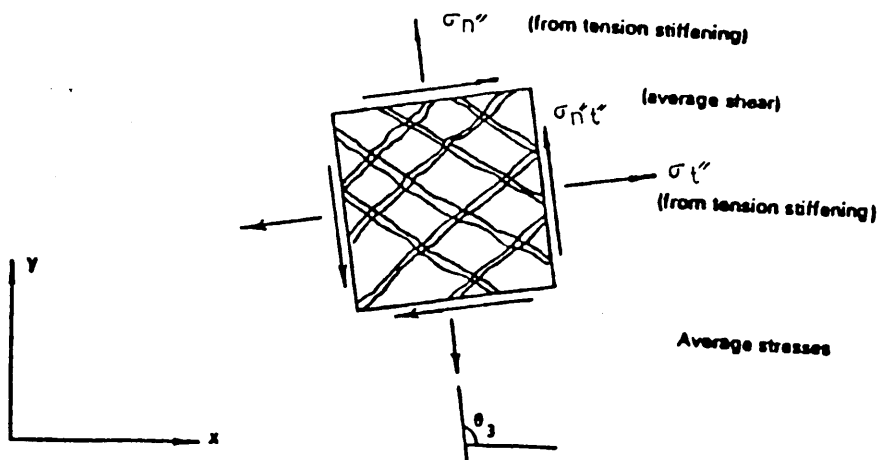


Figure (3-16) Stresses in doubly cracked concrete

referring to the global (X,Y) coordinate systems can be obtained as :

$$\left\{ \sigma \right\} = D^* \left\{ \epsilon \right\} \quad \dots(3.52)$$

An interesting point to notice with fixed crack analysis is the problem arising from retaining  $\tau_{xy}$  on cracked planes ( $\beta$  factor). The fact that  $\tau_{xy} \neq 0$  on the cracked plane implies that it is not a principal plane. Therefore there is a possibility of the true principal plane not coinciding with the assumed crack plane. Consequently, the angle of crack is not necessarily at right angle to the previous one, and thus the hypothesis made earlier that we allow only another set of smeared cracks normal to the initial ones, is violated.

#### B- Steel :

Figure (3.17) shows three possible representation of reinforcement :

- (1) Distributed : The steel is assumed to be distributed over the concrete element, with a particular orientation  $\alpha$ . A composite concrete-reinforcement constitutive relation is used in this case, as explained in sec- (3.3.3.1) assuming full bond. A stiffness matrix is built for the distributed steel separately then added to the stiffness matrix due to concrete to form the global stiffness matrix of an element.
- (2) An embedded representation may be used in connection with higher order isoparametric concrete elements. The reinforcement bar is considered to be an axial member built into the isoparametric element such that its displacements are consistent with those of the element.
- (3) A discrete representation of the reinforcement, using one dimensional elements, has been most widely used. Axial force members, or bar links, may

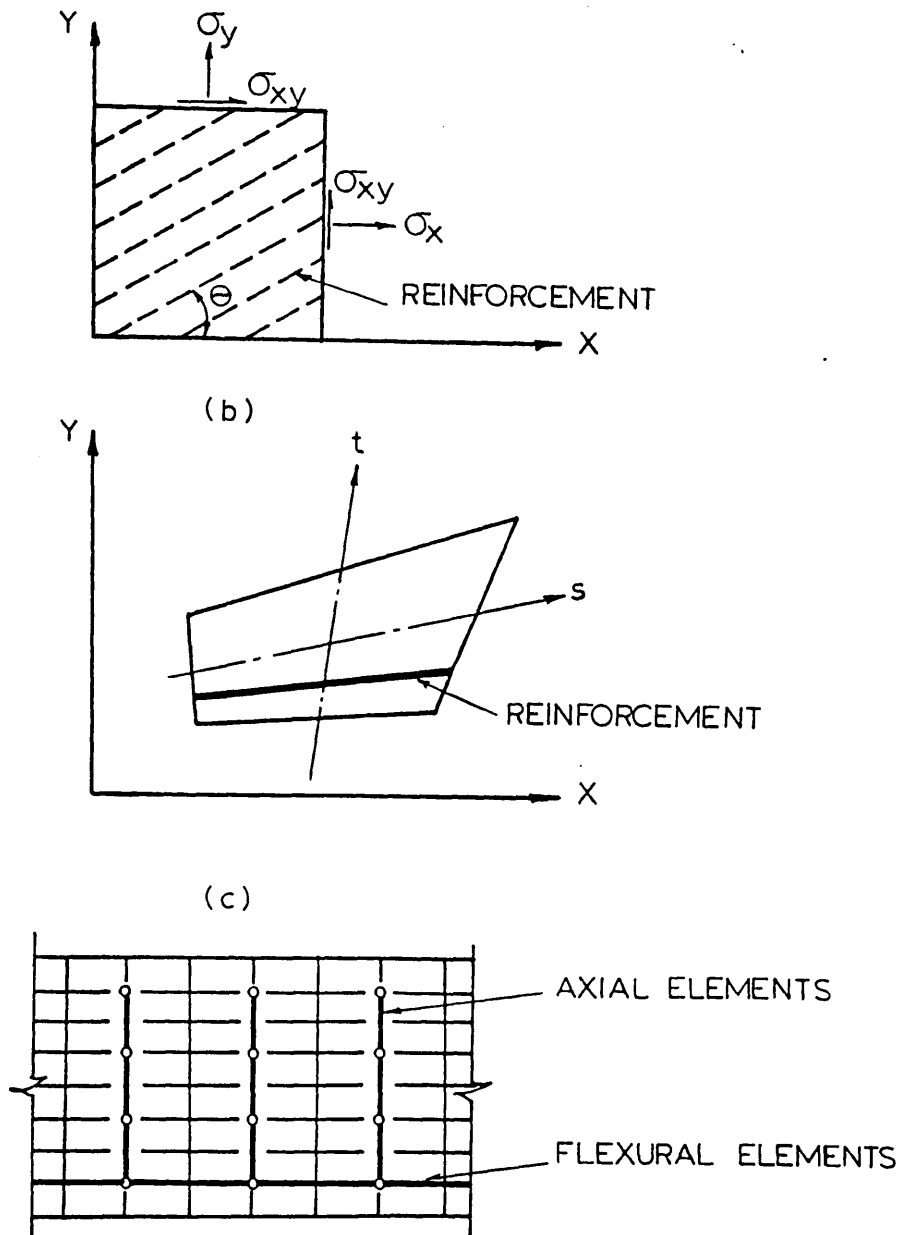


**Figure (3-17) Alternative representation of steel**

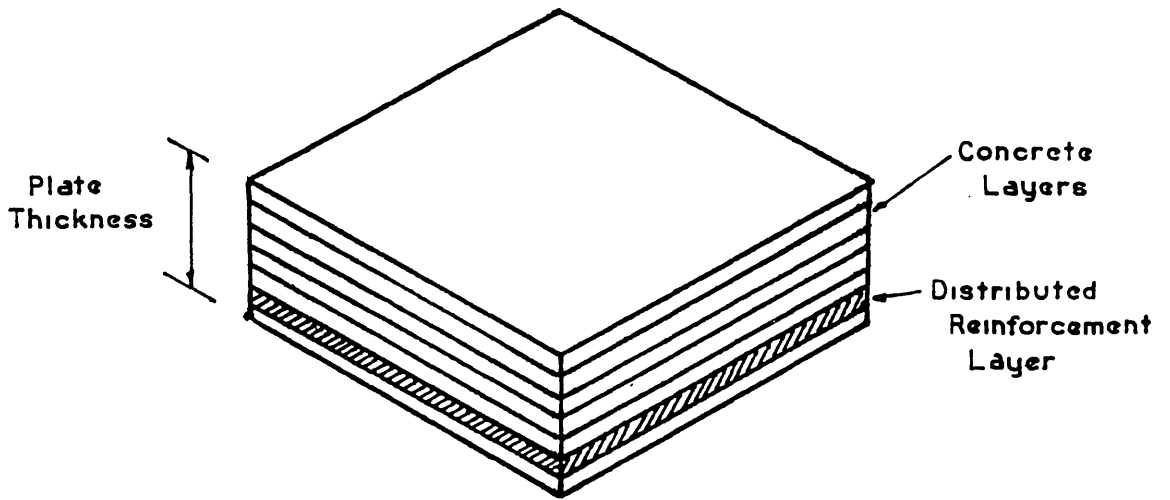


Figure (3-18) Layered plate bending element

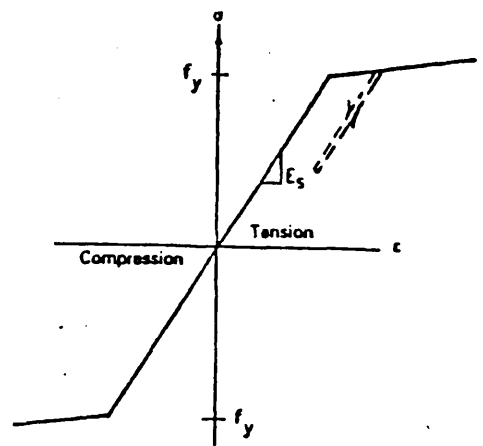
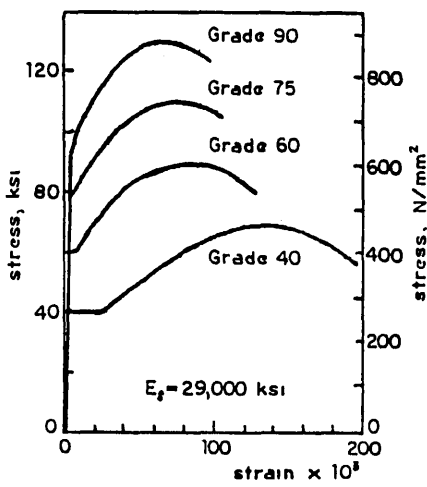


Figure (3-20) Idealized stress-strain curve for steel

Figure (3-19) Typical strain curves for steel

be used and assumed to be pin connected with two degrees of freedom at nodal points. In some cases the one-dimensional reinforcement elements are easily superimposed on a two-dimensional finite element mesh.

As mentioned, for surface-type structural members such as plates in which bending may be important, a layered finite element scheme shown in Fig- (3.18) is usually adopted. This permits the inclusion of the steel at the proper level in the surface element. A distributed representation is used for the layer containing the reinforcement. This is particularly valid for slabs where the reinforcement is uniformly spread over the whole surface or in bands which may be visualized by finite element meshes. Consequently, in this study the steel reinforcement is smeared into equivalent steel layer with uniaxial properties. A typical stress-strain curve for steel reinforcing bar, loaded monotonically in tension, is shown in Fig- (3.18), and the idealization taken in this model is shown in Fig- (3.19).

An elastic-plastic behaviour with possible strain hardening is assumed. The incremental elastic stress-strain relationship is given by:

$$\Delta\sigma = E_s \cdot \Delta\epsilon \quad \dots(3.53)$$

and when the uniaxial steel stress reaches its yield value  $f_y$ , the incremental elastic-plastic stress-strain relationship takes the form:

$$\Delta\sigma = E_s [ 1 - E_s / (E_s + H) ] \cdot \Delta\epsilon \quad \dots(3.54)$$

in which H is the strain hardening parameter for steel, and  $E_s$  is the elastic modulus for steel material.

### 3.3.3.3 Solution of the nonlinear problem :

Since there are a number of different conditions for the two constituent materials of the plate, it is evident that a step-by-step solution procedure is required.(Fig- 3.6b)

The present model uses a modified version of the mixed procedure , where a load is applied in increments and the solution at that load is obtained iteratively until equilibrium is satisfied to a specific accuracy.

Thus the nonlinear stiffness equation :

$$F = K. \delta \quad \dots(3.55)$$

where  $K$  = stiffness matrix , and  $\delta, F$  = displacement and load respectively.

is solved by a succession of linear approximations.

The stiffness matrix is updated at the first iteration for first increment and subsequent load increments at iteration number 2, 5, 8, 11, 15 and 20 , so that the nonlinear effects are reflected more accurately in the stiffness matrix. As the stiffness matrix is not updated at each iteration, economies in computation are gained. As additional measure of economy, only the stiffness matrix of the layer where yielding has occurred within the element is updated and added to the element stiffness using the direct access file.

### 3.3.3.4 Solution procedure :

The solution procedure remains almost the same as the one described in the first section of this chapter.

### 3.3.3.5 Convergence criterion :

Layer program uses the following criterion to check the convergence of the solution which is based on the force norms :

$$\frac{\left( \sum_{i=1}^N [F_{u,i}^i]^2 \right)^{0.5}}{\left( \sum_{i=1}^N [R_i]^2 \right)^{0.5}} 100 \leq \text{tolerance}$$

where N is the total number of nodal points of non-zero displacement in the structure, r denotes the iteration number,  $F_{u,i}$  is the residual force at the  $i^{\text{th}}$  displacement and  $R_i$  is the total external applied load at the  $i^{\text{th}}$  displacement.

### 3.3.4 Conclusion :

The nonlinear finite element model just reviewed, which is based on the layer approach, has been tested using experimental data and good agreement between the predicted behaviour and the experimental results was reported.<sup>(1)</sup>

CHAPTER FOUR :

ELASTO- PLASTIC STRESS FIELD

4.1 Introduction:

In the first section of the previous chapter a reliable finite element program was presented. In this chapter, the direct design approach using the non- elastic stress field will be examined. In particular the effect of using non- elastic stress field on the distribution of the moments of resistance ( $M_x^*, M_y^*$ ) over the slab which will be examined.

In order to analyse in detail this effect, some numerical experiments were conducted using the Mindlin program.

4.2 Description of the analysis:

The design procedure used in this study is dependent on the finite element program (Mindlin) described, and can be summarized as follows:

- (1) The geometric details, material properties and the design loads are used as input data for the program. The program performs an elasto- plastic analysis on the slab using Von- Mises criterion. The analysis establishes the stress distribution ( $M_x, M_y, M_{xy}$ ) at each increment of the design load.
- (2) Using the design equations (sect.2.2.3) the required resisting moments are calculated automatically at each increment and at each Gauss point.

The resulting ( $M_x, M_y, M_{xy}$ ) from step one are in equilibrium with the applied incremental load, let it be  $\alpha.P_d$  , where  $P_d$  represents the design load and  $\alpha \geq 1.0$  .



Consequently, in order to obtain a stress field in equilibrium with the design load, the moment triad obtained from (1) should be scaled by a factor which is equal to  $1 / \alpha$ .

As a result of these steps, one will obtain a design moment in accordance with the elastic distribution of the stresses, and a set of alternative design moments in accordance with non-elastic distribution for each degree of plastification.

Note that for each slab analysed with this program, it is required to define its plastic moment  $M_p$  which is used to define the onset of yielding. The plastic moment is given by the maximum value of the "Von- Mises moments" obtained at each Gauss point over the slab using the Eq- (3.18) :

$$M_p = \text{Max} \left\{ M \text{ (Von- Mises)} = \left[ M_x^2 + M_y^2 - M_x \cdot M_y + 3 \cdot M_{xy}^2 \right]^{\frac{1}{2}} \right\}$$

over the whole slab.

where  $(M_x, M_y, M_{xy})$  are the elastic moment triad.

#### 4.3 Analysis and results:

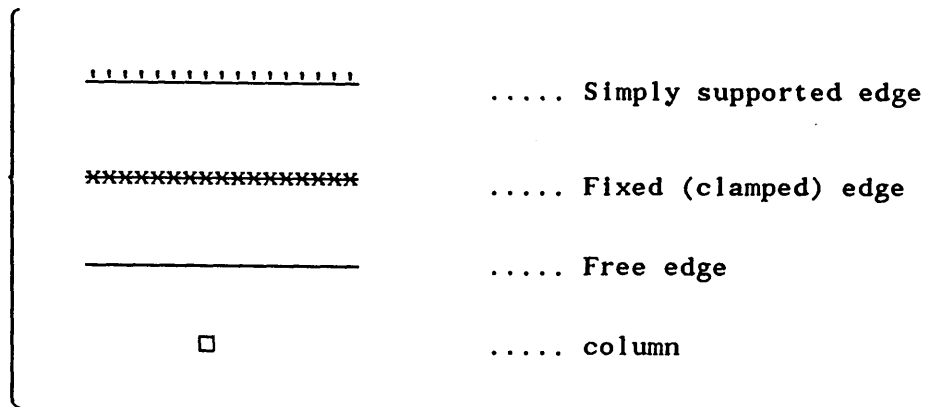
A series of slabs with various boundary conditions and differing aspect ratios were investigated by the technique described in the previous section.

The slabs were all analysed under a uniformly distributed lateral load. Table (4.1) summarizes the cases considered, and gives the results obtained.

The different levels of plasticity spread are shown in figure (4.1) for a typical slab. The results for the design moments  $(M_x^*, M_y^*)$  are plotted in figures (4.3) to (4.6), and here only some typical results are presented.

The results for the moment volumes which represent the total volume of reinforcement (both at top and at bottom) over the structural element to sustain the design load, given by this analysis have been plotted in figure (4.2).

In all the figures the following convention has been taken:



For general use, the results had been expressed in a nondimensional form. The sign convention for the moments is that those causing tension on the underside of the slab are positive.

#### 4.4 Discussion of results:

##### 4.4.1 – Load deflection curve:

Figure (4.1) shows a typical load– deflection curve obtained from elasto– plastic analysis (Mindlin program). This curve is used to compute the different degrees of plasticity or in other terms the percentage of plasticity spread over the slab. The scaling factor is automatically given by the load– increment corresponding to each degree of plasticity considered as shown in the figure.

In the present study, the following convention is adopted:

At the onset of yielding the zero percent (0 %) degree of plasticity is assigned, and at the fully plastic stage (ultimate load reached by the analysis), hundred percent (100%) of plasticity is assigned. Then from these definitions, the different degrees of plasticity are calculated in consequence.

#### 4.4.2 – Table (4.1) and Figures (4.2):

The table (4.1) gives the results obtained for total design moment volume by using stress values at various levels of plasticity. The last column of each table shows the (Elastic – Elasto–Plastic)moment volume to elastic moment volume ratio. Figures (4.2a) to (4.2c) show the variation of the moment volume as the degree of plasticity is increased.

##### a– case of simply supported: (SLB.1.)

Figure (4.2a) for the case of SLB.1.A and SLB.1.B, show little variation of the moment volume with various levels of plasticity.

For the case of SLB.1.C the variation of the moment volume remains insignificant up to 60% of plasticity spread then it starts to grow up very smoothly until reaching + 6% at 80% of plasticity spread.

In the case of SLB.1.D the variation of the moment volume shows an increase in the moment volume as the degree of plasticity grows until reaching + 15% at 84% of plasticity spread.

##### b– case of fixed edge:

In this case, we notice a considerable increase in the moment volume for SLB.2.B and SLB.2.C . The change in the moment volume is dramatically increased in the case of SLB.2.D , where it reaches 50.46% at the level of 93.65% of plasticity spread.

When plasticity spreads to the edges, the rotation at the edge is not zero. However, the present analysis assumes that the edge rotations equal zero at any stage of loading.

Some possible schemes to overcome this problem were proposed such as by W.Duncan and T.Johnarry<sup>(21)</sup> but this is still far from complete and further work needs to be done in this specific area.

The case of clamped edge slabs will not be considered further in this study.

c— case of SLB.3: (Three sides simply supported, one side free)

In this case the variation of the moment volume with the degree of plasticity is negligible.

#### 4.4.3 Isometric views:

Figure (4.3a) shows the distribution of the bottom design moment  $M_x^*$  over the slab as a function of the degree of plasticity spread.

The important points which can be seen from this figure are :

(i) The peak shown at the corner of the slab or the peak shown at the centre of the plate, tend to flatten as the degree of plasticity spread goes up.

At the corner for example, the maximum design moment as shown in Table (4.2a) has decreased by 15.4% at a level of plasticity of 17.5% and by 30.43% at a level of 70% of plasticity spread from the elastic stress field case.

One important practical advantage of using non elastic stress field is that it leads to more convenient layout of bars. For example the area covered by the design moment at the corner has grown considerably as shown in the Table (4.2a) , where for the case of elasto— plastic stress field at a level of 52.5% is about 15 times the area covered by the design moment given by the elastic stress field.

The same phenomenon is repeated at the centre of the slab, but here the design moment has increased slightly as the degree of plasticity goes up , an average of 2% was recorded.

This is due to the fact that in a simply supported slab the twisting moment  $M_{xy}$  is very large at the corners and in consequence the yielding starts in this region of the slab. Since we have noticed a decrease in the design moment at the corners of the plate so the increase of the design moment at the centre of the plate was expected in order to maintain equilibrium.

However, the design moment (the one corresponding to non elastic stress field ) is covering a broader area of the slab than the one corresponding to elastic stress

field.(as shown in the Table 4.2b)

(ii) the distribution of the design moment tends to be more uniform as the degree of plasticity spread goes up.

(iii) Apart from the practical benefit of having a uniform distribution of the design moment, there is another advantage which is related to the choice of bar diameters and their distribution to envelope the theoretical design moment. Obviously, the more uniform distribution pattern the more close envelope of the design moment can be obtained.

Figure (4.3b) shows the distribution of the top reinforcement over the slab as a function of the degree of plasticity spread. Similar conclusions are drawn from this figure and also they can be easily checked through the figures (4.4) to (4.6) where two other types of slab have been analysed.

#### 4.5 Conclusions:

On the basis of the results presented, the following conclusions can be drawn:

(1) The use of non elastic stress field with the direct design method has shown to have some advantages which are:

(i) The design moment distribution is more uniform.

(ii) the peaks are smoothed out with the consequence that congestion of reinforcement is avoided. Thus, it is also easier in this case to approximate the design moment envelope by a real choice of reinforcing bars.

(iii) In some cases and in some particular regions of a slab the design moment reduces considerably and remains largely constant over a broad area of the slab.

(2) As far as the economy on steel areas is concerned, the difference between the moment volumes obtained by using elastic stress field and by non elastic stress field in the direct design method is not significant.

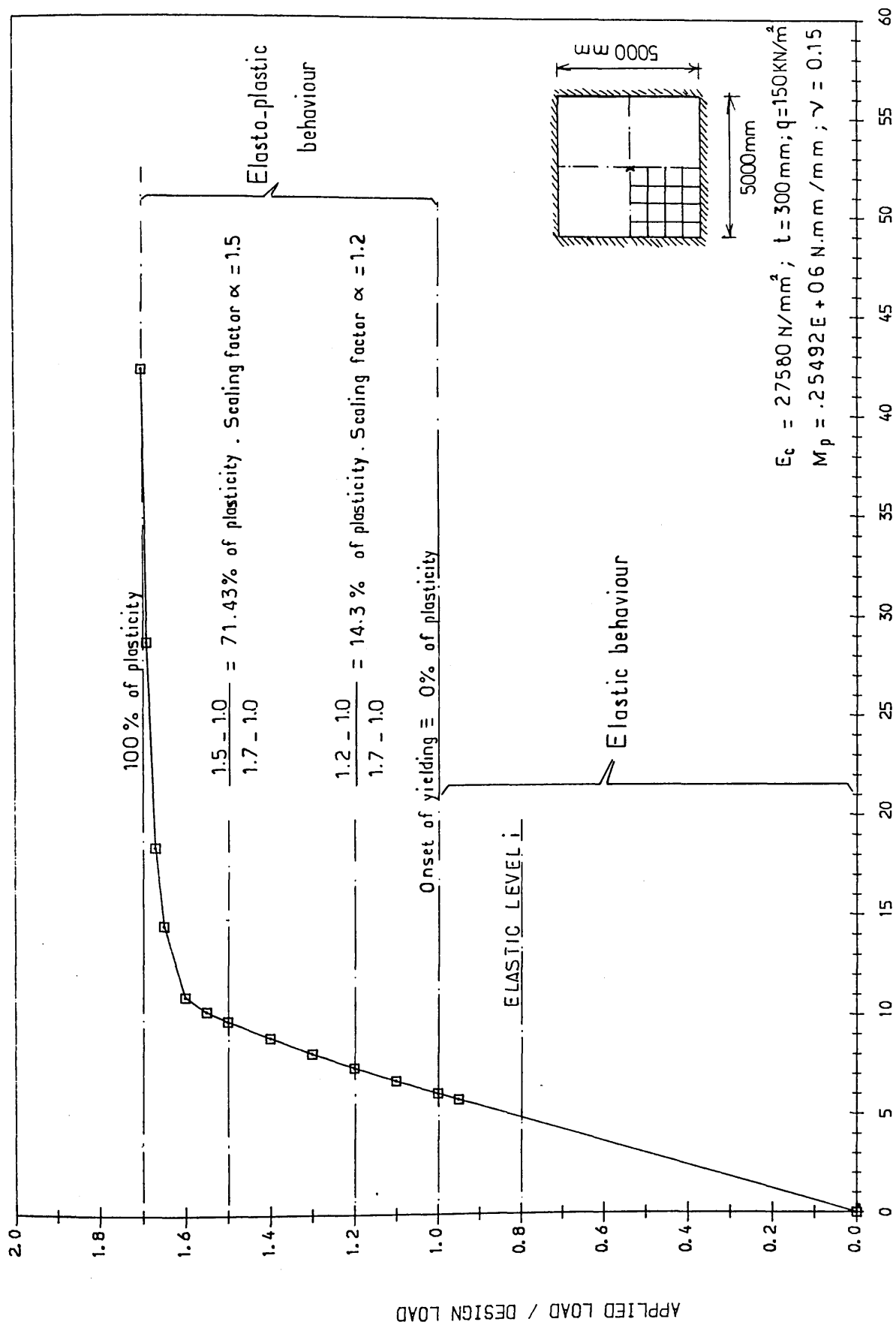


FIG. (4.1) LOAD-DEFLECTION CURVE FOR A GIVEN SLAB  
ANALYSED THROUGH MINDLIN PROGRAM

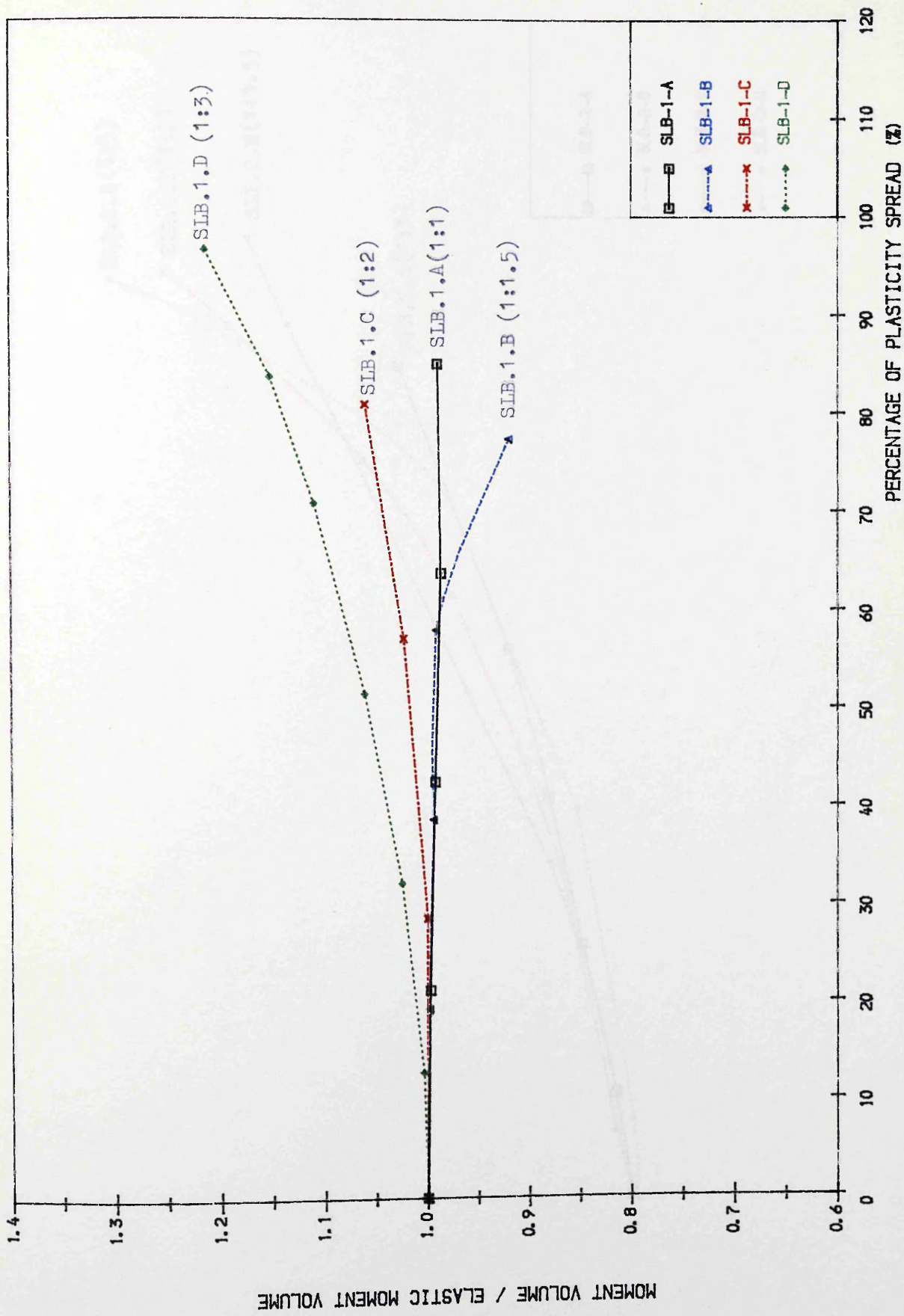


FIG-(4.2A) RATIO OF THE MOMENT VOLUME AT DIFFERENT LEVELS OF PLASTICITY SPREAD FOR VARIOUS ASPECT RATIOS OF THE SLABS-1-

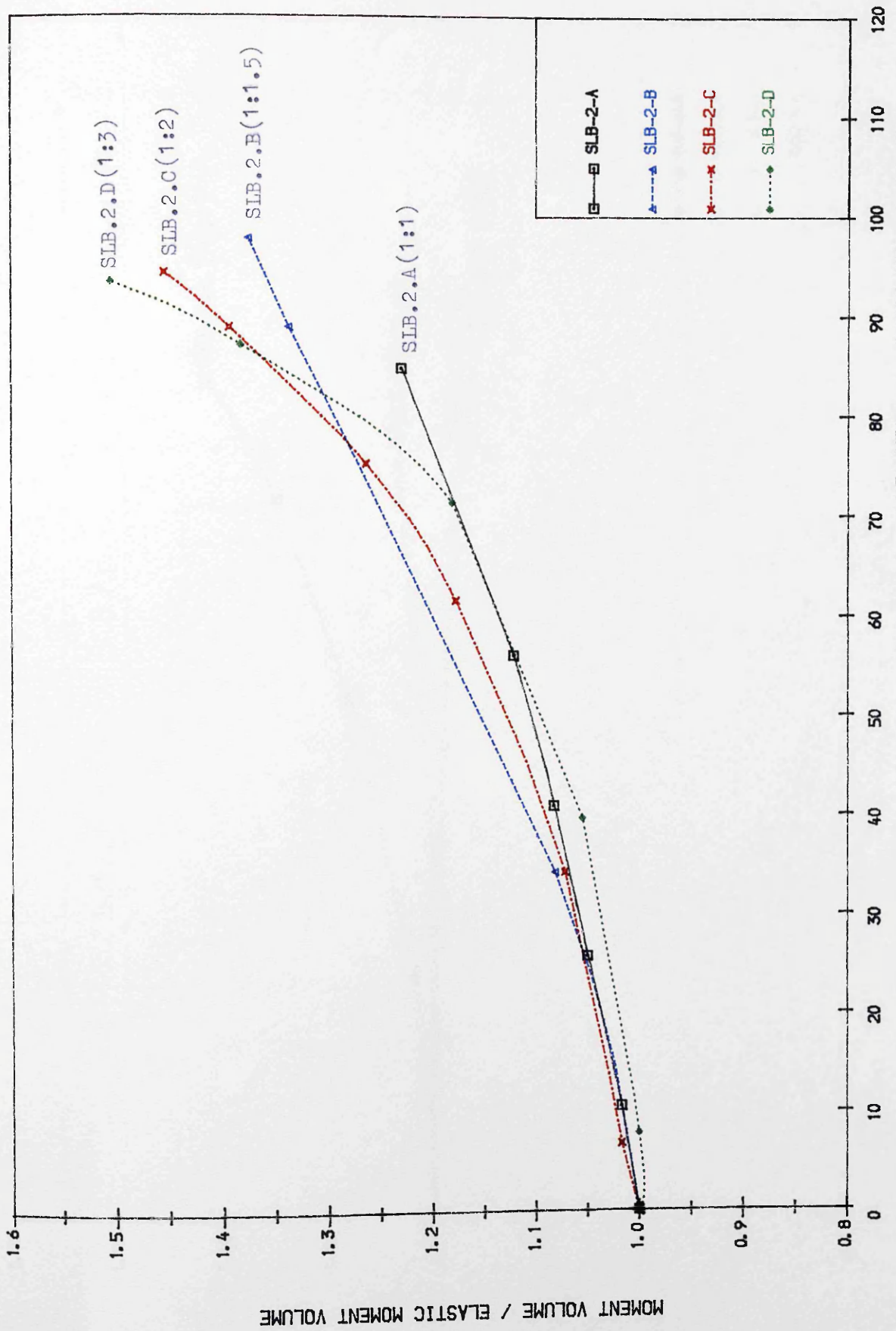


FIG- (4-2B) RATIO OF THE MOMENT VOLUME AT DIFFERENT LEVELS OF PLASTICITY SPREAD FOR VARIOUS ASPECT RATIOS OF THE SLABS-2-



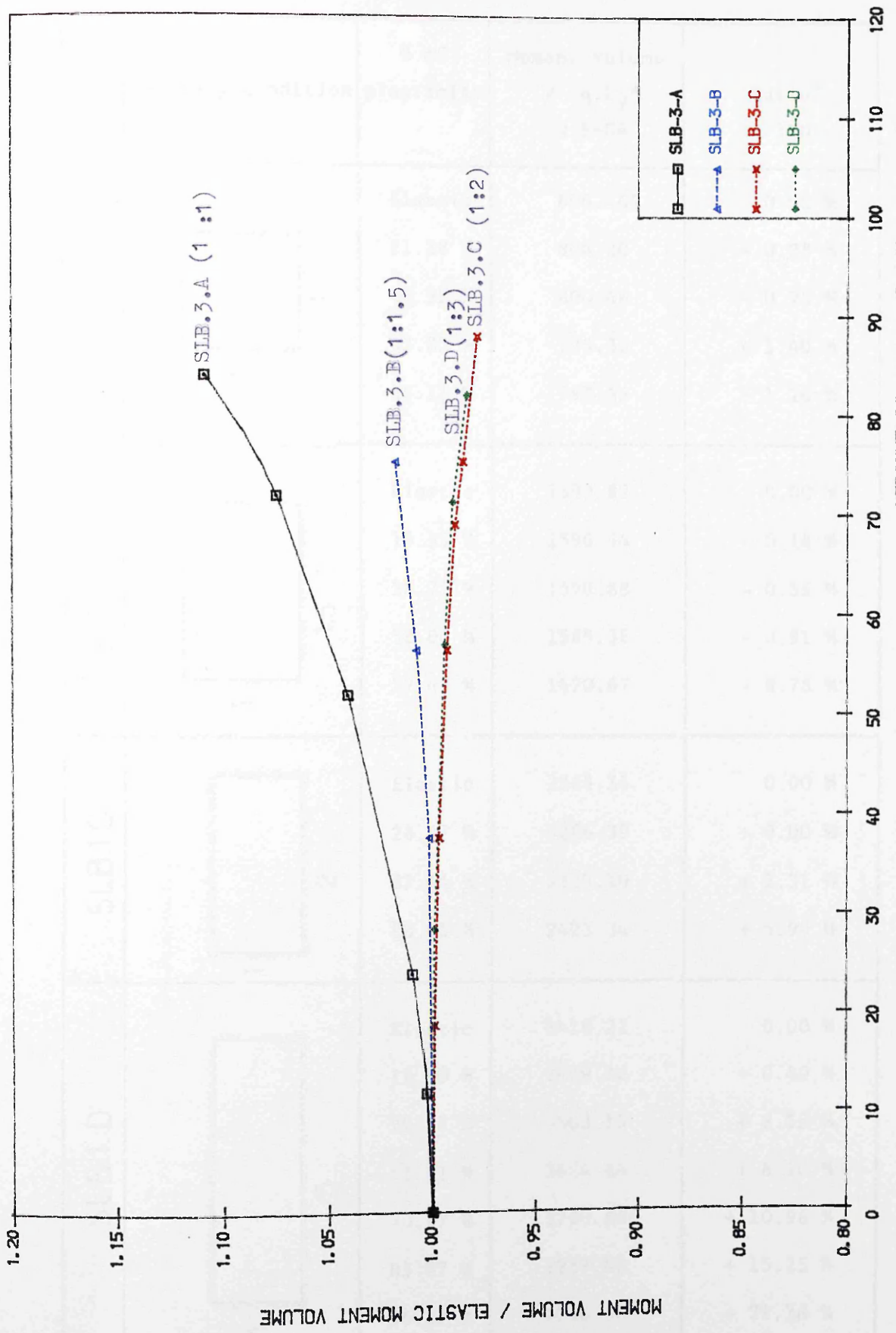


FIG- (4-2C) RATIO OF THE MOMENT VOLUME AT DIFFERENT LEVELS OF PLASTICITY SPREAD FOR VARIOUS ASPECT RATIOS OF THE SLABS-3-

TABLE (4-1)

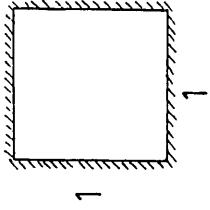
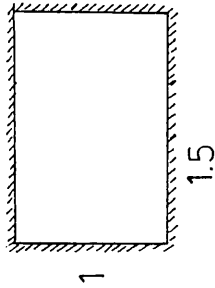
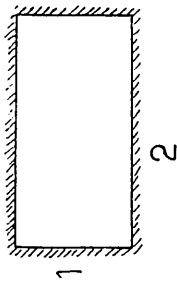
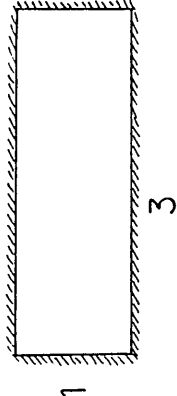
Case	Boundary condition	% of plasticity	Moment Volume / $q \cdot L_y^4$ $\times E+04$	Ratio* $\times 100$
SLB.1.A		Elastic	806.464	0.00 %
		21.28 %	804.20	- 0.28 %
		42.55 %	800.46	- 0.75 %
		63.83 %	795.36	- 1.40 %
		85.11 %	797.66	- 1.10 %
SLB.1.B		Elastic	1599.82	0.00 %
		19.35 %	1596.94	- 0.18 %
		38.71 %	1590.88	- 0.56 %
		58.06 %	1585.38	- 0.91 %
		77.42 %	1470.67	- 8.78 %
SLB.1.C		Elastic	2286.34	0.00 %
		28.57 %	2286.39	+ 0.00 %
		57.14 %	2339.10	+ 2.31 %
		80.95 %	2423.34	+ 5.99 %
SLB.1.D		Elastic	3416.22	0.00 %
		12.90 %	3429.76	+ 0.40 %
		32.26 %	3503.19	+ 2.55 %
		51.61 %	3624.64	+ 6.10 %
		70.97 %	3790.80	+ 10.96 %
		83.87 %	3937.06	+ 15.25 %
96.77 %	4146.50	+ 21.38 %		

TABLE (4-1) continued

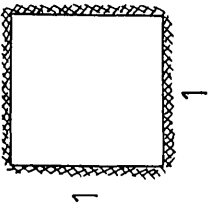
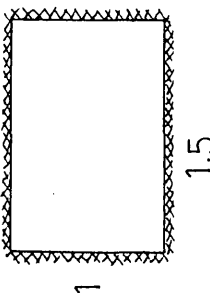
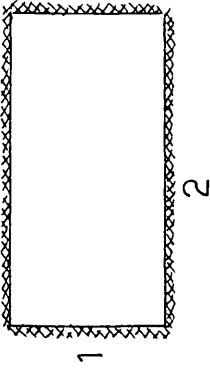
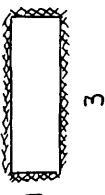
Case	Boundary condition	% of plasticity	Moment Volume / $q \cdot L_y^4$ x E+04	Ratio* x 100
SLB.2.A		Elastic	303.00	0.00 %
		10.61 %	308.17	+ 1.71 %
		25.76 %	318.07	+ 4.97 %
		40.91 %	328.25	+ 8.33 %
		56.06 %	340.09	+ 12.24 %
		84.85 %	372.74	+ 23.02 %
SLB.2.B		Elastic	574.48	0.00 %
		34.25 %	620.98	+ 8.18 %
		61.64 %	725.38	+ 26.30 %
		89.04 %	768.24	+ 33.76 %
		97.92 %	790.24	+ 37.59 %
SLB.2.C		Elastic	786.86	0.00 %
		6.85 %	800.16	+ 1.69 %
		34.25 %	843.560	+ 7.20 %
		61.64 %	926.77	+ 17.78 %
		75.34 %	995.00	+ 26.45 %
		89.04 %	1096.87	+ 39.40 %
		94.52 %	1145.22	+ 45.54 %
SLB.2.D		Elastic	1160.67	0.00 %
		7.94 %	1161.18	+ 0.04 %
		39.68 %	1225.07	+ 5.55 %

TABLE (4-1) continued

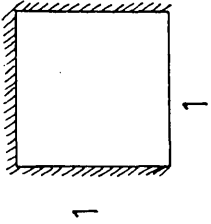
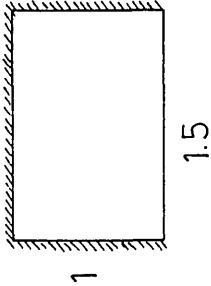
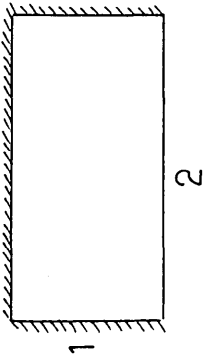
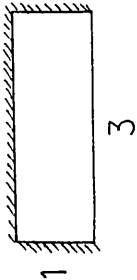
Case	Boundary condition	% of plasticity	Moment Volume / $q \cdot L_y^4$ x E+04	Ratio* x 100
		71.43 %	1370.68	+ 18.09 %
		87.30 %	1605.42	+ 38.32 %
		93.65 %	1746.37	+ 50.46 %
SLB.3.A		Elastic	1154.46	0.00 %
		12.02 %	1157.85	+ 0.29 %
		24.05 %	1166.47	+ 1.04 %
		52.10 %	1201.29	+ 4.06 %
		72.14 %	1241.15	+ 7.51 %
		84.17 %	1280.22	+ 10.89 %
SLB.3.B		Elastic	3637.33	0.00 %
		18.87 %	3631.72	- 0.15 %
		37.74 %	3646.12	+ 0.24 %
		56.60 %	3368.35	+ 0.85 %
		75.47 %	3701.65	+ 1.77 %
SLB.3.C		Elastic	7645.81	0.00 %
		18.87 %	7639.78	- 0.08 %
		37.74 %	7625.70	- 0.26 %
		56.60 %	7595.00	- 0.66 %
		69.18 %	7559.60	- 1.14 %
		75.47 %	7532.51	- 1.50 %
		88.05 %	7475.70	- 2.27 %

TABLE (4.1) continued

Case	Boundary condition	% of plasticity	Moment Volume / $q \cdot L_y^4$ x E+04	Ratio* x 100
SLB.3.D		Elastic	19857.78	0.00 %
		28.57 %	19839.85	- 0.09 %
		57.14 %	19746.03	- 0.57 %
		71.43 %	19668.94	- 0.96 %
		82.14 %	19539.16	- 1.63 %

\* : (Elastic - Elasto-plastic)moment volume / Elastic moment volume

Table (4.2a) Reduction of the peak design moment ( $p^t$ .A Fig- (4.3a) and the increase of the area covered by this design moment.

% of plasticity	Design Moment $M^*$ (units)	Moment ratio* x 100	Area Covered by the Design Moment (A in units)	Area ratio <sup>⊗</sup>
Elastic	15.00	0.00 %	3 x 3 = 9	1.00
17.50 %	≈ 13.00	- 15.38 %	8 x 8 = 64	7.11
35.00 %	≈ 12.00	- 25.00 %	11 x 11 = 121	13.44
52.50 %	≈ 11.10	- 35.14 %	$[11.5]^2 = 132.3$	14.72
70.00 %	≈ 11.50	- 30.43 %	13 x 13 = 169	18.78

\* : (Elasto-plastic - Elastic)design moment / Elasto-plastic design moment

⊗ : (Area covered by elastic / Area covered by elasto-plastic)design moment

Table (4.2b) Reduction of the peak design moment (p<sup>t</sup>.B Fig- (4.3a) and the increase of the area covered by this design moment.

% of plasticity	Design Moment M* (units)	Moment ratio* x 100	Area Covered by the Design Moment (A in units)	Area ratio <sup>⊗</sup>
Elastic	16.00	0.00 %	3 x 3 = 9	1.00
17.50 %	≈ 16.00	0.00 %	5 x 5 = 25	2.78
35.00 %	≈ 16.20	+ 1.25 %	5 x 5 = 25	2.78
52.50 %	≈ 16.50	+ 3.12 %	6 x 6 = 36	4.00
70.00 %	≈ 16.50	+ 3.12 %	8 x 8 = 64	7.11

Table (4.3a) Reduction of the peak design moment (p<sup>t</sup>.A Fig- (4.4a) and the increase of the area covered by this design moment.

% of plasticity	Design Moment M* (units)	Moment ratio* x 100	Area Covered by the Design Moment (A in units)	Area ratio <sup>⊗</sup>
Elastic	12.00	0.00 %	3 x 3 = 9	1.00
28.00 %	≈ 10.20	- 17.65 %	9 x 9 = 81	9.00
46.00 %	≈ 9.50	- 26.32 %	11 x 11 = 121	13.44
60.00 %	≈ 9.50	- 33.33 %	12 x 12 = 144	16.00
82.00 %	≈ 8.50	- 41.18 %	14 x 14 = 196	21.78

\* : (Elasto-plastic - Elastic) design moment / Elasto-plastic design moment

⊗ : (Area covered by elastic / Area covered by elasto-plastic) design moment

Table (4.3b) Reduction of the peak design moment ( $p^t$ .A Fig- (4.4b) and the increase of the area covered by this design moment.

% of plasticity	Design Moment $M^*$ (units)	Moment ratio* x 100	Area Covered by the Design Moment (A in units)	Area ratio <sup>⊗</sup>
Elastic	11.75	0.00 %	2 x 2 = 4	1.00
28.00 %	≈ 10.20	- 15.20 %	6 x 6 = 36	9.00
46.00 %	≈ 9.30	- 26.34 %	10 x 10 = 100	25.00
60.00 %	≈ 8.80	- 33.52 %	[10.5] <sup>2</sup> = 110.3	27.56
82.00 %	≈ 8.00	- 46.87 %	12 x 12 = 144	36.00

Table (4.4a) Reduction of the peak design moment ( $p^t$ .A Fig- (4.5a) and the increase of the area covered by this design moment.

% of plasticity	Design Moment $M^*$ (units)	Moment ratio* x 100	Area Covered by the Design Moment (A in units)	Area ratio <sup>⊗</sup>
Elastic	40.00	00.00 %	2 x 2 = 4	1.00
20.00 %	≈ 40.00	- 00.00 %	4 x 4 = 16	4.00
40.00 %	≈ 35.00	- 14.29 %	4 x 5 = 20	5.00
60.00 %	≈ 32.50	- 23.08 %	6 x 6 = 36	9.00
80.00 %	≈ 30.00	- 33.33 %	7 x 7 = 49	12.25

\* : (Elasto-plastic - Elastic) design moment / Elasto-plastic design moment

⊗ : (Area covered by elastic / Area covered by elasto-plastic) design moment

Table (4.4b) Reduction of the peak design moment ( $p^t$ .A Fig- (4.5b) and the increase of the area covered by this design moment.

% of plasticity	Design Moment $M^*$ (units)	Moment ratio* x 100	Area Covered by the Design Moment (A in units)	Area ratio <sup>⊗</sup>
Elastic	8.00	00.00 %	1	1.00
20.00 %	≈ 8.00	- 00.00 %	1 x 3 = 3	3.00
40.00 %	≈ 7.00	- 14.28 %	1 x 9 = 9	9.00
60.00 %	≈ 6.00	- 33.33 %	1.5 x 8 = 12	12.00
80.00 %	≈ 6.00	- 33.33 %	1.7 x 8 = 13.6	13.60

Table (4.5a) Reduction of the peak design moment ( $p^t$ .A Fig- (4.6a) and the increase of the area covered by this design moment.

% of plasticity	Design Moment $M^*$ (units)	Moment ratio* x 100	Area Covered by the Design Moment (A in units)	Area ratio <sup>⊗</sup>
Elastic	10.60	0.00 %	2 x 2 = 4	1.00
24.00 %	≈ 8.80	- 20.45 %	6 x 14 = 84	21.00
52.00 %	≈ 8.20	- 29.27 %	7 x 15 = 105	26.25
72.00 %	≈ 7.50	- 41.33 %	7 x 26 = 186	45.50

\* : (Elasto-plastic - Elastic)design moment / Elasto-plastic design moment

⊗ : (Area covered by elastic / Area covered by elasto-plastic)design moment



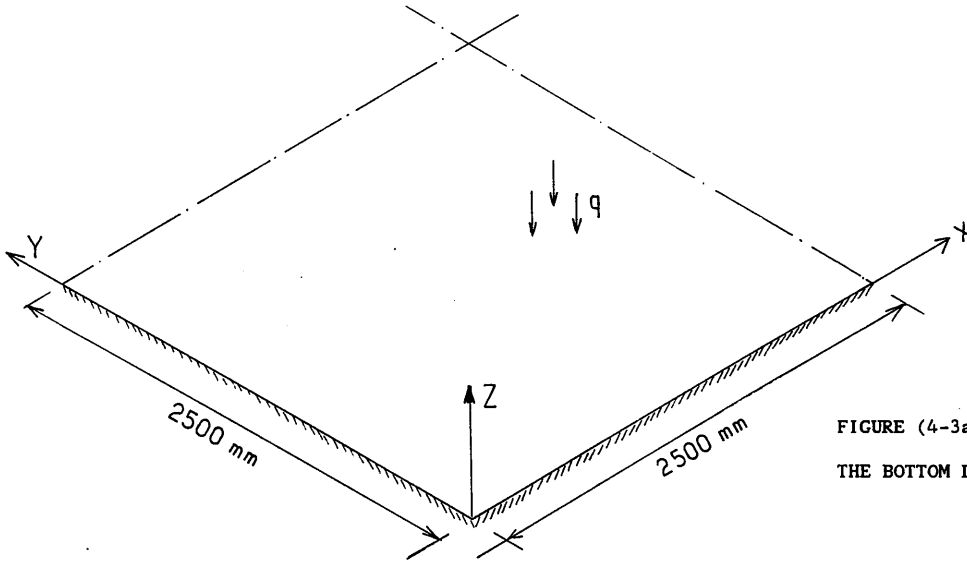
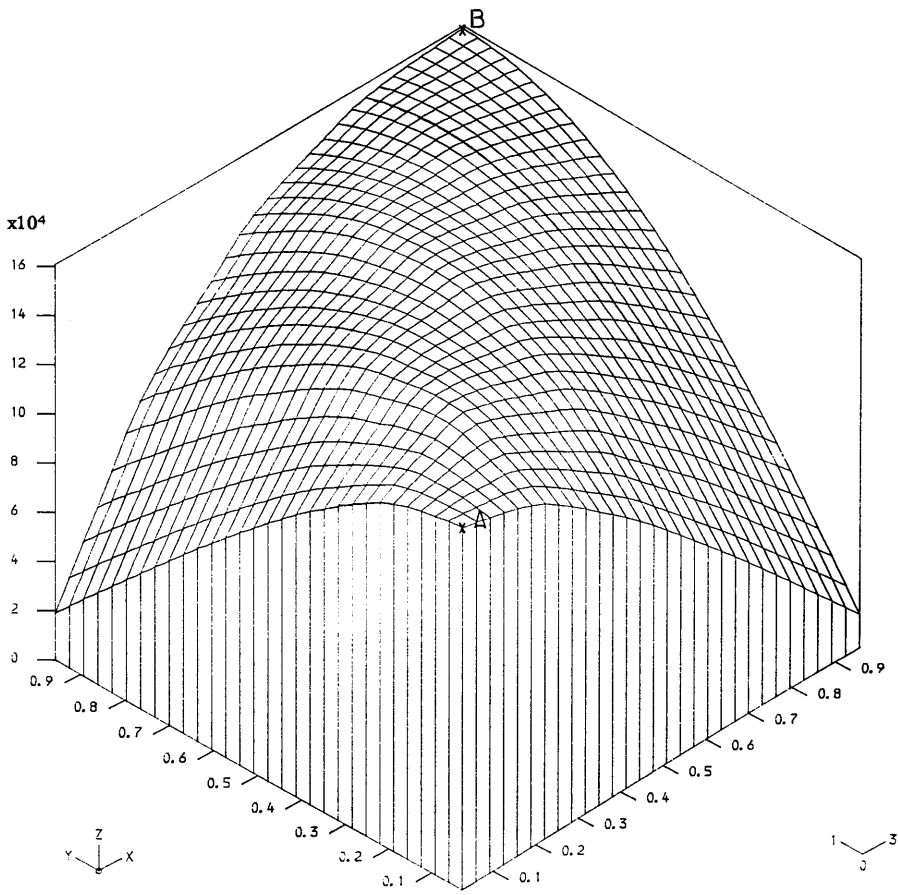
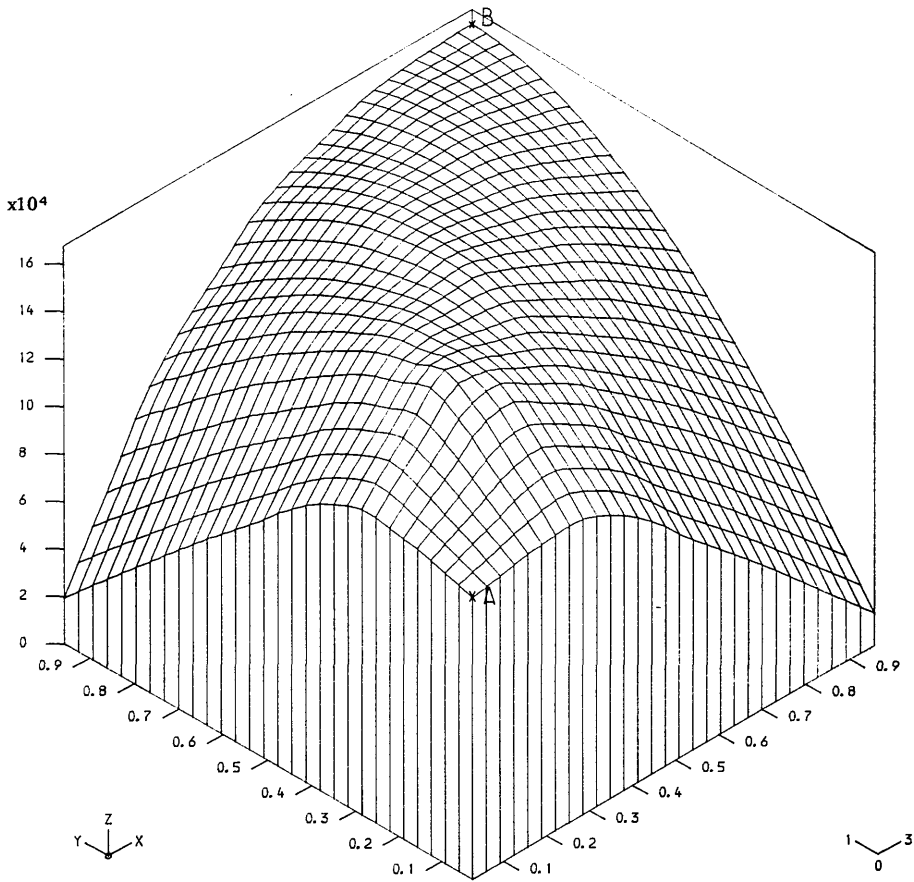


FIGURE (4-3a): DISTRIBUTION OF THE BOTTOM DESIGN MOMENT  $M_{xx}^*$

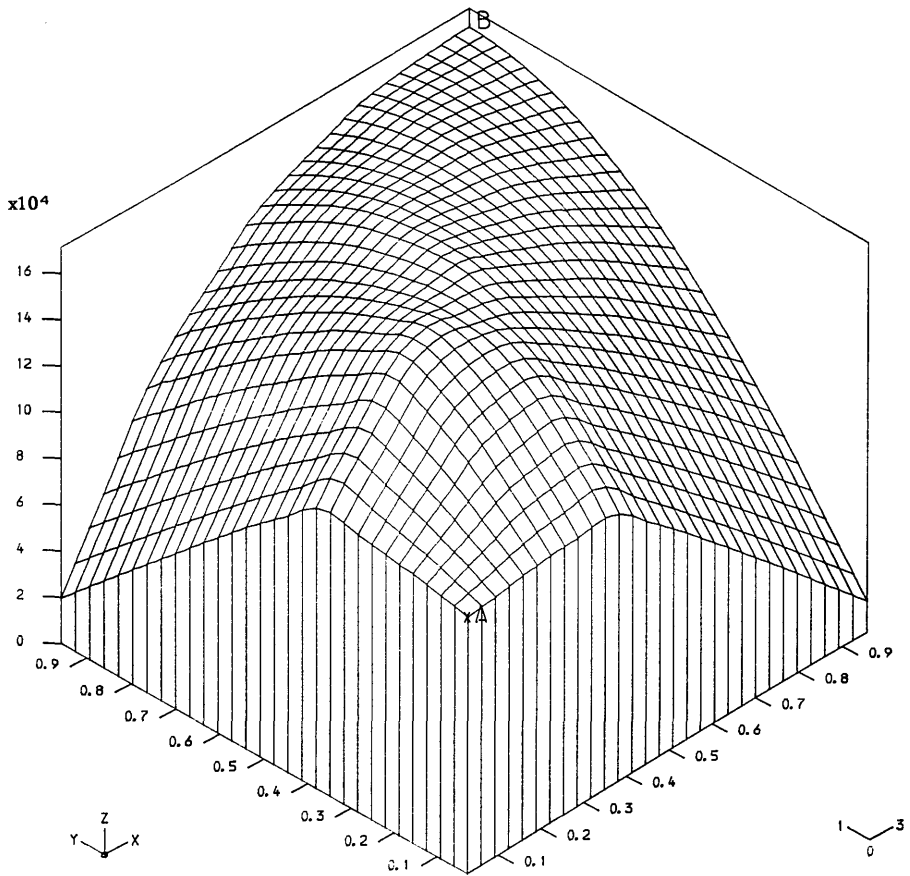
- $q = 0.15 \text{ N / mm}^2$
- $E = 27580 \text{ N / mm}^2$
- $\nu = 0.15$
- $M_p = 254920 \text{ N.mm / mm}$
- $t = 300 \text{ mm}$



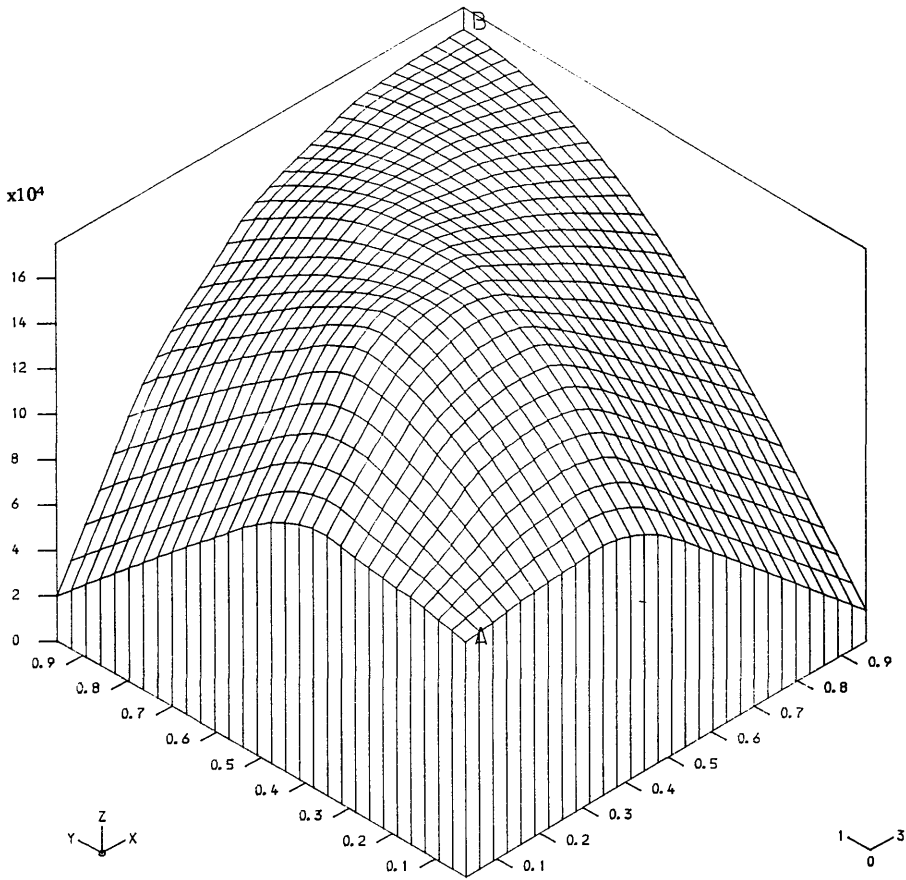
BOTTOM  $M_{xx}^*$  (ELASTIC)



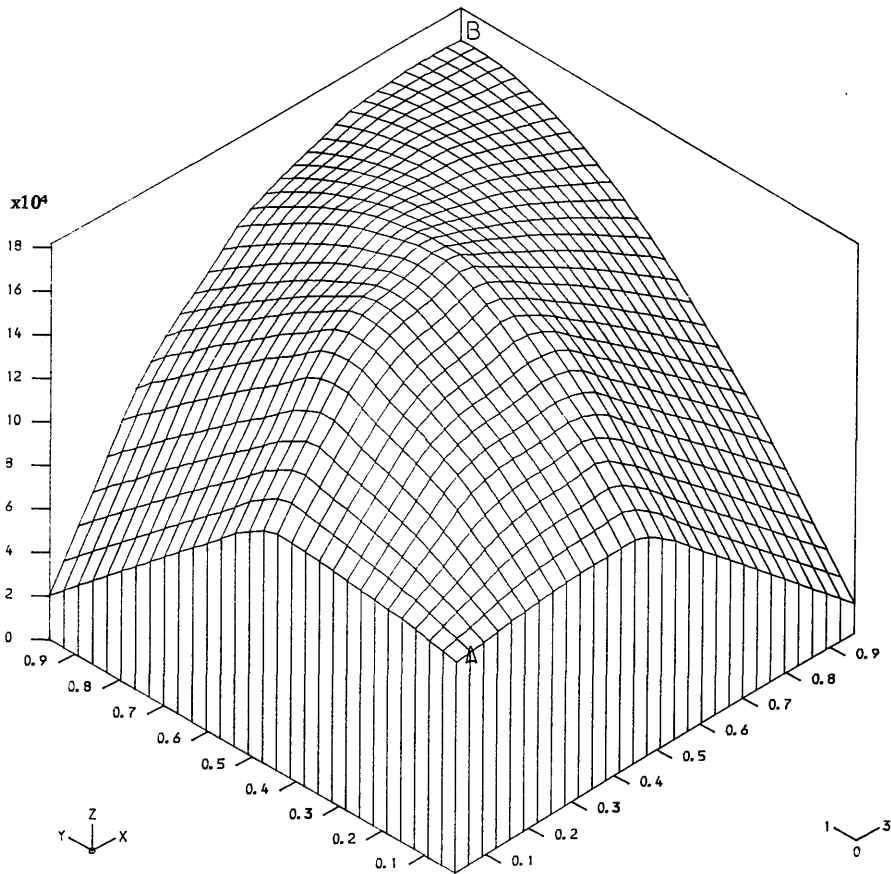
BOTTOM MX\* (17.5% of plasticity)



BOTTOM MX\* (35% of plasticity)



BOTTOM MX\* (52.5% of plasticity)



BOTTOM MX\* (70% of plasticity)

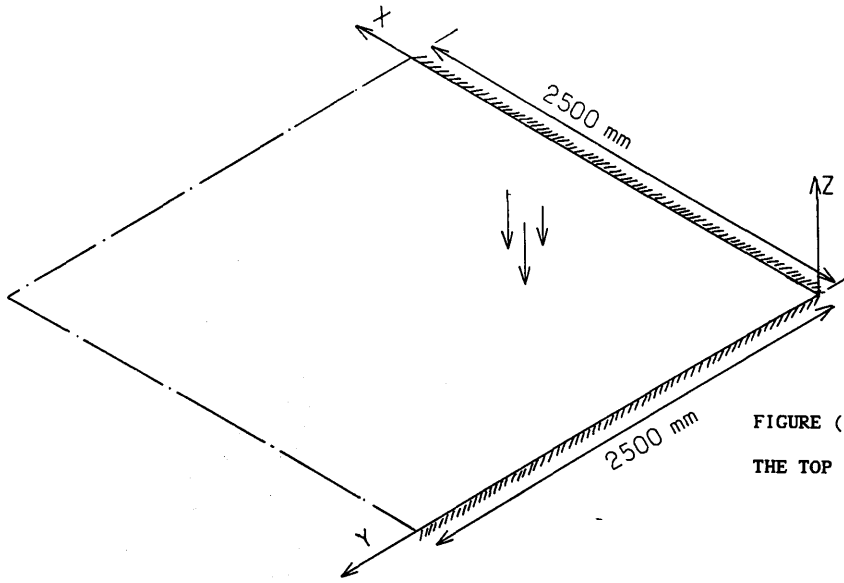
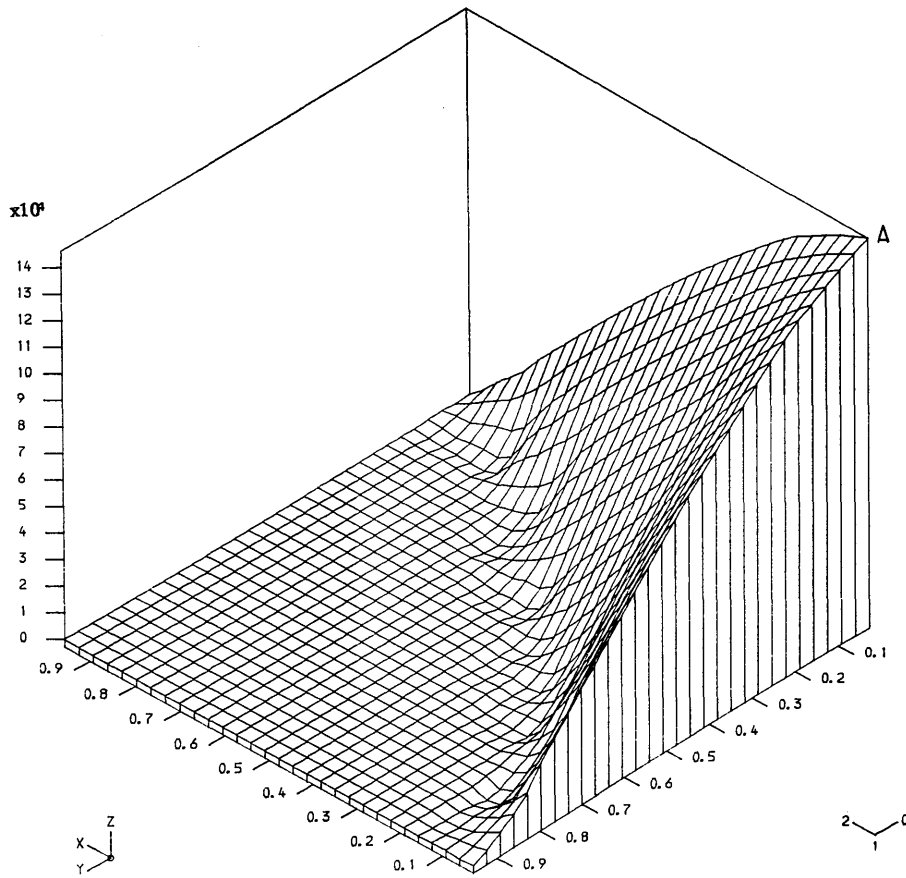
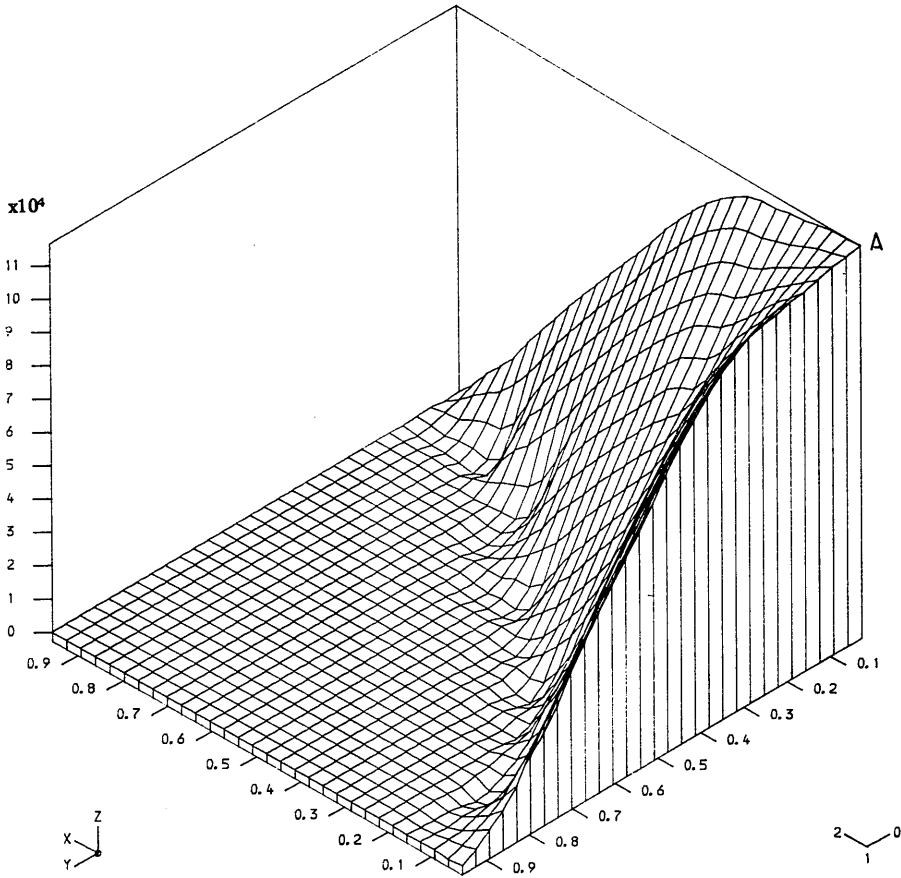


FIGURE (4-3b): DISTRIBUTION OF THE TOP DESIGN MOMENT  $M_x^*$

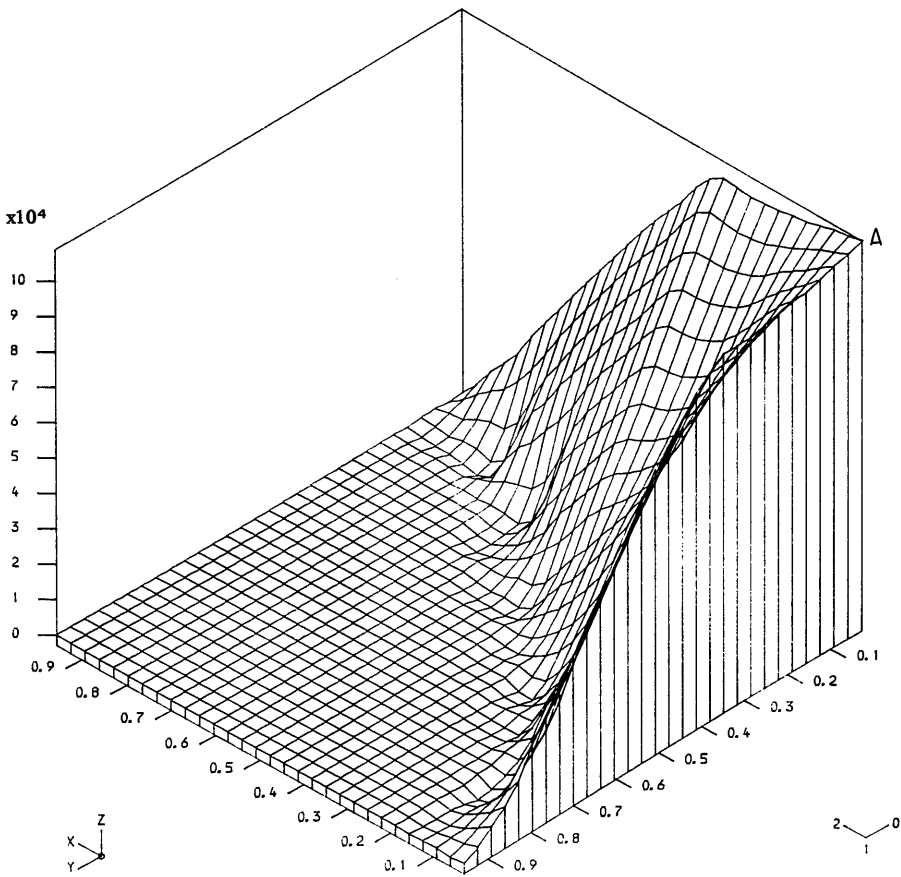
- $q = 0.15 \text{ N / mm}^2$
- $E = 27580 \text{ N / mm}^2$
- $\nu = 0.15$
- $M_p = 254920 \text{ N.mm / mm}$
- $t = 300 \text{ mm}$



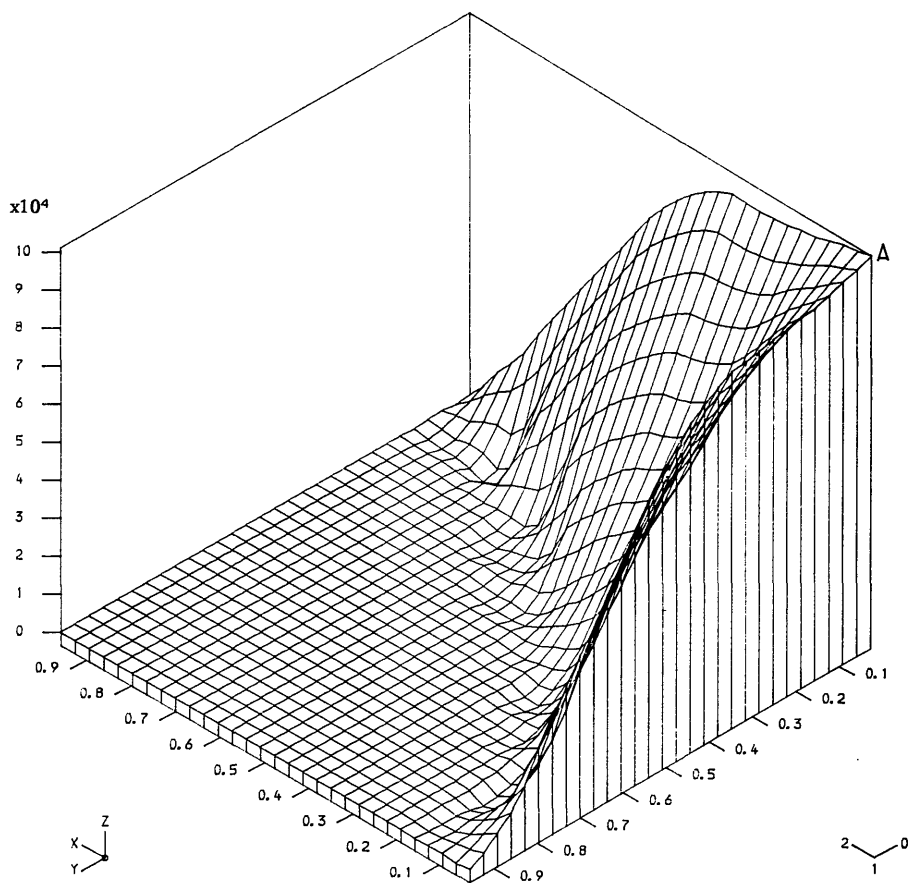
TOP  $M_x^*$  (ELASTIC)



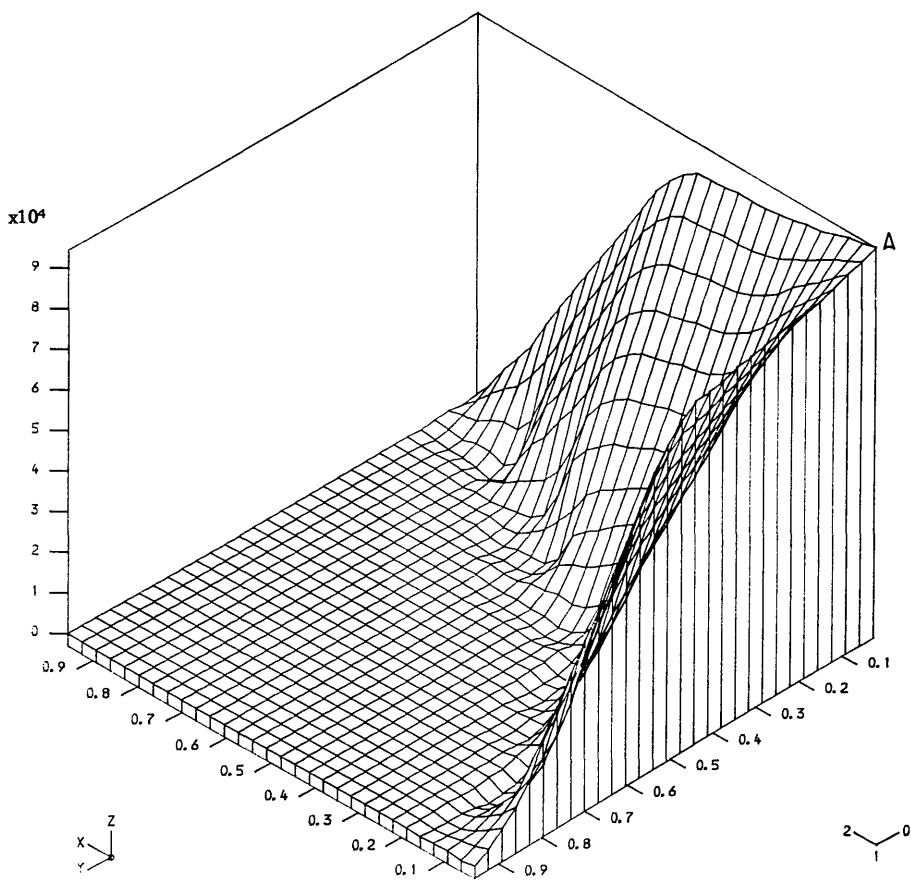
TOP MX\* (17.5% of plasticity)



TOP MX\* (35% of plasticity)



TOP MX\* (52.5% of plasticity)



TOP MX\* (70% of plasticity)

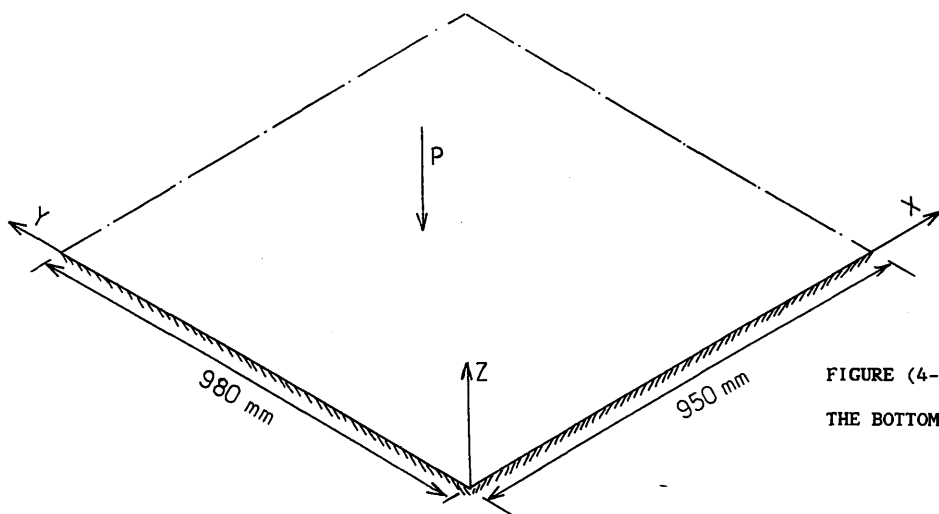
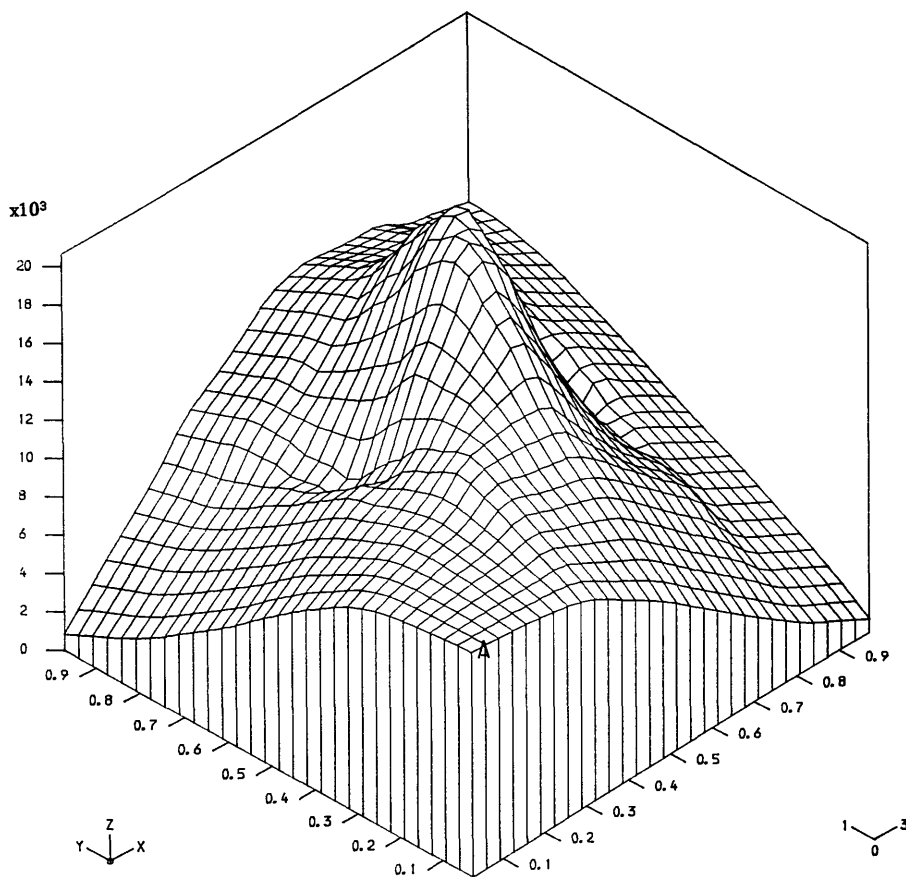
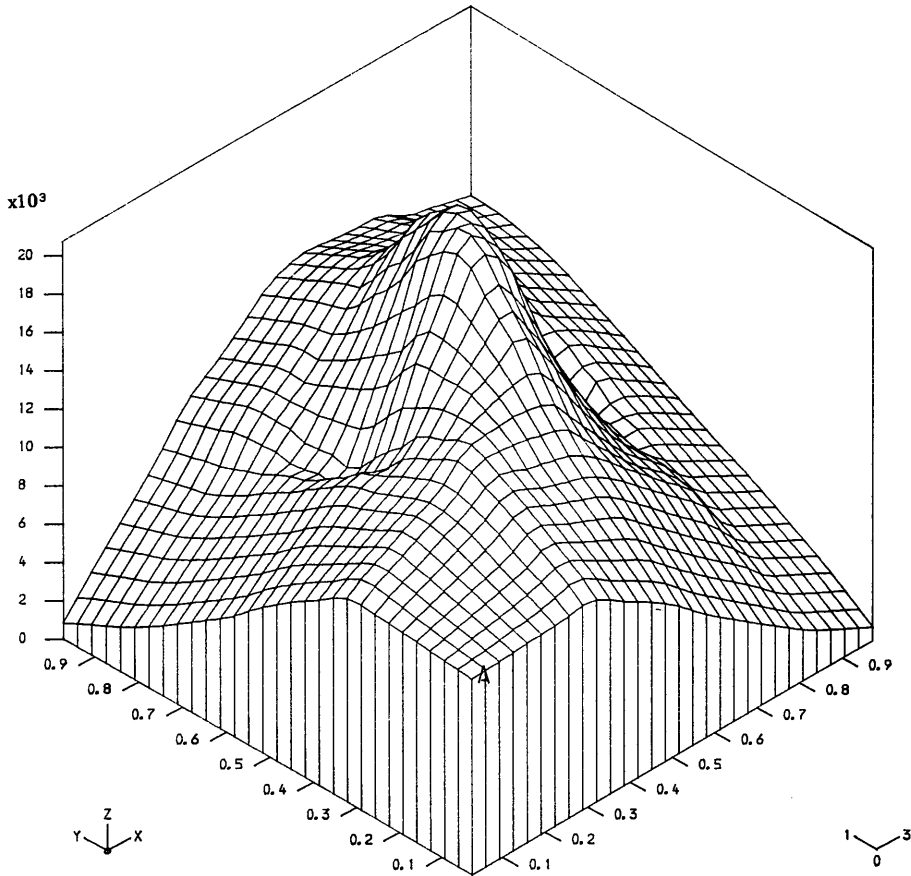


FIGURE (4-4a): DISTRIBUTION OF THE BOTTOM DESIGN MOMENT  $M_{xx}^*$

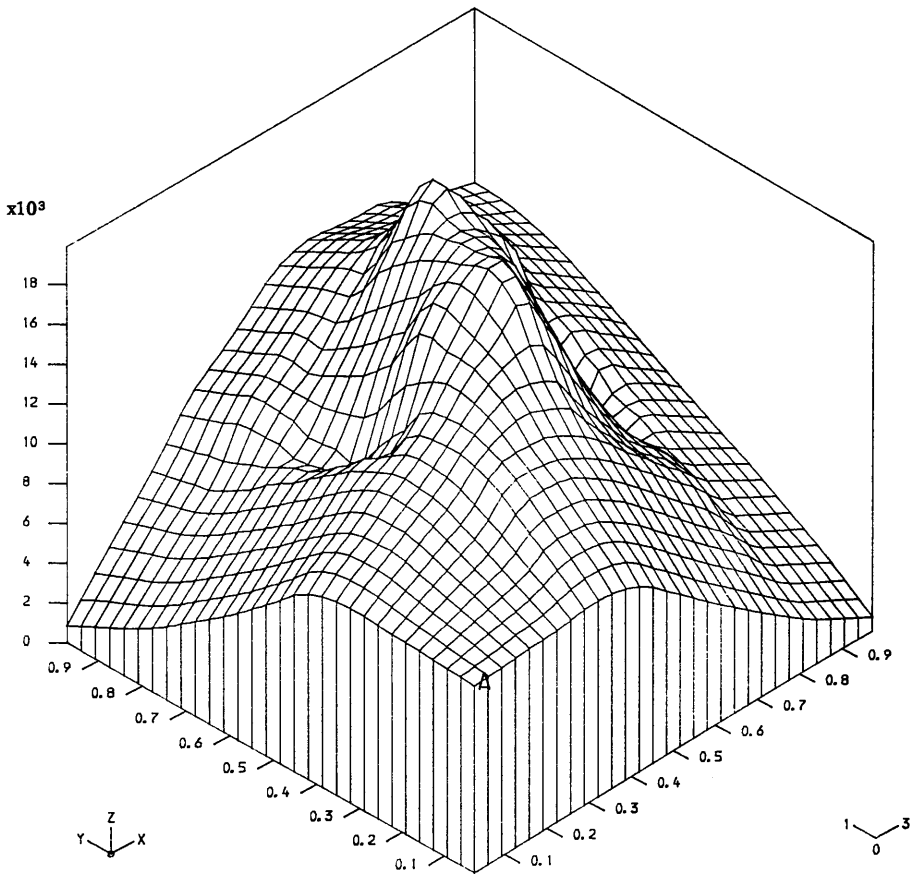
- P - 53325 N
- E - 21500 N / mm<sup>2</sup>
- $\nu$  - 0.15
- $M_p$  - 20422 N.mm / mm
- t - 100 mm



BOTTOM  $M_{xx}^*$  (ELASTIC)

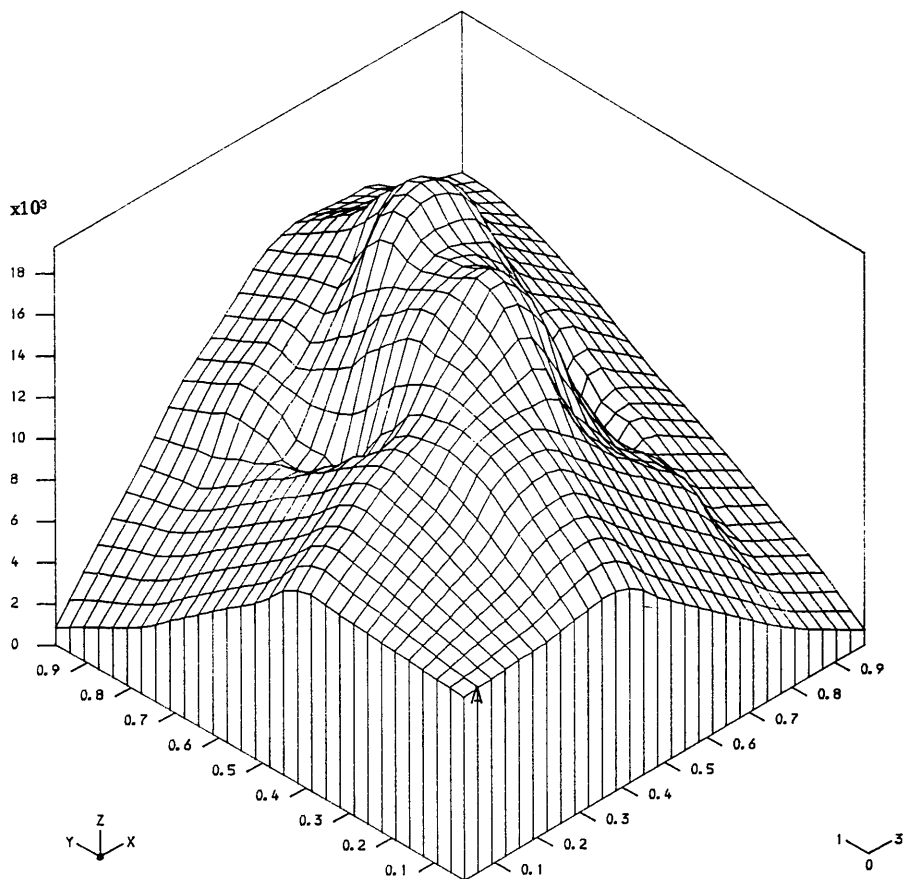


BOTTOM Mx\* (28% of plasticity)

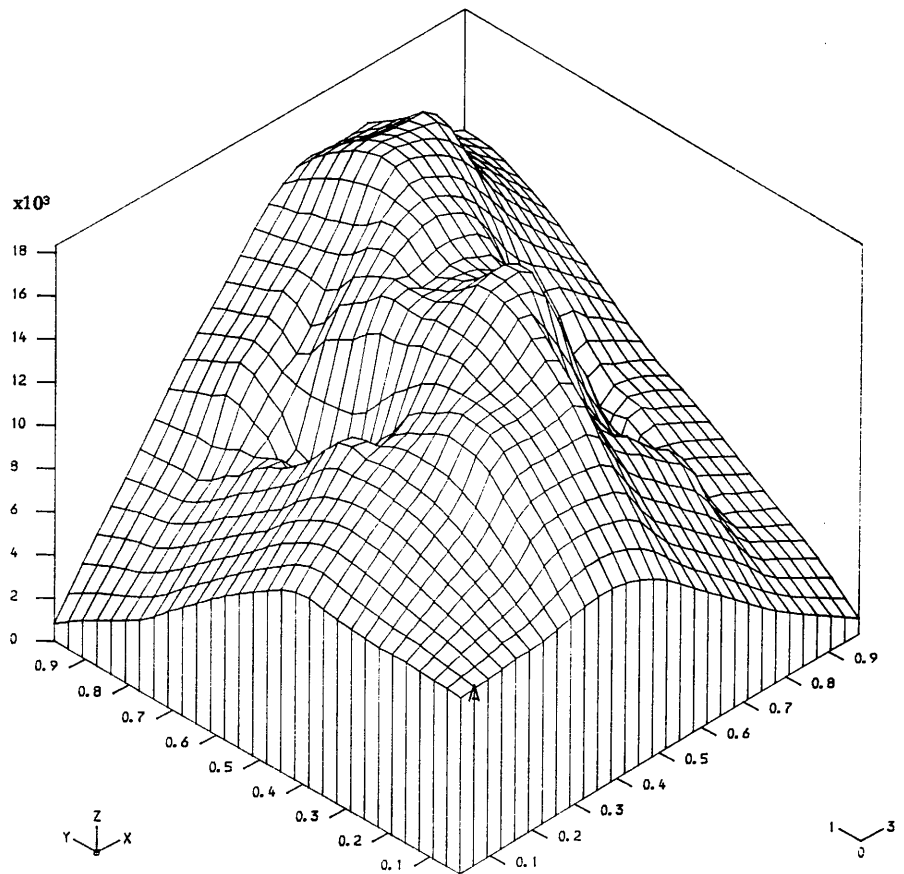


BOTTOM Mx\* (46% of plasticity)





BOTTOM  $M_{x^*}$  (60% of plasticity)



BOTTOM  $M_{x^*}$  (82% of plasticity)

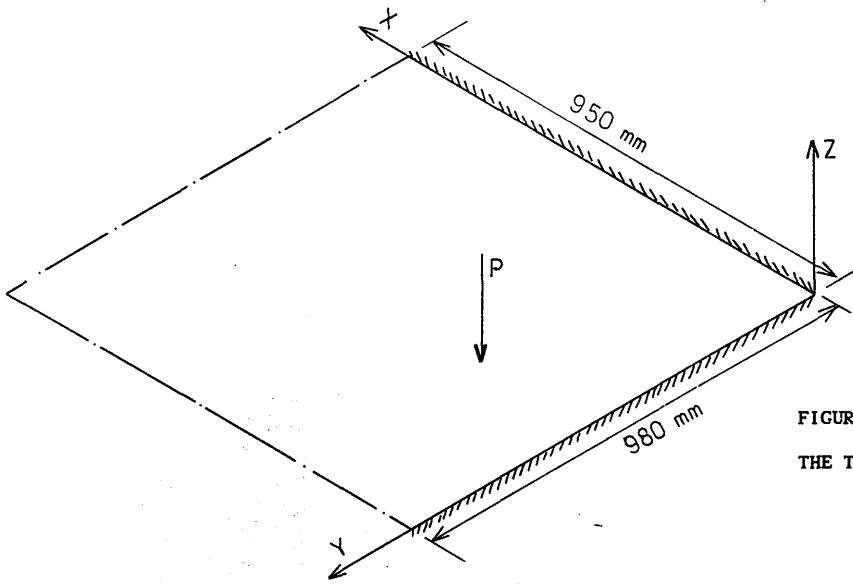
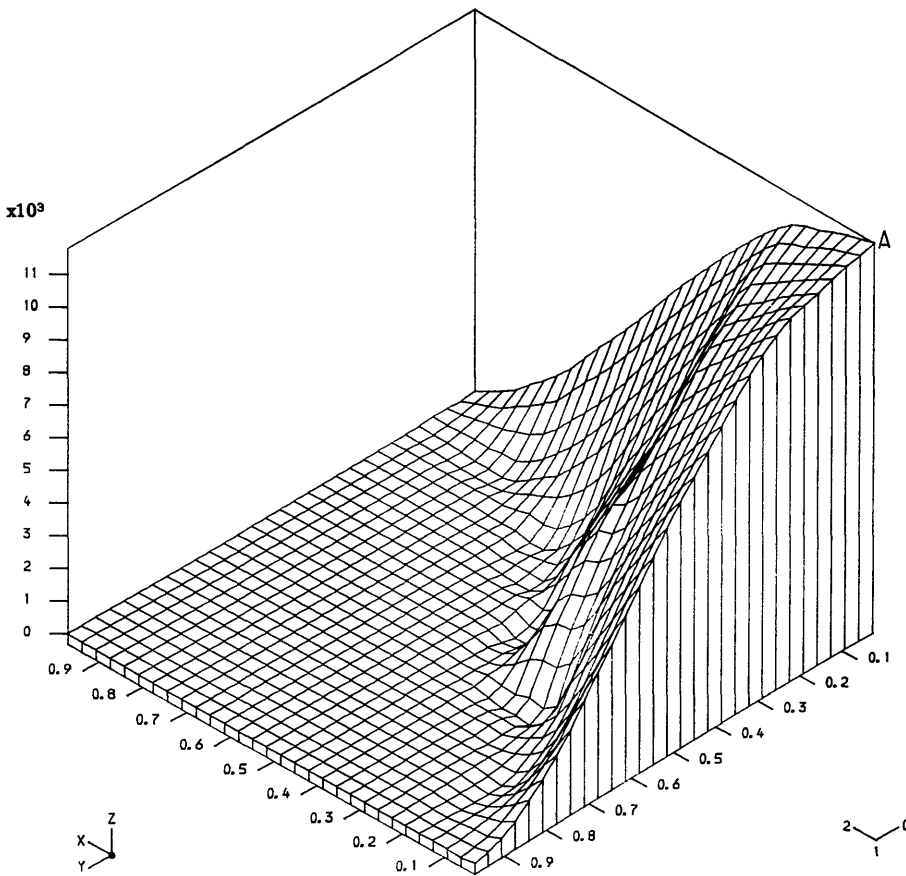
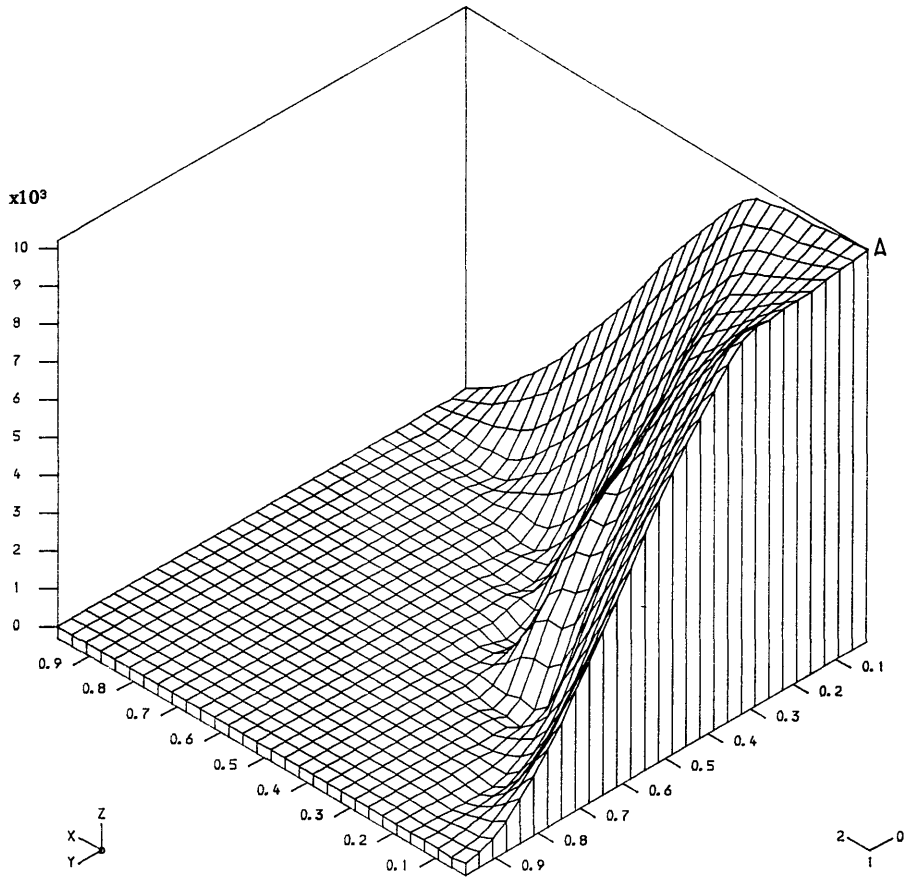


FIGURE (4-4b): DISTRIBUTION OF THE TOP DESIGN MOMENT  $M_x^*$

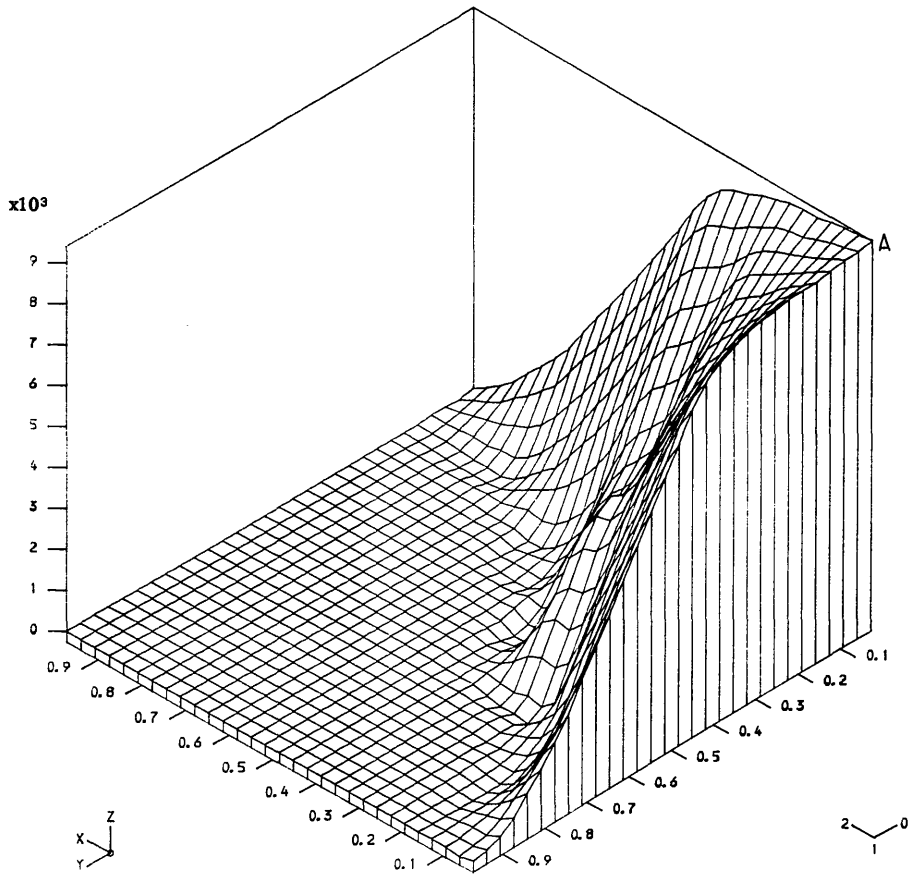
- P - 53325 N
- E - 21500 N / mm<sup>2</sup>
- $\nu$  - 0.15
- $M_p$  - 20422 N.mm / mm
- t - 100 mm



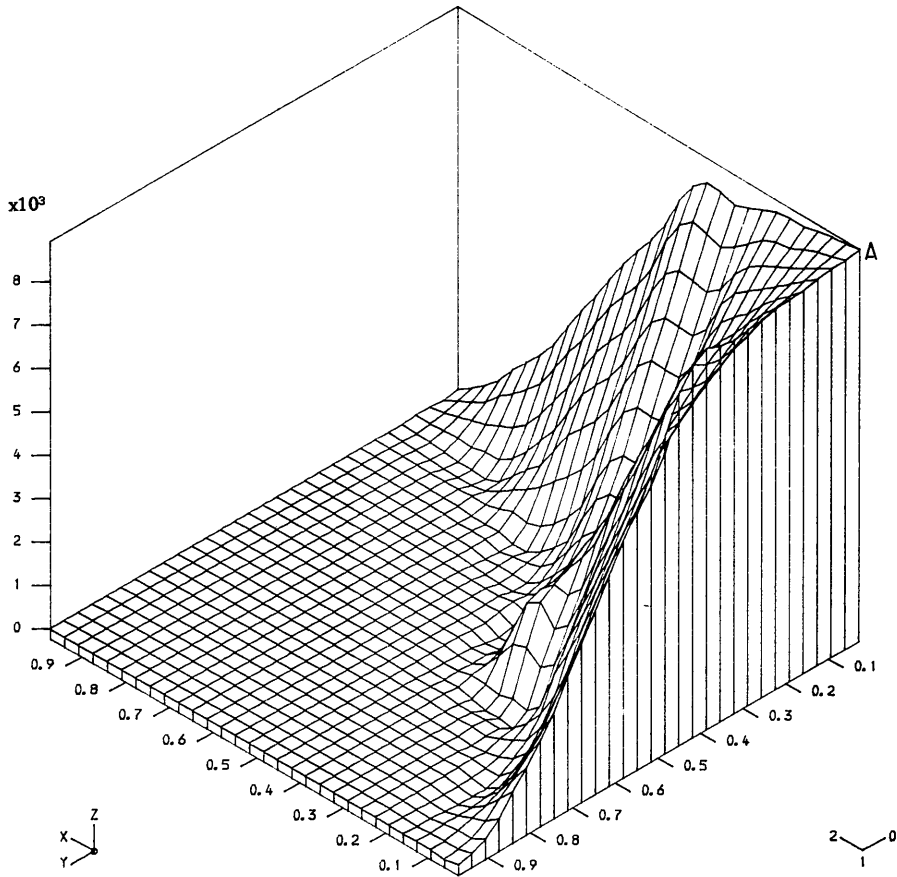
TOP  $M_{x^*}$  (ELASTIC)



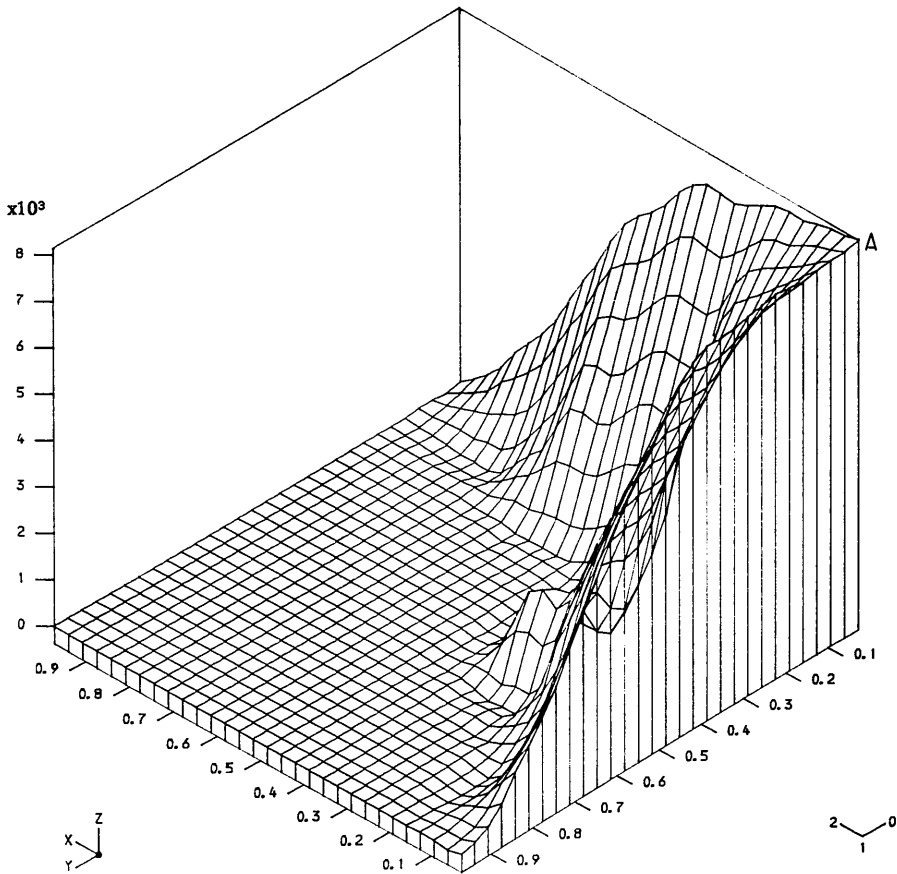
TOP Mx\* (28% of plasticity)



TOP Mx\* (46% of plasticity)



TOP Mx\* (60% of plasticity)



TOP Mx\* (82% of plasticity)

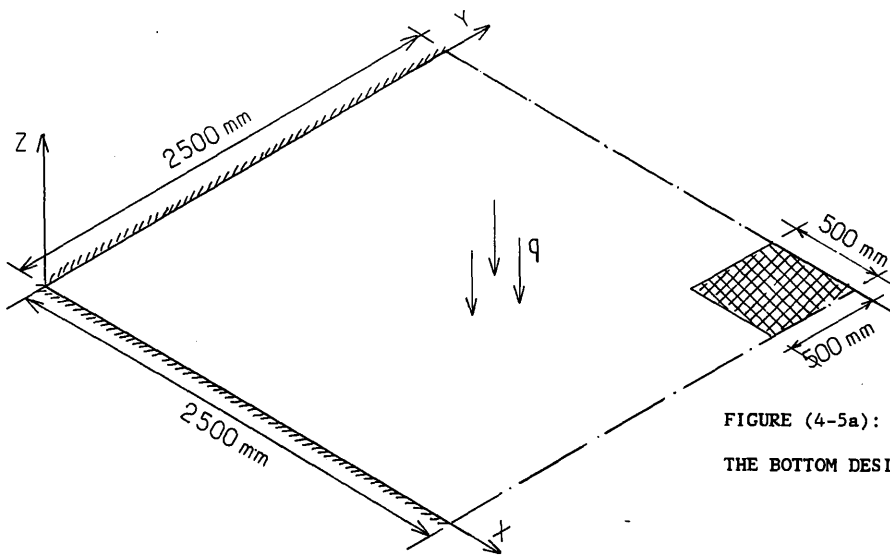
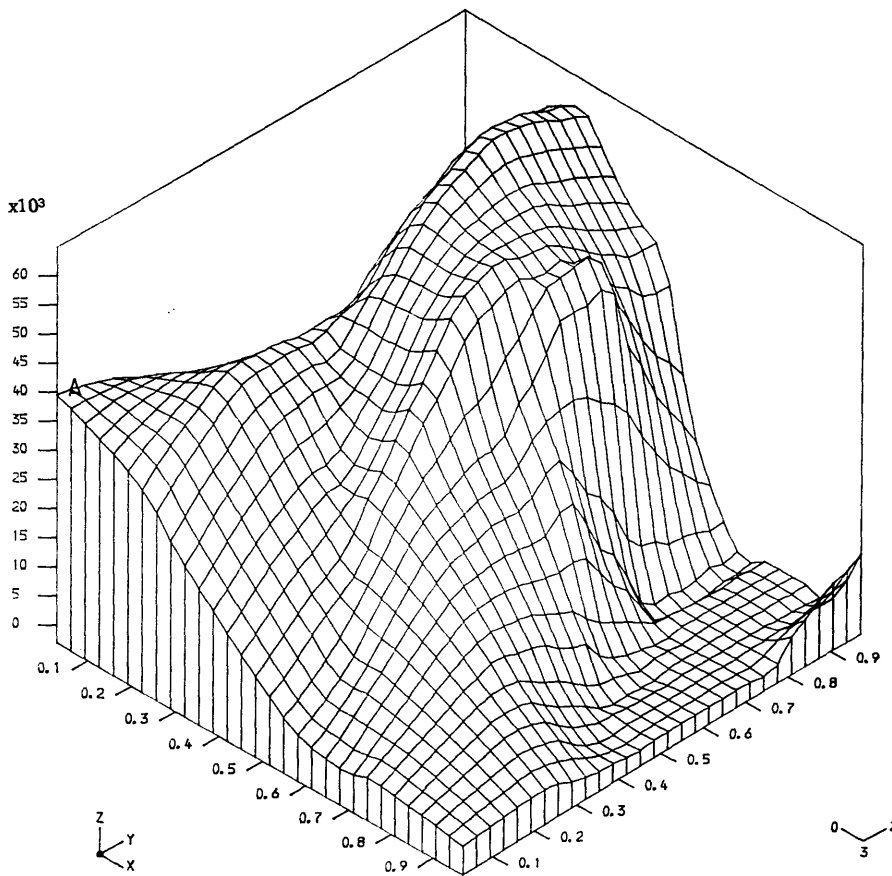
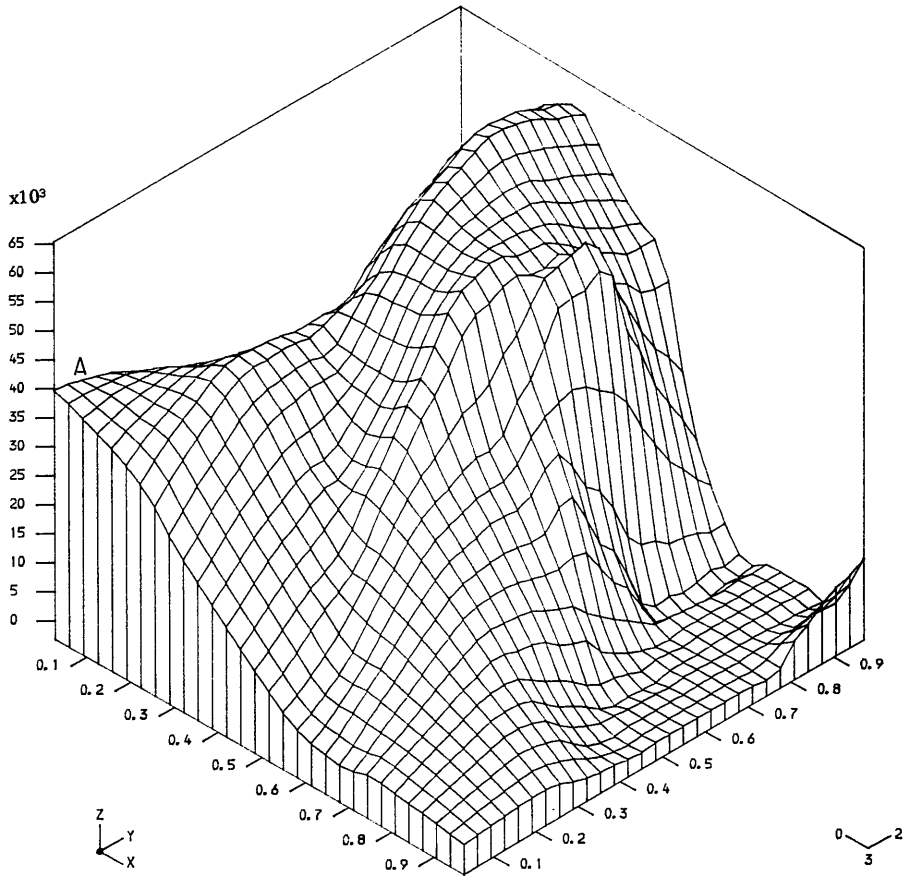


FIGURE (4-5a): DISTRIBUTION OF THE BOTTOM DESIGN MOMENT  $M_{x^*}$

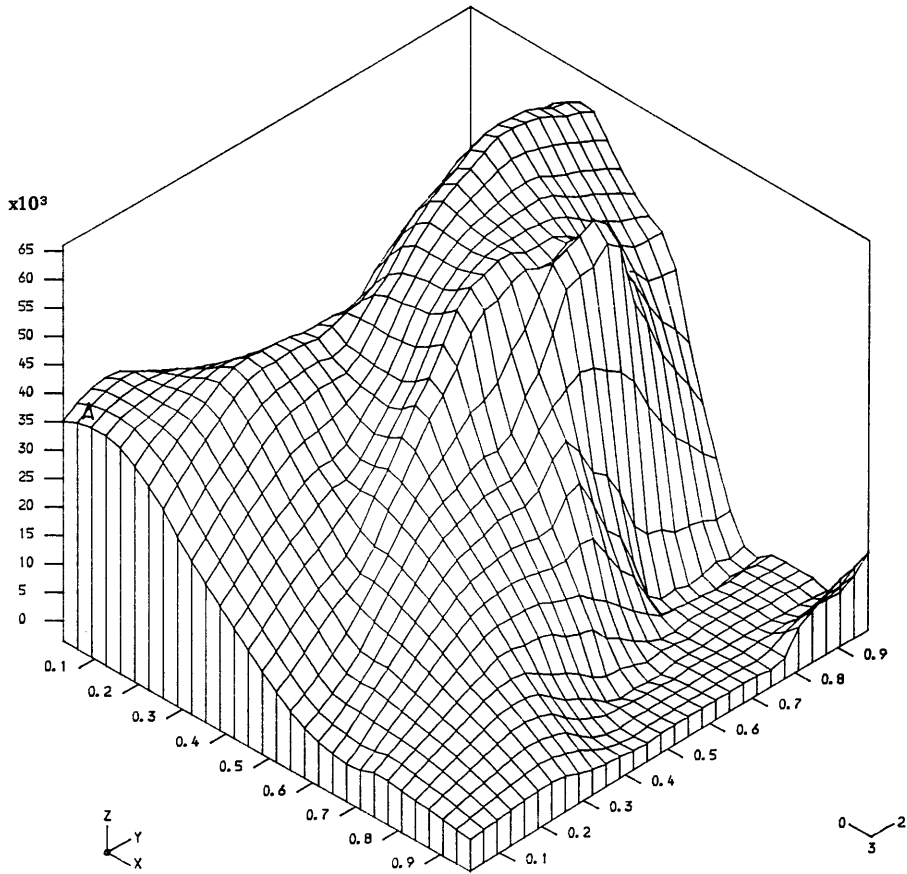
- $q = 0.17 \text{ N / mm}^2$
- $E = 26580 \text{ N / mm}^2$
- $\nu = 0.15$
- $M_p = 76950 \text{ N.mm / mm}$
- $t = 160 \text{ mm}$



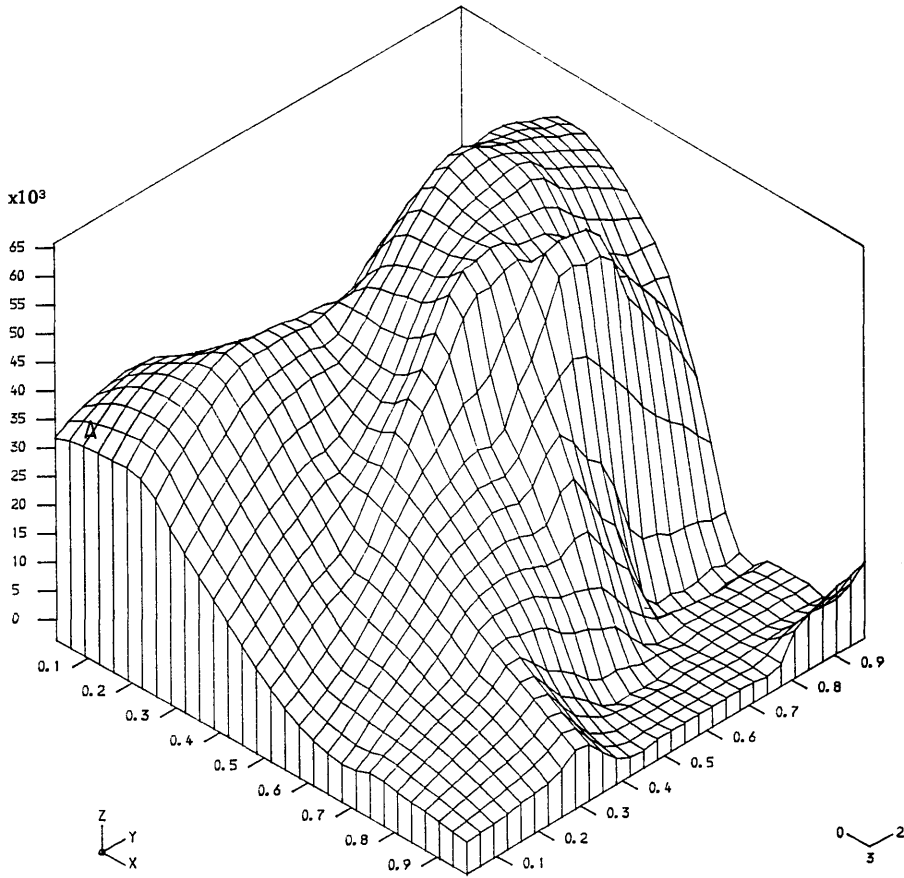
BOTTOM  $M_{x^*}$  (ELASTIC)



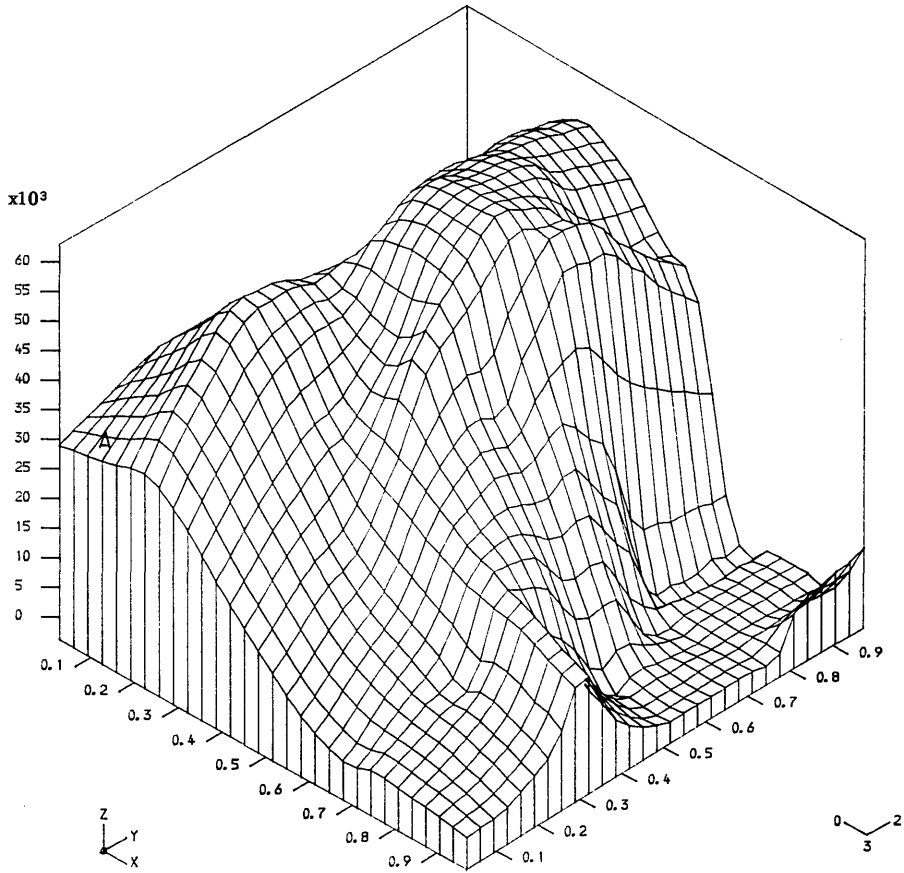
BOTTOM  $M_{x*}$  (20% of plasticity)



BOTTOM  $M_{x*}$  (40% of plasticity)



BOTTOM Mx\* (60% of plasticity)



BOTTOM Mx\* (80% of plasticity)

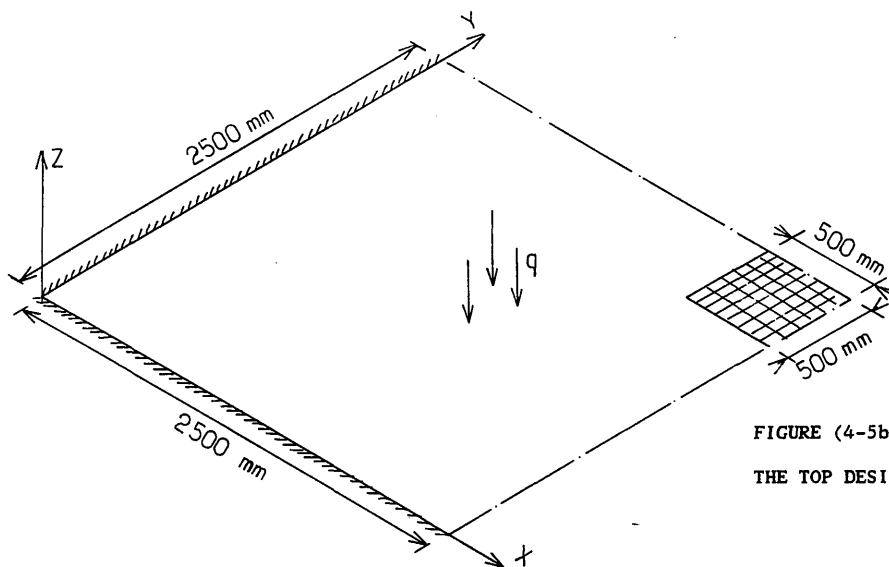
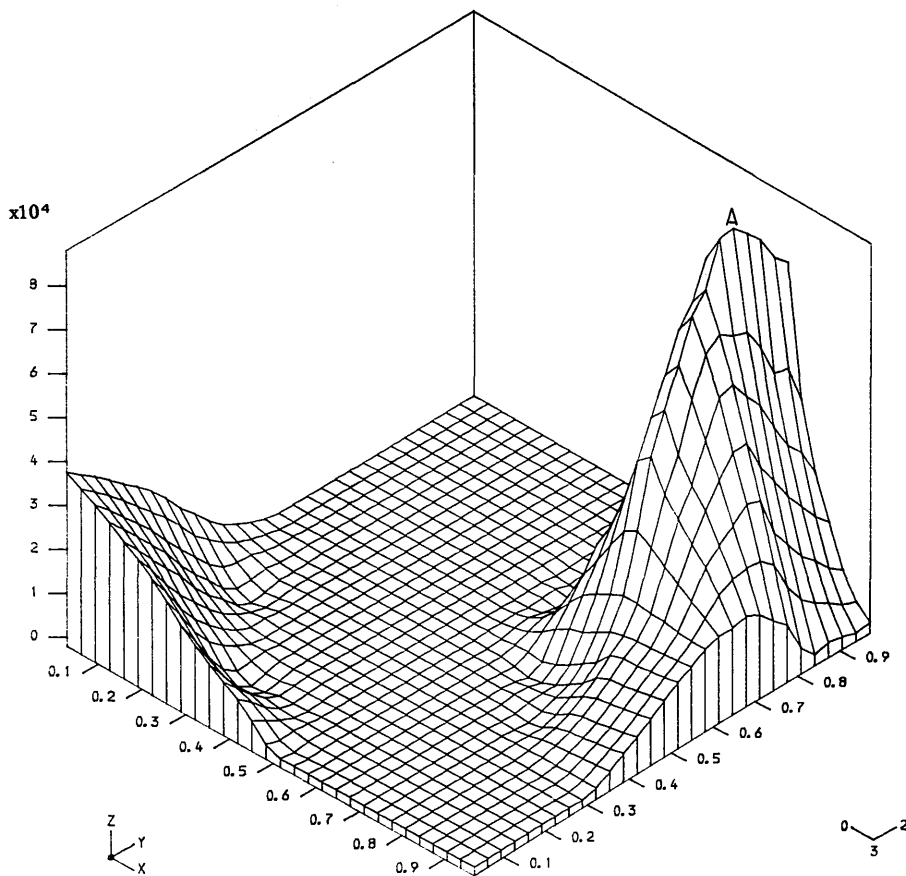


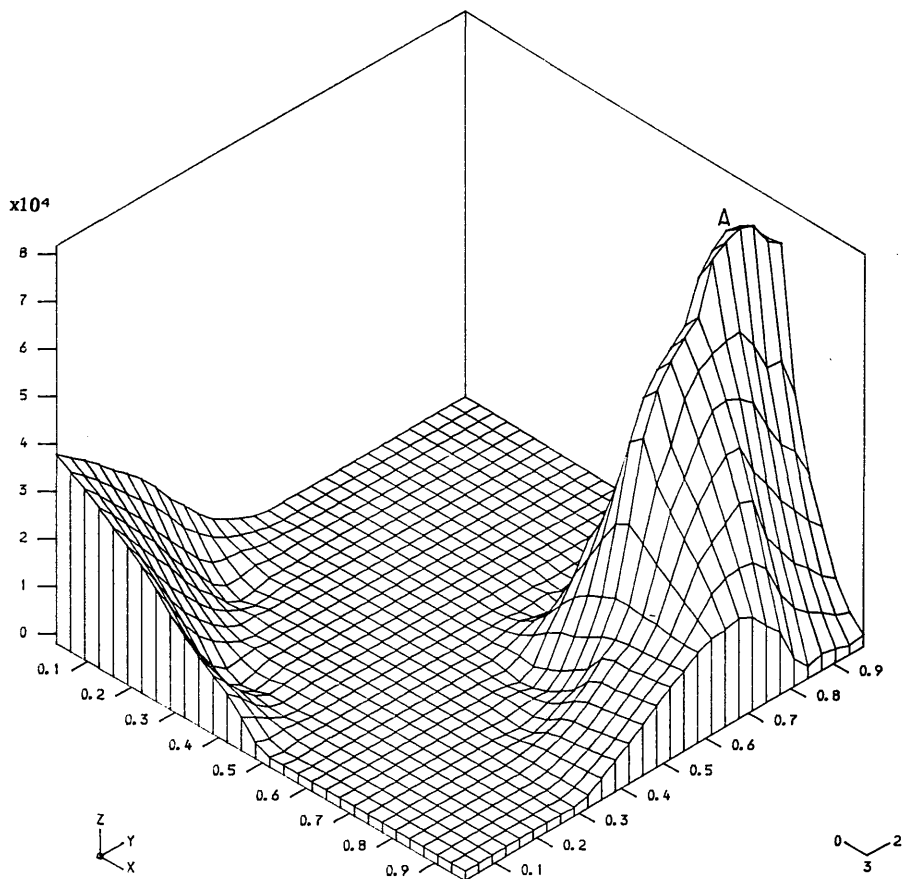
FIGURE (4-5b): DISTRIBUTION OF THE TOP DESIGN MOMENT  $M_x^*$

- $q = 0.17 \text{ N / mm}^2$
- $E = 26580 \text{ N / mm}^2$
- $\nu = 0.15$
- $M_p = 76950 \text{ N.mm / mm}$
- $t = 160 \text{ mm}$

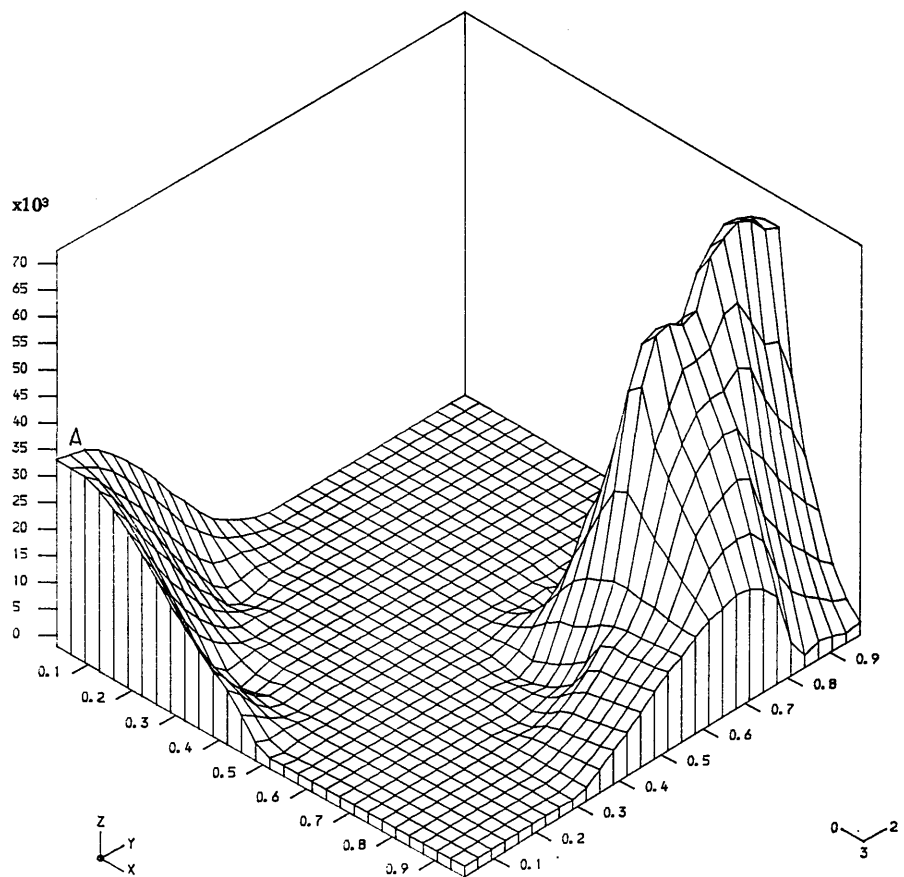


TOP  $M_x^*$  (ELASTIC)

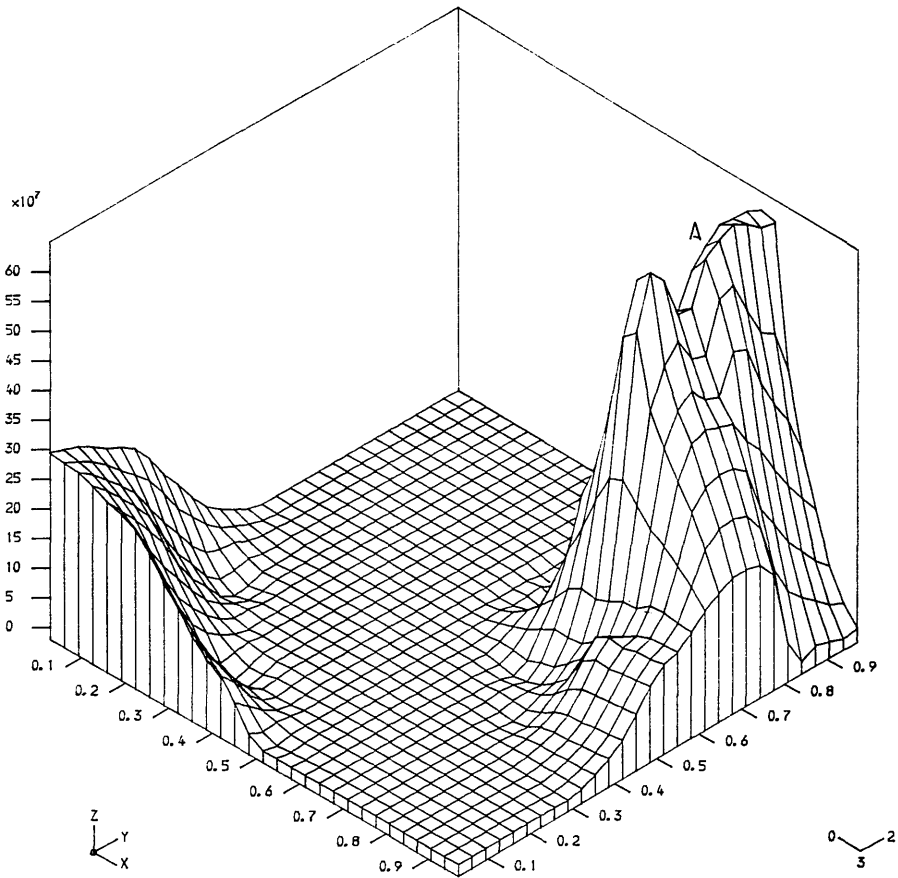




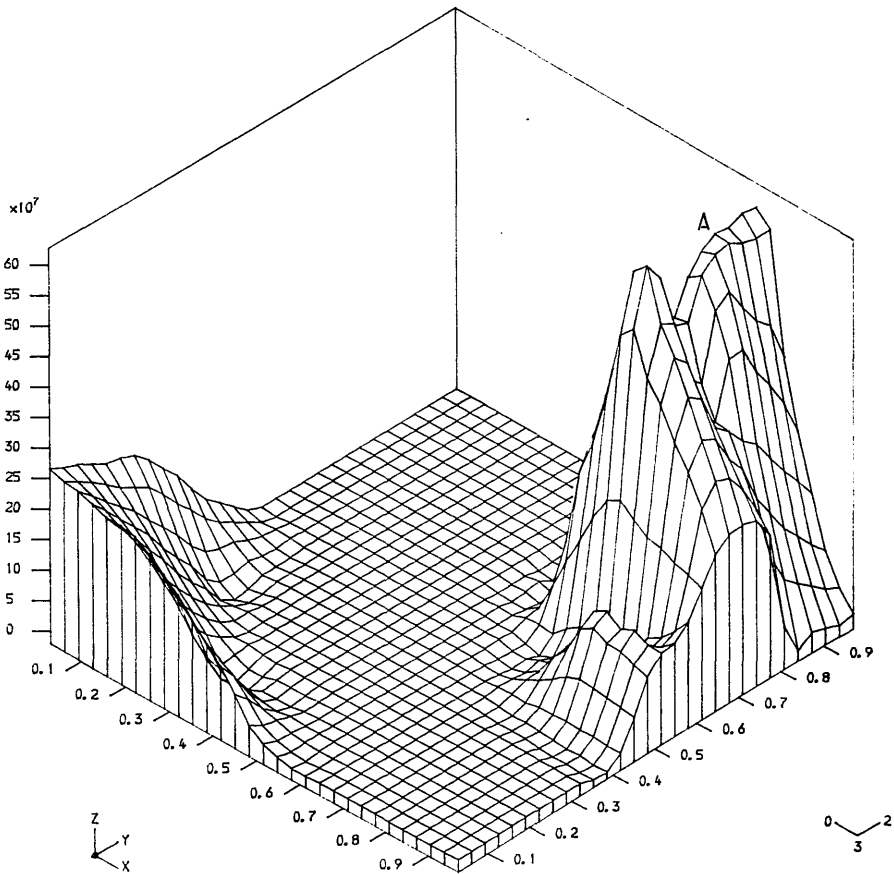
TOP Mx\* (20% of plasticity)



TOP Mx\* (40% of plasticity)



TOP Mx\* (60% of plasticity)



TOP Mx\* (80% of plasticity)

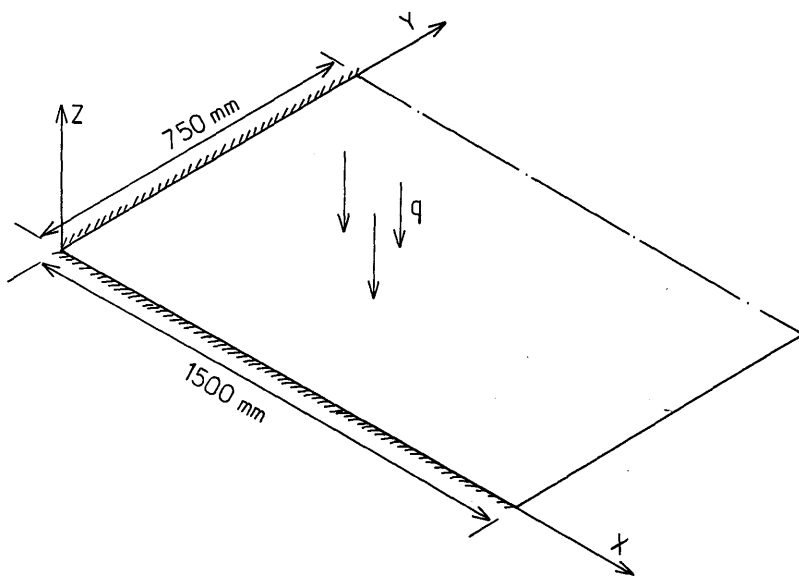
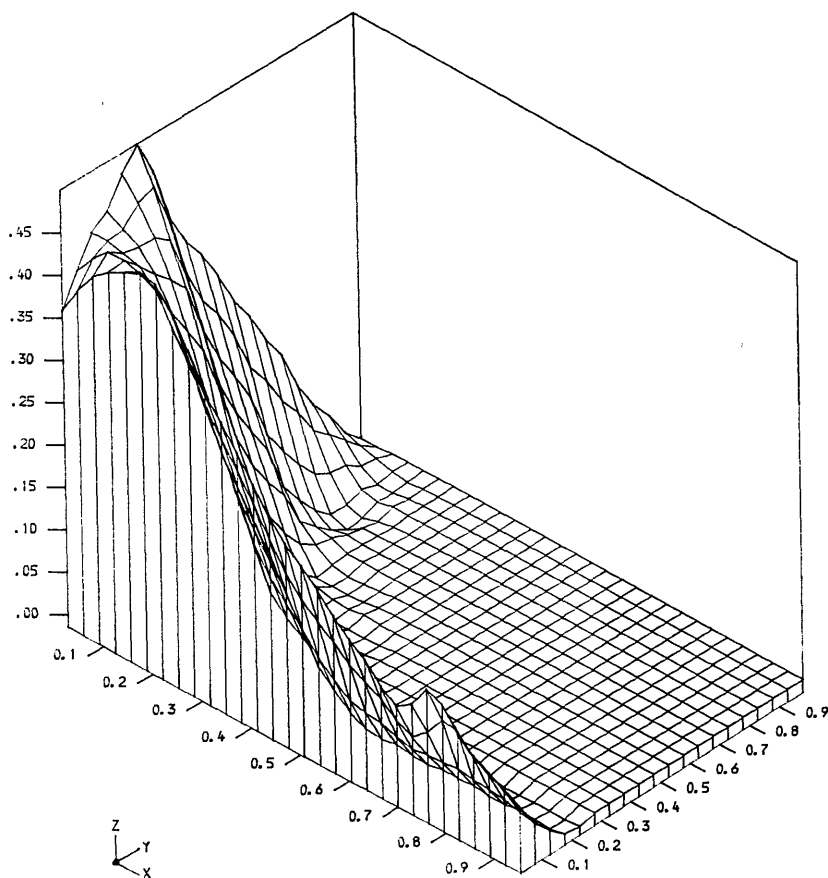
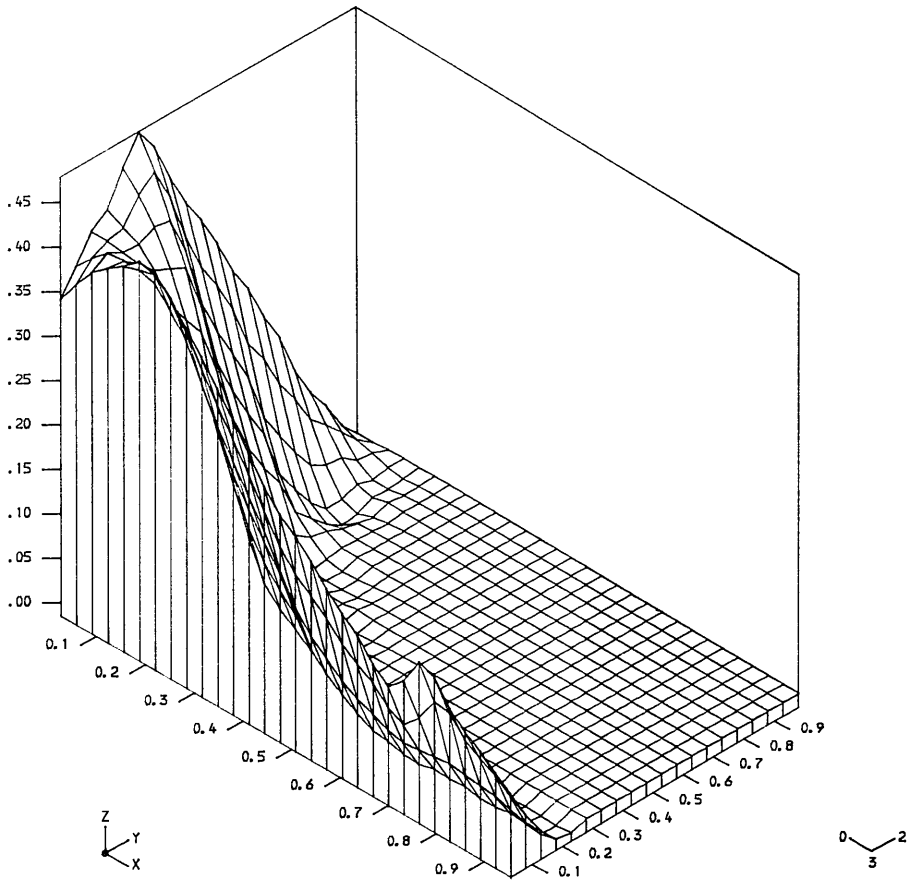


FIGURE (4-6a): DISTRIBUTION OF THE BOTTOM DESIGN MOMENT  $M_y^*$

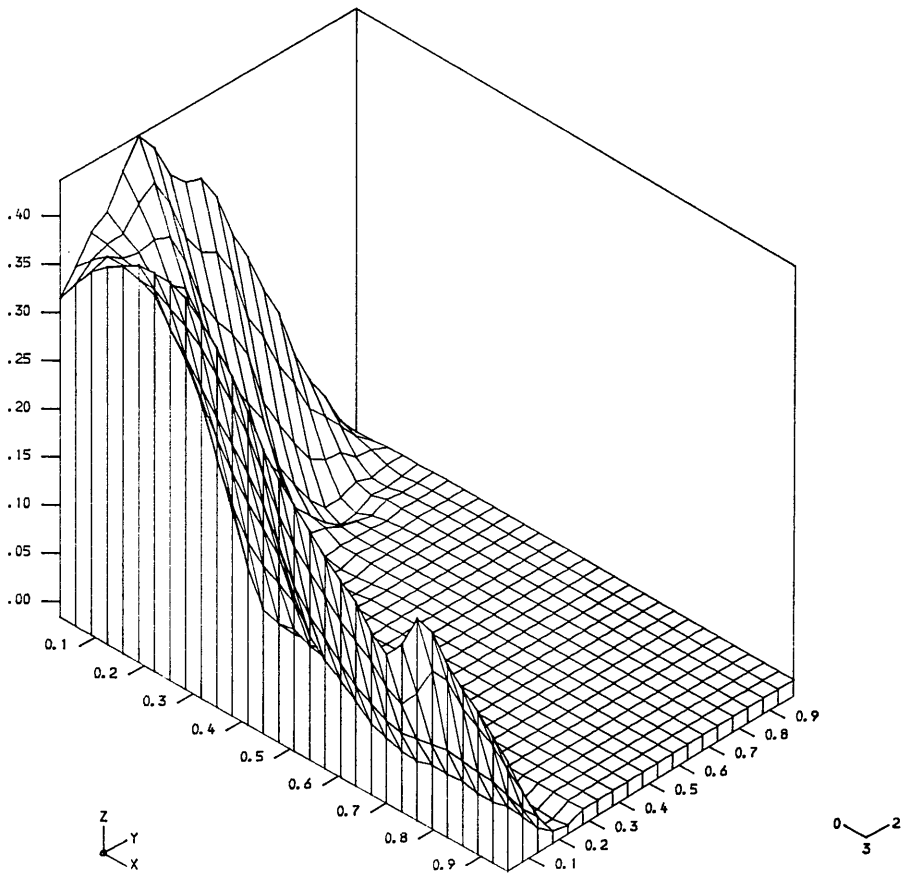
- $q = .4 \text{ E-}02 \text{ N / mm}^2$
- $E = 26580 \text{ N / mm}^2$
- $\nu = 0.15$
- $M_p = 874.80 \text{ N.mm / mm}$
- $t = 100 \text{ mm}$



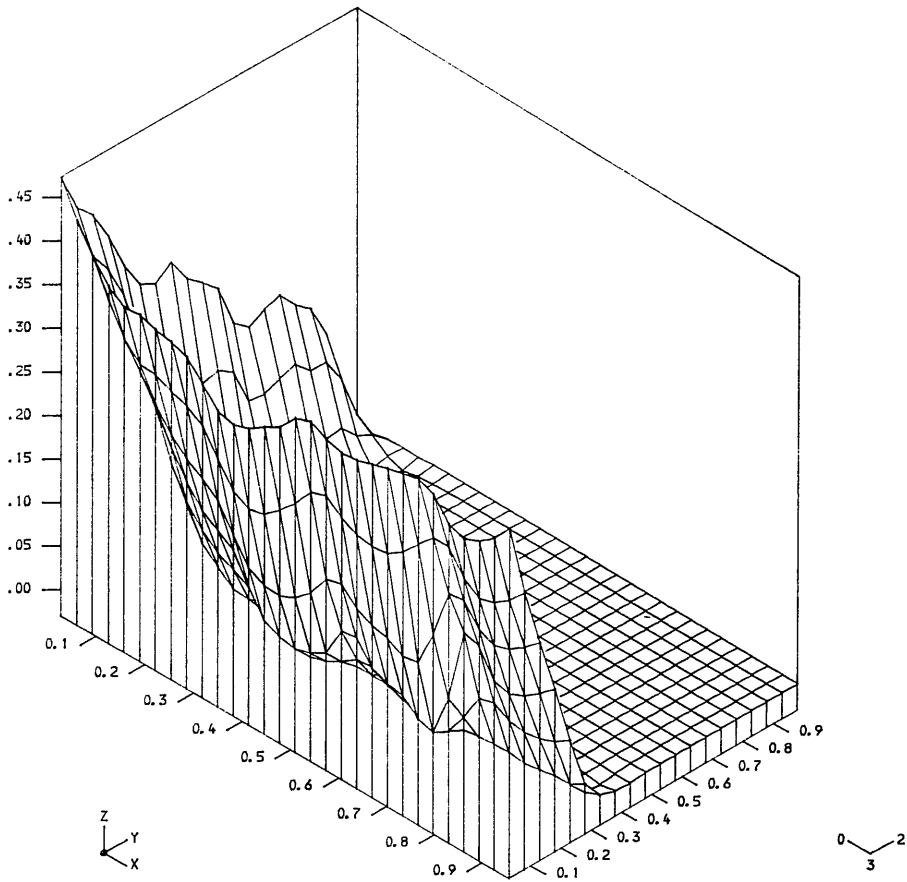
TOP  $M_y^*$  (ELASTIC)



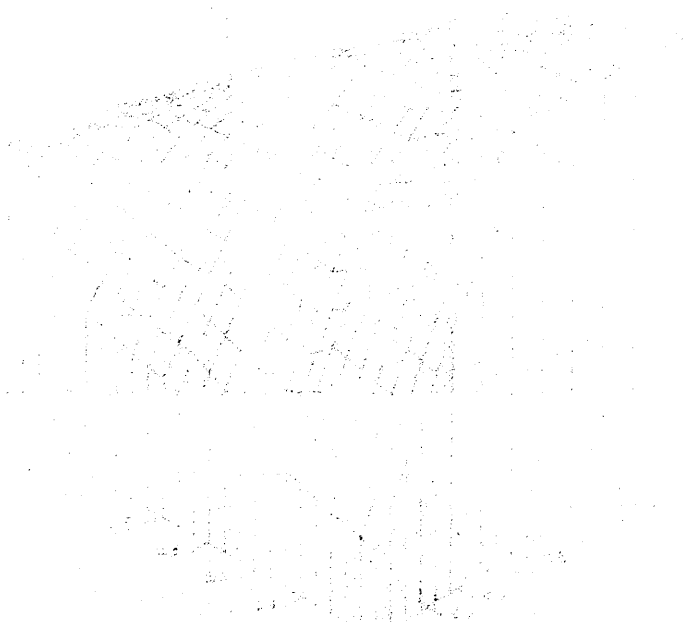
TOP My\* (24% of plasticity)



TOP My\* (52% of plasticity)



TOP My\* (72% of plasticity)



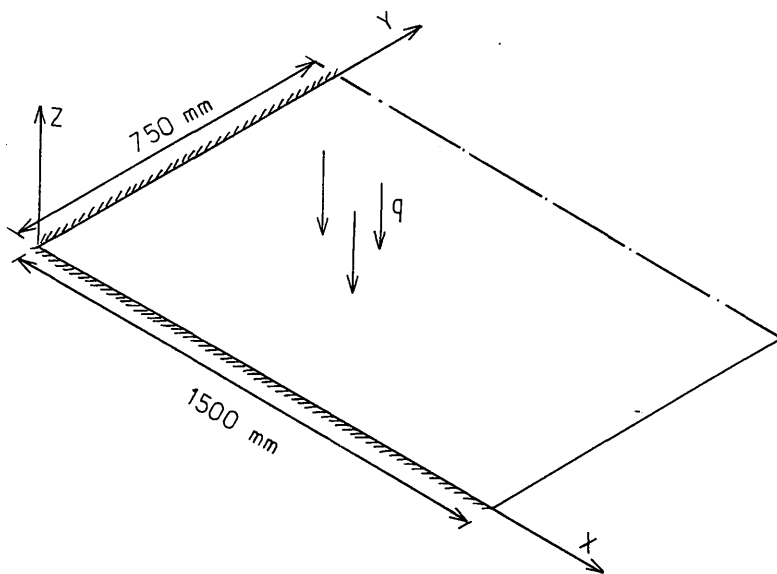
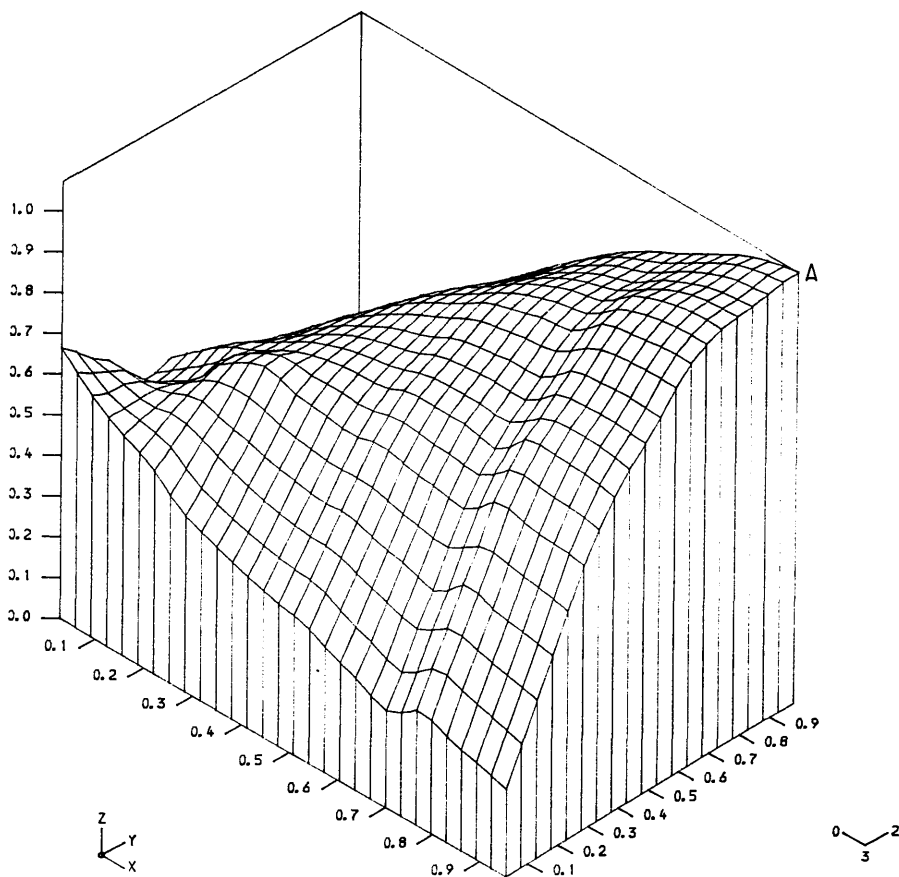
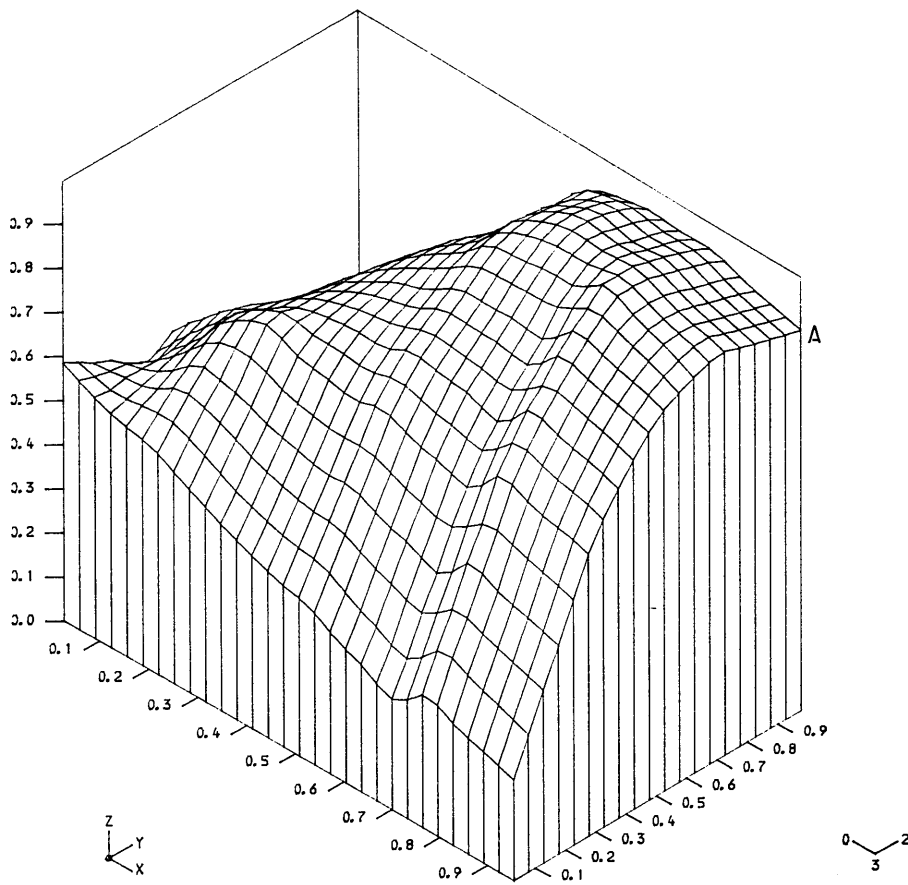


FIGURE (4-6b): DISTRIBUTION OF THE TOP DESIGN MOMENT  $M_y^*$

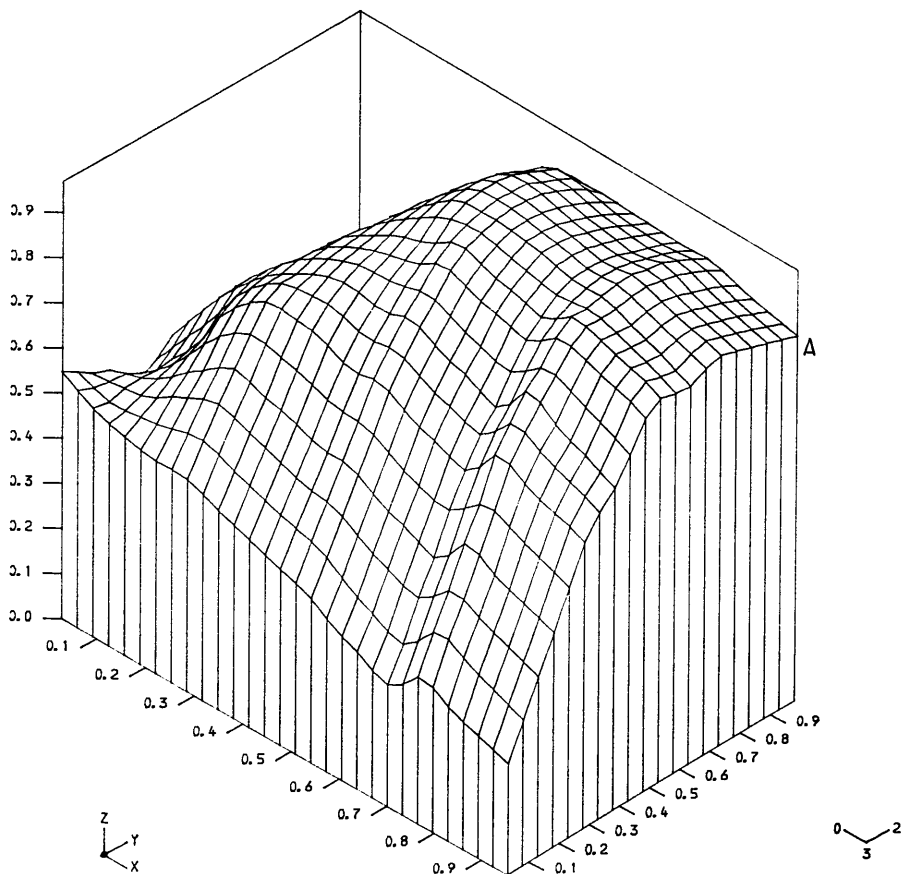
- $q = .4 \text{ E-}02 \text{ N / mm}^2$
- $E = 26580 \text{ N / mm}^2$
- $\nu = 0.15$
- $M_p = 874.80 \text{ N.mm / mm}$
- $t = 100 \text{ mm}$



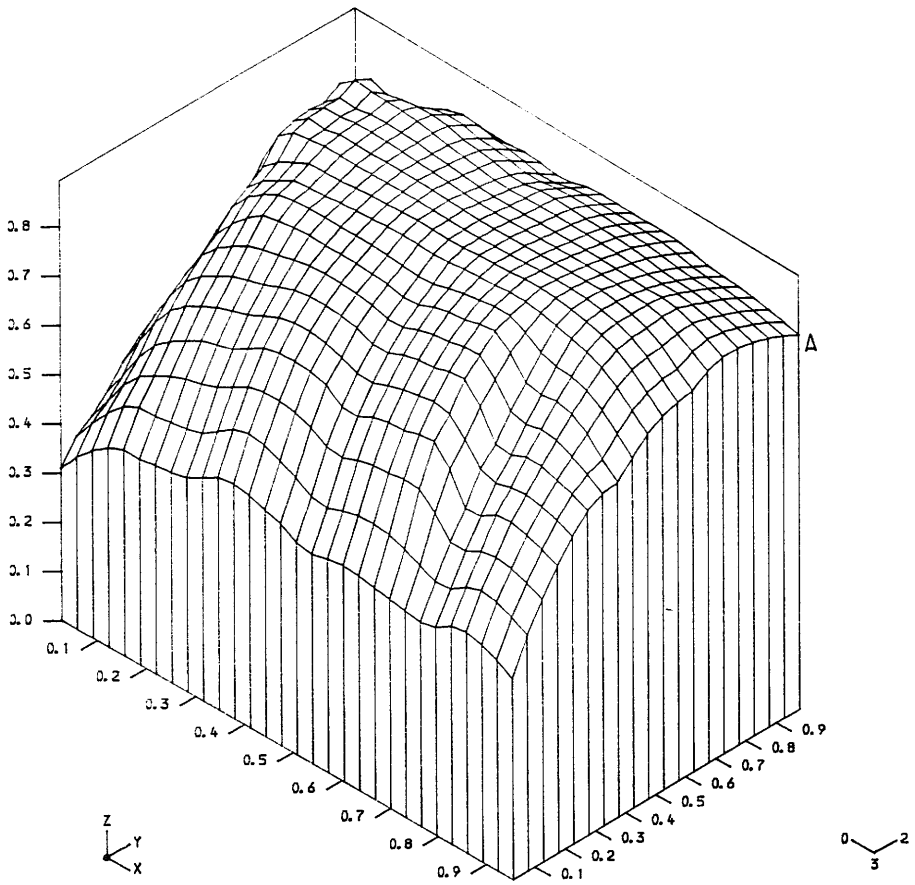
BOTTOM  $M_y^*$  (ELASTIC)



BOTTOM My\* (24% of plasticity)



BOTTOM My\* (52% of plasticity)



BOTTOM My\* (72% of plasticity)

The surface plot shows the distribution of the bottom moment  $M_y^*$  across the domain. The values range from approximately 0.0 at the front-right corner to 0.8 at the back-left corner. The surface is smooth and curved, indicating a non-uniform distribution of the moment. The plot is labeled "BOTTOM My\* (72% of plasticity)".

and boundary conditions.



## CHAPTER FIVE :

### NONLINEAR ANALYSIS

#### 5.1 Introduction:

In the previous chapter, it has been shown that the use of the elasto-plastic stress field in the direct design method presents many practical advantages. Here the behaviour of the slabs so designed is studied in detail using the layer approach reviewed in chapter three.

A series of numerical experiments using the layered finite element program will be conducted on a number of rectangular slabs.

The slabs were all designed by the direct design method using the non elastic stress field, except the first of each series which was designed using the elastic stress field. This was intended for comparison with the direct design method using non elastic stress field.

The main objective of these numerical experiments is to study the service and ultimate behaviour of the slabs when using non elastic stress field. By varying the reinforcement in accordance with the design moments ( $M_x^*$ ,  $M_y^*$ ), which depends on the state of the stress field chosen (elastic or elasto-plastic with different degrees of plasticity), the resulting behaviour in particular ductility demand and serviceability behaviour is studied.

The variables in the study are:

a- Loading and boundary conditions,

b- reinforcement layout (which result by varying the degree of plasticity of the stress field)

The slabs in this study can be divided into three series:

Test series 1 : Includes five simply supported square slabs  
under a uniform distributed load.

Test series 2 : Includes five simply supported square slabs  
loaded by four point loads.

Test series 3 : Includes five square slabs simply supported  
at the edges plus a central column  
support, subjected to a uniform  
distributed load.

### 5.2 Designation of slabs studied:

The numerical test slabs in test series 1 and 3 were designed to carry uniform loads only and in test series 2 the slabs were designed to carry point loads.

In each run, the slab was first designed for a specific ultimate load using the direct design method discussed in chapter four (using non elastic stress field) by means of Mindlin program (see Chapter three,sect- 1).

All the safety factors on the design load and the materials were taken as unity, the slab was then analysed under an incremental load till failure. This would constitute a full computer experiment.

### 5.3 Proportioning and loading:

The span depth in each case was taken as  $\text{span} / 20$  . The definition of the term "span" used in calculating the depths depends on the boundary

conditions of the problem. For slabs supported along four edges, the span length was taken as the length of the short side of the slab. For other cases involving free edges, the span length was taken as the length of the longer free edge.

An arbitrary design load was chosen, and an elasto-plastic analysis for the slab under the design load was obtained from the Mindlin program.(Chapter three,sect-2).

The output from such analysis would include the elastic design moments ( $M_x^*, M_y^*$ ), as well as elasto-plastic design moments at different levels of plasticity spread under the design load.

Finally the required steel areas in the X- and Y- directions respectively were calculated on the assumption of a rectangular stress block with an average stress in the block equal to 0.667 x cube strength of concrete (or approximately 0.83 x cylinder strength) and the stress in the steel equal to the yield strength  $f_y$ .

This assumption leads to the equation for the calculation of the steel area  $A_{st}$  to resist a given design moment  $M^*$ .

$$A_{st} = \frac{f_{cu}}{f_y} \frac{d}{1.5} \left[ 1.0 - \left[ 1.0 - \frac{3 M^*}{f_{cu} \cdot d^2} \right]^{\frac{1}{2}} \right] \dots (5.1)$$

where  $A_{st}$  = area of steel per unit width to resist  $M^*$ ,

$d$  = effective depth of the slab,

$f_{cu}$  = cube strength of concrete,

$f_y$  = yield strength of steel,

$M^*$  = design moment per unit width.

The value of the required area for each element of the finite element mesh of the slab is obtained by either averaging the design moments  $M^*$  obtained at each Gauss point of the element, or, by taking the maximum design moment  $M^*$  over

each element.

The severity of the variation of the design moment  $M^*$  over the whole slab will give an idea about what to adopt for the design moment, average or maximum values.

The effect of using the average values or the maximum values of the design moment  $M^*$  over each element for the slabs studied in this chapter are given in figures (5.1) to (5.3). On the basis of these plots, the slabs studied in test series 1 are designed using the maximum value of the design moments over each element and the average value of the design moments has been used in designing the slabs in test series 2 and 3.

#### 5.4 Steel layout:

For a better appreciation of the different steel patterns used in this study which vary with respect to the degree of plasticity of the stress field, the different distributions of the design moment are shown in figures (4-3a) to (4-5b).

#### 5.5 Analysis:

For each numerical experiment, the deformational behaviour resulting from various changes in the slab material due to progressive cracking and yielding under increasing loading, has been traced using the nonlinear finite element program, described in chapter three.

All the slabs are doubly symmetric, therefore only one quadrant was analysed using 4 x 4 subdivisions.

For all tested models, the slab thickness was divided into six concrete layers, plus two concrete layers representing the covers of steel, plus two to four steel layers as might be required by the reinforcement present.

All experiments were assigned the following material properties:

MATERIAL PROPERTIES	Test series 1&3	Test series 2
Concrete compressive strength, $f_{cu}$	47.7 N/mm <sup>2</sup>	44.2 N/mm <sup>2</sup>
Concrete tensile strength, $f_t$	3.5	3.4
Young's modulus for concrete, $E_c$	27580.0	21500.0
steel, $E_s$	206800.0	214000.0
Poisson's ratio for concrete, $\nu$	0.15	0.15
Yielding strength of steel, $f_y$	303.4	460.0

All experiments were designed to study the effect of taking non elastic stress field in the direct design method, on the behaviour of the slabs.

The slabs tested in "Test series 1" were simply supported with  $L_x / L_y = 1.0$  , and subjected to a uniform distributed load of 0.15 N/mm<sup>2</sup> .

The slabs tested in "Test series 2" were simply supported with  $L_x / L_y = 1.0$  , and subjected to four point loads of 52.5 KN each.

The slabs tested in "Test series 3" were simply supported on all the edges plus a central column support, subjected to a uniformly distributed load of 0.17 N/mm<sup>2</sup> .

As recommended in reference (1) , a load increment size of 0.10  $P_{cr}$  (the cracking load of the slab) was the maximum value used, for all slabs. A maximum number of 50 iterations was given at each increment. This was required only when the nonlinearity becomes important. 2 x 2 sampling points were used in each element. An average of 5.5% of the tolerance was adopted and near failure an average of 4.5% was allowable. A value of 0.4 of the shear retention is adopted during all the numerical experiments while the tension

stiffening has been ignored. The hardening parameter of steel has been ignored too. The fixed crack analysis (orthogonal) was used. Finally, for nonlinear solution, the combined algorithm where the stiffness matrix is updated at the 1<sup>st</sup> iteration for 1<sup>st</sup> increment and subsequent load increments at iteration number 2,5,8,11,15 and 20 was used.

In every test, the following aspects of structural behaviour have been investigated:

1- Deflections :

Short term deflections under increasing load till failure. For simplicity, only the point of maximum deflection which will be considered.

2- Redistribution of internal stresses :

The redistribution of bending moments in the reinforcement directions due to material nonlinearity will be considered.

3- Cracking and yielding :

A quantitative measure of cracks is not feasible by the present model, since the model employs a smeared crack approach. But, since crack widths can be related to steel strains ,they can be used as a measure of the crack widths. Accordingly steel strains will be investigated in this study.

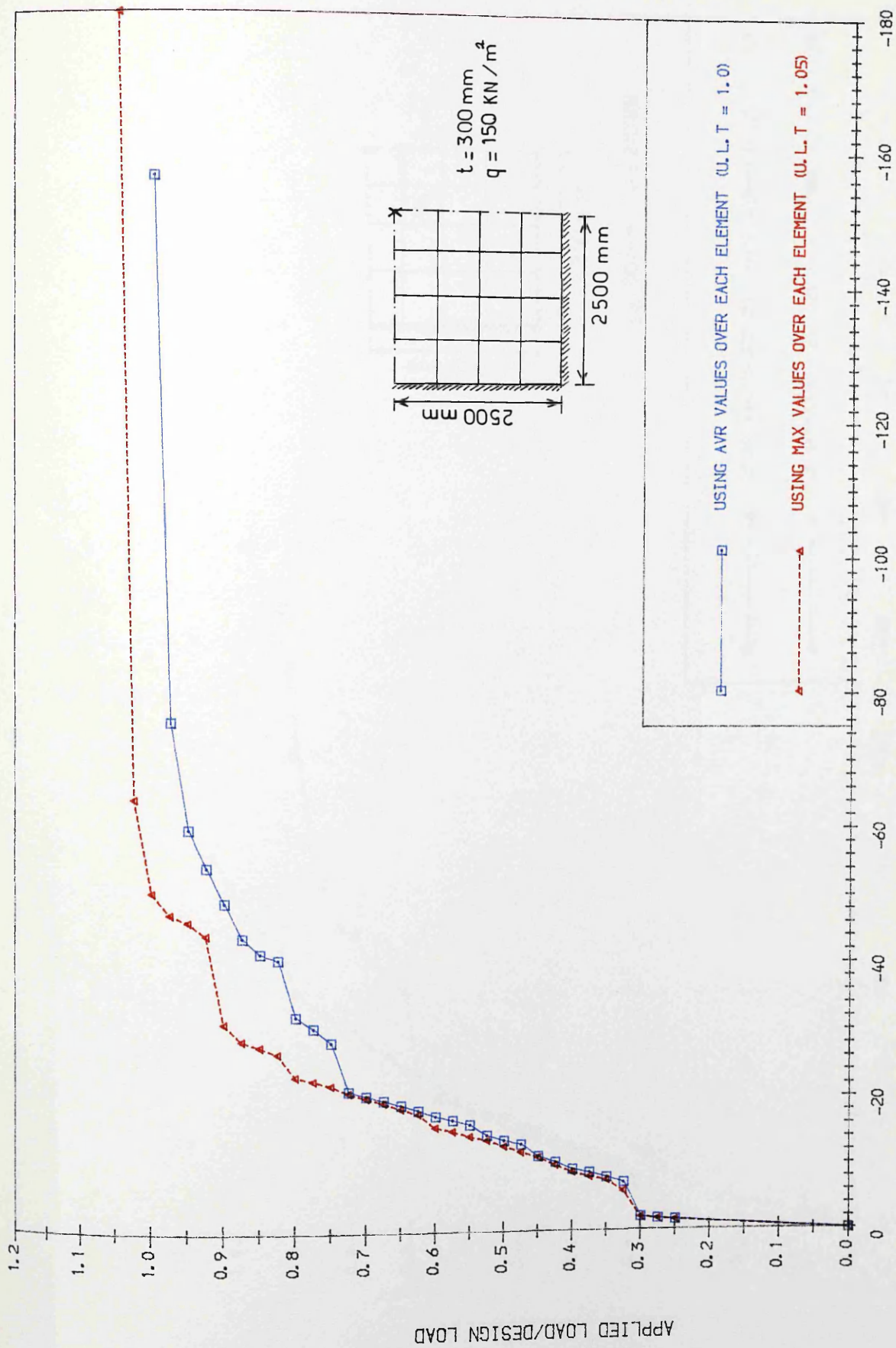


FIG. (5.1) LOAD-DEFLECTION CURVE FOR SLB1A

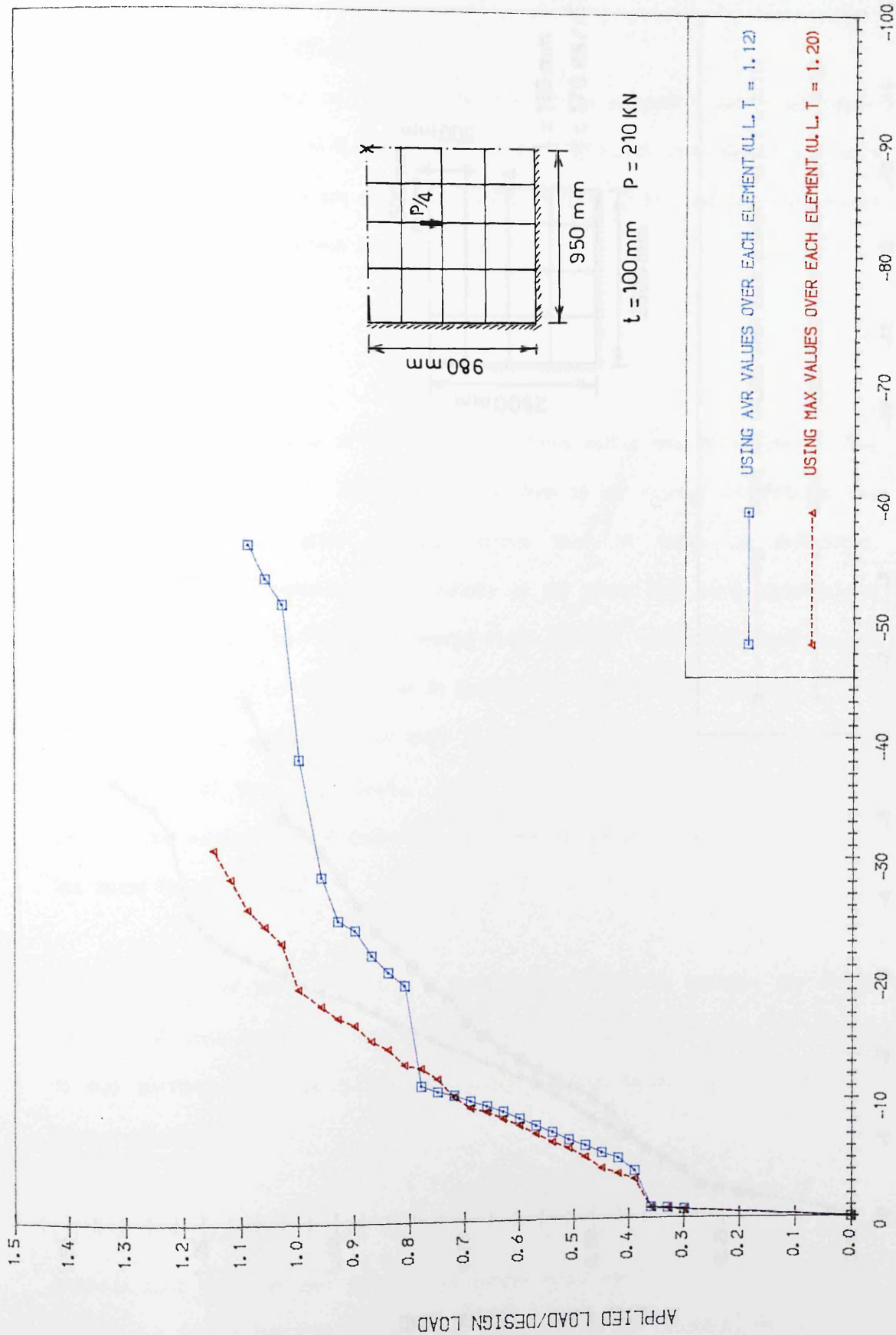
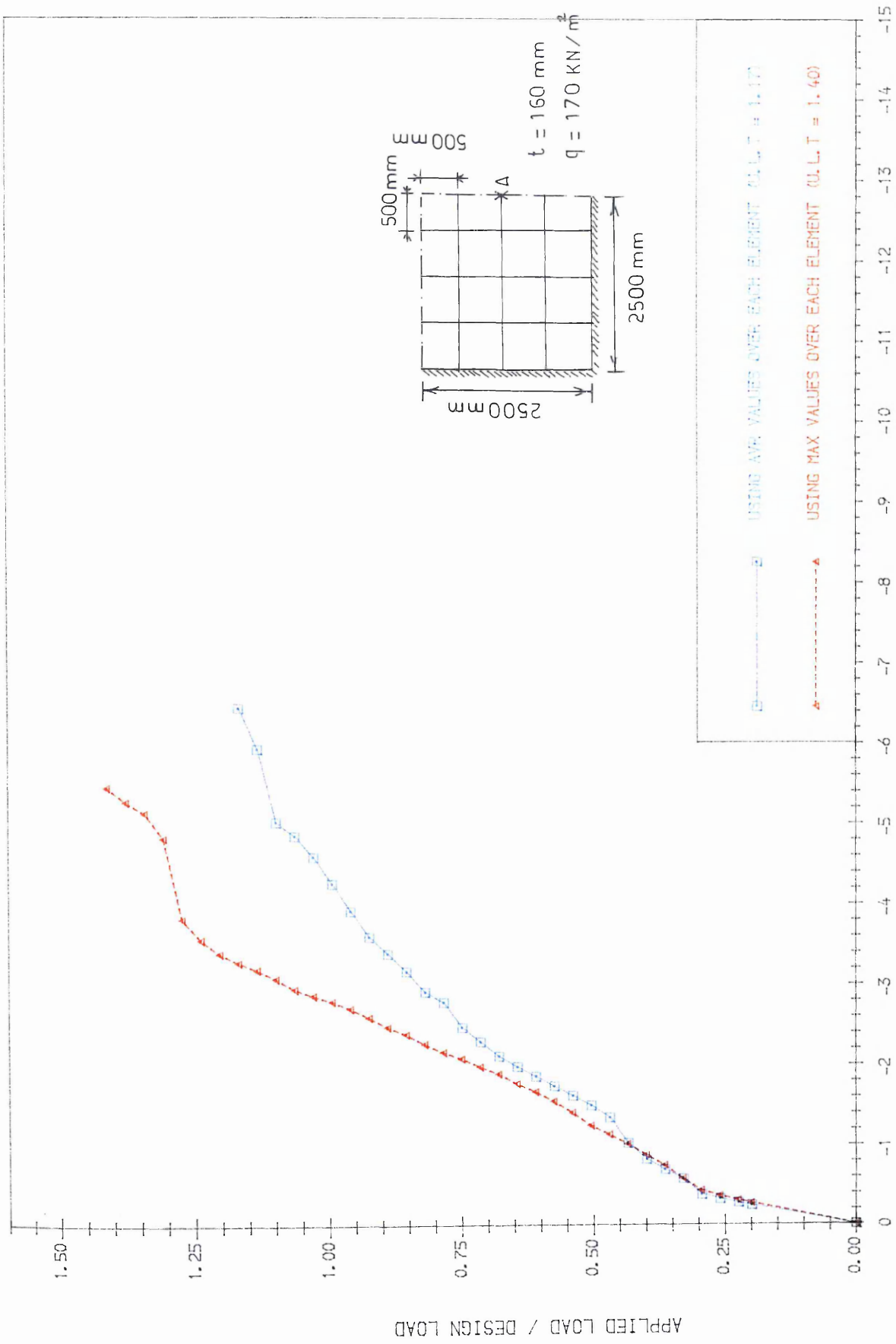


FIG. (5.2) LOAD-DEFLECTION CURVE FOR SLB2A





DEFLECTION OF THE POINT A (MM)

FIG. (5.3) LOAD-DEFLECTION CURVE FOR SLB34

## 5.6 Results, discussions and conclusions:

### 5.6.1 Test series 1:(SLB.1.A)

This series include tests on slabs which are simply supported along all edges. Five runs, SLB.1.A.0, SLB.1.A.1, SLB.1.A.2, SLB.1.A.3 and SLB.1.A.4 were performed. The results are shown in figures (5.4) to (5.8), and for convenience a summary is given in tables (5-1) and (5-2)

### 5.6.2 Conclusions:

- (1) The service behaviour of all the slabs in this series was satisfactory. The deflection limit of span / 250 has been reached at an average of 70% of the design load. This gives a high service load in terms of deflections. If we take now the percentage of plasticity of the stress field as a variable, the deflection at service load (0.625 x design load) shows a uniform decrease as this percentage goes up. (of about 5.2% in general) as shown in Fig- (5-19). In terms of steel strains, all the slabs in this series have recorded first yielding beyond 65% of the design load. Again as shown in table (5-1) and Fig- (5-20), the maximum steel strain has decreased as the percentage of plasticity of the stress field increases.
- (2) This series of tests show that in general the difference between the design load (or ultimate load as it is a lower bound method) and the onset of yielding in any particular element is not particularly sensitive to the level of plasticity spread adopted.
- (3) The slabs designed by non elastic stress field have recorded a slightly higher ultimate load than the one designed by elastic stress field ( around 4% higher). This is due to the fact that we have put more steel at the centre of the plate.

TABLE (5-1) " S L B - 1 - A "

CASE	% of pl <sup>t</sup> y	D <sub>ef.</sub> (s <sub>l</sub> )	D <sub>ef.</sub> (d)	$\epsilon_{s1} / \epsilon_0$	$\epsilon_d / \epsilon_0$	U.L.T
SLB.1.A0	0.00 %	17.71 mm	50.36 mm	.972	4.406	1.025
SLB.1.A1	17.50 %	17.23 mm	54.05 mm	.945	4.613	1.000
SLB.1.A2	35.00 %	16.89 mm	48.09 mm	.912	4.019	1.075
SLB.1.A3	52.50 %	17.38 mm	46.87 mm	.933	4.031	1.075
SLB.1.A4	70.00 %	15.86 mm	46.22 mm	.868	3.928	1.125

$\delta_{s1} = 5000 / 250 = 20$  mm ; Service Load = 0.625 x design load ;  $\epsilon_{s1}$  = max steel strain at service load ;  $\epsilon_d$  = max steel strain at design load ;  $\epsilon_0$  = yielding strength of steel = .145E-02 ; D<sub>ef.</sub>(s<sub>l</sub>) = max deflection at service load ; D<sub>ef.</sub>(d) = max deflection at the design load ; U.L.T = ultimate load / design load.

Table (5-2): The difference between the ultimate load ( $P_{ult}$ ) and the yielding load ( $P_y$ ) divided by the design load.  $(P_{ult} - P_y) / P_{ult}$

EI <sup>t</sup> . Case No	1	2	6	11	12	16
Elastic	5.00 %	5.00 %	5.00 %	15.00 %	20.00 %	30.00 %
17.50 %	5.00 %	5.00 %	5.00 %	15.00 %	15.00 %	32.00 %
35.00 %	7.50 %	2.50 %	2.50 %	15.00 %	20.00 %	32.50 %
52.50 %	2.50 %	2.50 %	2.50 %	10.00 %	20.00 %	30.00 %
70.00 %	5.00 %	0.00 %	0.00 %	5.00 %	12.50 %	27.50 %

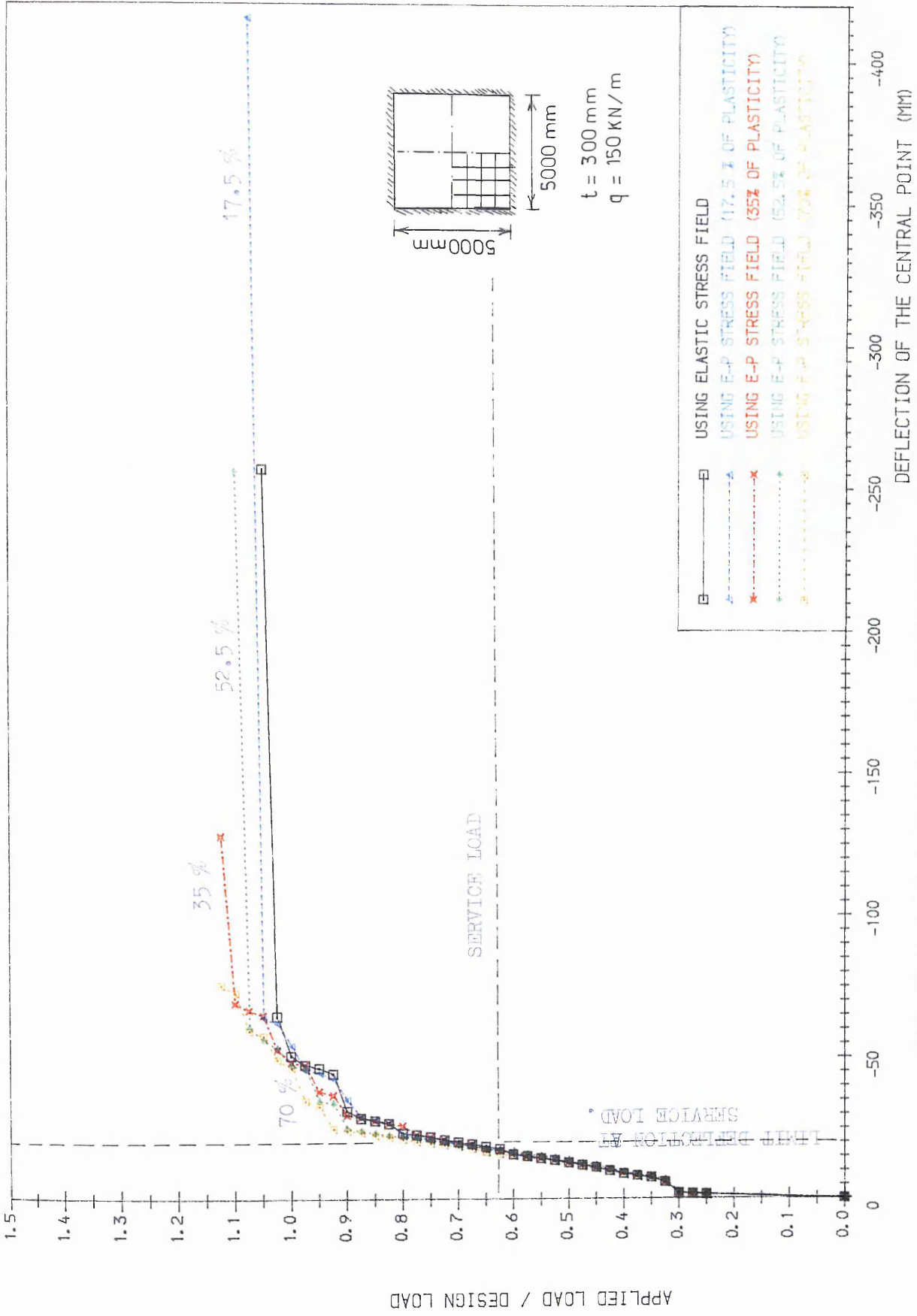


FIG. (5.4) LOAD-DISPLACEMENT CURVES FOR SIMPLY SUPPORTED SLAB UNDER UNIFORM DISTRIBUTED LOAD, DESIGNED BY VARIOUS TYPES OF STRESS FIELD.

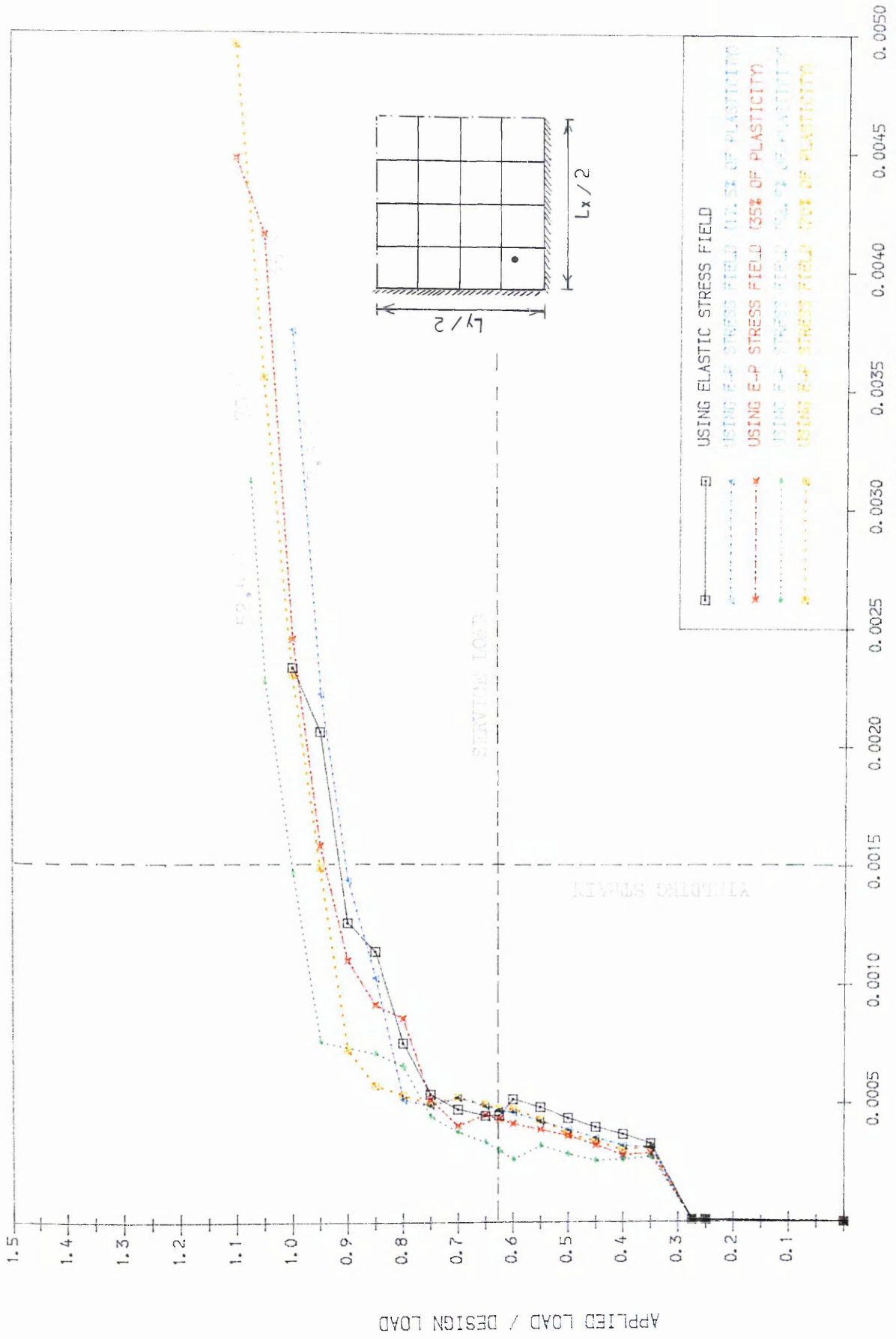


FIG. (5.5) STEEL STRAIN CURVES FOR BOTTOM STEEL (ELT. 1, L.YR. NO. 11, GP. NO. 4)  
FOR SLB1A

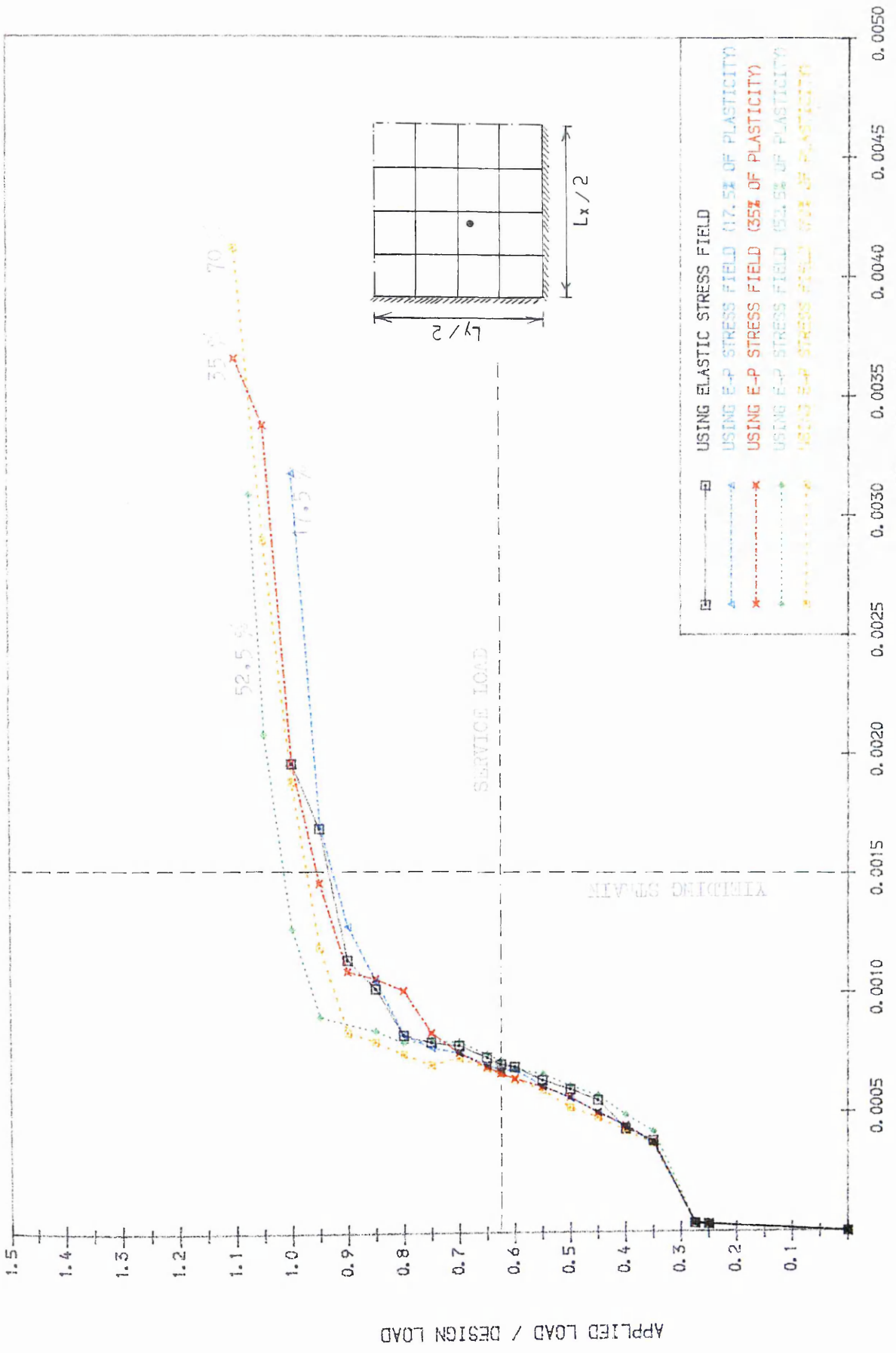


FIG. (5.6) STEEL STRAIN CURVES FOR BOTTOM STEEL (ELT. 6, LYR. NO. 11, GP. NO. 4) FOR SLB1A

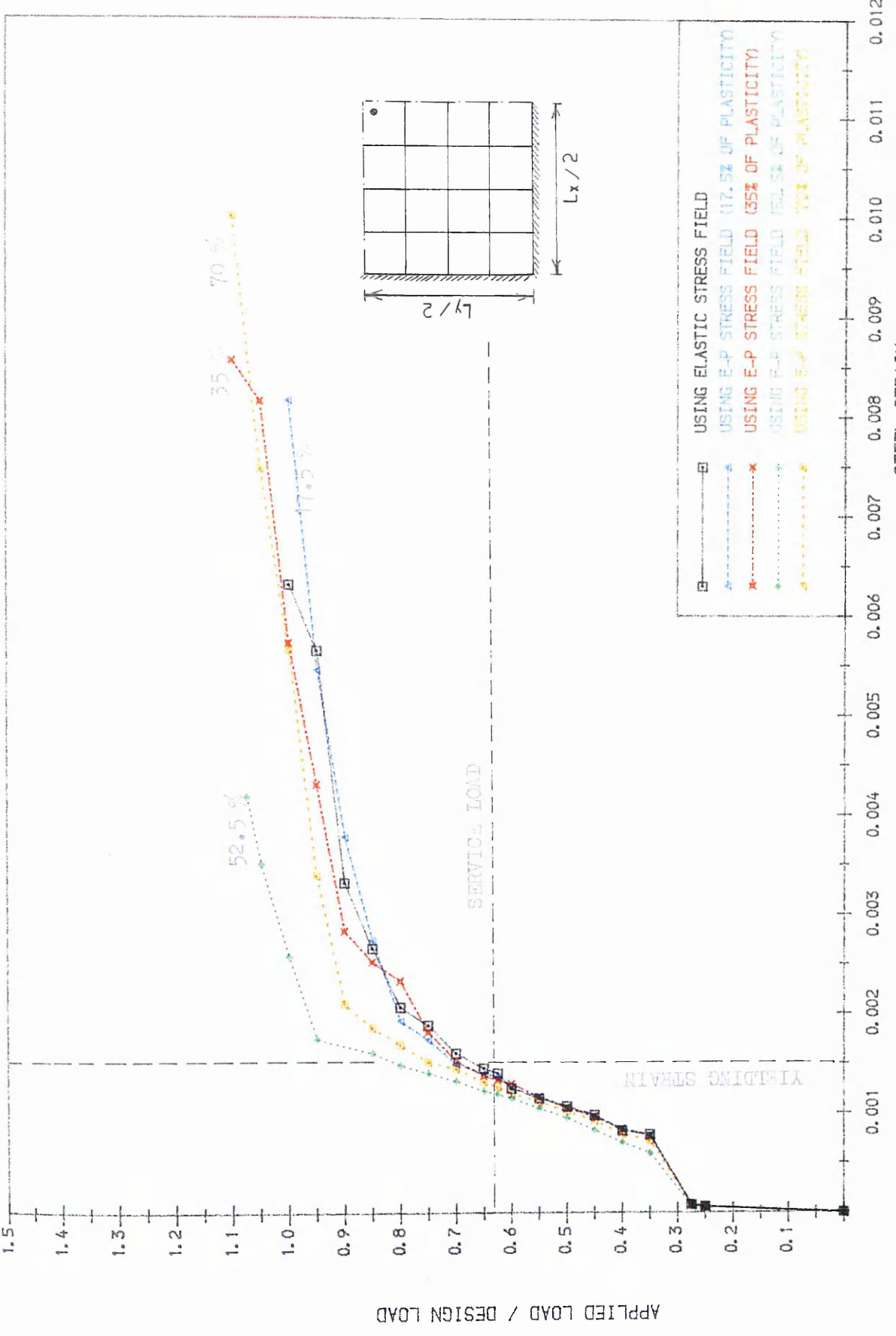


FIG. (5.7) STEEL STRAIN CURVES FOR BOTTOM STEEL (ELT. 16, L.YR. NO. 11, GP. NO. 4) FOR SLB1A

		0.800	0.700	C . L
		0.850		
0.950	0.950			
0.950				

SLB.1.A0 (Elastic Stress Field)

		0.850	0.675	C . L
		0.850		
0.950	0.950			
0.950				

SLB.1.A1 (E-P stress field of 17.5% plasticity)

Figure (5-8) Spread of yield (yielding load / design load)



		0.800	0.675	C . L
		0.850		
0.975	0.975			
0.925				

SLB.1.A2 (E-P stress field of 35.0% of plasticity)

		0.800	0.700	C . L
		0.900		
0.975	0.975			
0.975				

SLB.1.A3 (E-P stress field of 52.5% plasticity)

Figure (5-8) Spread of yield (yielding load / design load)

		0.875	0.725
		0.950	
1.000	1.000		
0.950			

C . L

SLB.1.A4 (E-P stress field of 70.0% plasticity)

Figure (5-8) Spread of yield (yielding load / design load)

### 5.6.3 Test series "2":

This series include tests on slabs which are simply supported along all the edges but loaded with four point loads. Five runs, SLB2.A.1 , SLB2.A.2 , SLB2.A.3 and SLB2.A.4 were performed. The results are shown in Figures (5-9) to (5-13), and are summarized in tables (5-3) and (5-4).

### 5.6.4 Conclusions:

(1) The service behaviour of all the slabs in this series was satisfactory. The deflection limit of span / 250 was reached at an average of 60% of the design load. This gives a reasonable service behaviour in terms of deflections. Here again the deflection at service load has decreased slightly as the degree of plasticity of the stress field increases (see table 5-3 and figure 5-19). Steel strain curves show an onset of yielding of an average of 75% of the design load, and the maximum steel strain in the case of non elastic stress field is in general less than that of an elastic stress field as shown in figure (5-20).

(2) In general the yielding load recorded during the numerical experiments for the slabs designed by non elastic stress field has been higher than the one corresponding to elastic stress field.

(3) Table (5-4) shows that the difference between the ultimate load and the onset of yielding remained in general stable as the degree of plasticity of the stress field increases. This difference at the centre of the plate (under the design load) is larger than the one at the corners.

(4) As far as the ultimate load is concerned, the slabs designed by non elastic stress field have recorded an ultimate load slightly smaller than the one of an elastic stress field ( $\approx 4\%$ ), this is due to the fact of smoothing the peak under the point load.

TABLE (5-3) " S L B - 2 - A "

CASE	% of plty	D <sub>ef.</sub> (sl)	D <sub>ef.</sub> (d)	$\epsilon_{sl} / \epsilon_0$	$\epsilon_d / \epsilon_0$	U.L.T
SLB.2.A0	0.00 %	9.10 mm	38.29 mm	.722	3.254	1.120
SLB.2.A1	27.00 %	9.05 mm	50.31 mm	.724	4.256	1.090
SLB.2.A2	45.00 %	8.90 mm	29.93 mm	.714	2.471	1.060
SLB.2.A3	61.00 %	8.70 mm	29.82 mm	.714	2.523	1.060
SLB.2.A4	82.00 %	7.60 mm	37.76 mm	.697	4.069	1.090

$\delta_{sl} = 1980 / 250 \approx 8.0$  mm ; Service Load = 0.630 x design load ;  $\epsilon_{sl}$  = max steel strain at service load ;  $\epsilon_d$  = max steel strain at design load ;  $\epsilon_0$  = yielding strength of steel = .215E-02 ; D<sub>ef.</sub>(sl) = max deflection at service load ; D<sub>ef.</sub>(d) = max deflection at the design load ; U.L.T = ultimate load / design load.

Table (5-4): The difference between the ultimate load ( $P_{ult}$ ) and the yielding load ( $P_y$ ) divided by the design load.  $(P_{ult} - P_y) / P_{ult}$

EI <sup>t</sup> . Case No	1	2	6	11	12	16
Elastic	16.00 %	4.00 %	16.00 %	16.00 %	16.00 %	16.00 %
27.00 %	13.00 %	10.00 %	16.00 %	16.00 %	16.00 %	16.00 %
45.00 %	13.00 %	4.00 %	16.00 %	25.00 %	25.00 %	25.00 %
61.00 %	10.00 %	4.00 %	16.00 %	16.00 %	16.00 %	16.00 %
82.00 %	12.00 %	12.00 %	16.00 %	16.00 %	16.00 %	16.00 %

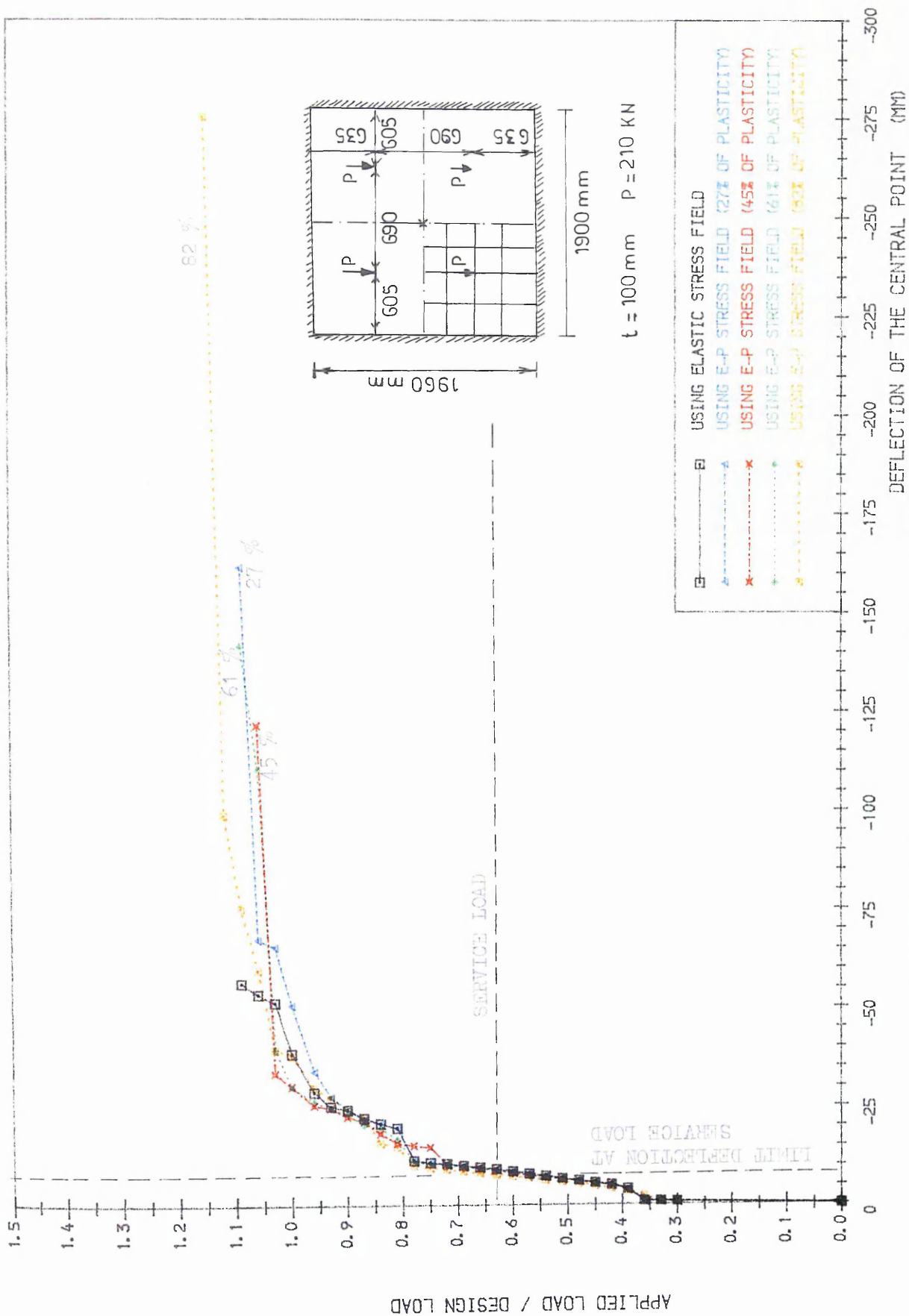


FIG. (5.9) LOAD-DISPLACEMENT CURVES FOR SIMPLY SUPPORTED SLAB UNDER FOUR POINT LOADS, DESIGNED BY VARIOUS TYPES OF STRESS FIELD.

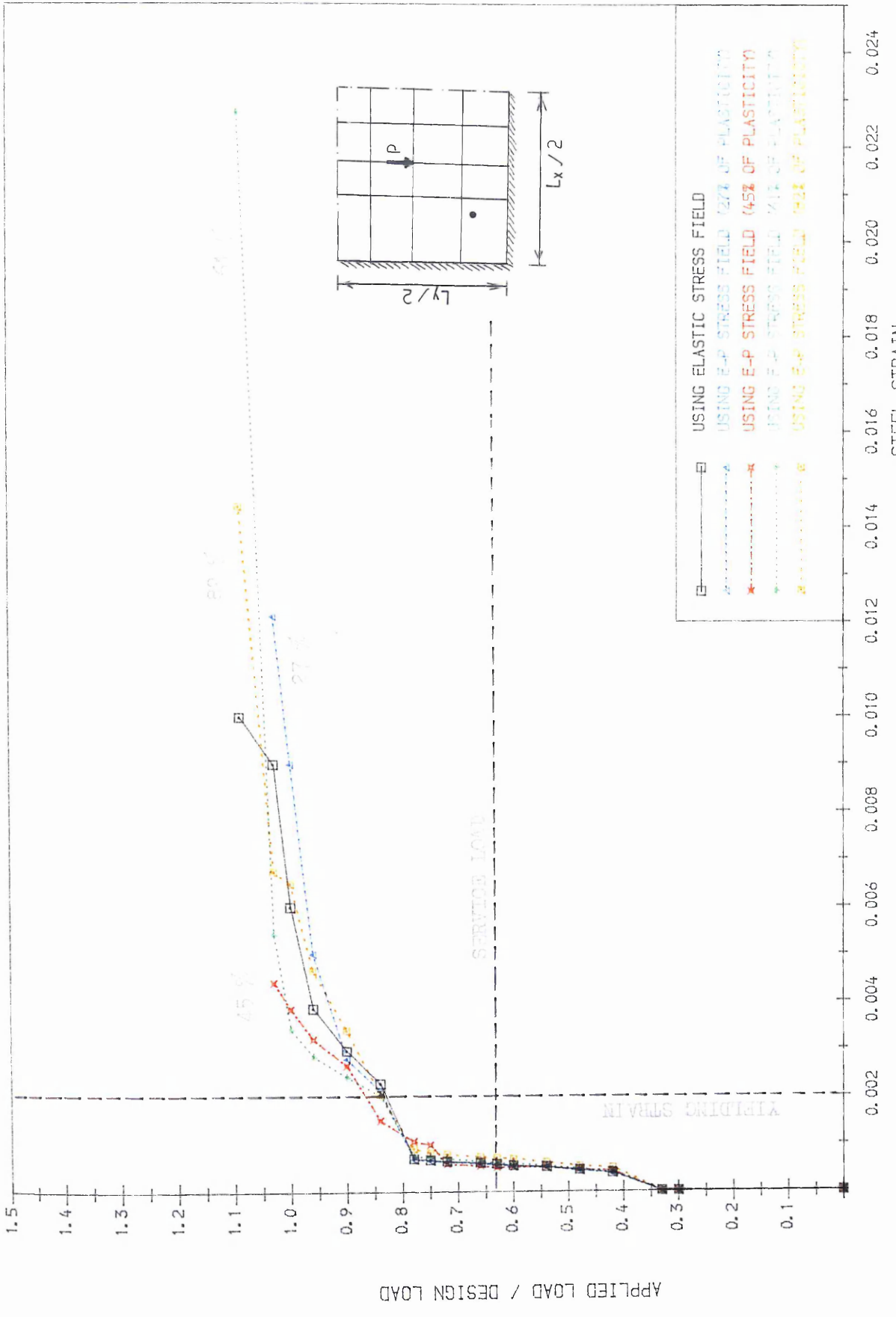


FIG. (5.10) STEEL STRAIN CURVES FOR BOTTOM STEEL (ELT. 1, L.YR. NO. 11, GP. NO. 4) FOR SLB2A

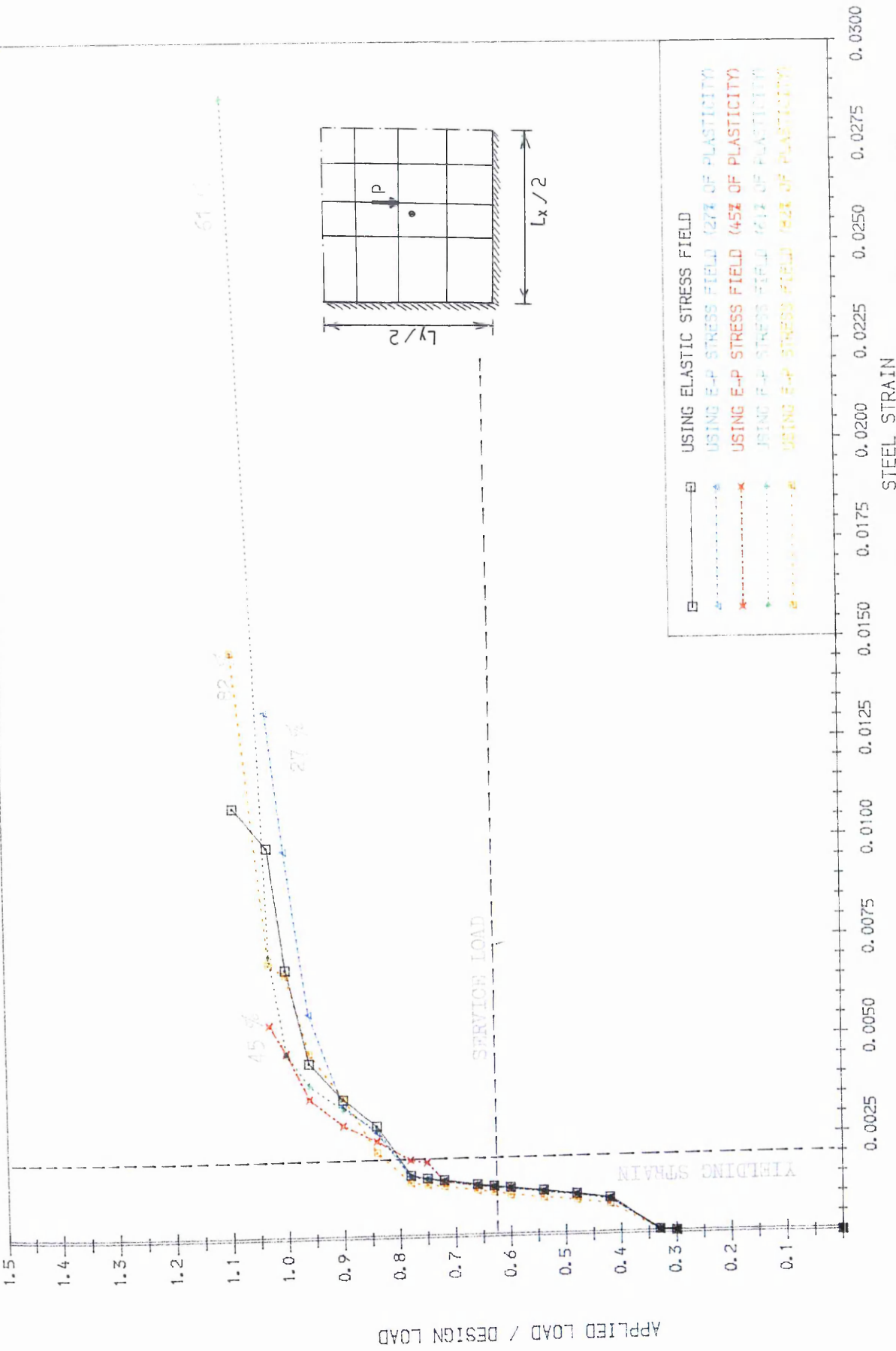


FIG. (5.11) STEEL STRAIN CURVES FOR BOTTOM STEEL (ELT. 6, L.YR. NO. 11, GP. NO. 4) FOR SLB2A

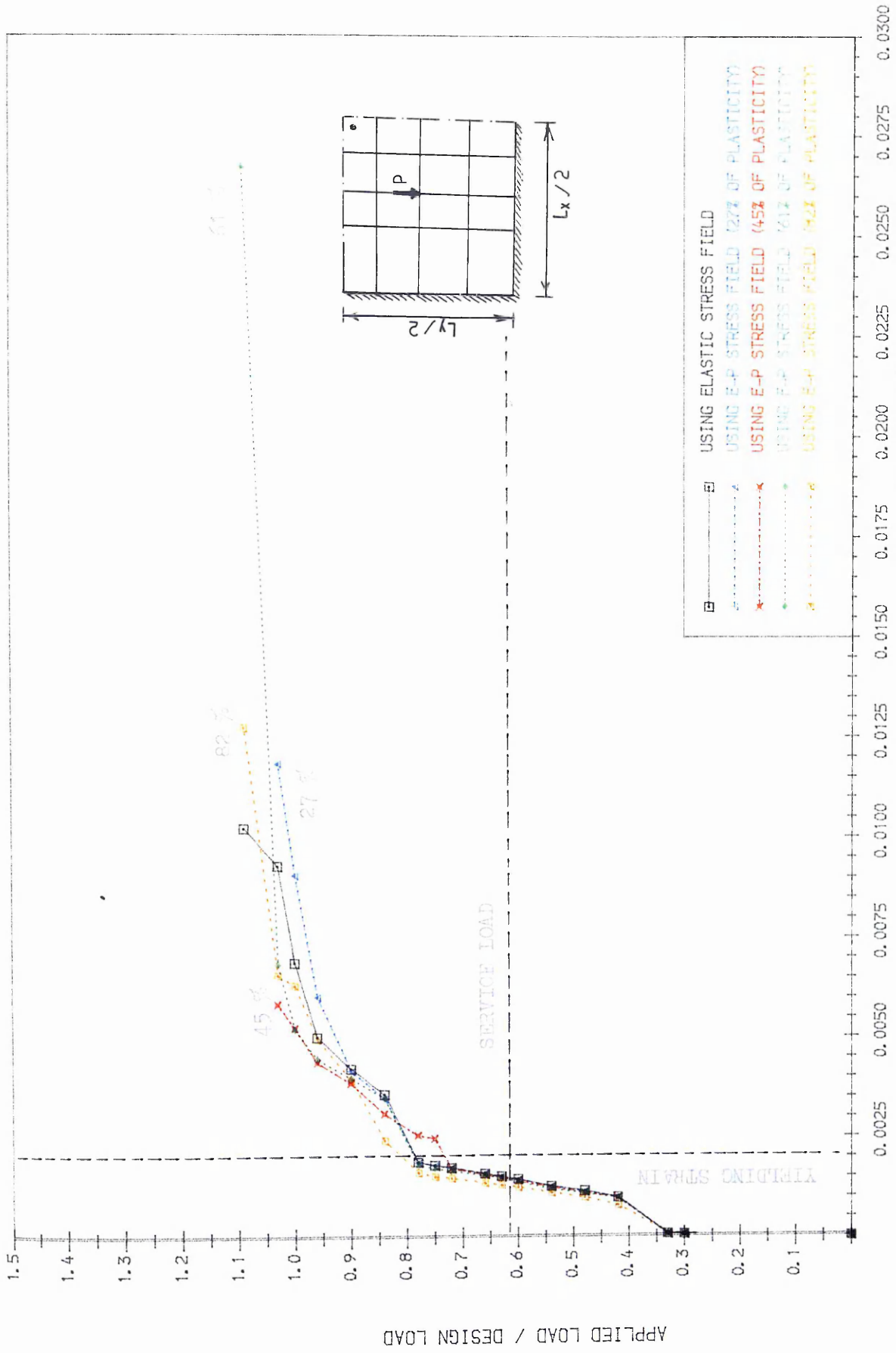


FIG. (5. 12) STEEL STRAIN CURVES FOR BOTTOM STEEL (ELT. 16, L.YR. NO. 11, GP. NO. 4) FOR SLB2A



		0.840	0.840	C . L
	0.840	0.840		
0.960	0.840			
0.840				

SLB.2.A0 (Elastic Stress Field)

		0.840	0.840	C . L
	0.840	0.840		
0.900	0.840			
0.870				

SLB.2.A1 (E-P stress field of 27% plasticity)

Figure (5-13) Spread of yield (yielding load / design load)

		0.750	0.750	C . L
	0.840	0.750		
0.960	0.840			
0.870				

SLB.2.A2 (E-P stress field of 45% plasticity)

		0.840	0.840	C . L
	0.840	0.840		
0.960	0.840			
0.900				

SLB.2.A3 (E-P stress field of 61% plasticity)

Figure (5-13) Spread of yield (yielding load / design load)

		0.840	0.840	C . L
	0.840	0.840		
0.870	0.840			
0.870				

SLB.2.A4 (E-P stress field of 82.0% plasticity)

Figure (5-13) Spread of yield (yielding load / design load)

### 5.6.5 Test series"3"

This series include the tests SLB.3.A.0, SLB.3.A.1, SLB.3.A.2, SLB.3.A.3, and SLB.3.A.4 . The slabs were all simply supported at the edges plus a central column support. The slabs were designed for a uniform distributed load of  $0.17 \text{ KN/mm}^2$  . The results are shown in figures (5-14) to (5-18) and again summarized in tables (5-5) and (5-6).

### 5.6.6 Conclusions:

In this series of numerical experiments, the effect of using non elastic stress field in the direct design method on the service behaviour has been found to be satisfactory.

(1) The deflection limit of span / 250 has not been reached. However, this deflection has increased of an average of 17% as the degree of plasticity of the stress field is increased (see figure 5-19).

In terms of steel strains, the bottom steel has yielded just near failure at 1.17 the design load in the case of elastic stress field and didn't yield in the remaining cases of non elastic stress field. However, for the top steel the onset of yielding has been recorded between 60% and 70% of the design load, which is satisfactory too.

The maximum steel strain at service load has increased as the degree of plasticity increases (see figure 5-20). This is due to the fact that we have put less steel at the top near the column.

In general this series of slabs have behaved differently from the previous slabs tested. This is due to a general early yielding of the whole slab.

(2)The difference between the ultimate load and the onset of yielding remained in general stable as the degree of plasticity of the stress field increases and in all cases it didn't exceed 25%.

(3) In terms of ultimate load, a negligible reduction of the ultimate load in comparison with the one of elastic stress field ( $\approx 4\%$ ) is noticed.

TABLE (5-5) " S L B - 3 - A "

CASE	% of ply	D <sub>ef.</sub> (s1)	D <sub>ef.</sub> (d)	$\epsilon_{s1} / \epsilon_0$	$\epsilon_d / \epsilon_0$	U.L.T
SLB.3.A0	0.00 %	2.67 mm	6.61 mm	.645	1.880	1.170
SLB.3.A1	20.00 %	3.13 mm	9.53 mm	.724	2.593	1.012
SLB.3.A2	40.00 %	3.14 mm	9.90 mm	.731	2.809	1.012
SLB.3.A3	60.00 %	3.11 mm	9.14 mm	.731	2.655	1.047
SLB.3.A4	73.33 %	3.14 mm	10.28 mm	.741	3.055	1.047

$\delta_{s1} = 5000 / 250 = 20$  mm ; Service Load = 0.610 x design load ;  $\epsilon_{s1}$  = max steel strain at service load ;  $\epsilon_d$  = max steel strain at design load ;  $\epsilon_0$  = yielding strength of steel = .145E-02 ; D<sub>ef.</sub>(s1) = max deflection at service load ; D<sub>ef.</sub>(d) = max deflection at the design load ; U.L.T = ultimate load / design load.

Table (5-6): The difference between the ultimate load ( $P_{ult}$ ) and the yielding load ( $P_y$ ) divided by the design load.  $(P_{ult} - P_y) / P_{ult}$   
(b) = bottom steel ; (t) = top steel

EI <sup>t</sup> . Case No	1(b)	2(b)	6(b)	11(t)	12(t)	16(t)
Elastic	/	4.00 %	/	11.00 %	21.50 %	/
20.00 %	/	18.00 %	/	21.50 %	21.50 %	/
40.00 %	18.00 %	7.50 %	/	21.50 %	21.50 %	/
60.00 %	18.00 %	11.00 %	/	21.50 %	21.50 %	/
73.33 %	18.00 %	11.00 %	4.00 %	25.00 %	25.00 %	/



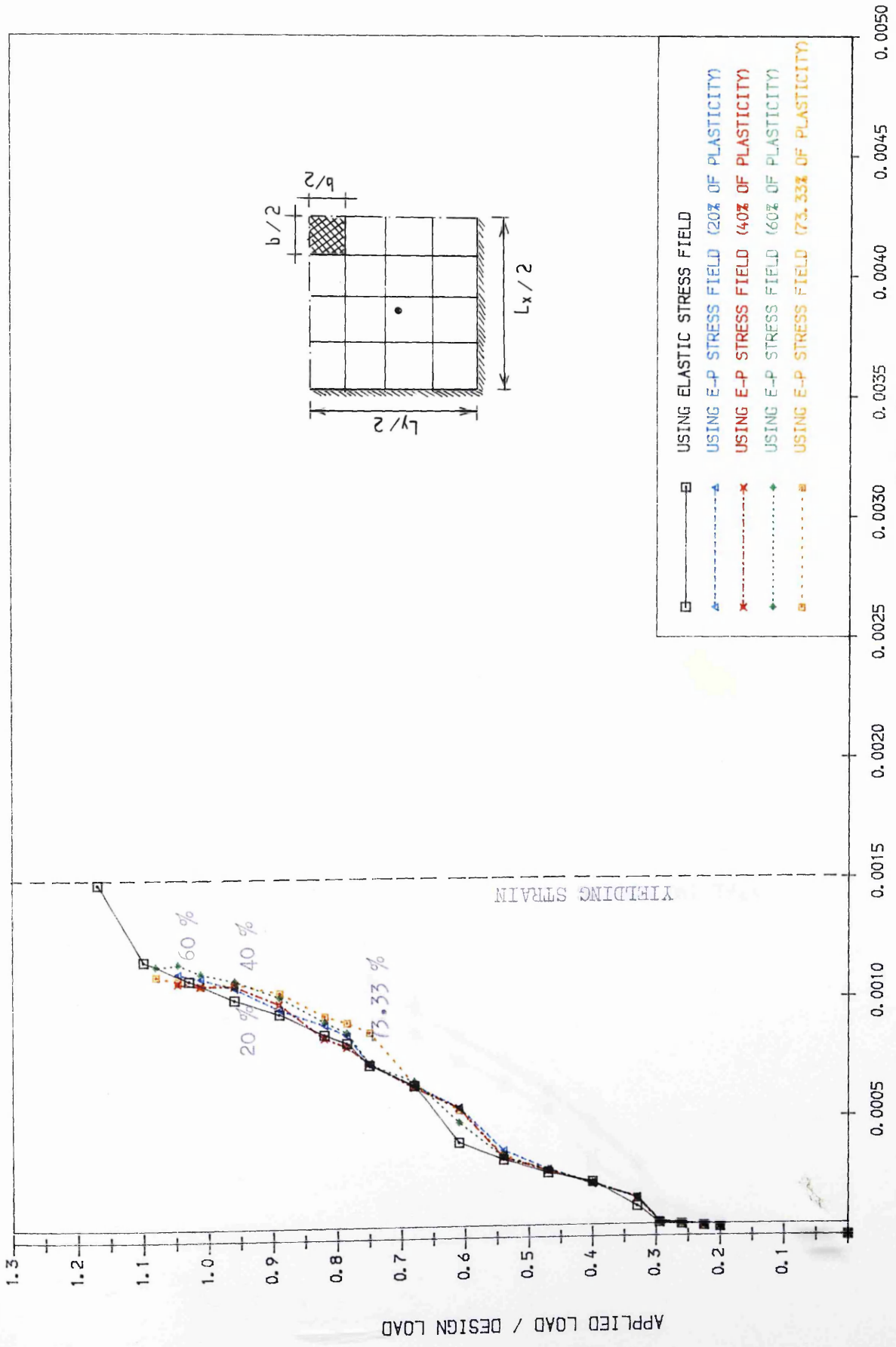


FIG. (5.15) STEEL STRAIN CURVES FOR BOTTOM STEEL (EL.T. 6, L.YR. NO. 11, GP. NO. 4) FOR SLB3A



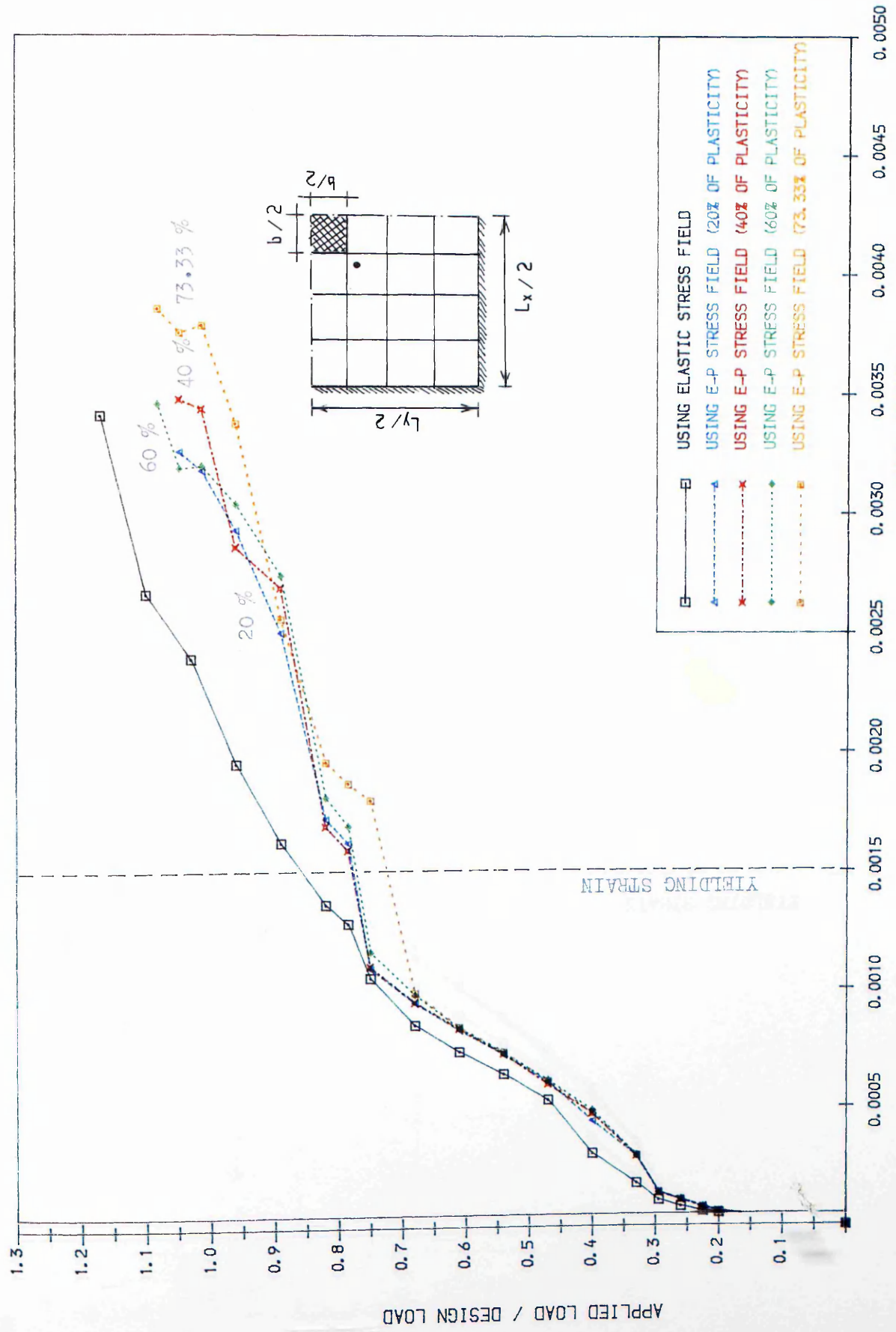


FIG. (5. 16) STEEL STRAIN CURVES FOR TOP STEEL (ELT. 11, L.YR. NO. 2, GP. NO. 4) FOR SLB3A

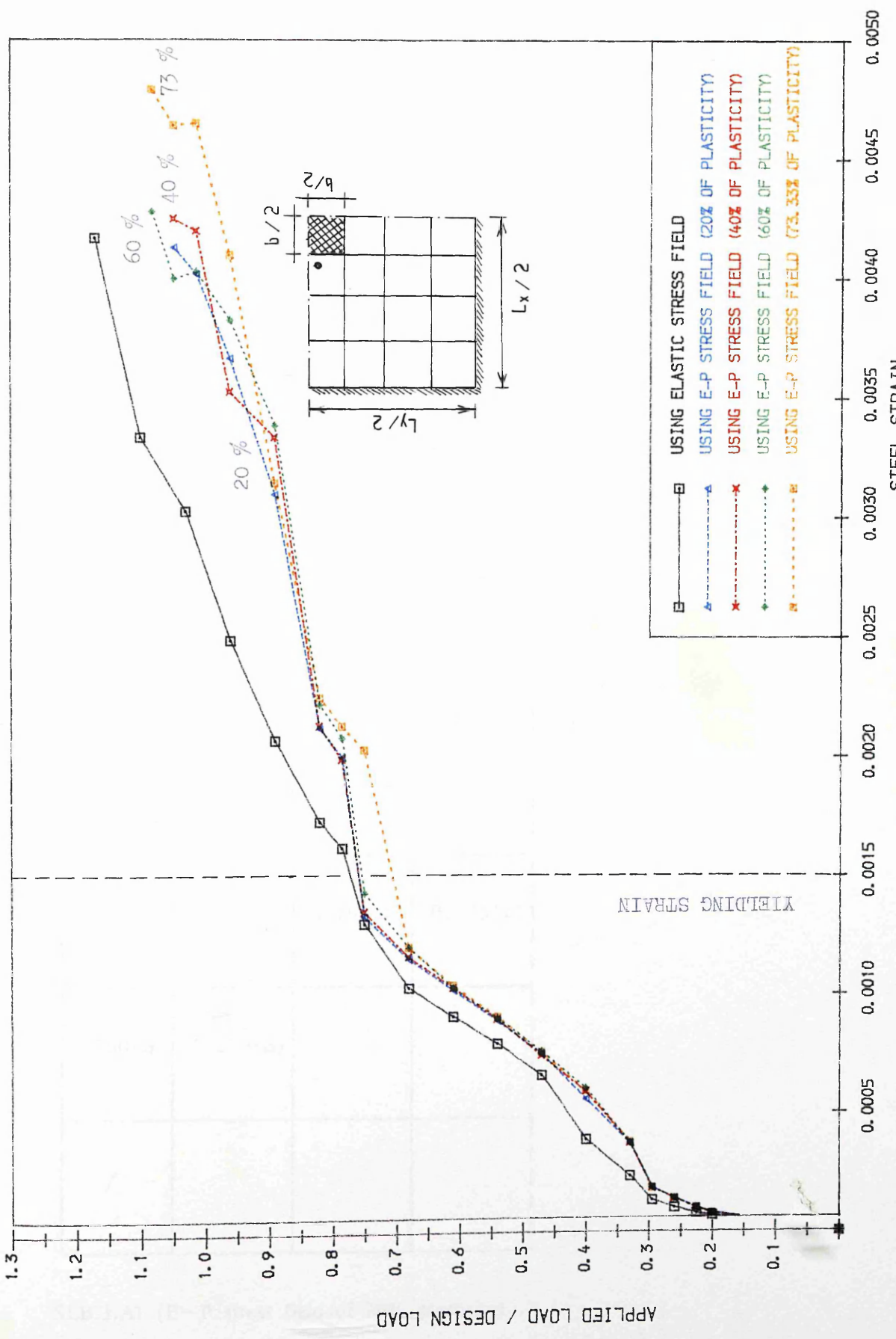


FIG. (5. 17) STEEL STRAIN CURVES FOR TOP STEEL (ELT. 12, L.YR. NO. 2, GP. NO. 4) FOR SLB3A

(b) = bottom steel ; (t) = top steel

C . L

		0.785(t)	/
		0.890(t)	0.785(t)
0.960(b)	1.170(b)		
/			

SLB.3.A0 (Elastic Stress Field)

C . L

		0.785(t)	/
		0.785(t)	0.785(t)
0.960(b)	1.170(b)		
/			

SLB.3.A1 (E-P stress field of 20% plasticity)

Figure (5-18) Spread of yield (yielding load / design load)

		0.785(t)	/	C . L
		0.785(t)	0.785(t)	
0.925(b)	/			
0.820(b)				

SLB.3.A2 (E-P stress field of 40% of plasticity)

		0.750(t)	/	C . L
		0.785(t)	0.785(t)	
0.890(b)	/			
0.820(b)				

SLB.3.A3 (E-P stress field of 60% plasticity)

Figure (5-18) Spread of yield (yielding load / design load)

		0.750(t)	/	C . L
		0.750(t)	0.785(t)	
0.890(b)	0.960(b)			
0.820(b)				

SLB.3.A4 (E-P stress field of 73.33% plasticity)

Figure (5-18) Spread of yield (yielding load / design load)

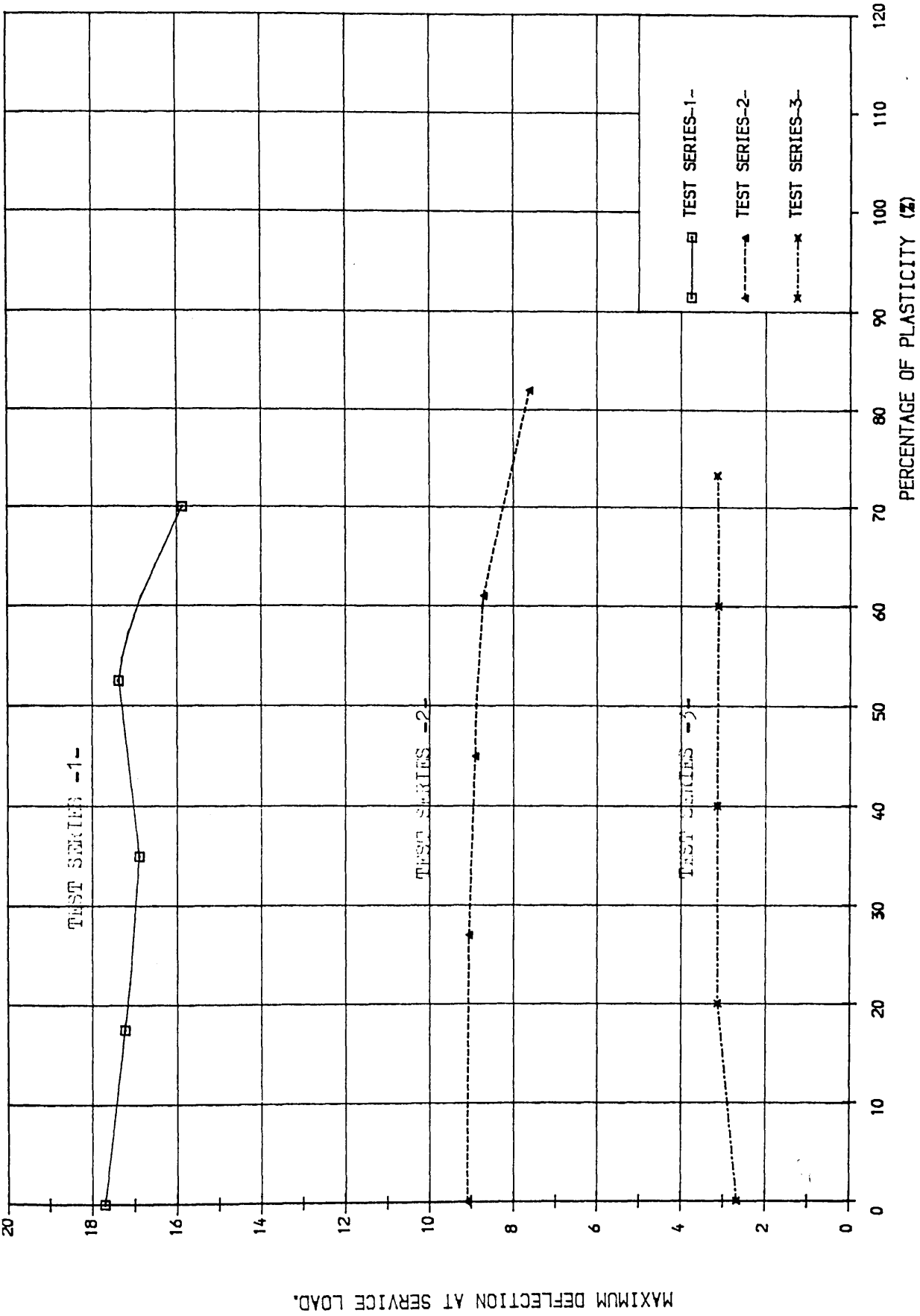


FIG. (5. 19) VARIATION OF THE DEFLECTION AT SERVICE LOAD WITH THE % OF PLASTICITY.

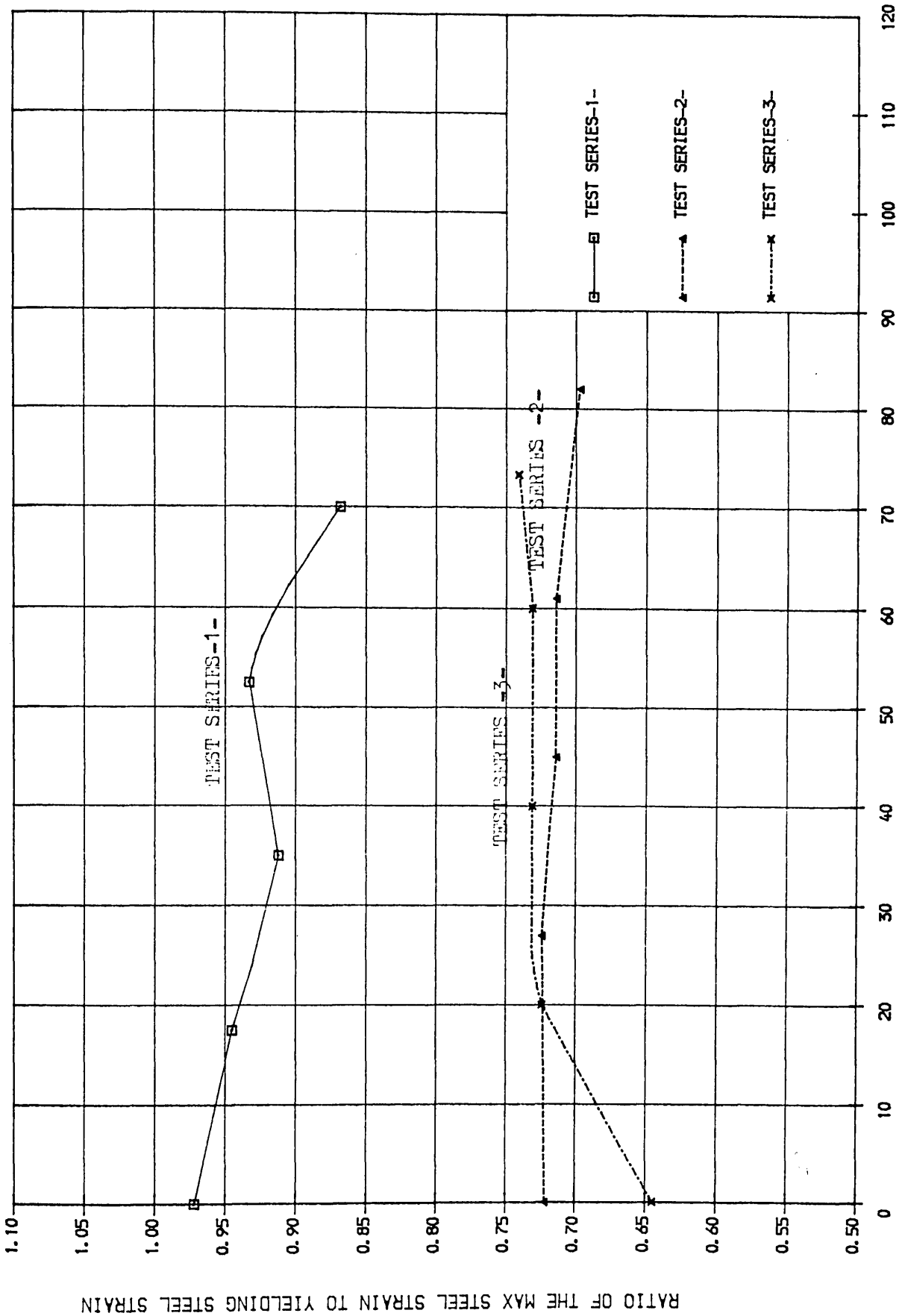


FIG. (5.20) VARIATION OF THE RATIO OF THE MAX STEEL STRAIN TO YIELDING STRAIN AT SERVICE LOAD WITH THE % OF PLASTICITY.

RATIO OF THE MAX STEEL STRAIN TO YIELDING STEEL STRAIN

**CHAPTER SIX :****ELASTO- PLASTIC ANALYSIS OF REINFORCED CONCRETE SLABS****BASED ON WOOD-ARMER YIELD CRITERION.****6.1 Introduction:**

In the previous chapter a detailed nonlinear analysis has been carried out in order to predict the behaviour of the slab both at service load and ultimate load. Such analysis gives realistic evaluation of deflections, stresses and strains for the whole range of loading till failure. This has been made by modelling the nonlinear behaviour of the individual material of which a reinforced concrete slab is made.

In general, such analysis is research rather than practical analysis oriented. One important aspect that will concern any designer is to find out the ultimate load of a given reinforced slab without going into details of cracks etc. Consequently, a development of a simple computer program to predict the ultimate load of reinforced concrete slabs is undoubtedly useful.

This chapter summarizes the steps of the development of such finite element program and some examples demonstrating the accuracy of this program will be given as well.

**6.2 Program:**

The structure of the program developed in this study is same as the Mindlin program (see sec.3.2). A flow chart of this program is given in figure (6-1).

Originally Mindlin program used Tresca and Von Mises laws, which closely approximate metal behaviour.



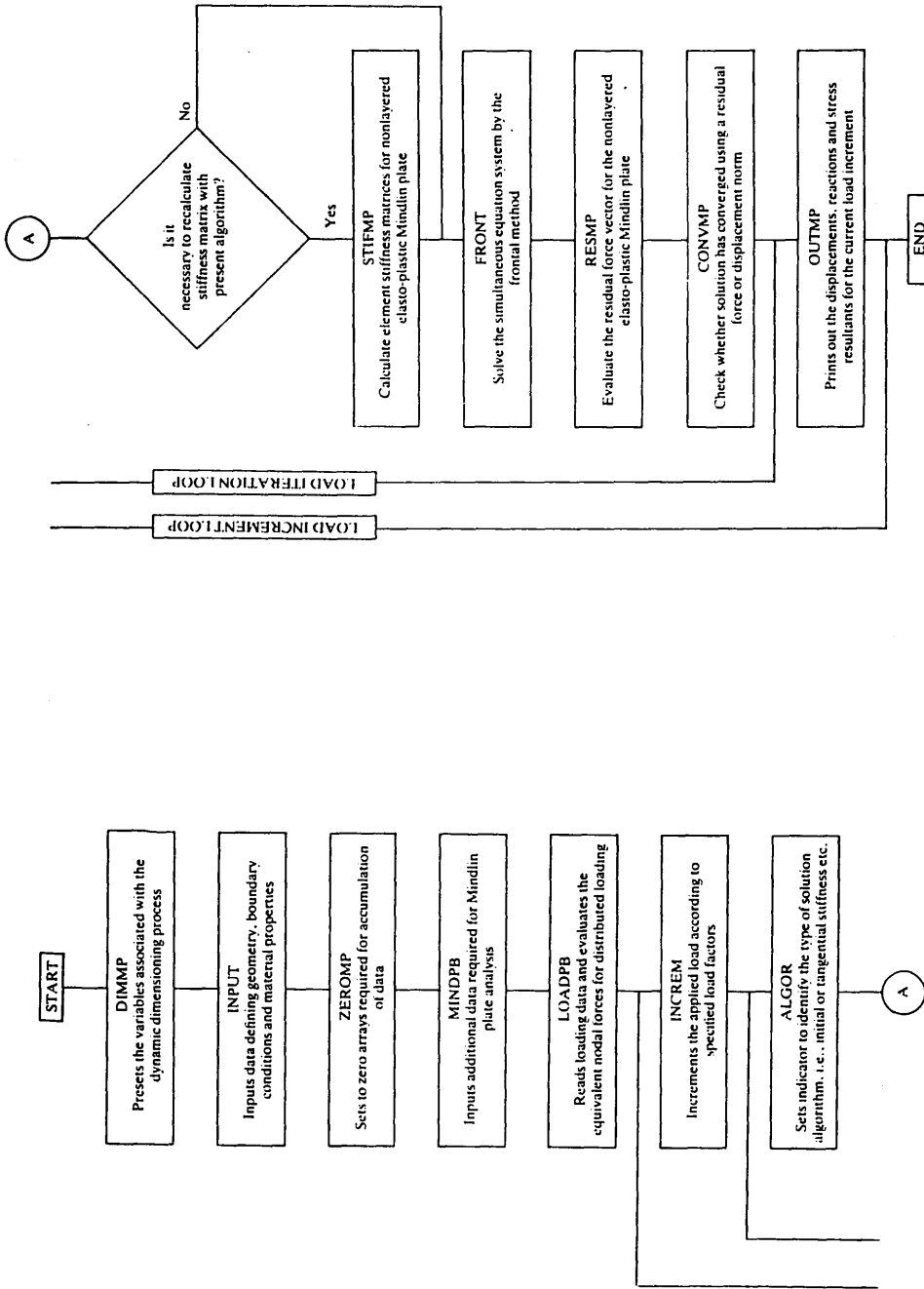


Figure (6-1) Overall structure of the WOOD-ARMER program

The yield criterion which can be shown to be easy to implement in such finite element program and which has been proved to give good results, is Wood-Armer criterion (Sec.2.2.2).

The derivation of this yield criterion was given in detail in Sec(2.2.2), and the finite element formulation in chapter three. Therefore only the mathematical formulation of the yield criterion and the alterations made in consequence will be given in the following.

### 6.2.1 The mathematical formulation of the yield criterion:

$$(i) F_1 = -(M_x^{*b} - M_x + M_\alpha^{*b} \cdot \cos^2 \alpha)(M_\alpha^{*b} \cdot \sin^2 \alpha - M_y) + (M_{xy} + M_\alpha^{*b} \cdot \sin \alpha \cdot \cos \alpha)^2 \leq 0 \quad \dots(6.1)$$

$$F_2 = -(M_x^{*t} + M_x - M_\alpha^{*t} \cdot \cos^2 \alpha)(M_\alpha^{*t} \cdot \sin^2 \alpha + M_y) + (M_{xy} - M_\alpha^{*t} \sin \alpha \cdot \cos \alpha) \leq 0.0 \quad \dots(6.2)$$

where  $F_i$  = yield function ( $i = 1$  for bottom steel and  $i = 2$  for top steel ),

$(M_x^*, M_y^*)$  = Representing moments developed by the reinforcement in the slab in X- and  $\alpha$ - direction respectively.

This will be provided as Input Data to the program.

b = stands for bottom steel

t = stands for top steel

$(M_x, M_y, M_{xy})$  = Direct bending moments and twisting moment resulting from the analysis

$\alpha$  = direction of the skew reinforcement taken as clockwise from the X- axis ( $\alpha = 90^\circ$  for the case of orthogonal reinforcement).

(ii) The normality rule:

$$a_b = \begin{bmatrix} \frac{\partial F_1}{\partial M_x} \\ \frac{\partial F_1}{\partial M_y} \\ \frac{\partial F_1}{\partial M_{xy}} \end{bmatrix} = \begin{bmatrix} + (M_\alpha^{*b} \cdot \sin^2 \alpha - M_y) \\ + (M_x^{*b} - M_x + M_\alpha^{*b} \cdot \cos \alpha) \\ 2(M_{xy} + M_\alpha^{*b} \cdot \sin \alpha \cdot \cos \alpha) \end{bmatrix} \quad \dots (6.3)$$

which is an outward normal vector.

$$a_t = \begin{bmatrix} \frac{\partial F_2}{\partial M_x} \\ \frac{\partial F_2}{\partial M_y} \\ \frac{\partial F_2}{\partial M_{xy}} \end{bmatrix} = \begin{bmatrix} -(M_\alpha^{*t} \cdot \sin^2 \alpha + M_y) \\ -(M_x^{*t} + M_x - M_\alpha^{*t} \cdot \cos \alpha) \\ 2(M_{xy} - M_\alpha^{*t} \cdot \sin \alpha \cdot \cos \alpha) \end{bmatrix} \quad \dots (6.4)$$

which is an outward normal vector.

### 6.2.2 Alterations to the Mindlin program:

The main subroutines which have been modified are subroutine FLOWMP, subroutine INVMP and subroutine RESMP. Subroutines INPUT and STIFMP have been only accomodated to these changes.(All these subroutines are presented in the appendix A )

#### i- Subroutine FLOWMP:

This subroutine evaluates the following prameters for both  $F_1$  and  $F_2$ :

- Flow vector  $a$  ( $a_b$  and  $a_t$ )
- the vector  $D.a$
- the scalar  $a^T.D.a$  and  $a / a^T.D.a$

where  $D$  is the constitutive elastic matrix.

ii- Subroutine INVMP:

This subroutine evaluates the following parameters:

- $F_1$  as given by Eq- (6.1)
- $FBT1 = M_x^{*b} - M_x + M_\alpha^{*b} \cdot \cos^2 \alpha$
- $FBT2 = M_\alpha^{*b} \cdot \sin^2 \alpha - M_y$
- $F_2$  as given by Eq- (6.2)
- $FTP1 = M_x^{*t} + M_x - M_\alpha^{*t} \cdot \cos^2 \alpha$
- $FTP2 = M_\alpha^{*t} \cdot \sin^2 \alpha + M_y$

The above equations represent the conditions of yielding, ie yielding occurs if :

$$\left\{ \begin{array}{l} F_1 > 0 \quad \text{or,} \\ FBT1 < 0 \quad \text{or,} \\ FBT2 < 0 \end{array} \right. \quad \dots \text{ for positive yield surface}$$

or

$$\left\{ \begin{array}{l} F_2 > 0 \quad \text{or,} \\ FTP1 < 0 \quad \text{or,} \\ FTP2 < 0 \end{array} \right. \quad \dots \text{ for negative yield surface}$$

In addition to the check for yielding, this subroutine is called to evaluate the reduction factor 'ALPHA' once yielding occurs.

'ALPHA' is a factor by which the stress components ( $M_x, M_y, M_{xy}$ ) are multiplied to determine what fraction of the stresses will be requested to keep on the yield surface.

iii- Subroutine RESMP:

This subroutine evaluates the residual forces as:

$$\left[ f^e \right]^r = \int_{A^e} [ B ]^T \sigma^r dv \quad \dots (6.5)$$

where  $B$  = strain matrix and  $\sigma^r$  = stress at Gauss point  $(M_x, M_y, M_{xy})$ , at the iteration  $(r)$  for the element  $(e)$ .

One feature of this subroutine is that after evaluating the incremental stress  $(dM_x, dM_y, dM_{xy})$  it checks if :

$$\left. \begin{array}{l} (1) F_1(M_x + dM_x, M_y + dM_y, M_{xy} + dM_{xy}) \\ \quad FBT1(M_x + dM_x) \\ \quad FBT2(M_y + dM_y) \end{array} \right\} \dots \text{have been violated}$$

or

$$\left. \begin{array}{l} (2) F_2(M_x + dM_x, M_y + dM_y, M_{xy} + dM_{xy}) \\ \quad FTP1(M_x + dM_x) \\ \quad FTP2(M_y + dM_y) \end{array} \right\} \dots \text{have been violated}$$

If the latest checks are positive in respect of one or both functions ( $F_1$  and  $F_2$ ), the stresses are corrected and brought on to the yield surface by allowing plastic strain.

Example of stress correction:

Step-1- Computation of ALPHA:

$$F_1 = -(M_x^* - \text{ALPHA} \cdot M_x + M_{\alpha}^* \cdot \cos^2 \alpha)(M_{\alpha}^* \cdot \sin^2 \alpha - \text{ALPHA} \cdot M_y) + (\text{ALPHA} \cdot M_{xy} + M_{\alpha}^* \cdot \sin \alpha \cdot \cos \alpha)^2 = 0.0$$

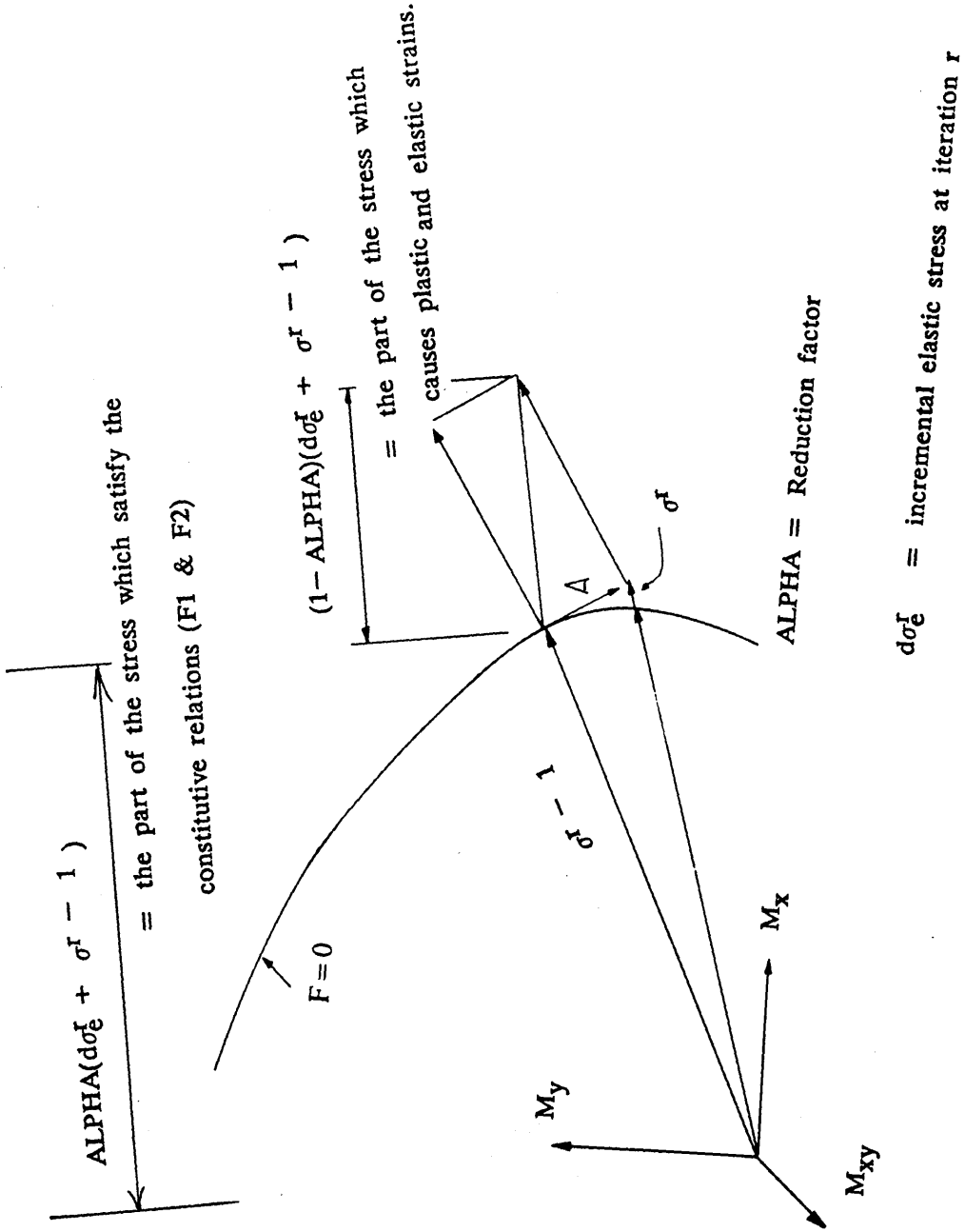


Figure (6-2) Stress correction  $\sigma^r - 1$  = state of the stress at the previous iteration.

Let  $A^* = M_x^* + M_\alpha^* \cos^2 \alpha$ ,  $B^* = M_\alpha^* \sin^2 \alpha$  and  $C^* = M_\alpha^* \sin \alpha \cos \alpha$

Then  $F_1$  reduces to :

$$\text{ALPHA}^2(M_{xy}^2 - M_x \cdot M_y) + \text{ALPHA}(A^* \cdot M_y + B^* \cdot M_x + 2 \cdot C^* \cdot M_{xy}) + (Z^2 - A^* \cdot B^*) = 0.0$$

Thus with  $A1 = M_{xy}^2 - M_x \cdot M_y$

$$B1 = A^* \cdot M_y + B^* \cdot M_x + 2 \cdot C^* \cdot M_{xy}$$

$$C1 = C^{*2} - A^* \cdot B^*$$

the solution of the second order equation gives:

$$\text{ALPHA}_{1,2} = \frac{-B1 \pm \sqrt{B1^2 - 4A1 \cdot C1}}{2A1} \quad \dots(6.6)$$

ALPHA is then chosen such as the following condition is verified :

$$\left\{ \begin{array}{l} \text{ALPHA} \times M_x \leq M_x^{*b} + M_\alpha^{*b} \cdot \cos^2 \alpha \\ \text{and} \\ \text{ALPHA} \times M_y \leq M_\alpha^{*b} \cdot \sin^2 \alpha \end{array} \right.$$

The same procedure as above is used with  $F_2$  in the case of negative yield surface (top steel).

Step-2- Computation of the part of the stress which causes elastic strains only on the yield surface:

$$A = (1 - \text{ALPHA})(d\sigma_e^r + \sigma^r - 1) - d\sigma_p^r \quad \dots(6.7)$$

where  $d\sigma_p^r = d\lambda D a$

where  $d\lambda$  = plastic multiplier (as given in 3.2.3)

$D$  = matrix of elastic rigidity.

$a$  = flow vector (as defined in sect.6.2.1)

Step-3- Computation of the total stress  $\sigma^r$  :

$$\sigma^r = (\sigma^{r-1} + d\sigma_e^r) \text{ALPHA} + [(1 - \text{ALPHA})(\sigma^{r-1} + d\sigma_e^r) - d\lambda D a] \quad \dots(6.8)$$

This represents the correct stress  $\sigma^r$  at the iteration  $r$  .

Note that with plate bending cases the term stress  $\sigma$  stand for the bending and twisting moments ( $M_x, M_y, M_{xy}$ ).

iv- Curved boundaries:

To allow slab systems presenting curved or inclined boundary supports to be analysed by 'WOOD-ARMER' program, the necessary changes have been incorporated within this program.

These changes consist of transforming the variables at nodes of curved or inclined boundary to  $(w, \theta_n, \theta_t)$  see Fig- (6-3), using the transformation matrix,  $[T_b]$ , so that:

$$\begin{bmatrix} P_i \\ C_{ni} \\ C_{ti} \end{bmatrix} = [T_b]^T \begin{bmatrix} P_i \\ C_{xi} \\ C_{yi} \end{bmatrix} \quad \text{and} \quad \begin{bmatrix} w_i \\ \theta_{xi} \\ \theta_{yi} \end{bmatrix} = [T_b] \begin{bmatrix} w_i \\ \theta_{ni} \\ \theta_{ti} \end{bmatrix} \quad \dots(6.9)$$

where  $(P_i, C_{ni}, C_{ti})$  and  $(P_i, C_{xi}, C_{yi})$  are the vectors of the nodal force and nodal couples related to the local axes  $(n, t)$  and the global axes  $(x, y)$  respectively,  $(w_i, \theta_{xi}, \theta_{yi})$  and  $(w_i, \theta_{ni}, \theta_{ti})$  are the vectors of displacements related to the global axes  $(x, y)$  and local axes  $(n, t)$  respectively, and finally  $[T_b]$  is the transformation



matrix given by :

$$[T_b] = \begin{bmatrix} 1 & 0 & 0 \\ 0 & \cos\alpha^* & -\sin\alpha^* \\ 0 & \sin\alpha^* & \cos\alpha^* \end{bmatrix} \quad \dots(6.10)$$

$\alpha^*$  is the angle of inclination of the curved or inclined edge to X axis.

Since the nodal forces and displacements are linked through the stiffness matrix by :

$$\begin{bmatrix} P_i \\ C_{xi} \\ C_{yi} \end{bmatrix} = [K] \begin{bmatrix} w_i \\ \theta_{xi} \\ \theta_{yi} \end{bmatrix} \quad \dots(6-11)$$

where  $[K]$  is the stiffness matrix, and the equivalent expression with respect to the local axes (n,t) is given as:

$$\begin{bmatrix} P_i \\ C_{ni} \\ C_{ti} \end{bmatrix} = [K] \begin{bmatrix} w_i \\ \theta_{ni} \\ \theta_{ti} \end{bmatrix} \quad \dots(6-12)$$

$$\text{where } [K]' = [T_b]^T [K] [T_b] \quad \dots(6-13)$$

Thus the steps used in the solution can be summarised as follows:

(1) For any node to be restrained in local directions, transform the applied nodal forces to coincide with the local axes.

(2) Transform the relevant element stiffness submatrices according to (6-13).

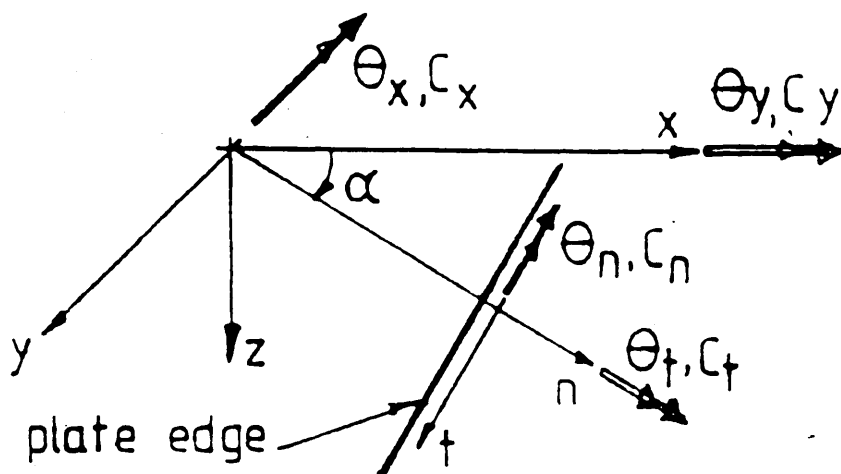


**Figure (6-3) Positive directions of  
moment and couple vectors.**

(3) Assemble the loads and stiffnesses in the usual way and solve for the displacements. The resulting displacements and reactions are then transformed to the global axes (x,y) before evaluating the stresses.

### 6.3 Convergence study:

In order to have confidence in the accuracy of the results obtained from the finite element analyses, a convergence study in the elastic– plastic domain must be carried out. The main objective of this part of the work is to reduce the computer cost while maintaining good accuracy. The sensitivity of the solution of the mesh size and convergence tolerance were studied for the case of a simply supported square slab under a uniformly distributed load. The slabs were orthogonally reinforced using the direct design method with elastic stress field.

#### 6.3.1 Mesh size:

Figure (6– 4a) shows the load– displacement curves for the 2 x 2 , 4 x 4 and 6 x 6 element meshes for the simply supported square slab.

The curves show that there isn't a great difference between using 4, 16 and 36 elements.

This is due to the fact that the design method used evaluates the reinforcement with the ultimate flexural moments ( $M_x^*$ ,  $M_y^*$ ), so that all points of the slab start yielding at about the same load and with small redistribution the whole slab will turn into a mechanism simultaneously and then fails.

#### 6.3.2 Tolerance:

The convergence criterion used in this program is the same as the one given by Eq– (3.28) which is based on a 'tolerable' value of the residual forces.

Figure (6– 4b) depicts load– displacement curves for three different values of tolerance :  $t_1 = 5\%$ ,  $t_2 = 2\%$  and  $t_3 = 1\%$ . Here also the results in respect to the ultimate load are not greatly affected.

The error on the ultimate load ( $P_{ult}$ ) was 2.2% when 5% of tolerance is used.

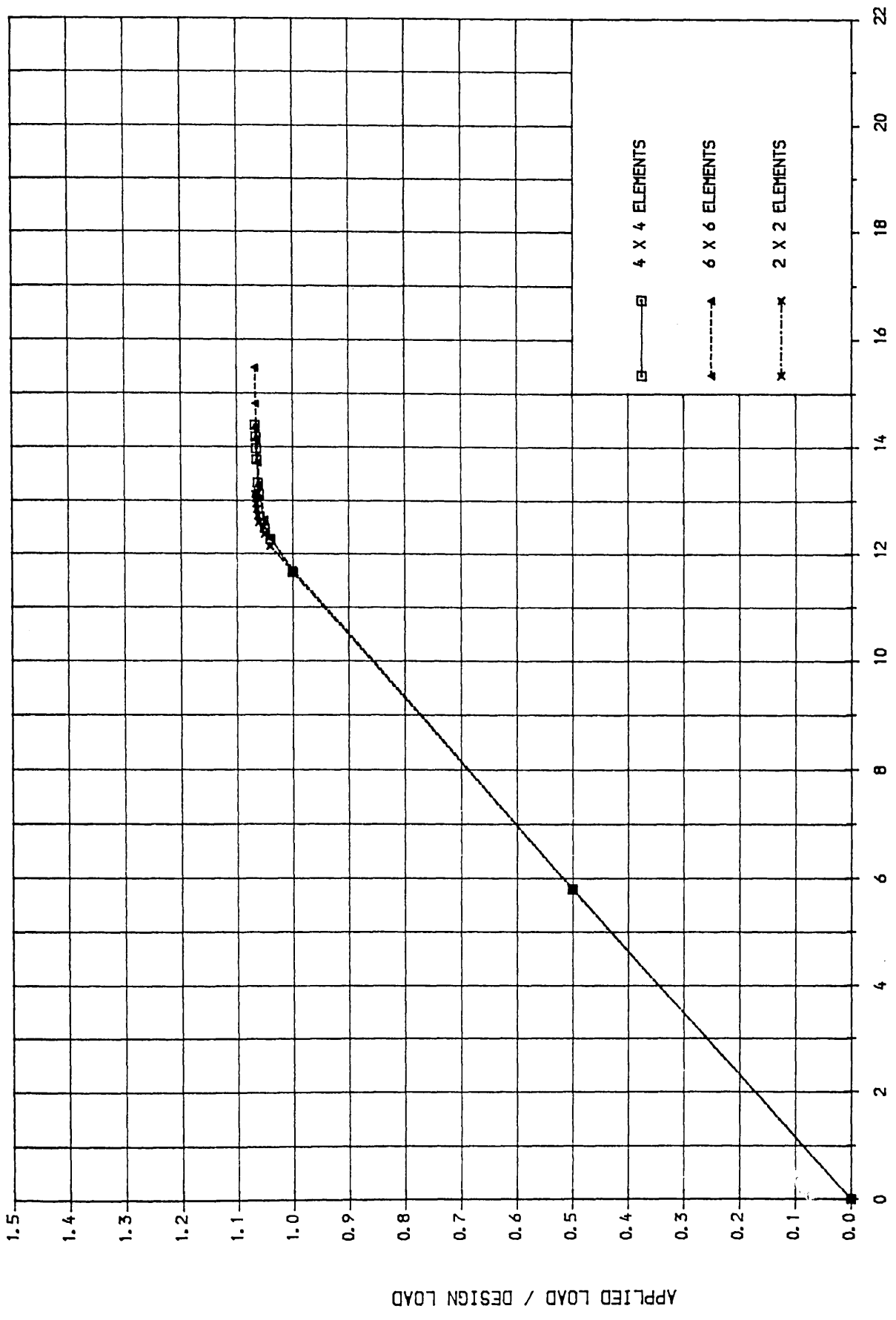


FIG-(6-4A) LOAD-DISPLACEMENT CURVE FOR THE MESH SIZE STUDY

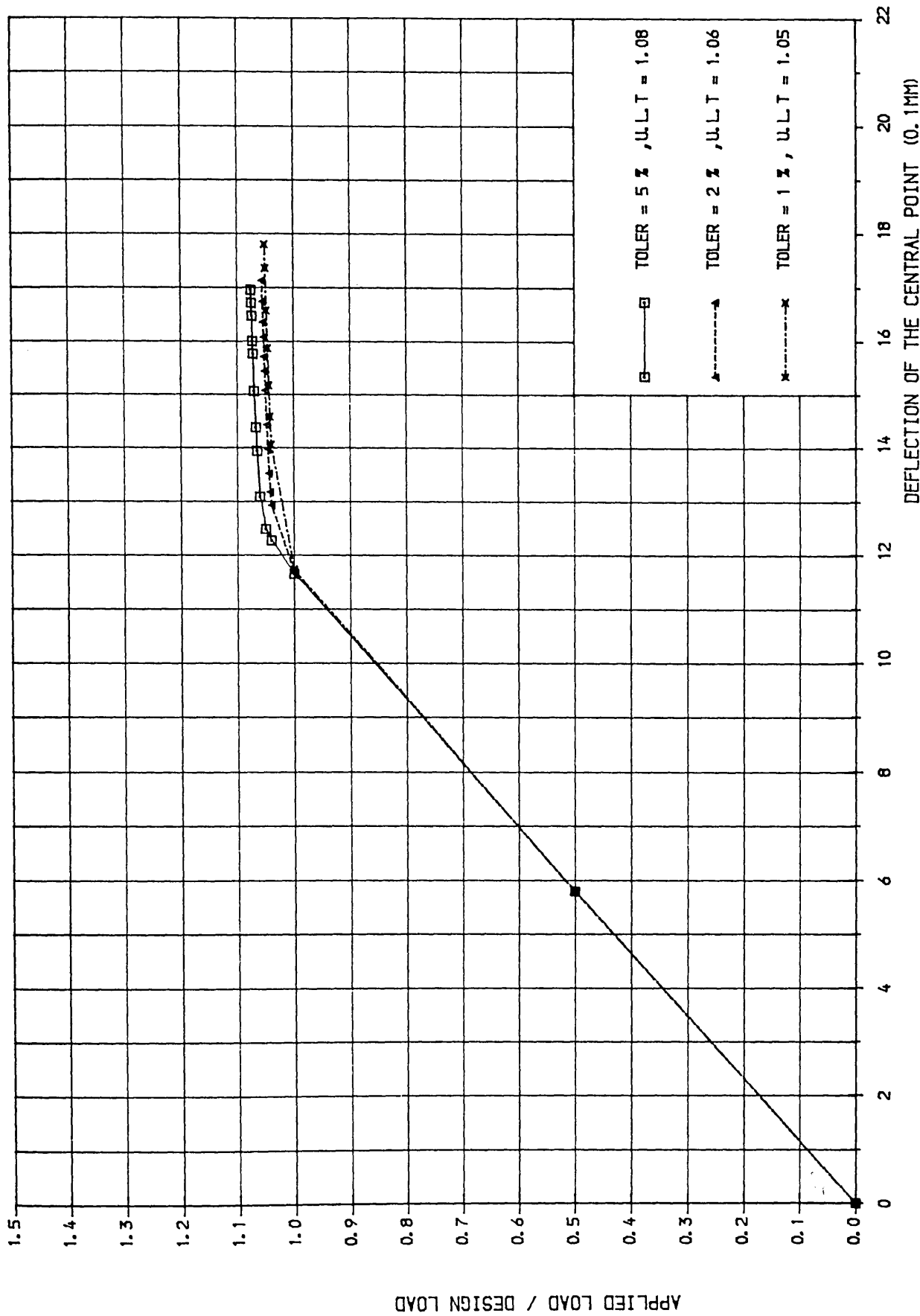


FIG- (6-4B) DISPLACEMENT CONVERGENCE CRITERION

So we can conclude that a tolerance value of 4% is sufficient to evaluate the ultimate load with good accuracy.

#### 6.4 Numerical application:

The object of this section is to demonstrate the reliability of the developed computer program 'WOOD-ARMER' and to conduct some selected numerical experiments.

The basic idea is that if over a wide range of experimental problems this model can produce an accurate prediction for the ultimate load, the program can then be used to predict the ultimate load of similar problems.

##### 6.4.1 A simply supported slab under a central point load:

This experimental slab is taken from tests performed by the Portland Cement Association in 1954. Results for this test may be found in reference (20).

The slab is 1828.8 mm square, 139.7 mm thick and is reinforced with an isotropic mesh of 0.99% reinforcing steel.(Fig- (6-5))

The load is centrally applied on a small column cast integrally with the slab as is also shown in figure (6-5). While figure (6-6) shows the grid used in the finite element analysis, together with the material properties.

In the nonlinear solution, the combined algorithm was used, with the maximum number of iterations limited to 50. A convergence force tolerance of 3.5% was adopted. The average number of iterations to reach the specified convergence tolerance varied from 2 to 5. The load was applied in 11 increments as shown in the load- displacement curve (Fig.6-7).

This figure shows also the ultimate load predicted, which was 1.5% higher than the experimental failure load. While figure (6-8) shows the spread of yielding. (The Gauss points which were at a yielding prior failure)

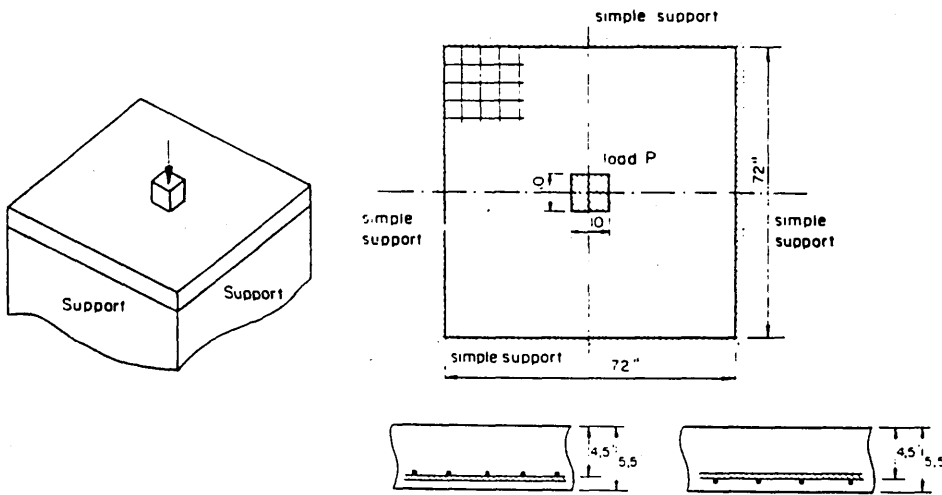


**Figure (6-5) Loading system and reinforcement mesh for the simply supported square slab.**

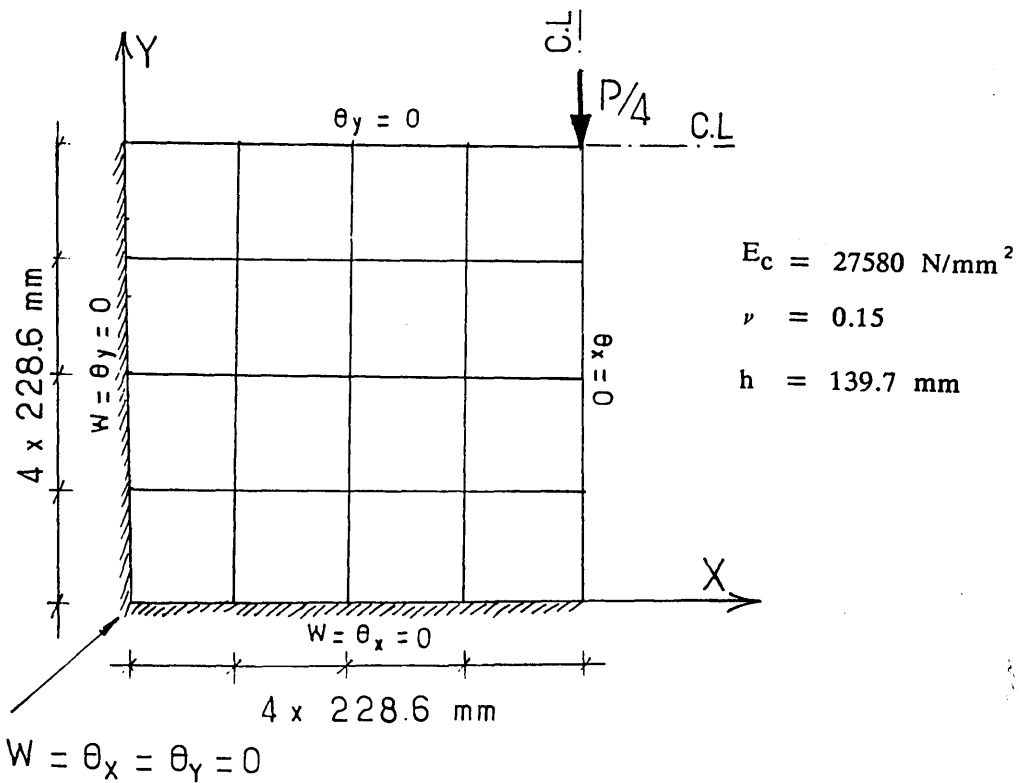


**Figure (6-6) Mesh idealization**

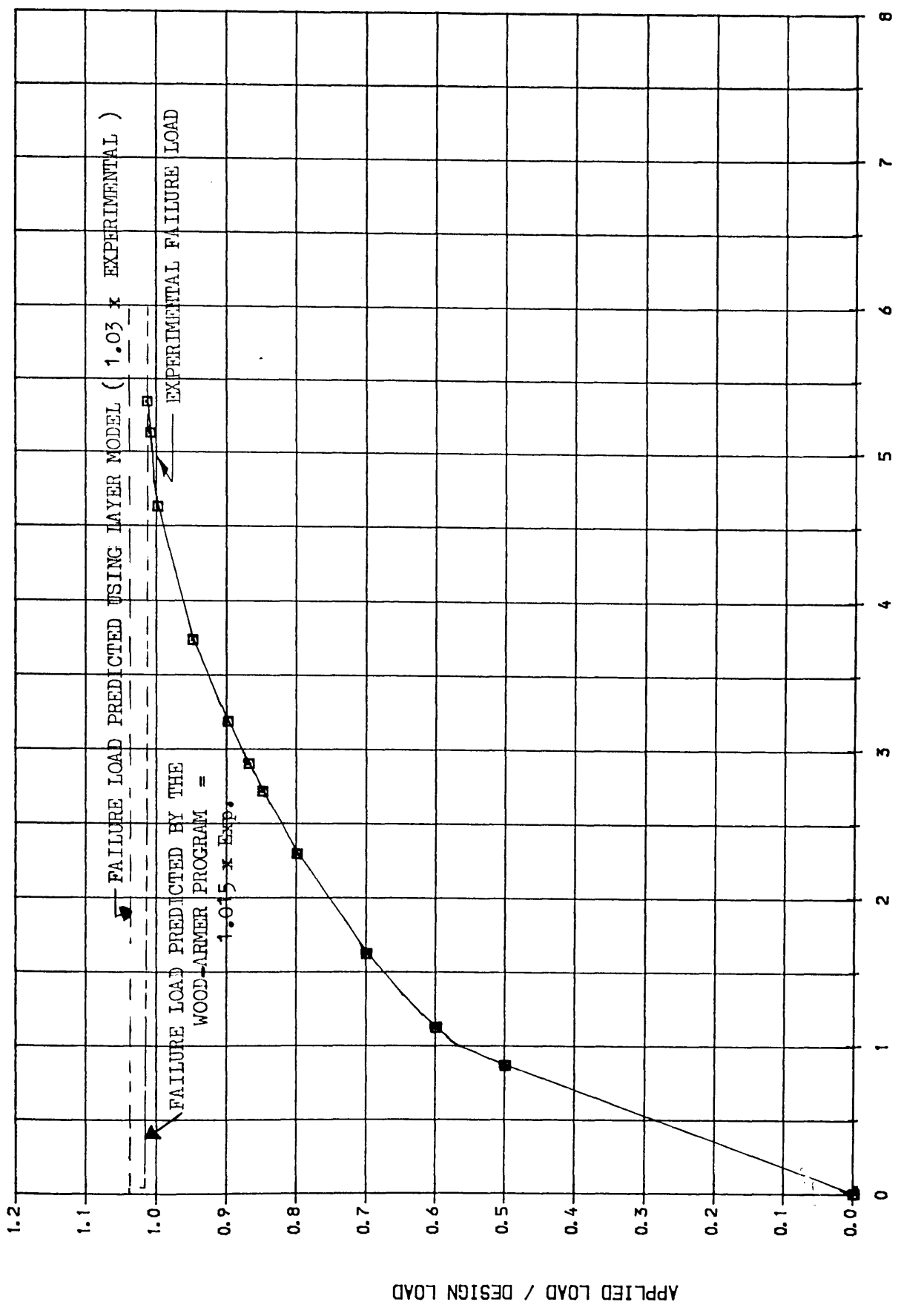


FIG-(6-7) LOAD-DISPLACEMENT CURVE FOR DDTREPE SLAB

APPLIED LOAD / DESIGN LOAD

DEFLECTION OF THE CENTRAL POINT (MM)

FAILURE LOAD PREDICTED USING LAYER MODEL ( 1.03 x EXPERIMENTAL )

FAILURE LOAD PREDICTED BY THE WOOD-ARMER PROGRAM = 1.015 x Exp.

EXPERIMENTAL FAILURE LOAD



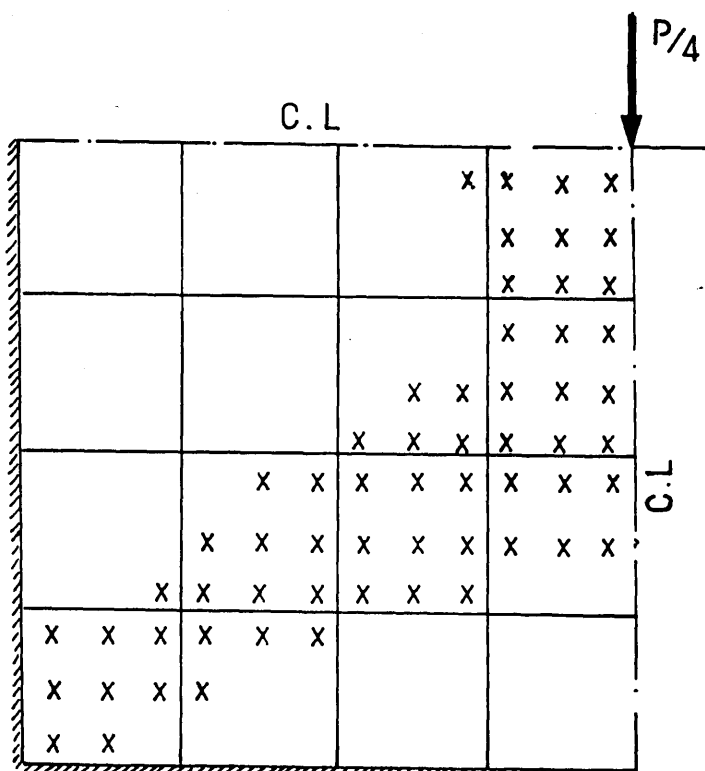


Figure (6-8) Spread of yielding

#### 6.4.2 Hago's slab:

The model No.3 of the five slabs tested by Hago<sup>(30)</sup> has been chosen for this analysis.

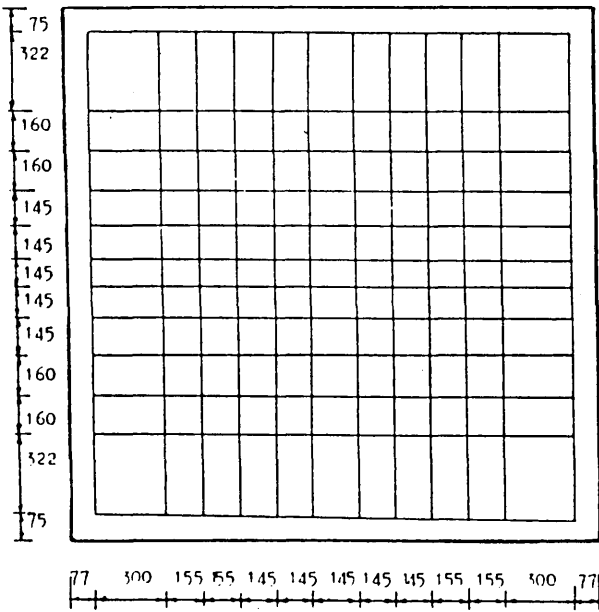
The slab is 2100 x 2160 mm square and is simply supported along each edge to give 1900 x 1960 mm spans. The thickness of the slab is 100 mm, with orthotropic reinforcement as shown in Fig- (6-9). The slab was loaded with four point loads as shown in Fig- (6-9c ).

Figure (6-9d ) shows the grid used in the finite element solution together with the material properties.

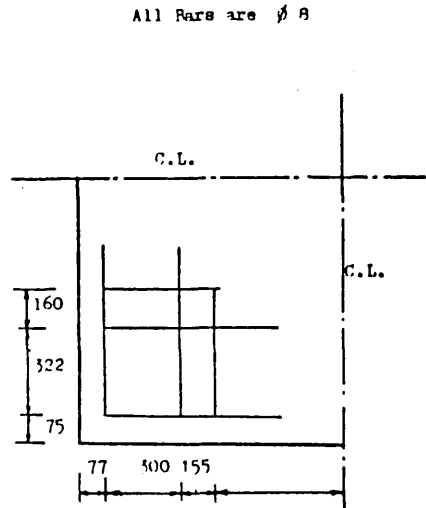
Taking advantage of symmetry, only one quarter of the plate using 2x2 element mesh was analysed. This subdivision is dictated by the idealization of the steel reinforcement.

The combined algorithm was used to solve the nonlinear equations, with the maximum number of iterations limited to 50. A convergence force tolerance of 3.5% was adopted. The specified convergence tolerance was reached with an average number of iterations of 2. The load was applied in 11 increments as shown in figure (6-10). This figure shows the load- displacement curve and from which we can see the ultimate load reached. This was 6% less than the experimental one. This is due to the fact that within this program the check of yielding is done for each Gauss point and thus the subdivision of the slab into finite element meshes and their equivalent design moments computed from the steel areas provided, have an important effect on the ultimate load.

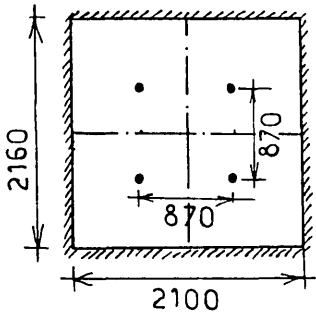
Figure (6-11) shows the spread of yielding for this example which represents the yielding lines constituting the mechanism pattern.



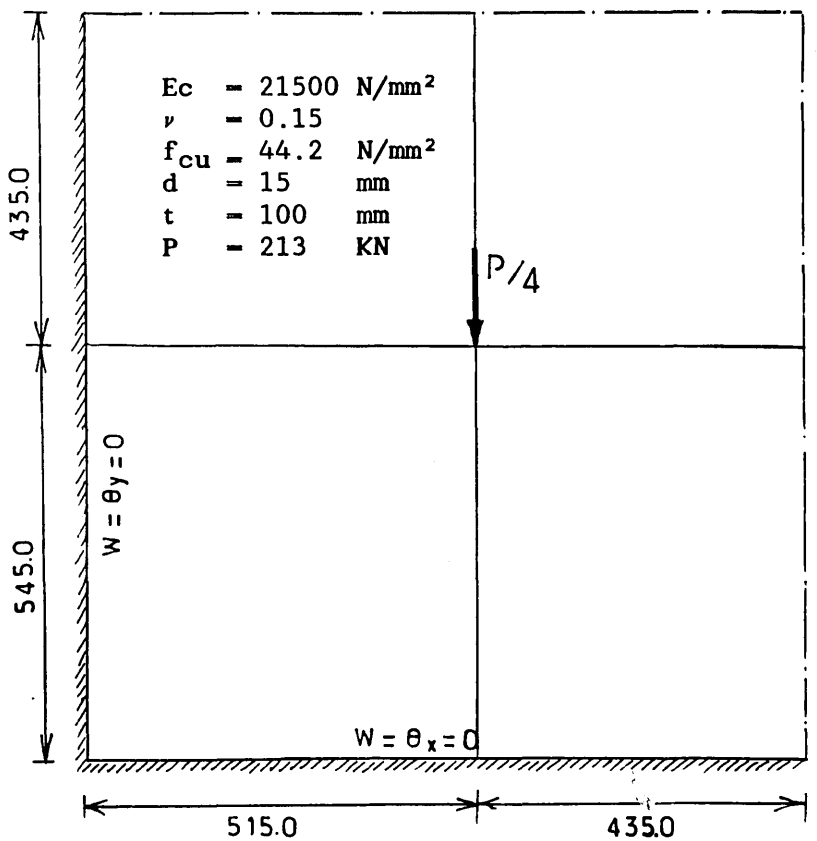
(a) Bottom steel



(b) Top steel



(c) Four point loading system



(d) Finite element idealisation.

Figure (6-9) Details of Hago's model three

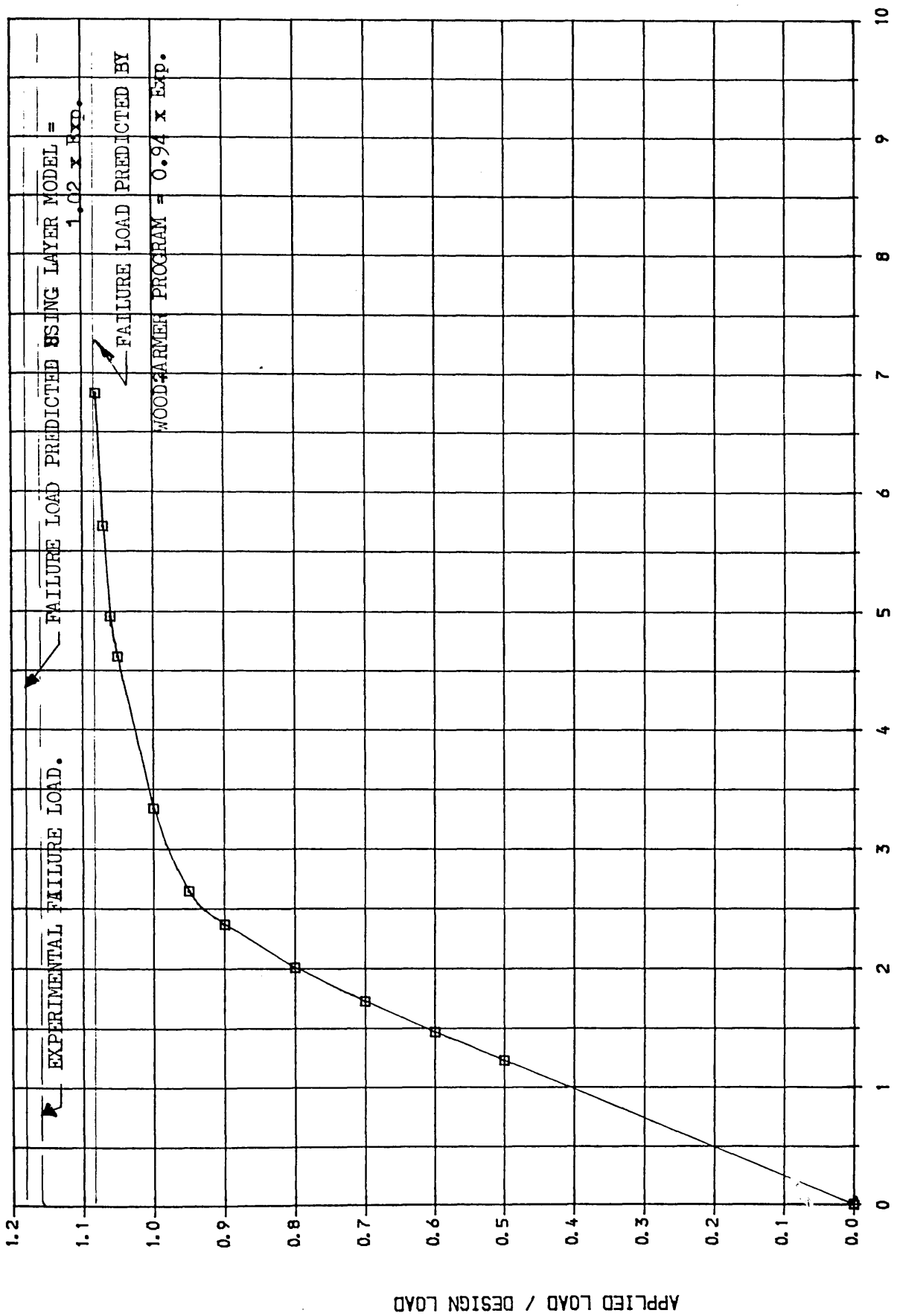


FIG. (6.10) LOAD-DISPLACEMENT CURVE FOR HAGO'S MODEL NO. 3

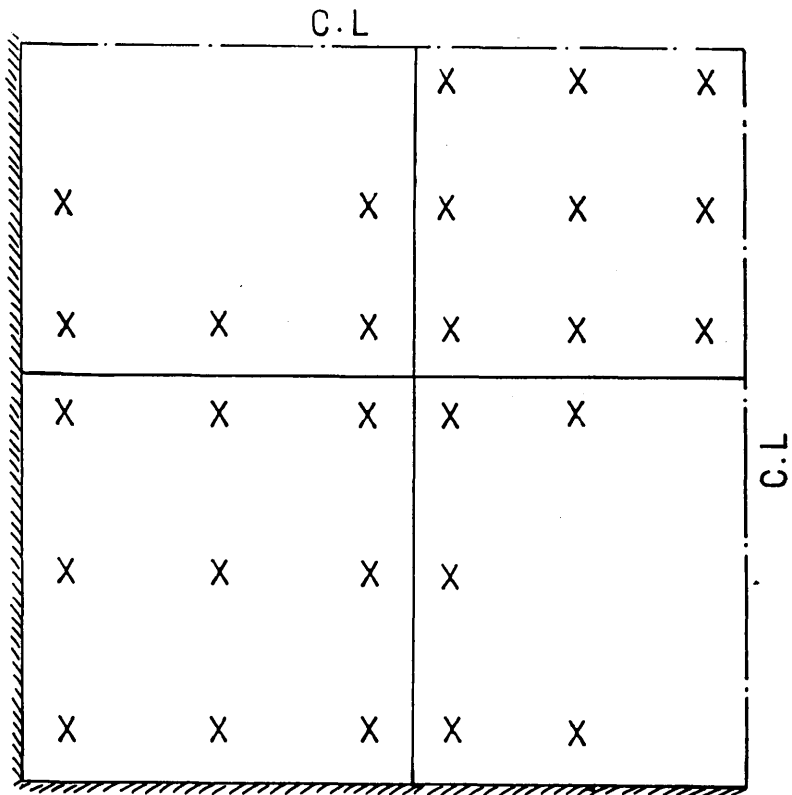


Figure (6-11) Spread of yielding

### 6.5 Conclusion:

This finite element program presented in this chapter proved to be an interesting tool for predicting failure load of reinforced concrete slabs . Furthermore the cost of this analysis in terms of time processing is much cheaper than the layer program for example.

The analysis of the two experimental slabs have given a result which is close to the experimental but during other numerical tests the results were far from the experimental failure load. This shows that a detailed investigation into this problem is necessary but because of lack of time it has prevented further investigations.

CHAPTER SEVEN :

GENERAL CONCLUSIONS AND SUGGESTIONS FOR FUTURE WORK

7.1 General conclusions:

From the theoretical investigations reported in this thesis, the following conclusions can be drawn:

1- The use of non elastic stress field with the direct design method has shown the following practical advantages :

1- a) The distribution of the design moments ( $M_x^*, M_y^*$ ) is more uniform.

1- b) The congestion of reinforcement is avoided due to the fact that peaks are smoothed out. Since design moment surface presents large flat area, this leads to convenient layout of reinforcement.

1- c) In general the maximum design moment is reduced by an average of 26% of the design moment associated with elastic stress field. Additionally it covers in average an area 15 times broader than the elastic design moment area.

1- d) The total design moment volume is not sensitive to the degree of plasticity spread.

2- The conclusions drawn from the nonlinear analysis conducted on the slabs designed by the elasto- plastic stress field are as follows:

2- a) The results indicate that at service load (0.625 x design load) the limiting deflection of span / 250 has not been reached for all the tested slabs except in the series No.2, in which the deflection at service load was about 11% more than the span / 250 . This is due to a general early yielding of the slab.

2- b) No steel yielded within the service load limit. The average load at first

yield of steel for all the tested slabs was 0.86 times the design load.

2- c) Compared to the slabs using elastic stress field , the yielding load ( $P_y$ ) has increased by an average of 2% for the test series "1" and decreased by an average of 5.2% in the case of test series 2 and 3 .

These results indicate also that the ductility demand is not much different for all the slabs designed by elasto- plastic stress field.

2- d) The average ultimate load for all the analysed slabs was 1.07 times the design load. This confirms that this method is a lower bound method.

2- e) In general the sensitivity of the results to the level of plasticity of the stress field used in the design was insignificant.

3- The elasto- plastic analysis based on Wood- Armer criterion (Wood- Armer program) proved to be an interesting tool of predicting failure load of reinforced concrete slabs with a reasonable accuracy. This analysis is, for example much cheaper than the layer program in terms of time processing. But although the good agreement reached for the two experimental slabs analysed, this program needs further arrangements.

## 7.2 Recommendations for futur work:

1- The investigation presented in this thesis pertains only to non elastic stress field obtained from the analysis of metallic plates. It is recommended to extend this work to other possible non elastic stress fields such as :

Elastic-plastic stress fields obtained from the analysis of reinforced concrete plates using Wood- Armer criterion:

$$(M_x^* - M_x)(M_y^* - M_y) - M_{xy}^2 = 0.0$$

where  $M_x^*$  and  $M_y^*$  are the design moments which are predetermined for large sections of the slab.



2- Slab systems presenting fixed edge boundaries have not been considered in this study due to the difficulty of simulation of these boundaries beyond the elastic conditions. It is recommended to investigate this problem in detail in order to be able in the future to analyse clamped edge slabs using finite element programs.

3- Since the service and ultimate behaviour of the tested slabs have been checked numerically only, it is recommended to carry out an experimental work to confirm the results obtained in this thesis.

4- The deflections predicted by Wood-Armer program are not real due to the fact that the matrix of elastic rigidities is not affected by the deterioration of the concrete properties (cracking). It is recommended to take into account the cracking of concrete within this program by using a pseudo thickness of the slab as given in the appendix. This pseudo-thickness ( $h_p$ ) simulates the cracked concrete in the elasto plastic analysis.

## REFERENCES

- 1 - ABD-EL-HAFEZ, L.M.  
Direct Design of Reinforced Concrete Skew Slabs.  
*Ph.D Thesis, Dept of Civ. Eng, University of Glasgow, Oct 1986.*
- 2 - AL MAHAIDI, R.S.H.  
Nonlinear finite element analysis of reinforced concrete deep members.  
*Report No.79-1, Dept of Structural Eng., Cornell University, January , 1979.*
- 2' - American Society of Civil Engineers Committee  
State of the art report on finite element analysis of reinforced concrete.  
*ASCE, New York, 1982*
- 3 - BAZANT, P.Z.  
Comment on Orthotropic models for Concrete and geomaterials  
*Journal of Engineering Mechanics, Vol.109, No.3, June 1983, PP 850-865*
- 4 - BRAESTRUP, C.M.W.  
Yield-line theory and limit analysis of plates and slabs.  
*Magazine of Concrete Research : Vol.22, No.71 , June 1970, PP 99-106*
- 5 - BELL, J.C. and ELMS, D.G.  
Nonlinear analysis of reinforced concrete slabs.  
*Magazine of concrete research, Vol.24, No.79, June 1972.*
- 6 - BELL, J.C. and ELMS, D.G.  
A finite element approach to post- elastic slab behaviour.  
*ACI special publications, SP 30-15, March 1971, PP 325-344*
- 7 - BUYUKOZTURK, O.  
Nonlinear analysis of reinforced concrete structures.  
*Computers & structures, Vol.7, 1977, PP 149-156*

- 8 - CARDENAS, A.E. and SOZEN, M.A.  
Flexural Yield Capacity of Slabs.  
*ACI Journal, February 1973, PP 124-126*
  
- 9 - CHEN, W.F. and TING, E.C.  
Constitutive Models for Concrete Structures.  
*Journal of the Eng. Mech. Division, Proc. of the ASCE, Vol. 106, No. EM 1, Feb 1979, PP 1-19*
  
- 10 - CHEN, W.F.  
Plasticity in reinforced concrete.  
*McGraw-Hill Book Company, 1982*
  
- 11 - CHEN, W.F. and SALEEB, A.F.  
Constitutive equations for engineering materials  
Volume 1 : Elasticity and modeling.  
*A Wiley- Interscience publication, 1981*
  
- 12 - CHEUNG, Y.K. and YEO, M.F.  
A Practical Introduction to Finite Element Analysis.  
*Pitman Publication Ltd, 1979*
  
- 13 - CLARK, L.A. and SPEIRS, D.M.  
Tension stiffening in reinforced concrete beams and slabs  
under short term loads.  
*Technical report 42.521, Cement and Concrete Association, London, 1978*
  
- 14 - CLYDE, D.H.  
Yield-line theory and plasticity.  
*Magazine of Concrete Research : Vol. 24, No. 78, March 1972, PP 37-42*
  
- 15 - COPE, R.J., RAO, P.V. and EDWARDS, K.R.  
Nonlinear finite element analysis techniques for concrete  
slabs.  
*Proceedings of the Third Int Conf in Australia on Finite Element methods, July 1979, The University of South Wales. PP 445-455*

- 16 - COPE, R.J. , RAO, P.V. , CLARK, L.A. and NORRIS, P.  
 Modelling of reinforced concrete behaviour for finite element analysis of bridge slabs.  
*Proceedings of the Third Int. Conf. in Australia on finite Element Methods, July 1979, the University of South Wales.*  
 PP 457-469
- 17 - COPE, R.J. and RAO, P.V.  
 Non-linear finite element analysis of concrete slab structures.  
*Proc. Instn Civ. Engrs, Part 2, No. 63, March 1977, PP 159-179*
- 18 - COPE, R.J. and CLARK, L.A.  
 Concrete Slabs - Analysis and Design  
*Elsevier Applied Science Publishers Ltd. 1984*
- 19 - DHIR, R.K. and MUNDAY, J.G.L.  
 Advances in Concrete Slab technology.  
*Pergamon Press Ltd 1980*
- 20 - DOTREPPE, J.C. , SCHNOBRICH, W.C. and PECKNOLD, D.A.  
 Layered Finite Element Procedure for inelastic Analysis of Reinforced Concrete Slabs.  
*Publications of the Int. Association for Bridges and Struc. Engrs, Vol. 33, No. 2, 1973, PP 53-68*
- 21 - DUNCAN, W. and JOHNARRY, T.  
 Nonlinear analysis of calmped concrete slab by a progressive relaxation of rotational restraints.  
*Proc. of 3<sup>rd</sup> Int. conf. in Australia on Finite Element Methods, July 1979, University of South Wales.*
- 22 - BS 8110 : Part one and two : 1985  
 Structural use of concrete.  
*British Standards Institution.*
- 23 - EBIRERI, J.O.  
 Direct Design of Beams for Combined Bending and Torsion  
*Ph.D Thesis, Dep of Civ. Eng, University of Glasgow, Feb, 1985*

- 24 - ERGATOUDIS, J.G. , IRONS, B.M. and ZIENKIEWICZ, O.C.  
Curved isoparametric quadrilateral elements for  
finite element analysis.  
*International Journal of Solids and Structures*, Vol.4,  
1968, PP 31-42
- 25 - FERNANDO, J.S. and KEMP, K.O.  
A generalized strip deflection method of reinforced  
concrete slab design.  
*Proc. Instn Civ. Engrs, Part 2*, Vol 65, Mar 1978, PP 163-174
- 26 - FERNANDO, J.S. and KEMP, K.O.  
The strip method of slab design : unique or lower-bound  
solutions.  
*Magazine of Concrete Research* , Vol.27, No.90, March 1975,  
PP 23-29
- 27 - GRAYSON, R. and STEVENS, L.K.  
Nonlinear analysis of structural systems of steel and  
concrete.  
*Proceedings of the Third Int. Conf in Australia on Finite  
Element Methods, July 1979, The University of South Wales.*  
PP 179-196
- 28 - GUPTA, A.K. and AKBAR, H.  
Cracking in Reinforced Concrete Analysis.  
*Journal of Structural Engineering*, Vol. 110, No.8, August 1984  
PP 1735-1746
- 29 - HAGO, A.W. and BHATT, P.  
Direct Design of reinforced Concrete Slabs.  
*ACI Journal*, Nov-Dec 1986, NO.6. *Proceedings Vol.83*,  
PP 916-924
- 30 - HAGO, A.W.  
Direct Design of Reinforced Concrete Slabs.  
*Ph.D Thesis, Dept of Civ. Eng, University of Glasgow, May 1982*

- 31 - HAND, F.R. , PECKNOLD, D.A. and SCHNOBRICH, W.C.  
Nonlinear Layered Analysis of RC Plates and Shells.  
*Journal of the Structural Division, Proc. of the ASCE, Vol. 99*  
*No. ST7, July 1973, PP 1491-1505*
- 32 - HILLERBORG, A.  
The advanced strip method - a simple design tool.  
*Magazine of Concrete Research : Vol. 34, No. 121, December 1982*  
*PP 175, 181*
- 33 - HILLERBORG, A.  
Equilibrium theory of concrete slabs.  
*Betong, Vol. 41, No. 41, 1956, PP 171-182*
- 34 - HINTON, E. , RAZZAQUE, A. , ZIENKIEWICZ, O.C. and DAVIES, J.D.  
A simple finite element solution for plates of homogeneous,  
sandwich and cellular construction.  
*Proc. Instn Civ. Engrs, Part 2, Vol. 59, March 1975, PP 43-65*
- 35 - HINTON, E. and OWEN, D.R.J.  
Finite Element Software for Plates and Shells.  
*Pineridge Press, 1984*
- 36 - HINTON, E and OWEN, D.R.J.  
Finite Element in Plasticity (Theory & Practice)  
*Pineridge Press, 1980*
- 37 - HINTON, E and OWEN, D.R.J.  
Finite Element Programming.  
*Academic Press, 1977*
- 38 - HOFBECK, J.A. , IBRAHIM, I.O. and MATTOCK, A.H.  
Shear transfer in reinforced concrete.  
*ACI Journal, Title No. 66-13, Feb 1969, PP 119-128*
- 39 - IABSE Colloquium Copenhagen, 1979  
Plasticity in reinforced concrete.  
*Report of the working commissions, Vol. 28*

- 40 - JAIN, S.C. and KENNEDY, J.B.  
Yield Criterion for Reinforced Concrete Slabs.  
*Journal of the Structural division, Proc. of the ASCE, Vol. 100*  
*No. ST3, March 1974, PP 631-644*
- 41 - JOHNARRY, T.  
Elasto-plastic analysis of concrete structures using  
the finite elements.  
*Ph.D Thesis, University of STRATHCLYDE, May 1979.*
- 42 - JIMENEZ, R. , WHITE, R.N. and GERGELY, P.  
Bond and Dowel Capacities of Reinforced Concrete.  
*ACI Journal, Title No. 76-4, Jan 1979, PP 73-93*
- 43 - JOFRIET, J.C. and Mc NIECE, G.M.  
Finite element analysis of reinforced concrete slabs.  
*Journal of the Str.Div., ASCE, Vol. 97, No. ST3, March 1971,*  
*PP 785.*
- 44 - JONES, L.L. and WOOD, R.H.  
Yield Line Analysis of Slabs  
*Thames & Hudson, Chatto & Windus, London, 1967*
- 45 - KEMP, K.O.  
The Yield Criterion for Orthotropically Reinforced Concrete  
Slabs.  
*Int. J. Mech. Sci., 1965, Vol. 7, PP 737-746*
- 46 - KEMP, K.O.  
Optimum Reinforcement in a Concrete Slab Subjected to  
Multiple Loadings  
*Publications of the Int. Association for Bridge and*  
*Structural Engineering, Vol. 31, 1971, PP 93-105*
- 47 - KUPFER, H.B. and GERSTLE, K.H.  
Behaviour of Concrete Under Biaxial Stresses.  
*Journal of the Eng. Mech. division, Proc of the ASCE, Vol. 99,*  
*No. EM4, August 1973, PP 853-866*

- 48 - KUPFER, H.B. , HILSDORF, H.K. and RUSH, H.  
Behaviour of Concrete Under Biaxial Stresses.  
*ACI Journal*, Title No. 66-52, August 1969, PP 656-666
- 49 - LENSCHOW, R. and SOZEN, M.A.  
A Yield Criterion for Reinforced Concrete Slabs.  
*ACI Journal*, Title No. 64-27, May 1967, PP 266-273
- 50 - CARDENAS, A. , CLYDE, D.H. , HILLERBORG, A. , LENKEI, P. , and AUTHORS  
Discussion of the reference 49.  
*ACI Journal*, Nov 1967, PP 783-789
- 51 - LIU, T.C.Y. , NILSON, A.H. , and SLATE, F.O.  
Stress-Strain Response and Fracture of Concrete in Uniaxial  
and Biaxial Compression.  
*ACI Journal*, Title No. 69-31, May 1972, PP 291-295
- 52 - MARCAL, P.V.  
Finite element analysis with material nonlinearities.  
ed. by, R.H. Gallagher, Y. Yamada and J.T. Oden, Univ. of.  
Alabama, 1971
- 53 - MORLEY, C.T. and GULVANESSIAN, H.  
Optimum reinforcement of concrete slab elements.  
*Proc. Instn. Civ. Engrs*, Part 2, Vol. 63, June 1977, PP 441-454
- 54 - MORLEY, C.T.  
Equilibrium design solutions for torsionless grillages or  
Hillerborg slabs under concentrated loads.  
*Proc. Instn Civ, Engrs*, Part 2, Vol. 81, Sept 1986, PP 447-460
- 55 - MELCHERS, R.E. , WOOD, R.H. , GURLEY, C.R. , MORLEY, C.T.  
Discussion of Ref. 54 by MORLEY, C.T.  
*Proc. Instn Civ, Engrs*, Part 2, Vol. 83, Sept 1987, PP 669-682
- 56 - NAYAK, G.C. and ZIENKIEWICZ, O.C.  
Convenient form of stress invariants for plasticity.  
*Journal of the Structural division, Proc. of the ASCE*, Vol. 98,  
No. ST4, April 1972, PP 949-954



- 57 - NIELSON, M.P.  
Limit Analysis and Concrete Plasticity.  
Prentice-Hall, 1984
- 58 - NIELSON, M.P.  
Limit Analysis of Reinforced Concrete Slabs  
*Acta Polytechnica Scandinavica,*  
*Civ. Eng and Building Construction series, No. 26, Copenhagen 1964*
- 59 - PARK, R. and GAMBLE W.L.  
Reinforced concrete slabs  
Wiley, 1980
- 60 - PARKHILL, D.L.  
The flexural behaviour of slabs at ultimate load.  
*Magazine of Concrete Research : Vol. 18, No. 56, Sept 1966,*  
*PP 141-146*
- 61 - SAVE, M.  
A consistent limit- analysis theory for reinforced  
concrete slabs.  
*Magazine of concrete research, Vol. 19, No. 58, March 1967,*  
*PP 3-12*
- 62 - SUIDAN, M. and SCHNOBRICH, W.C.  
Finite Element Analysis of Reinforced Concrete.  
*Journal of the Structural division, Proc. of the ASCE, Vol. 99,*  
*No. ST10, October, 1973, PP 2109-2122*
- 63 - SZILARD, R.  
Theory and analysis of plates  
Classical and numerical methods.  
Prentice-Hall, INC., 1974
- 64 - TASUJI, M.E. , SLATE, F.O. and NILSON, A.H.  
Stress strain response and fracture of concrete  
in biaxial loading.  
*Proceedings of the ACI, July 1978, Vol. 75,*  
*No. 7, PP 306-312*

- 65 - TASUJI, M.E. , NILSON, A.H. and SLATE, F.O.  
Biaxial stress-strain relationships for concrete.  
*Magazine of Concrete Research : Vol.31, No.109, December, 1979*  
PP 217-224
- 66 - TIMOSHENKO, S. and WOINOSKY-KRIEGER, S.  
Theory of plates and shells.  
*Mc Graw-Hill, New York, Second edition 1959.*
- 67 - WANCHOO, M.K. and MAY, G.W.  
Cracking Analysis of Reinforced Concrete plates.  
*Journal of the Structural division, Proc. of the ASCE, Vol.101*  
*No.ST1, Jan 1975, PP 201-215*
- 68 - WANG, B.  
Application of finite element methods in Civ.Eng  
*Vanderbilt University, Nashville, Tenn., Nov 1969.*
- 69 - WEGMULLER, A.W.  
Elastic-plastic finite element analysis of plates.  
*Proc. Instn Civ, Engrs, part 2, Vol.57, Sept 1974, PP 535-543*
- 70 - WOOD, R.H.  
Slab design : past, present and future.  
*American Concrete Institute Int. Symposium on Slabs, Denver,*  
*March 1971, and is reprinted from 'Cracking, deflection and*  
*ultimate load of concrete slab systems', ACI Publication*  
*SP-30, PP 203-221*
- 71 - WOOD, R.H.  
The reinforcement of slabs in accordance with a  
pre-determined field of moments.  
*Concrete, Vol.2, No.2, Feb 1968, PP 69-75*
- 72 - ARMER, G. S. T.  
Correspondance on Ref.71  
*Concrete, August 1968, PP 319-320*

73 - ZIENKIEWICZ, O.C. , VALLIAPPAN, S. and KING, I.P.

Stress analysis of rock as a 'no tension' material.

*Geotechnique*, Vol.18, March 1968, PP 56-66

74 - ZIENKIEWICZ, O.C.

The Finite Element Method.

McGraw Hill, Book Company (UK) Limited, 1977



C  
C\*\*\*\*\*

PROGRAM WXA

C\*\*\*\*\*

C  
C\*\*\* ELASTO PLASTIC ANALYSIS OF NON-LAYERED REINFORCED  
C\*\*\* CONCRETE SLABS USING WOOD-ARMER YIELD CRITERION

C  
C\*\*\*\*\*

C  
C\*\*\* THIS PROGRAM HAS BEEN DEVELOPED BY Mr M.BENREDOUANE  
C\*\*\* AT THE DEPARTEMENT OF CIVIL ENGINEERING AT  
C\*\*\* GLASGOW UNIVERSITY 1987/1988

C  
C\*\*\*\*\*

COMMON/BLOC6/KINCS(20), SHAPE(8), NPLLOT, MNODE  
COMMON/TAPE/IREW1, IREW2, IREW4, IREW8,  
. AREW1(46656), AREW2(53120), AREW4(640), LREW8(8640)  
COMMON/DAT/BEETA, CBEETA, C2BEETA, SBEETA, S2BEETA, CSBEETA  
COMMON/DATA/IBOU(80), BOUNG(80), ICHANG(64)  
DIMENSION ASDIS(867), COORD(289, 2), ELOAD(64, 27),  
. PSTNI(5, 576), ESTIF(27, 27),  
. EQRHS(10), EQUAT(80, 10), FIXED(867),  
. IFFIX(867), GLOAD(80), GSTIF(3240), LNODS(64, 9), LOCEL(27),  
. MATNO(64), NACVA(80), NAMEV(10), NCDIS(4), NCRES(4),  
. NDEST(27), NDFRO(64), NOFIX(80), NOUTP(2), NPIVO(10),  
. POSGP(4), PRESC(80, 3), PROPS(10, 8), REFOR(867),  
. RLOAD(64, 27), STRSG(5, 576), TOFOR(867),  
. TDISP(867), TLOAD(64, 27), TREAC(80, 3), VECRV(80),  
. WEIGP(4), BRMX(64), BRMY(64), TRMX(64), TRMY(64),  
. GPCODS(64, 2, 9), KIS(576)

C  
C\*\*\* PRESET VARIABLES ASSOCIATED WITH DYNAMIC DIMENSIONS

C  
CALL DIMMP (MBUFA, MELEM, MEVAB, MFRON, MMATS, MPOIN,  
. MSTIF, MTOTG, MTOTV, MVFIX, NDIME, NDOFN,  
. NPROP, NSTRE)

C  
C\*\*\* CALL THE SUBROUTINE WHICH READS MOST OF THE PROBLEM DATA

C  
CALL INPUT (COORD, IFFIX, LNODS, MATNO, MELEM, MEVAB,  
. MFRON, MMATS, MPOIN, MTOTV, MVFIX, NALGO,  
. NDFRO, NDIME, NDOFN, NELEM, NEVAB,  
. NGAUS, NLAPS, NINCS, NMATS, NNODE, NOFIX,  
. NPOIN, NPROP, NSTRE, NSTR1, NSWIT, NTOTG,  
. NTOTV, NTYPE, NVFIX, POSGP, PRESC, PROPS,  
. WEIGP, BRMX, BRMY, TRMX, TRMY, INMESH,  
. INCVRT)

C  
C\*\*\* INITIALIZE ARRAYS TO ZERO

C  
CALL ZEROMP (ELOAD, PSTNI, MELEM, MEVAB, MTOTG,  
. MTOTV, MVFIX, NDOFN, NELEM, NEVAB, NGAUS,  
. NTOTG, NTOTV, NVFIX, STRSG, TDISP, TFACT,  
. TLOAD, TREAC)

C  
C\*\*\*  
C

```

CALL          MINDPB      (IFDIS, IFFIX, IFRES, LNODS, MELEM, MTOTV,
.                  - NCDIS, NCRES, NELEM, NTYPE)
C
C*** COMPUTE LOAD AFTER READING RELEVANT EXTRA DATA
C
CALL          LOADPB      (COORD, LNODS, MATNO, MELEM, MMATS, MPOIN,
.                  NELEM, NEVAB, NGAUS, NNODE, NPOIN, PROPS,
.                  RLOAD, NOFIX, NVFIX)
C
C*** LOOP OVER EACH INCREMENT
C
DO 70 IINCS=1, NINCS
C
C*** READ DATA FOR CURRENT INCREMENT
C
CALL          INCREM      (ELOAD, FIXED, IINCS, MELEM, MEVAB, MITER,
.                  MTOTV, MVFIX, NDOFN, NELEM, NEVAB, NOUTP,
.                  NOFIX, NTOTV, NVFIX, PRESC, RLOAD, TFACT,
.                  TLOAD, TOLER)
C
C*** LOOP OVER EACH ITERATION
C
DO 90 IITER=1, MITER
PRINT*, 'IINCS=', IINCS, '*** IITER= ', IITER
C
C*** CALL ROUTINE WHICH SELECTS SOLUTION ALGORITHM VARIABLE
C*** KRESL
C
CALL          ALGOR      (FIXED, IINCS, IITER, KRESL, MTOTV, NALGO,
.                  NTOTV)
C
C*** CHECK WHETHER A NEW EVALUATION OF THE STIFFNESS MATRICES
C*** IS NEEDED
C
IF(KRESL.EQ.1)
CALL          STIFMP      (COORD, PSTNI, IINCS, LNODS, MATNO, MELEM,
.                  MEVAB, MMATS, MPOIN, MTOTG, NELEM,
.                  NEVAB, NGAUS, NNODE, PROPS, STRSG, BRMX, BRMY,
.                  TRMX, TRMY, KIS, GPCODS, NOFIX, NVFIX)
C
C*** SOLVE EQUATIONS
C
CALL          FRONT      (ASDIS, ELOAD, EQRHS, EQUAT, ESTIF, FIXED,
.                  IFFIX, IINCS, IITER, GLOAD, GSTIF, KRESL,
.                  LNODS, LOCEL, MBUFA, MELEM, MEVAB, MFRON,
.                  MSTIF, MTOTV, MVFIX, NACVA, NAMEV, NDEST,
.                  NDOFN, NELEM, NEVAB, NNODE, NOFIX, NPIVO,
.                  NPOIN, NTOTV, TDISP, TLOAD, TREAC, VECRV, NVFIX)
C
C*** CALCULATE RESIDUAL FORCES
C
CALL          RESMP      (ASDIS, COORD, ELOAD, PSTNI, LNODS,
.                  MATNO, MELEM, MMATS, MPOIN, MTOTG, MTOTV,
.                  NELEM, NEVAB, NGAUS, NNODE, PROPS,
.                  STRSG, BRMX, BRMY, TRMX, TRMY, KIS, IINCS)
C
C*** CHECK FOR CONVERGENCE
C

```

```

CALL      CONVMP      (ASDIS , ELOAD, IITER, IFDIS , IFRES , LNODS ,
.          .          MELEM , MEVAB , MTOTV , NCHEK , NCDIS , NCRES ,
.          .          NDOFN , NELEM , NEVAB , NNODE , NPOIN , NTOTV ,
.          .          REFOR , TOFOR , TDISP , TLOAD , TOLER)

```

C

C\*\*\* OUTPUT RESULTS IF REQUIRED

C

```

IF(IITER.EQ.1.AND.NOUTP(1).GT.0)
.CALL      OUTMP      (PSTNI , IITER , MTOTG , MTOTV , MVFIX , NELEM ,
.          .          NGAUS , NOFIX , NOUTP , NPOIN , NVFIX , STRSG ,
.          .          TDISP , TREAC , NCHEK , GPCODS , KIS)

```

C

C\*\*\* IF SOLUTION HAS CONVERGED STOP ITERATING AND OUTPUT

C\*\*\* RESULTS

C

```

IF(NCHEK.EQ.0) GO TO 100
90 CONTINUE

```

C

C\*\*\*

C

```

IF(NALGO.EQ.2) GO TO 100
STOP
100 CALL      OUTMP      (PSTNI , IITER , MTOTG , MTOTV , MVFIX , NELEM ,
.          .          NGAUS , NOFIX , NOUTP , NPOIN , NVFIX , STRSG ,
.          .          TDISP , TREAC , NCHEK , GPCODS , KIS)
70 CONTINUE
20 CONTINUE
10 CONTINUE
STOP
END

```





```
ABETA2=1.0/DENOM2
```

```
RETURN
```

```
C
```

```
C*** VECTOR A WHEN YIELD1-YIELD2=0.0
```

```
C
```

```
3 AVECT3(1)=(YY-STEMP(2))-(YY1+STEMP(2))
```

```
AVECT3(2)=(XX-STEMP(1))-(XX1+STEMP(1))
```

```
AVECT3(3)=2.0*(STEMP(3)+ZZ)+2.0*(STEMP(3)-ZZ1)
```

```
C
```

```
DENOM3=0.0
```

```
DO 130 ISTRE=1,3
```

```
DVECT3(ISTRE)=0.0
```

```
DO 135 JSTRE=1,3
```

```
135 DVECT3(ISTRE)=DVECT3(ISTRE)+DMATX(ISTRE,JSTRE)*AVECT3(JSTRE)
```

```
130 DENOM3=DENOM3+AVECT3(ISTRE)*DVECT3(ISTRE)
```

```
ABETA3=1.0/DENOM3
```

```
RETURN
```

```
END
```

```

SUBROUTINE INVMP      (STEMP, YIELD1, YIELD2, BRMX, BRMY, TRMX, TRMY,
                      IELEM, ALPHA, KIS, KYIELD, IND, FBT1,
                      FBT2, FTP1, FTP2, KGAUS)
C*****
C
C***   CALCULATE YIELD VALUES FOR BOTTOM AND TOP STEEL RESP.
C***   EVALUATION OF THE REDUCTION FACTORS ALPHAB & ALPHAT IF NEEDED
C
C*****
COMMON/DAT/BEETA, CBEETA, C2BEETA, SBEETA, S2BEETA, CSBEETA
DIMENSION STEMP(5), BRMX(64), BRMY(64),
           TRMX(64), TRMY(64), KIS(576)
XX=BRMX(IELEM)+BRMY(IELEM)*C2BEETA
YY=BRMY(IELEM)*S2BEETA
ZZ=BRMY(IELEM)*CSBEETA
XX1=TRMX(IELEM)-TRMY(IELEM)*C2BEETA
YY1=TRMY(IELEM)*S2BEETA
ZZ1=TRMY(IELEM)*CSBEETA
C
C***   WOOD-ARMER CREITERION FOR ORTHOGONALLY REINFORCED SLABS
C
C
C***   POSITIVE YIELD SURFACE (BOTTOM STEEL)
C
      FBT1=XX-STEMP(1)
      FBT2=YY-STEMP(2)
      YIELD1=-((FBT1*FBT2)+((STEMP(3)+ZZ)**2))
C
C***   NEGATIVE YIELD SURFACE(TOP STEEL)
C
      FTP1=XX1+STEMP(1)
      FTP2=YY1+STEMP(2)
      YIELD2=-((FTP1*FTP2)+((STEMP(3)-ZZ1)**2))
C
C***   IND INDICE FOR COMPUTING THE REDUCTION FACTOR OR NOT
C
      IF (IND.EQ.0) RETURN
      GOTO(1,2,3) KYIELD
C
C***   EVALUATE THE REDUCTION FACTOR FOR BOTTOM STEEL
C
1     A=(STEMP(3)*STEMP(3))-(STEMP(1)*STEMP(2))
      B=XX*STEMP(2)+YY*STEMP(1)+2.0*ZZ*STEMP(3)
      C=ZZ*ZZ-XX*YY
      Z=MAX(A,B,C)
      A=A/Z
      B=B/Z
      C=C/Z
      DELTA=(B*B)-(4.0*A*C)
      IF(DELTA.LT.0.0.AND.DELTA.GE.-0.1) DELTA=0.0
      ALFA1=(-B+SQRT(DELTA))/(2.0*A)
      ALFA2=(-B-SQRT(DELTA))/(2.0*A)
      X=ALFA1*STEMP(1)
      Y=ALFA1*STEMP(2)
      X2=ALFA2*STEMP(1)
      Y2=ALFA2*STEMP(2)
      IF(X.LE.XX.AND.X2.LE.XX.AND.Y.LE.YY.
* AND.Y2.LE.YY) THEN
      ALPHAB=MAX(ALFA1,ALFA2)

```

```

ELSE IF(X.LE.XX.AND.Y.LE.YY) THEN
ALPHAB=ALFA1
ELSE
ALPHAB=ALFA2
END IF
ALPHA=ALPHAB
KIS(KGAUS)=1
RETURN

```

C

C\*\*\* REDUCTION FACTOR FOR YIELD2 (TOP STEEL)

C

```

2   A=STEMP(3)*STEMP(3)-STEMP(1)*STEMP(2)
    B=- (XX1*STEMP(2)+YY1*STEMP(1)+ZZ1*STEMP(3))*2.0)
    C=ZZ1*ZZ1-XX1*YY1
    Z=MAX(A,B,C)
    A=A/Z
    B=B/Z
    C=C/Z
    DELTA=B*B-4.0*A*C
    IF(DELTA.LT.0.0.AND.DELTA.GE.-0.1) DELTA=0.0
    ALFA1=(-B+SQRT(DELTA))/(2.0*A)
    ALFA2=(-B-SQRT(DELTA))/(2.0*A)
    X=ALFA1*STEMP(1)
    Y=ALFA1*STEMP(2)
    X2=ALFA2*STEMP(1)
    Y2=ALFA2*STEMP(2)
    V=-XX1
    W=-YY1
    IF(X.GE.V.AND.X2.GE.V.AND.Y.GE.W.AND.Y2.GE.W) THEN
    ALPHAT=MAX(ALFA1,ALFA2)
    ELSE IF(X.GE.V.AND.Y.GE.W) THEN
    ALPHAT=ALFA1
    ELSE
    ALPHAT=ALFA2
    END IF
    ALPHA=ALPHAT
    KIS(KGAUS)=2
    RETURN

```

C

C\*\*\* REDUCTION FACTOR WHEN BOTH YIELD1 AND YIELD2 ARE VIOLATED

C

```

3   A=STEMP(3)*STEMP(3)-STEMP(1)*STEMP(2)
    B=XX*STEMP(2)+YY*STEMP(1)+2.0*STEMP(3)*ZZ
    C=ZZ*ZZ-XX*YY
    Z=MAX(A,B,C)
    A=A/Z
    B=B/Z
    C=C/Z
    DELTA=B*B-4.0*A*C
    IF(DELTA.LT.0.0.AND.DELTA.GE.-0.1) DELTA=0.0
    ALFA1=(-B+SQRT(DELTA))/(2.0*A)
    ALFA2=(-B-SQRT(DELTA))/(2.0*A)
    X=ALFA1*STEMP(1)
    Y=ALFA1*STEMP(2)
    X2=ALFA2*STEMP(1)
    Y2=ALFA2*STEMP(2)
    IF(X.LE.XX.AND.X2.LE.XX.AND.Y.LE.YY.
* AND.Y2.LE.YY) THEN
    ALPHAB=MAX(ALFA1,ALFA2)

```

```
ELSE IF(X.LE.XX.AND.Y.LE.YY) THEN
ALPHAB=ALFA1
ELSE
ALPHAB=ALFA2
END IF
ALPHA1=ALPHAB
A=STEMP(3)*STEMP(3)-STEMP(1)*STEMP(2)
B=-(XX1*STEMP(2)+YY1*STEMP(1)+2.0*STEMP(3)*ZZ1)
C=ZZ1*ZZ1-XX1*XX1
Z=MAX(A,B,C)
A=A/Z
B=B/Z
C=C/Z
DELTA=B*B-4.0*A*C
IF(DELTA.LT.0.0.AND.DELTA.GE.-0.1) DELTA=0.0
ALFA1=(-B+SQRT(DELTA))/(2.0*A)
ALFA2=(-B-SQRT(DELTA))/(2.0*A)
X=ALFA1*STEMP(1)
Y=ALFA1*STEMP(2)
X2=ALFA2*STEMP(1)
Y2=ALFA2*STEMP(2)
V=-XX1
W=-YY1
IF(X.GE.V.AND.X2.GE.V.AND.Y.GE.W.AND.Y2.GE.W) THEN
ALPHAT=MAX(ALFA1,ALFA2)
ELSE IF(X.GE.V.AND.Y.GE.W) THEN
ALPHAT=ALFA1
ELSE
ALPHAT=ALFA2
END IF
ALPHA2=ALPHAT
ALPHA=MAX(ALPHA1,ALPHA2)
IF(ALPHA.EQ.ALPHA1) KIS(KGAUS)=1
IF(ALPHA.EQ.ALPHA2) KIS(KGAUS)=2
RETURN
END
```

```

      SUBROUTINE RESMP      (ASDIS,COORD,ELOAD,PSTNI, LNODS,
      .                    MATNO,MELEM,MMATS,MPOIN,MTOTG,MTOTV,
      .                    NELEM,NEVAB,NGAUS,NNODE,PROPS,
      .                    STRSG,BRMX,BRMY,TRMX,TRMY,KIS,IINCS)
C*****
C
C***  EVALUATES EQUIVALENT NODAL FORCES FOR THE STRESS RESULTANTS
C***  IN MINDLIN PLATES DURING EP ANALYSIS
C
C*****
      DIMENSION ASDIS(MTOTV),AVECT(5),CARTD(2,9),AVECT3(5),DVECT3(5),
      .          COORD(MPOIN,2),DERIV(2,9),DESIG(5),DEVIA(4),
      .          DVECT(5),AVECT1(5),AVECT2(5),DVECT1(5),DVECT2(5),
      .          ELCOD(2,9),
      .          ELDIS(3,9),ELOAD(MELEM,27),PSTNI(5,MTOTG),GPCOD(2,9),
      .          LNODS(MELEM,9),MATNO(MELEM),POSGP(4),
      .          PROPS(MMATS,8),SGTOT(5),SHAPE(9),SIGMA(5),
      .          STRES(5),STRSG(5,MTOTG),WEIGP(4),
      .          DFLEX(3,3),DSHER(2,2),BFLEI(3,3),BSHEI(2,3),
      .          DUMMY(3,3),FORCE(3),DGRAD(6),
      .          BRMX(64),BRMY(64),TRMX(64),TRMY(64),KIS(576)
      DO 680 ILI=1,576
680    KIS(ILI)=0
      DO 10 IELEM=1,NELEM
      DO 10 IEVAB=1,NEVAB
10    ELOAD(IELEM,IEVAB)=0.0
      KGAUS=0
      LGAUS=0
      DO 20 IELEM=1,NELEM
      LPROP=MATNO(IELEM)
C
C***  COMPUTE COORDINATE AND INCREMENTAL DISPLACEMENTS OF THE
C      ELEMENT NODAL POINTS
C
      DO 190 INODE =1,NNODE
      LNODE=IABS(LNODS(IELEM,INODE))
      NPOSN=(LNODE-1)*3
      DO 30 IDOFN=1,3
      NPOSN=NPOSN+1
30    ELDIS(IDOFN,INODE)=ASDIS(NPOSN)
      DO 180 IDIME=1,2
180    ELCOD(IDIME,INODE)=COORD(LNODE,IDIME)
190    CONTINUE
      KGASP=0
      CALL      MODPB      (DFLEX,DUMMY,DSHER,LPROP,MMATS,PROPS,
      .                    0, 1, 1)
      CALL GAUSSQ      (NGAUS,POSGP,WEIGP)
      DO 40 IGAUS=1,NGAUS
      DO 40 JGAUS=1,NGAUS
      KBOT=0
      KTOP=0
      NTIME=0
      KGAUS=KGAUS+1
      EXISP=POSGP(IGAUS)
      ETASP=POSGP(JGAUS)
      CALL      SFR2      (DERIV,ETASP,EXISP,NNODE,SHAPE)
      KGASP=KGASP+1
      CALL      JACOB2      (CARTD,DERIV,DJACB,ELCOD,GPCOD,IELEM,
      .                    KGASP,NNODE,SHAPE)

```

```

DAREA=DJACB*WEIGP(IGAUS)*WEIGP(JGAUS)
CALL      GRADMP      (CARTD,DGRAD,ELDIS,      3,NNODE)
CALL      STRMP       (CARTD,DFLEX,DGRAD,DSHER,ELDIS,NNODE,
.           SHAPE,STRES,      1,      0)
DO 150 ISTORE=1,3
DESIG(ISTRE)=STRES(ISTRE)
SIGMA(ISTRE)=STRSG(ISTRE,KGAUS)+STRES(ISTRE)
150 CONTINUE
CALL      INVMP       (SIGMA,YIELD1,YIELD2,BRMX,BRMY,TRMX,TRMY,
.           IELEM,ALPHA,KIS,0,0,FBT1,FBT2,FTP1,FTP2,KGAUS)
500 IF(YIELD1.GT.0.0.OR.FBT1.LT.0.0.OR.FBT2.LT.0.0) KBOT=1
IF(YIELD2.GT.0.0.OR.FTP1.LT.0.0.OR.FTP2.LT.0.0) KTOP=1
C
C*** CHECK IF THIS GP STILL ELASTIC OR NO CORRECTION ON THE STRESSES IS
NEEDED
C
IF(KBOT.EQ.0.AND.KTOP.EQ.0) GOTO 50
C
C*** CHECK IF THIS GP HAS YIELDED IN RESPECT OF BOTTOM STEEL
C
IF(KBOT.EQ.1.AND.KTOP.EQ.0) CALL INVMP (SIGMA,YIELD1,YIELD2,BRMX,
.   BRMY,TRMX,TRMY,IELEM,ALPHA,KIS,1,1,FBT1,FBT2,FTP1,FTP2,KGAUS)
C
C*** CHECK IF THIS GP HAS YIELDED IN RESPECT OF TOP STEEL
C
IF(KBOT.EQ.0.AND.KTOP.EQ.1) CALL INVMP (SIGMA,YIELD1,YIELD2,BRMX,
.   BRMY,TRMX,TRMY,IELEM,ALPHA,KIS,2,1,FBT1,FBT2,FTP1,FTP2,KGAUS)
C
C*** CHECK IF THIS GP HAS YIELDED IN RESPECT OF BOTH BOTTOM AND TOP STEE
L
C
IF(KBOT.EQ.1.AND.KTOP.EQ.1) CALL INVMP (SIGMA,YIELD1,YIELD2,BRMX,
.   BRMY,TRMX,TRMY,IELEM,ALPHA,KIS,3,1,FBT1,FBT2,FTP1,FTP2,KGAUS)
60 ASTEP=50.0
C*** ASTEP HAS BEEN SET ARBITRARILY
DO 70 ISTORE=1,3
SGTOT(ISTRE)=(STRSG(ISTRE,KGAUS)+STRES(ISTRE))*ALPHA
STRES(ISTRE)=((STRSG(ISTRE,KGAUS)+STRES(ISTRE))*(1.0-ALPHA))/
.   ASTEP
70 CONTINUE
DO 650 ISTEP=1,50
CALL FLOWMP (ABETA1,ABETA2,ABETA3,AVECT1,AVECT2,AVECT3,DFLEX,
*   DVECT1,DVECT2,DVECT3,
.   BRMX,BRMY,TRMX,TRMY,SGTOT,IELEM,KIS,KGAUS)
GOTO (1,2,3) KIS(KGAUS)
2 DO 11 ISTORE=1,3
AVECT(ISTRE)=AVECT2(ISTRE)
11 DVECT(ISTRE)=DVECT2(ISTRE)
ABETA=ABETA2
GOTO 80
1 DO 22 ISTORE=1,3
AVECT(ISTRE)=AVECT1(ISTRE)
22 DVECT(ISTRE)=DVECT1(ISTRE)
ABETA=ABETA1
GOTO 80
3 DO 33 ISTORE=1,3
AVECT(ISTRE)=AVECT3(ISTRE)
33 DVECT(ISTRE)=DVECT3(ISTRE)
ABETA=ABETA3

```

```

80   AGASH=0.0
      DO 100 ISTORE=1,3
100  AGASH=AGASH+AVECT(ISTRE)*STRES(ISTRE)
      DLAMD=AGASH*ABETA
      IF(DLAMD.LT.0.0) DLAMD=0.0
      DO 110 ISTORE=1,3
110  SGTOT(ISTRE)=SGTOT(ISTRE)+STRES(ISTRE)-DLAMD*DVECT(ISTRE)
650  CONTINUE
      CALL INVMP (SGTOT, YIELD1, YIELD2, BRMX, BRMY, TRMX, TRMY, IELEM,
                ALPHA, KIS, 0, 0, FBT1, FBT2, FTP1, FTP2, KGAUS)
      IF((YIELD1.GT..1E+00.OR.YIELD2.GT..1E+00.OR.FBT1.LT.0.0.OR.
        . FBT2.LT.0.0.OR.FTP1.LT.0.0.OR.FTP2.LT.0.0).AND.(
        . NTIME.LT.1010)) THEN
C*** THIS LAST CHECK HAS BEEN SET ARBITRARILY TO GIVE GOOD RESULT
      NTIME=NTIME+1
      DO 450 ISTORE=1,3
      STRES(ISTRE)=SGTOT(ISTRE)-STRSG(ISTRE,KGAUS)
450  SIGMA(ISTRE)=SGTOT(ISTRE)
      KBOT=0
      KTOP=0
      GOTO 500
      ELSE
      CONTINUE
      END IF
      DO 400 ISTORE=1,3
      PSTNI(ISTRE,KGAUS)=PSTNI(ISTRE,KGAUS)+DLAMD*AVECT(ISTRE)
400  DESIG(ISTRE)=SGTOT(ISTRE)-STRSG(ISTRE,KGAUS)
50   DO 120 ISTORE=1,3
      SGTOT(ISTRE)=STRSG(ISTRE,KGAUS)+DESIG(ISTRE)
120  STRSG(ISTRE,KGAUS)=SGTOT(ISTRE)
C
C*** CALCULATE THE EQUIVALENT NODAL FORCES AND ASSOCIATE WITH THE
C   ELEMENT NODES
C
250  CONTINUE
      DO 140 INODE=1, NNODE
C*** ZERO FORCE VECTOR
      CALL VZERO (3, FORCE)
      CALL BMATPB (BFLEI, DUMMY, BSHEI, CARTD, INODE, SHAPE,
                0, 1, 0)
      FORCE(2)=(BFLEI(1,2)*SGTOT(1)+BFLEI(3,2)*SGTOT(3))*DAREA
        +FORCE(2)
      FORCE(3)=(BFLEI(2,3)*SGTOT(2)+BFLEI(3,3)*SGTOT(3))*DAREA
        +FORCE(3)
      IPOSN=(INODE-1)*3+1
      DO 135 IDOFN=2,3
      IPOSN=IPOSN+1
135  ELOAD(IELEM, IPOSN)=ELOAD(IELEM, IPOSN)+FORCE(IDOFN)
      140 CONTINUE
      40 CONTINUE
C
C*** CALCULATE FORCES ASSOCIATED IF(IELEM.EQ.1) WITH SHEAR DEFORMATION
C
      NGAUM=NGAUS-1
      CALL GAUSSQ (NGAUM, POSGP, WEIGP)
C
C*** ENTER LOOPS FOR AREA NUMERICAL INTEGRATION
C
      KGASP=0

```

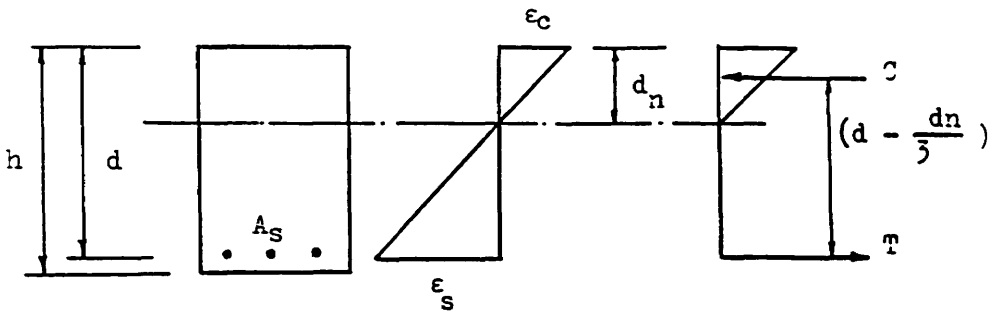
```

DO 300 IGAUS=1, NGAUM
DO 300 JGAUS=1, NGAUM
LGAUS=LGAUS+1
EXISP=POSGP(IGAUS)
ETASP=POSGP(JGAUS)
CALL      SFR2      (DERIV, ETASP, EXISP, NNODE, SHAPE)
KGASP=KGASP+1
CALL      JACOB2    (CARTD, DERIV, DJACB, ELCOD, GPCOD, IELEM,
                    KGASP, NNODE, SHAPE)
DAREA=DJACB*WEIGP(IGAUS)*WEIGP(JGAUS)
CALL      GRADMP    (CARTD, DGRAD, ELDIS,      3, NNODE)
CALL      STRMP     (CARTD, DFLEX, DGRAD, DSHER, ELDIS, NNODE,
                    SHAPE, STRES,      0,      1)
DO 310 ISTRE=4, 5
SGTOT(ISTRE)=STRSG(ISTRE, LGAUS)+STRES(ISTRE)
310 STRSG(ISTRE, LGAUS)=SGTOT(ISTRE)
C
C*** CALCULATE THE EQUIVALENT NODAL FORCES
C
DO 320 INODE=1, NNODE
C*** ZERO FORCE VECTOR
CALL VZERO(3, FORCE)
CALL      BMATPB    (BFLEI, DUMMY, BSHEI, CARTD, INODE, SHAPE,
                    0,      0,      1)
FORCE(1)=(BSHEI(1,1)*SGTOT(4)+BSHEI(2,1)*SGTOT(5))*DAREA
          +FORCE(1)
FORCE(2)=(BSHEI(1,2)*SGTOT(4))*DAREA+FORCE(2)
FORCE(3)=(BSHEI(2,3)*SGTOT(5))*DAREA+FORCE(3)
IPOSN=(INODE-1)*3
DO 315 IDOFN=1, 3
IPOSN=IPOSN+1
315 ELOAD(IELEM, IPOSN)=ELOAD(IELEM, IPOSN)+FORCE(IDOFN)
320 CONTINUE
300 CONTINUE
20 CONTINUE
RETURN
END

```



## APPENDIX (B)

CALCULATION OF THE PSEUDO THICKNESS ( $b_p$ )

For equilibrium:  $C = T$

$$\therefore 1/2 \epsilon_c \cdot E_c \cdot d_n = A_s \cdot E_s \cdot \epsilon_s \quad \dots (1)$$

$$\therefore d_n = 2 \frac{E_s}{E_c} \cdot \frac{\epsilon_s}{\epsilon_c} \cdot A_s = 2 \cdot m \cdot A_s \cdot \frac{\epsilon_s}{\epsilon_c} \quad \dots (2)$$

where  $m$  = modular ratio =  $E_s/E_c$ .

But from the strain diagram:

$$\frac{\epsilon_s}{\epsilon_c} = \frac{d - d_n}{d_n} \quad \dots (3)$$

$$\therefore d_n^2 + 2 \cdot m \cdot A_s \cdot d_n - 2 \cdot m \cdot A_s \cdot d = 0 \quad \dots (4)$$

Solving gives:

$$d_n = \left( -m.A_s + \sqrt{(m.A_s)^2 + 2(m.A_s)d} \right) \quad \dots(5)$$

The gross moment of inertia is

$$I_g = \frac{bh^3}{12} + (m-1)A_s \left( d - \frac{h}{2} \right)^2 \quad \dots(6)$$

and the fully cracked transformed section gives:

$$I_{cr} = \frac{b.d_n^3}{3} + m.A_s(d - d_n)^2 \quad \dots(7)$$

Then by assuming  $I_{cr} = (b.h_p^3) / 12$  , a pseudo-thickness ( $h_p$ ) of a cracked section is calculated from:

$$h_p = \left\{ (12 I_{cr}) / b \right\}^{3/2} \quad \dots(8)$$